Pain behaviour, locomotor activity, inflammation and muscle metabolic dysregulation in pre-clinical animal models of OA and RA and the impact of PPARɣ agonism intervention

Nuria Casanova Vallve, BSc, MSc

ARUK Centre for sports, exercise and osteoarthritis

School of Life Sciences

Thesis submitted to the University of Nottingham for the degree of Doctor of Philosophy

2018

Declaration

This is to certify that I conducted the original research submitted in this thesis. Any help received with *in-vivo* studies here has been fully acknowledged, and referenced where appropriate.

I conducted the study design, data collection, analysis and writing. The MNX surgeries were performed by James Burston and myself. The majority of knee and ankle joints were processed and embedded by Roger Hill in King's Mill Hospital. Dr Tim Constantin-Teodosiu introduced the mRNA expression data in the Ingenuity Pathway Analysis (IPA).

The supervision of this thesis was undertaken by Professors Victoria Chapman and Paul Greenhaff and Dr Tim Constantin-Teodosiu. This thesis has not been already accepted for any degree.

Acknowledgements

I would like to thank a big number of people that made possible this PhD helping professionally and emotionally throughout all these years.

I would like to thank the most my supervisors Professors Victoria Chapman and Paul Greenhaff for giving me this opportunity and for their supervision and guidance throughout the PhD. I would like to thank Dr Tim Constantin-Teodosiu for sharing his knowledge on muscle physiology and training in all the biochemical, molecular and muscle dissection techniques I have learnt. I would like to thank the Pain Centre team and especially those I have shared the lab with, helping with the animal work, and for their support.

To my family and friends. Most importantly to my parents, my sister and my brother. Their support and encouragement have been essential for me.

Abstract

Background: Osteoarthritis (OA) and rheumatoid arthritis (RA) are degenerative joint diseases accompanied by pain and inflammation, which can lead to a sedentary lifestyle. Skeletal muscle inflammation and inactivity can lead to increased muscle insulin resistance and atrophy, which are associated with the dysregulation of muscle carbohydrate metabolism and changes in the expression of genes and proteins known to regulate muscle mass. This study aimed to identify the impact of OA and RA on pain behaviour, locomotor activity, inflammation and muscle metabolic dysregulation and atrophy in two animal models and the effects of the PPARɣ agonist (rosiglitazone) on these study end-points. Additionally, muscle mRNA isolated from RA patients was used to identify potential commonality of muscle gene expression between clinical and pre-clinical RA. The hypothesis of the thesis was that joint inflammation in arthritis will impact behavioural pain and activity, and skeletal muscle function.

Methods: In two independent studies, using medial meniscus transection (MNX) model of OA and the collagen-induced arthritis (CIA) model of RA levels of pain, locomotor activity, joint pathology, and inflammation, and changes in extensor digitorum longus (EDL) muscle mass and intermediary metabolism were assessed. Additionally, expression levels of 46 gene transcripts associated with muscle inflammation, and carbohydrate and protein metabolism were assessed using TaqMan low-density array (TLDA) cards in the EDL muscle in the CIA model. Ingenuity Pathway Analysis (IPA) was used to predict changes in cellular functions. A cohort of genes altered

in the CIA model was also assessed in quadriceps muscle biopsy samples from RA patients, which were normalised to a healthy age-matched control volunteer group. Effects of the PPARɣ agonist rosiglitazone on pain behaviour, locomotor activity, inflammation, joint pathology, and muscle mass and metabolism was also determined in the CIA model. Again, muscle gene expression was assessed using TLDA cards and IPA was used to predict changes in cellular functions.

Results: Increased pain (WB $p<0.01$ at day 28, 42; WB $p<0.05$ at day 49; PWT $p<0.01$ at day 21, 42, 55; PWT $p<0.05$ at day 28, 35) and joint pathology (chondropathy $p<0.001$ days 28, 55; osteophytosis $p<0.001$ day 28, $p<0.01$ day 55; synovitis $p<0.001$ day 28, $p<0.01$ day 55) were identified in the MNX model. The magnitude of systemic and muscle inflammation and locomotor activity was similar to control animals, and no difference in muscle metabolites and the muscle protein:DNA ratio was identified between groups. In the CIA model, increased pain behaviour ($p<0.01$), reduced locomotor activity (horizontal $p<0.001$; vertical $p<0.05$) and greater levels of plasma IL-6 ($p<0.01$) was observed compared to control, which was accompanied by incremented paw thickness ($p<0.001$) and synovitis ($p<0.01$). An increase in muscle lactate content relative to control ($p<0.01$) was in line with the IPA predicted change in carbohydrate metabolism based on differences in muscle mRNA expression, exemplified by reduced expression IRS1, Glut4 and PPARgc1β mRNAs relative to control ($p<0.01$). The muscle protein:DNA ratio tended to be less in the CIA model compared to control, a finding in line with the IPA prediction of an altered protein metabolism, suggested for example by increased expression levels of

FOXO1, Eif4ebp1, MAFbx, MuRF1 and Cathepsin-L mRNA in CIA model ($p<0.05$). Rosiglitazone reduced inflammation and the paw thickness ($p<0.001$) in CIA relative to the CIA rats treated with vehicle. Rosiglitazone tended to reduce plasma IL-6 and muscle lactate accumulation, while differences in mRNA expression predicted activation of lipid oxidation, carbohydrate metabolism and protein synthesis using IPA. In clinical RA muscle samples, levels of inflammatory cytokine IL-6, myostatin, Mt1A and PDK4 were higher and PPARgc1β lower than healthy controls.

Conclusion: Muscle atrophy and metabolic dysregulation in the CIA model of RA could result from a decline in locomotor activity, secondary to pain, and inflammation, which were not identified in the MNX model of OA. The CIA model exhibited significant differences on the expression of various genes in muscle, which were also modified in muscle from RA patients. PPARɣ agonism is worthy of further investigation as a strategy to treat inflammation and muscle metabolic dysregulation in RA.

Presentations

Poster

Casanova-Vallve N, Constantin-Teodosiu D, Greenhaff PL and Chapman V. The impact of osteoarthritis development on locomotor activity and muscle inflammation and metabolism in a rodent pain model. – Physical Activity and Osteoarthritis Conference, Loughborough University, UK. December 2015

Casanova-Vallve N, Constantin-Teodosiu D, Greenhaff PL and Chapman V. Modulation of pain, muscle energy metabolism and muscle mass in a collagen-induced arthritis model in the rat. – 5th World Congress on Controversies, Debates and Consensus in Bone, Muscle and Joint Diseases (BMJD), Gold Coast, Australia. August 2017

List of figures

Figure 1.1: Description of normal joint and joint with osteoarthritis. 6

Figure 1.2: Description of the healthy joint and its changes with rheumatoid arthritis 17

Figure 1.3: Inflammatory and immune response in the joint of RA. 24

Figure 1.4: Representation of the ATP-dependent ubiquitin-proteasome system (UPS) pathway for protein degradation. 33

Figure 1.5: IGF1-PI3K-Akt signalling pathway regulating protein synthesis and degradation in the skeletal muscle. 35

Figure 1.6: Signalling pathway regulating carbohydrate metabolism. 39

Figure 2.1: Zones of articular cartilage important to distinguish for accurate scoring. 61

Figure 2.2: Typical real-time PCR plot showing the three main steps of the reaction; the exponential, linear and plateau phase 73

Figure 3.1: Experimental design scheme for *in vivo* study of the meniscus transacted model of osteoarthritis. 82

Figure 3.2: Weight-bearing and paw withdrawal thresholds in MNX, sham and naïve rats. 87

Figure 3.3: Locomotor activity during the dark cycle in MNX, sham and naïve rats. 88

Figure 3.4: Plasma concentrations of IL-10, IL-6 and TNFα in MNX, sham and naïve rats. 89

Figure 3.5: Scoring of cartilage damage, osteophytosis and synovitis of the tibiofemoral joint at the end of the study. 90

Figure 3.6: Histology of the medial tibiofemoral joint at days 28 and 55 after surgery. 92

Figure 3.7: Muscle metabolites in the EDL muscle from MNX, sham and naïve rats. 93

Figure 3.8: Alkaline-soluble protein to DNA ratio in EDL muscle MNX, sham and naïve rats at 55 days after surgery. 94

Figure 4.1: Experimental design scheme for *in vivo* study of the collagen-induced model of arthritis. 106

Figure 4.2: Paw withdrawal thresholds and thickness at baseline and after treatment with CIA or control rats. 114

Figure 4.3: Locomotor activity at baseline and after treatment with CIA or control group. 115

Figure 4.4: Plasma inflammatory cytokine concentrations from CIA rats and control rats at the end of the study. 116

Figure 4.5: Histology and synovitis scoring of the tibiatarsal joint at the end of the study. 117

Figure 4.6: Correlations of paw withdrawal threshold as indicative of pain with systemic inflammation and activity. 118

Figure 4.7: Levels of intermediate metabolites in the EDL muscle of CIA and control rats. 119

Figure 4.8: Alkaline-soluble protein to DNA ratio in the EDL muscle of CIA and control rats at the end of the study. 120

Figure 4.9: Fold-change in EDL mRNA abundance from control in CIA rats at day 18. 121

Figure 4.10: IPA prediction of energy metabolism including fatty acid and carbohydrate metabolism and metabolism of protein in EDL muscle based upon changes in mRNA expression from CIA rats compared to control rats. 123

Figure 4.11: Expression of different clusters of genes in quadriceps from patients with RA versus controls. 124

Figure 4.12: Proposed signalling pathway regulated by rheumatoid arthritis induced inflammation in the rodent model of CIA. 132

Figure 5.1: Experimental design scheme for *in vivo* study of the collagen-induced model of arthritis with daily treatment with rosiglitazone/vehicle. 138

Figure 5.2: Effects of vehicle versus rosiglitazone on paw withdrawal thresholds and paw thickness in CIA rats. 145

Figure 5.3: Correlation of paw withdrawal thresholds and paw thickness as indicative of pain responses and paw swelling. 145

Figure 5.4: Effects of rosiglitazone treatment on locomotor activity in CIA rats..... 146

Figure 5.5: Correlation of horizontal activity with paw withdrawal thresholds and paw thickness, indicative of pain responses and paw swelling respectively..... 147

Figure 5.6: Plasma concentrations of IL-6 in CIA and control rats treated with rosiglitazone or vehicle on day 17. 148

Figure 5.7: Correlation of plasma concentrations of IL-6 and paw withdrawal thresholds and paw thickness as indicative of pain and paw swelling. .. 148

Figure 5.8: Synovitis scoring of the tibiatarsal joint at the end of the study. 149

Figure 5.9: Histology of the tibiatarsal joint in CIA and control treated with rosiglitazone and vehicle at day 17..... 151

Figure 5.10: Glycogen and intermediate metabolite content in the EDL muscle of CIA rats. 152

Figure 5.11: Alkaline-soluble protein to DNA ratio in EDL muscle of CIA rats. 153

Figure 5.12: Cellular functions identified by IPA as being different from control + vehicle in control + rosiglitazone, CIA + vehicle and CIA + rosiglitazone..... 155

Figure 5.13: IPA prediction of oxidation of lipid in EDL muscle based upon changes in mRNA expression from control + rosiglitazone, CIA + vehicle and CIA + rosiglitazone compared to control + vehicle rats. 157

Figure 5.14: IPA prediction of oxidation of lipid moieties (energy production) in EDL muscle based upon changes in mRNA expression from control + rosiglitazone, CIA + vehicle and CIA + rosiglitazone compared to control + vehicle rats. 158

Figure 5.15: IPA prediction of metabolism of carbohydrates in EDL muscle based upon changes in mRNA expression from control + rosiglitazone, CIA + vehicle and CIA + rosiglitazone compared to control + vehicle rats.... 159

Figure 5.16: IPA prediction of protein synthesis in EDL muscle based upon changes in mRNA expression from control + rosiglitazone, CIA + vehicle and CIA + rosiglitazone compared to control + vehicle rats. 160

Figure 6.1: Comparison of locomotor activity in MNX rats with knee OA and CIA rats with RA 174

Figure 6.2: Comparison of systemic inflammatory markers in MNX rats with knee OA and CIA rats with RA 174

Figure 6.3: Comparison of lactate accumulation in EDL muscle from MNX rats with knee OA ad CIA rats with RA 174

Figure 6.4: Schematic diagram of RA-induced muscle metabolic function in the EDL from CIA rats..... 182

List of tables

Table 1.1: Prevalence of radiographic and symptomatic knee OA in Rotterdam, NHANES III and Framingham studies. 3

Table 1.2: Summary of the main features of osteoarthritis and rheumatoid arthritis. 20

Table 1.3: Summary of immune cells present in synovium of OA joint as a response to inflammation 22

Table 3.1: Description of group size over the time-course of weight bearing test. 86

Table 3.2: Description of group size for cytokine measurement for each group. 89

Table 3.3: Correlation of knee joint pathology to pain behaviour and activity tests. 91

Table 4.1: Clinical features from patients with rheumatoid arthritis whose muscle mRNA was used for gene expression quantification. 106

Table 4.2: Genes included in the TaqMan low-density array with its catalogue number. 110

Table 4.3: Genes selected to be quantified by TaqMan probes in muscle from RA patients. 112

Table 4.4: Description of group size and end-point based on paw swelling in each treatment group. 113

Table 4.5: Group size during the time-course of paw withdrawal thresholds test..... 113

Table 4.6: Group size during the time-course of the locomotor activity test..... 113

Table 4.7: Correlation of inflammatory synovitis and paw thickness with *in vivo* parameters in CIA rats. 118

Table 5.1: Description of group size and end-point based on paw swelling in each treatment group..... 143

Table 5.2: Description of group size over the time-course of PWT measurement..... 143

Table 5.3: Correlation of synovitis score with PWTs, horizontal activity and paw thickness. 150

Abbreviations

4E-BP1: 4E binding protein 1

ACLT: anterior crucial ligament transection

ACPA: anti-citrullinated protein antibodies

ADP: adenosine diphosphate

AGDase: amyloglucosidase

AIA: adjuvant-induced arthritis

AKT: protein kinase B (PKB)

APC: antigen-presenting cell

ASP: alkaline soluble protein

ASPA: Animal Scientific Procedures Act

ATP: adenosine tri-phosphate

B: baseline

BMI: body mass index

BSA: bovine serum albumin

cDNA: complementary DNA

CFA: complete Freund’s adjuvant

CIA: collagen-induced arthritis

CK: creatine kinase

CKD: chronic kidney disease

Slc2a4: solute carrier 2a4

CNS: central nervous system

COPD: chronic obstructive pulmonary disease

COX-2: cyclooxygenase-2

CPT1A: carnitine palmitoyltransferase 1a

Cr: creatine

CRP: C-reactive protein

Ct: cycle threshold

Ctsl: cathepsin L

DMARD: disease-modifying anti-rheumatic drug

DMM: destabilisation of medial meniscus

DMOAD: disease-modifying OA drug

EDL: extensor digitorum longus

EDTA: ethylenediaminetetra acetic acid

EF: extraction factor

eiF2B: eukaryotic initiation factor 2B

eiF3-f: eukaryotic initiation factor 3 subunit 5

eiF-4E: eukaryotic initiation factor 4E

EIF4EBP1: eukaryotic initiation factor 4E binding protein 1

ELISA: Enzyme-linked immunosorbent assay

ESR: erythrocyte sedimentation rate

EULAR: European league against rheumatism

FOXO: Forkhead box O

G6PDH: glucose-6-phosphate dehydrogenase

GLUT4: glucose transporter-4

GS: glycogen synthase

GSK3β: glycogen synthase kinase 3β

H&E: haematoxylin and eosin

HK: hexokinase

HLA: human leukocyte antigen

HMBS: hydroxymethylbilane synthase

HPMC: Hydroxypropylmethyl cellulose

IFA: incomplete Freund’s adjuvant

IGF-1: insulin-like growth factor 1

IgG: immunoglobulin G

IL-10: interleukin 10

IL-1β: interleukin 1β

IL-6: interleukin 6

IL-8: interleukin 8

INSR: insulin receptor

IPA: Ingenuity pathway analysis

IR: insulin resistance

IRS1: insulin receptor substrate 1

JAK: Janus kinase

LASA: Laboratory animal science association

LDH: lactate dehydrogenase

LMA: locomotor activity

LPS: lipopolysaccharide

MAFbx: muscle atrophy F-box

MCL: medial collateral ligament

MCP-1: monocyte chemoattractant protein 1

MHC: major histocompatibility complex

MIA: monosodium iodoacetate

MMP: metalloproteinases

MNX: medial meniscus transection

mRNA: messenger RNA

MSTN: myostatin

MT1A: metallothionein 1A

mTOR: mammalian target of rapamycin

MuRF1: muscle-specific RING-finger 1

MyoD: Myogenic differentiation antigen

NAD: nicotinamide adenine dinucleotide

NADH: nicotinamide adenine dinucleotide hydrogen

NADP: nicotinamide adenine dinucleotide phosphate

NADPH: nicotinamide adenine dinucleotide phosphate hydrogen

NGF: neurotrophic growth factor

NICE: National Institute for Health and Care Excellence guidelines

NSAID: non-selective anti-inflammatory drug

Ntrk1: neurotrophic receptor kinase 1

O_2: oxygen

OA: osteoarthritis

OARSI: Osteoarthritis research international

OD: optical density

PBS: phosphate-buffered saline

PCA: perchloric acid

PCR: polymerase chain reaction

PCr: phosphocreatine

PDC: pyruvate dehydrogenase complex

PDH: pyruvate dehydrogenase

PDK1: phosphoinositide-dependent kinase 1

PDK4: pyruvate dehydrogenase kinase 4

PGC1α: proliferator-activated receptor gamma cofactor 1 alpha

PGC1β: proliferator-activated receptor gamma cofactor 1 beta

PI3K:phosphatidylinositol-3-kinase

PIP: phosphoinositide-3,4,5-triphosphate

PK: pyruvate kinase

pMMX: partial medial meniscectomy

PPAR: peroxisome proliferator-activated receptor

PPARa: peroxisome proliferator-activated receptor alpha

PPARD: peroxisome proliferator-activated receptor delta

PPARɣ: peroxisome proliferator-activated receptor gamma

PPARGC1a: proliferator-activated receptor gamma cofactor 1 alpha

PPARGC1β: proliferator-activated receptor gamma cofactor 1 beta

PVP: polyvinylpyrrolidone

PWT: paw withdrawal thresholds

qPCR: quantitative polymerase chain reaction

RA: rheumatoid arthritis

RANKL: receptor activator of nuclear factor Kβ ligand

RF: rheumatoid factor

RIN: RNA integrity number

RMIA: rodent models of immune-mediated arthritis

Rosi: rosiglitazone

TCA: tricarboxylic acid cycle

TGFβ: tumour growth factor-beta

TLDA: TaqMan low-density array

TNFα: tumour necrosis factor alpha

tRNA: transfer RNA

TZD: thiazolidinediones

Ub: ubiquitin

UCP3: uncoupling protein 3

UPP: ubiquitin-proteasome pathway

UPS: ubiquitin-proteasome system

Vegfa: vascular endothelial growth factor alpha

Table of contents

Declaration 1

Acknowledgements 2

Abstract 3

Presentations 6

List of figures 7

List of tables 12

Abbreviations 14

Chapter 1: 1

General Introduction 1

1.1. Osteoarthritis 2

1.1.1. Epidemiology of knee OA 2

1.1.2. Risk factors 3

1.1.3. Pathophysiology of knee OA 5

1.1.4. Symptoms of knee OA 8

1.1.5. Treatments for knee OA 10

1.2. Rheumatoid arthritis 12

1.2.1. Epidemiology 13

1.2.2. Risk factors 13

1.2.3. Pathophysiology of RA 15

1.2.4. Symptoms and treatments of RA 17

1.3. Inflammation 21

1.3.1. Osteoarthritis 21

1.3.2. Rheumatoid arthritis 22

1.4. Animal models of arthritis 25

1.4.1. Animal models of OA 25

1.4.2. Animal models of RA 27

1.5. Regulation of skeletal muscle mass 28

1.5.1. Muscle protein synthesis 30

1.5.1.1.The IGF1-PI3k-Akt signalling pathway 31

1.5.1.2. Myostatin 32

1.5.2. Muscle protein breakdown 32

1.5.2.1.Ubiquitin-proteasome system 33

1.5.2.2.Lysosome-autophagy system 35

1.5.3. Cross-talk between muscle protein synthesis and breakdown 36

1.6. Regulation of skeletal muscle carbohydrate metabolism 37

1.6.1. Inflammation and muscle disuse-induced insulin resistance 39

1.7. Muscle atrophy and insulin signalling in inflammation and arthritis 40

1.8. Aims of thesis 45

Chapter 2: 47

General methods 47

2.1.Animals and subjects 48

2.1.1.Anaesthesia 49

2.1.2.Medial meniscus transection 50

2.1.3.Intradermal injection of Bovine Collagen type II..... 51

2.1.4.Blood withdrawal from the tail vein 52

2.2.Oral gavage 52

2.3.Joint swelling 54

2.4.Pain behaviour measurements 54

2.4.1.Weight-bearing 54

2.4.2.Hind paw withdrawal thresholds 55

2.5.Physical activity measurements..... 55

2.6.Tissue collection 56

2.6.1.Muscle dissection under terminal anaesthesia 56

2.6.2.Dissection and mounting of rat tibiofemoral joint 57

2.6.3.Dissection and mounting of rat tibiotarsal joint 58

2.7.Histopathology of joints 58

2.7.1.Histology..... 58

2.7.2.Joint microscopic scoring..... 60

2.8.Enzyme-linked immunosorbent assay (ELISA) to determine cytokines in plasma 62

2.9.*Ex vivo* analysis of muscle intermediary metabolites..... 63

2.9.1.Muscle metabolite extraction 63

2.9.2.Muscle adenosine triphosphate and phosphocreatine determination..... 64

2.9.3.Muscle free creatine assay determination 65

2.9.4.Muscle lactate determination 65

2.9.5.Calculations 66

2.9.6.Muscle glycogen 66

2.10.Muscle alkaline-soluble protein:DNA ratio 68

2.10.1.Muscle extraction 68

2.10.2.Protein quantification 69

2.10.3.DNA quantification 70

2.11.Gene expression quantification in muscle tissue 71

2.11.1.Muscle total mRNA extraction 71

2.11.2.cDNA synthesis by reverse transcription PCR (RT-PCR) 72

2.11.3.Quantitative PCR (qPCR) 73

2.11.3.1.Quantitative PCR (qPCR) by TaqMan® 75

2.11.3.2.Quantitative PCR (qPCR) by TaqMan® low-density array (TLDA) ... 75

2.11.4.Ingenuity Pathway Analysis 76

2.12.Statistical analysis 76

Chapter 3: 78

Unaffected muscle mass and energy metabolism in the MNX model of knee OA 78

3.1.Introduction 79

3.2.Methods 81

3.2.1.Experimental design 81

3.2.2.MNX model of osteoarthritis 82

3.2.3.Pain behaviour 83

3.2.4.Locomotor activity 83

3.2.5.Plasma cytokines concentration 84

3.2.6.Knee joint histopathology 84

3.2.7.Muscle analysis 84

3.2.7.1.Muscle metabolites 85

3.2.7.2.Protein and DNA quantification 85

3.2.8.Statistical analysis 85

3.3. Results 86

3.3.1.Pain behaviour in MNX model of OA 86

3.3.2.Locomotor activity in MNX rats 87

3.3.3.Plasma inflammatory cytokine concentrations and EDL mRNA expression89

3.3.4.Histopathology of tibiofemoral joint and scoring 90

3.3.5.Muscle metabolites 93

3.3.6.Muscle alkaline-soluble protein to DNA ratio 94

3.4.Discussion 95

Chapter 4: 102

Dysregulation of indices for muscle metabolism and wasting in a rat model and patients with rheumatoid arthritis 102

4.1.Introduction 103

4.2.Methods 105

4.2.1.Experimental design 105

4.2.1.1.Rodent study 105

4.2.1.2.Human volunteer study 106

4.2.2.Collagen-induced model of arthritis 107

4.2.3.Pain behaviour 107

4.2.4.Paw thickness 107

4.2.5.Locomotor activity 108

4.2.6.Plasma cytokines 108

4.2.7.Ankle histopathology 108

4.2.8.Muscle analysis 109

4.2.8.1.Muscle metabolites 109

4.2.8.2.Protein and DNA quantification 109

4.2.8.3.RNA extraction and quantitative PCR 109

4.2.9.Statistical analysis 112

4.3. Results 113

4.3.1.Rodent study 113

4.3.1.1.Pain behaviour and paw thickness in the CIA model of RA 114

4.3.1.2.Locomotor activity in CIA rats 115

4.3.1.3.Plasma inflammatory cytokine concentrations 116

4.3.1.4.Histopathology of tibiotalus joint results in synovitis 116

4.3.1.5.Muscle glycogen and metabolites..... 119

4.3.1.6.Alkaline-soluble protein to DNA ratio 120

4.3.1.7.Muscle mRNA expression 120

4.3.2.Human volunteer study..... 124

4.4.Discussion 125

Chapter 5: 133

Peroxisome proliferator-activated receptor ɣ agonist ameliorates inflammation and modifies muscle metabolism and lactate accumulation in a rat model of rheumatoid arthritis..... 133

5.1. Introduction..... 134

5.2.Methods..... 137

5.2.1.Experimental design 137

5.2.2.Oral gavage 138

5.2.3.Collagen-induced model of arthritis 138

5.2.4.Pain behaviour..... 139

5.2.5.Paw thickness..... 139

5.2.6.Locomotor activity..... 139

5.2.7.Plasma cytokine concentration 140

5.2.8.Ankle histopathology 140

5.2.9.Muscle analysis 140

5.2.9.1.Muscle metabolites..... 141

5.2.9.2.Protein and DNA quantification..... 141

5.2.9.3.RNA extraction and quantitative PCR..... 141

5.2.9.4.Statistical analysis 142

5.3. Results 143

5.3.1.Rosiglitazone reduced pain behaviour and blunted paw thickness 144

5.3.2.Effects of rosiglitazone treatment on locomotor activity in CIA rats 146

5.3.3.Plasma levels of the inflammatory cytokine IL-6..... 147

5.3.4.Histopathology of tibiotalus joint and synovitis..... 149

5.3.5.Muscle glycogen and metabolites..... 152

5.3.6.Alkaline-soluble protein to DNA ratio 153

5.3.7.Effects of rosiglitazone treatment on muscle mRNA expression 154

5.4.Discussion 163

Chapter 6: General discussion..... 172

6.1. Overview of findings..... 173

6.1.1. Inflammation and physical inactivity in arthritis 176

6.1.1.1.Inflammation 176

6.1.1.2.Physical activity 177

6.1.2. Muscle atrophy and metabolic flux in arthritis 178

6.1.2.1.Regulation of muscle mass in CIA rats, a cross-talk with insulin signalling 180

6.2. Future directions for research 183

6.2.1. Adapting the MNX model of OA to human disease symptoms 183

6.2.2. Muscle disuse, fatigue and disability 184

6.2.3. Effects on muscle function in CIA by inhibiting pain 184

6.2.4. Overview of body homeostasis and the origin of metabolic dysregulation and inflammation in CIA 185

6.2.5. Molecular analysis for muscle atrophy in the CIA model..... 186

6.2.6. *In vitro* models..... 186

6.3. Limitations in this study 187

6.4. Conclusions 191

Annexe 1 192

Annexe 2 193

References 194

Chapter 1:

General Introduction

1.1. Osteoarthritis

Osteoarthritis (OA) is the most common type of arthritis in the worldwide population (Lawrence et al. 2008) and has a serious socioeconomic impact on public health. It is a chronic degenerative disease that involves the whole joint, mainly characterised by the degradation of articular cartilage and synovium inflammation (Aurich et al. 2005; Loeser et al. 2012) associated to comorbidities and disabilities resulting in poor quality of life (Nelson 2018). Out of all the types of OA, being hand, hip and knee the most common, knee OA has been extensively associated to muscle weakness (Alnahdi, Zeni, and Snyder-Mackler 2012) and, therefore, this thesis was focused on knee OA.

1.1.1. Epidemiology of knee OA

Knee OA is the most prevalent type of arthritis and is common in ageing (>50 years old) (Litwic et al. 2013) and obesity (Chu, Lim, and Ng 2018). Knee OA is classified on the basis of the radiographic changes in joint structure and whether the patients are symptomatic. It is widely accepted that structural changes to the joint are not always accompanied by symptoms and *vice versa*. The prevalence of OA is higher in women and increase with ageing, starting from 40 years in women and from 50 years in men (Meulenbelt et al. 1997). A radiographic evidence study in Dutch population (Rotterdam study), in people aged ≥80 the prevalence was 53% in women and 33% in men (Dahaghin et al. 2005). Different studies done in the US (Framingham and NHANES III) looked at the prevalence by radiographic and symptomatic changes (Felson et al. 1987; Dillon et al.

2006). Radiographic prevalence in Framingham study, where participants were ≥45 years old, was 18.6% in men and 19.3% in women. In NHANES III study, the prevalence in participants ≥60 years was 31.2% in men and 42.1% in women. Symptomatic prevalence was 5.9% in male and 7.2% in women ≥45 years whereas it was 10% in male and 13.6% in women aged ≥60 years (Table 1.1).

Table 1.1: Prevalence of radiographic and symptomatic knee OA in Rotterdam, NHANES III and Framingham studies.

	Study	Age	Men	Women
Radiographic	Rotterdam	≥80	33%	53%
	NHANES III	≥60	31.2%	42.1%
	Framingham	≥45	18.6%	19.3%
Symptomatic	NHANES III	≥60	10%	13.6%
	Framingham	≥45	5.9%	7.2%

The sex- and age-standardised incidence of OA is 240/100,000 person-years in the US. Changes in lifestyle increase the predisposition to risk factors, increasing the prevalence and incidence of OA.

1.1.2. Risk factors

OA can be primary or secondary depending on the predisposition to risk factors. Primary or idiopathic OA begins from an unknown cause, and there are many systemic factors contributing to its development causing injury in joint tissues or preventing its repair process. As mentioned, age and sex

are systemic factors that affect primarily to elderly and with high prevalence in women after menopause. Thus, hormonal and endocrine are also systemic risk factors poorly understood in the appearance of OA (Lawrence, Bremner, and Bier 1966). There is strong evidence of genetic components with the discovery of the mutation of 80 genes involved with the pathogenesis of OA (Ryder et al. 2008). Diet can be a systemic risk factor increasing susceptibility to develop secondary OA. Nutritional deficiencies may cause important consequences resulting in metabolic disorders and secondary diseases such as obesity, increasing predisposition to develop OA. Bad dietary habits due to busy life style increases the consumption of fast food and snacks attributed to the accumulation of fat and glucose and lack of nutritional factors essential for our body, causing metabolic responses that activates the degradation of tissues in the joint (Sartori-Cintra, Aikawa, and Cintra 2014; Thijssen, van Caam, and van der Kraan 2015). It can lead to different comorbidities associated with OA such as diabetes, cardiac, vascular problems and obesity (Griffin et al. 2010). The increase of body mass index (BMI) rises the prevalence of OA due to loading and mechanical stress on the joints. Subjects with a BMI>30 kg/m^2 were 6.8 times more likely to develop knee OA than normal-weight controls (Coggon D 2001). The overload can lead to local risk factors such as mechanical tear and wear and inflammation. Local factors are those physical alterations of the joint that are a risk to develop OA due to mechanical friction or instability, such as misalignment, muscle weakness, and alterations of the structure of the joint (Hunter and Felson 2006).

1.1.3. Pathophysiology of knee OA

In both systemic and local factors mentioned above, inflammation occurs and is a major contributor to OA development and its consequences independently of the origin. OA was used to be considered as a tear and wear disease remodelling joint tissues, and now more evidence points to inflammation as a contributor to joint degeneration. The release of cytokines and chemokines stimulates inflammatory mechanisms in synovium disturbing cartilage homeostasis (Scanzello and Goldring 2012). The knee joint is structured by the femur condyles and tibia plateaus with its respective subchondral bone, articular cartilage, meniscus, muscle ligaments and synovium. Knee OA is characterised of developing synovium inflammation as first symptom and progressing to cartilage degradation. It can start by systemic factors and injured of any of the structures of the joint. In late stages, the cartilage degradation leads to bone resorption and scleroses as well as osteophytes formation, accompanied by frayed meniscus and weak muscles (Figure 1.1).

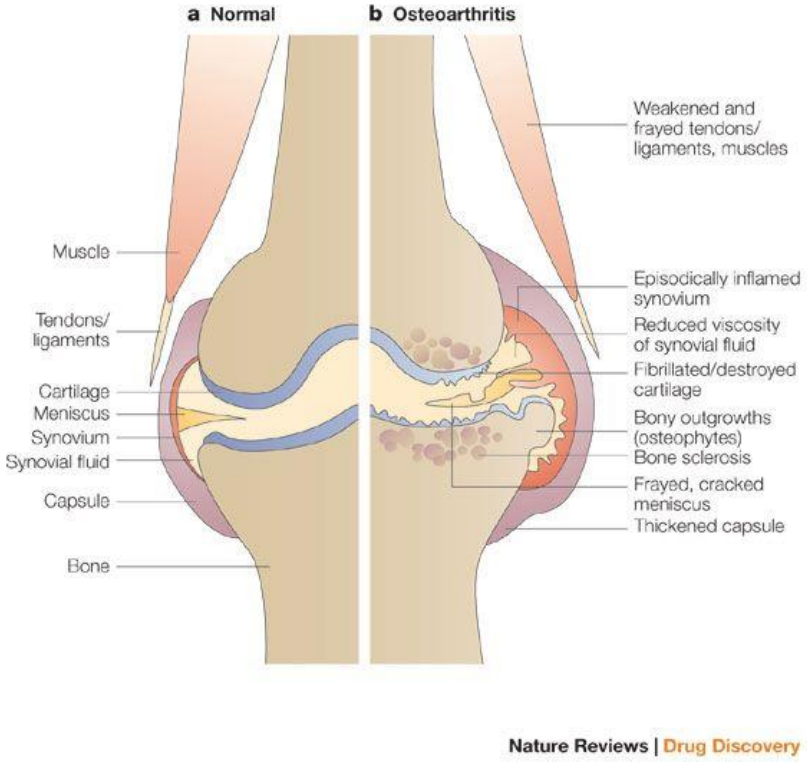


Figure 1.1: Description of normal joint (a) and joint with osteoarthritis (b). In the picture a) it can be appreciated a healthy joint with cartilage, meniscus and synovium in normal conditions. In picture b), the joint with osteoarthritis presents inflamed synovium, fibrillated and degraded cartilage, osteophytes formation and frayed meniscus accompanied with weak muscles. Image from (Wieland et al. 2005).

The articular cartilage protects the condyles of the femur and plateaus of tibia allowing a smooth movement of the joint. Chondrocytes are the only cell type in the cartilage, and they synthesise and maintain the extracellular matrix comprised of collagens type II, IX and XI and proteoglycans (Bruckner and van der Rest 1994). There is a balance between synthesis and degradation of cartilage under healthy conditions whereas degradation activity predominates in OA (Sandell and Aigner 2001). The pathology when cartilage degenerates is also called chondropathy. The breakdown of cartilage matrix is complex because it involves different factors such as environmental, genetic, mechanical and biochemical. The most evidenced

process is by the activation of matrix metalloproteinases (MMP) that degrades collagen and proteoglycans (Aurich et al. 2005). It is believed that cytokines and chemokines are released from synovium and triggers the activation of MMPs by interleukins (IL) -1, 17, 18 and tumour necrosis factor alpha (TNFα) (Haseeb and Haqqi 2013). The degradation of cartilage is irreversible and it can end with total articular cartilage damage exposing the subchondral bone to mechanical erosion.

In OA there are also changes in the subchondral bones due to an imbalance of synthesis and degradation. Under healthy conditions, cell remodelling occurs. Bone resorption in cortical and trabecular bone is initiated by the activation of osteoclasts. Then, osteoblasts generate the new cortical and trabecular bone to maintain the balance (Tombran-Tink and Barnstable 2004). In OA, the mechanisms that impair this balance are poorly understood and it is not clear if cartilage loss leads to subchondral bone changes or *vice versa* (Goldring and Goldring 2010). The changes in subchondral bone can include thickening of the plate, bone sclerosis and osteophytes, which are new bone spurs invading the free space left by the loss of cartilage.

There are two menisci in the knee joint (lateral and medial) attached to the tibia plateaus. It is thought that their function is to improve joint stability and weight distribution. In patients of OA is common to see meniscal damaged (Englund et al. 2008), which destabilise the joint and may create articular friction and consequent erosion and inflammation.

As mentioned, inflammation is a major determinant that may start the degeneration of articular cartilage (Scanzello and Goldring 2012). Synovium is the outer part of the joint which serves to protect the joint and generate the synovial fluid to lubricate the joint, nourish the non-vascularised cartilage and regulate the immune activity. In contrast to cartilage, healthy synovium is highly vascularised and comprised by cellular layers. Synovial inflammation also called synovitis is less evident than in rheumatoid arthritis. However, an increase of thickness, vascularisation and inflammatory cells are detected in OA, especially in early stages (Benito et al. 2005) and after joint injuries (Scanzello et al. 2011). Inflammatory cells release mediators of inflammation, chemokines and cytokines which promote synovitis and activates the degeneration of the tissues in the joints in arthritis and post injured joints (Bondeson et al. 2006).

1.1.4. Symptoms of knee OA

Pain is often the first and predominant symptom of knee OA that causes patients to visit the general doctor (Thorstensson et al. 2009). It is intermittent and typically worst during and after physical weight-bearing activities. It may originate from the innervated tissues of the joint such as synovium, periosteum, subchondral bone, ligaments and muscle (Hunter, McDougall, and Keefe 2008). The loss of cartilage exposes the subchondral bone, which is vascularised and innervated, contributing to OA pain.

Additionally, during the progression of OA cartilage may become innervated by sympathetic and sensory nerves, which may also contribute to the pain experienced by OA patients (Suri et al. 2007). The local release of

inflammatory mediators from sensory fibres and immune cells can lead to inflammatory pain (Tore and Tuncel 2009). The release of cytokines and other inflammatory mediators such as bradykinin, histamine, prostaglandins, adipokines, lactic acid and substance P (amongst others) into the joint may reduce the firing threshold of the joint nociceptors, which triggers the response to non-noxious and noxious painful stimuli (Hunter, McDougall, and Keefe 2008). However, the mechanism and origin of pain in OA is unknown.

Patients with OA also experience stiffness normally in the morning, after a period of physical inactivity or in the evening, which is generally resolved in minutes. Knee pain is the principal factor that limits the normal daily activities that affect the quality of life (Dekker et al. 1993). This is a major problem as physical inactivity and disability can impact on skeletal muscle function (Fink et al. 2007). Reduced functional capacity is attributed to pain, stiffness and loss of muscle strength (Hurley et al. 1997) which has been correlated in knee OA patients with weak muscles compared to patients with normal muscles (Dekker et al. 1993). It has been shown however that weakness can also be found around knees in the absence of pain or muscle atrophy. This may be due to arthrogenous inhibition of muscle contraction (Slemenda et al. 1997). OA inflammation may also impact muscle integrity. Patients with knee OA have increased levels of inflammatory and atrophy markers in muscle, where the elevated gene expression of MCP-1 protein, TNFα and the atrophy marker atrogin-1 in Vastus Lateralis muscle were found to be negatively correlated to muscle strength (Levinger, Levinger, et al. 2011). It seems that the major muscle dysfunction is the loss of muscle

strength in patients with knee OA. Muscle weakness in quadriceps of patients with OA results with a reduction of muscle strength compared to age-matched healthy control volunteers and relative to BMI (Lewek, Rudolph, and Snyder-Mackler 2004).

1.1.5. Treatments for knee OA

There is no cure for OA yet no disease-modifying OA drug (DMOAD) has been approved. Therefore, the treatments used are aimed to ameliorate symptoms in knee OA. Treatments can be pharmacological or non-pharmacological, normally starting with non-pharmacological treatments and weak analgesics followed by stronger pharmacological interventions (Roubille, Pelletier, and Martel-Pelletier 2013).

Non-pharmacological treatments include education, rehabilitation, exercise and nutrition. It is important to encourage patients to attend self-management programmes organised by the hospital and foundations to get social support and instructions to better deal with the disease (Hunter and Felson 2006). Rehabilitation or physical therapy facilitates the resolution of symptoms and includes physical exercises aimed to muscle strengthening, stretching and soft tissue mobilisation (Hunter and Felson 2006). An exercise therapy protocol, consisting on exercise for strength and flexibility of lower limbs during 12 weeks, conducted in patients with knee OA (aged 50-65, n=22) reduced the perception of pain, IL-6 levels in serum and improved function and strengthening in quadriceps and hamstring in patients with knee OA (Aguiar et al. 2015). If the subjects present high BMI

or obesity, it is also encouraging to lose weight getting some advice from a nutritionist.

Pharmacological treatments in OA include the administration of analgesics and anti-inflammatory agents. The National Institute for Health and Care Excellence guidelines (NICE) recommends starting with paracetamol and topical non-selective non-steroidal anti-inflammatory drugs (NSAIDs) for moderate severity cases before NSAIDs oral administration. The NSAID typically used is ibuprofen, and together with cyclooxygenase-2 (COX-2) selective inhibitors, they have comparable effects reducing walking induced pain (Zhang et al. 2008). Generally, NSAIDs have the ability to supress COX expression and activity as well as the downstream signals. COX-1 and 2 are enzymes that catabolise the conversion of arachidonic acid to different products, including prostaglandins. The secretion of inflammatory cytokines induces COX-2 activation (J. R. Vane, Bakhle, and Botting 1998) promoting the generation of prostaglandins, known to mediate inflammation and pain, the production of vascular endothelial growth factor, platelet-derived growth factor and MMP (Simon 1999). They need to be used under caution, choosing the recommended dose and agent, taking into account individual risk factors, as NSAIDs and COX-2 inhibitors are associated with potential gastrointestinal, liver and cardio-renal toxicity (Trelle et al. 2011). When a lack of effectiveness or non-tolerated of NSAIDS, opioids are the alternative drug in severe stages (Zhang et al. 2008). More recent treatments include anti-NGF therapy, which reduces pain and improves function in patients with knee OA (Dimitroulas et al. 2017).

If pain and lack of mobility persist after the most aggressive pharmacological combination treatment, surgery is the alternative. The success of the available treatments is limited, and a joint replacement is often needed. Knee replacement is a cost-effective treatment improving global knee score of pain (63%), function (93%) and range of motion (100%) after 4-6 years of surgery (Zhang et al. 2008).

1.2. Rheumatoid arthritis

Rheumatoid arthritis (RA) is the most common autoimmune disease with chronic inflammation of synovial joints leading to the destruction of cartilage and bone. It is a heterogeneous and complex disease with various pathogenetic mechanisms involved between individuals and variable clinical pathology. RA is a degenerative disease that involves not only the whole joint but also systemic alterations with serious comorbidities (cardiovascular diseases, diabetes, hyperlipidaemia and obesity) (Radner et al. 2017) and disabilities resulting in poor quality of life and high rate of mortality (Sparks et al. 2016). It results from autoimmune disorder whereby there is a production of autoantibodies to immunoglobulin G (IgG or rheumatoid factor (RF)) and to citrullinated proteins, called anti-citrullinated protein antibodies (ACPAs) classified as seropositive RA (van Venrooij, Zendman, and Pruijn 2006). However, some patients are negative to these autoantibodies and environmental factors affect genetically susceptible individuals, classified as seronegative RA.

1.2.1. Epidemiology

In RA prevalence is less associated with age compared to OA. The prevalence in epidemiological studies comprises adults >18. Although most of the epidemiological studies have been done in Western countries, the reported rates seem to be constant in many populations (Myasoedova et al. 2010). The global prevalence of RA is in the range of 0.5-1% (Tobón, Youinou, and Saraux 2010; Malemba et al. 2012). However, it may differ between ethnicities and gender being more prevalent in women and American populations (5-6%) (Peschken and Esdaile 1999). For instance, the prevalence of women in the United States and the United Kingdom is 1.4% and 1.16% respectively whereas in males is 0.74% and 0.44% respectively. In Europe, this prevalence is lower being in a range of 0.45-0.8% in women and 0.19-0.2% in men (Tobón, Youinou, and Saraux 2010).

The incidence varies geographically being higher in North America (38/100,000). In Europe, the incidence is higher in Northern Europe with 29/100,000 than Southern Europe with 16.5/100,000 (Tobón, Youinou, and Saraux 2010).

Several longitudinal studies suggest that both incidence and prevalence seem to decline over time after the 1960s. The decline is more noticeable in women than in men (Doran et al. 2002).

1.2.2. Risk factors

RA is a multifactorial disease that results from interactions between genetic, environmental and systemic factors. Sex and age are systemic factors affecting more women than men with the ratio being 3:1. The mechanism

involved in the higher frequency of RA in women remains unclear although is likely to undergo by hormonal changes. It may be attributed to the stimulatory effects of oestrogens on the immune system, and low levels of testosterone have been reported in men with RA (Cutolo et al. 2002; Alpízar-Rodríguez et al. 2017). Indeed, ageing may also contribute to the hormonal changes, with women more susceptible to RA in their 50s (Tobón, Youinou, and Saraux 2010).

Genetic factors contribute 50-60% of the risk to develop RA. Specific class II human leukocyte antigen (HLA) loci encoding major histocompatibility complex (MHC) are the most associated with the risk of developing RA (Gregersen, Silver, and Winchester 1987). *HLA-DRB1* and *PTPN22* are the most important genes associated with RA in all the populations, However, other weaker risk loci have been identified, mainly associated with immune and inflammatory pathways (Okada et al. 2014). The manifestation of the genes strongly involved with RA are susceptible to environmental factors. Smoking is associated with RF and ACPA production. The risk of developing RF-positive RA was substantially higher in smokers with two copies of HLA shared-epitope (Risk Ratio 15.7) than in smokers with no copies (Risk Ratio 2.4) (Costenbader et al. 2008). The effect of smoking is likely to be due to the up-regulation of inflammatory cytokines IL-1β, IL-6 and IL-8 that exacerbate the pathophysiological mechanisms involved in RA (Kobayashi et al. 2008). Inhalation of pollutant particles and exposure to silica are recent identified environmental risk factors linked with diseases involving pulmonary and systemic inflammation and RA (Hart et al. 2009; Stolt et al. 2005). Other environmental risk factors include dietary habits. It

is seen that in Southern Europe they have milder forms of RA and this may be partly to the Mediterranean diet and vitamin D intake (Khanna, Jaiswal, and Gupta 2017). In patients with RA, the consumption of Mediterranean diet (including olive oil with antioxidant properties) reduced inflammation and improved physical functions (Sköldstam, Hagfors, and Johansson 2003). In a mouse CIA model of RA, the administration of extra virgin oil reduced the serum levels of MMPs and the expression of pro-inflammatory cytokines IL-1β, IL-17 and TNF-α (Rosillo et al. 2016). Additionally, deficiency of vitamin D was associated with RA and negatively correlated to disease activity in patients with RA (Kostoglou-Athanassiou et al. 2012).

1.2.3. Pathophysiology of RA

In both, production of autoantibodies and manifestation of susceptible variants of genes, an autoimmune response is activated before articular inflammation develops. Risk factors can induce post-translational modifications of proteins. Citrullination is the most common process that consists with the post-translational conversion of an amino acid (arginine) to citrulline in a range of proteins via induction of peptidyl arginine deiminases (Makrygiannakis et al. 2008). Following the post-translation modifications (citrullination, acetylation, etc) the altered peptide binds to MHC protein heterodimers to present the antigen to T cells, which stimulate B cells to synthesise the autoantibodies that recognise self-proteins such as RF and ACPAs (Holers 2013; Trouw, Huizinga, and Toes 2013). The presence of ACPAs alone is insufficient to cause synovitis, therefore, an additional hit (such as complement activation or microvascular insult) is

required (Arend and Firestein 2012) (See review Smolen et al. 2018)(Figure 1.3).

Early RA is characterised by synovial inflammation with inflammatory cells infiltration that release MMPs and autoantibodies (i.e., ACPA, RF, type II collagen, etc). The synovium produces the synovial fluid necessary to lubricate the joint and provide nutrients to the cartilage. The increase of inflammatory cells infiltration into the synovium is reflected with the thickened synovium layer and cellularity leading to the formation of pannus to protect the bones of the joint. First, there is a production of pro-inflammatory cytokines including IL-1, IL-6 and TNFα by macrophage-like synoviocytes and IL-6, MMPs, prostaglandins and leukotrienes by fibroblast-like synoviocytes (Bartok and Firestein 2010). Then, the invasion of the cartilage triggers an inflammatory response causing joint degeneration. Secondly, there is an infiltration of adaptive immune T cells and/or B cells to produce antibodies (Ziff 1974). The release of pro-inflammatory cytokines and production of receptor activator of nuclear factor kB ligand (RANKL) by T cells activates osteoclasts and degrades the bone matrix by producing proteases like cathepsin K (Schett and Gravallese 2012; Redlich and Smolen 2012) (Figure 1.2).

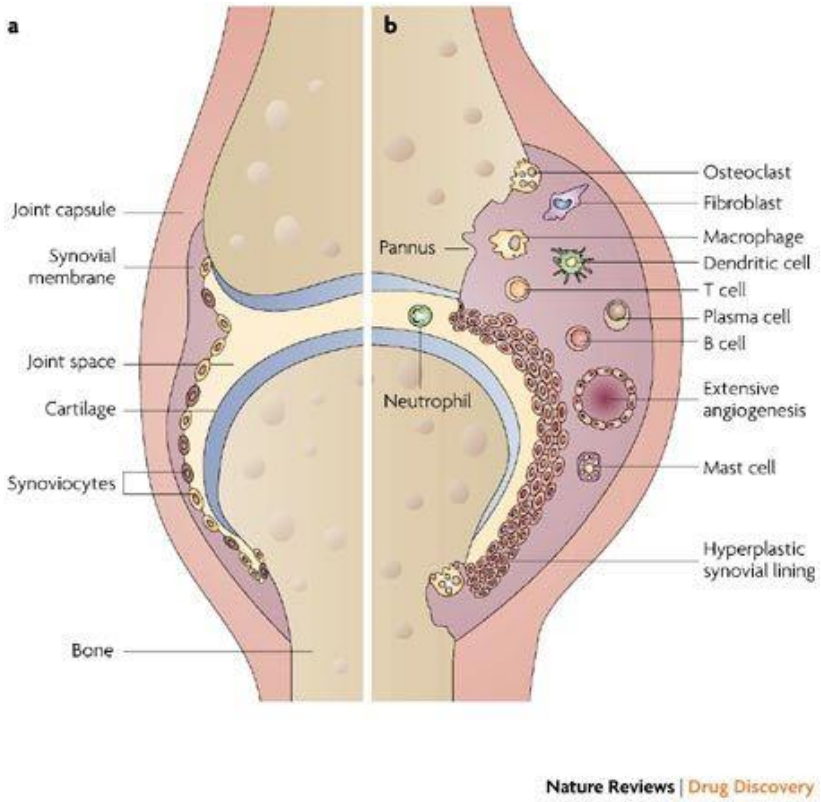


Figure 1.2: Description of the healthy joint (a) and its changes with rheumatoid arthritis (b). In the picture a) it can be appreciated healthy cartilage and bone with a single lining of cells (synoviocytes) in the synovial membrane (synovium). The RA joint, in picture b), starts a mechanism where synovium increases with thickness and hyperplastic synovial lining by the infiltration of inflammatory cells, innate and adaptive immune cells forming the pannus in the joint space. The activity of the infiltrated cells activates osteoclasts and starts bone resorption. Image from (Strand, Kimberly, and Isaacs 2007).

1.2.4. Symptoms and treatments of RA

Inflammation is the main and principal mechanism involved in RA. Joint swelling is the first symptom developed followed by pain and discomfort. There are some joints more predominant to develop RA than others, and it helps to distinct from other joint pathologies. These joints are the metacarpophalangeal and proximal interphalangeal of the hands and feet, the wrist, ankle and elbow and with less incidence in the shoulder, knee and hip (Smolen et al. 1995). Joint swelling is accompanied by stiffness in the

morning lasting >1h and pain (Lee and Weinblatt 2001). The progression of swelling and deterioration can end with joint deformation. The treatments to ameliorate symptoms are similar to those given to OA patients. Analgesics and anti-inflammatory drugs NSAIDs lessen pain and stiffness but do not interfere with the mechanisms leading to joint damage (Smolen, Aletaha, and McInnes 2016). They are widely used as a first treatment in RA patients before knowing the mechanisms involved, as different genetic risk factors and immune response are seen in RA.

To treat the disease, disease-modifying anti-rheumatic drugs (DMARDs) are the main established drugs. They reduce joint swelling and pain, decrease acute-phase markers, limit progressive joint damage, and improve physical function (Donahue et al. 2008). Methotrexate is a conventional synthetic DMARD with an unknown target, usually the first and most important drug administered in patients with early RA. A large proportion of patients (25%-40%) significantly improve with methotrexate monotherapy (Emery et al. 2017), and its adverse effects can be prevented (Van Ede et al. 2001). At the beginning of treatment, glucocorticoids may be given for a short period, due to its adverse effects, (Chatzidionysiou et al. 2017) until conventional synthetic DMARDs have exerted their full anti-inflammatory potential (Smolen, Aletaha, and McInnes 2016). When conventional synthetic DMARDs do not reach treatment targets, in the presence of poor prognostic markers, the European league against rheumatism (EULAR) recommends starting any biologic DMARD or a targeted synthetic DMARD in addition to methotrexate, with a current preference for biologic DMARDs because of long-term experience with

efficacy and safety profiles. Targeted synthetic DMARDs are for Janus kinase 1 and 2 (JAK1, JAK2). Different biological DMARDs acts to different targets: TNFα, IL-6 receptor, IL-6, CD80 and CD86 (involved in T cell co-stimulation) and CD20 (expressed by B cells) (Smolen et al. 2018).

In RA, the mentioned pharmacological treatments should be combined with non-pharmacological treatments. Education is important for social support and getting some advice to front a disease with a high incidence of depression (Kwiatkowska et al. 2018). Patients with RA tend to have sedentary behaviour (SB) or physical inactivity, feeling weak and fatigue. SB or physical inactivity aggravates inflammation affecting muscle density and weakness (Fenton et al. 2018). More recently, studies report that personalised exercise therapy improves the wellbeing and reduces pain in patients with RA (Strasser et al. 2011).

Table 1.2: Summary of the main features of osteoarthritis and rheumatoid arthritis.

	Osteoarthritis (OA)	Rheumatoid arthritis (RA)
Cause	Wear and tear, injury and inflammatory response	Autoimmune disorder and inflammatory response • Seropositive: production RF, ACPAs • Seronegative: genetic and environmental factors
Prevalence	Higher prevalence in women than men	Higher prevalence in women than men
Age	Most common age from >40 years (aging)	Most common age: 20-60 years
Symptoms	Localised in the joint: Pain, stiffness <1h, muscle weakness, physical disability	Throughout the body: Pain, stiffness >1h, muscle weakness, physical disability, fatigue, depression, joint swelling and deformation
Pathology	Synovium inflammation, cartilage degradation, bone spurs	Synovium inflammation, pannus, bone resorption, cartilage degradation
Treatment	• Pharmacological: paracetamol, NSAID, opioids • Non-pharmacological: personalised exercise, education, nutrition, surgery	• Pharmacological: NSAID, DMARD • Non-pharmacological: education, personalised exercise

1.3. Inflammation

1.3.1. Osteoarthritis

Even though inflammation in OA is lower than in RA, synovitis plays an important role in disease progression. It is unknown yet how inflammatory response starts in OA. There are more evidences suggesting that there is an autoimmune compound initiating inflammation (Scanzello et al. 2011). Matrix fragments and products released during cellular stress can activate the innate immune response via pattern-recognition receptors known as Toll-like receptors. The cellular response activates the specific transcription factors leading to the production of multiple pro-inflammatory mediators including cytokines and chemokines that can cause local tissue damage and activate macrophages and innate immune cells T and B (Benito et al. 2005). The immune and inflammatory response initiates the release of cytokines TNFα and IL1β in the synovium helping to initiate cartilage degeneration (Goldring 2001). It creates a vicious cycle provoking more inflammation and therefore more cartilage being degraded. TNFα and IL1β stimulate the synthesis of the enzymes responsible for inhibiting the synthesis of collagen and proteoglycans in the cartilage matrix and produces other cytokines (IL-6 and IL-8), stimulate proteases and prostaglandin production (Martel-Pelletier 2004). TNFα and IL1β are mainly released by macrophages in the synovium, and that initiates the activation of chondrocytes. The depletion of macrophages in vitro showed a reduced amount of the cytokines TNFα and IL1β as well as IL6 and IL8 by fibroblasts (Bondeson et al. 2006).

Table 1.3: Summary of immune cells present in synovium of OA joint as a response to inflammation.

Inflammatory cell	Function
Macrophage	The most predominant inflammatory cell in synovium. It possess pattern-recognition receptors (PRRs) such as TLRs that recognise endogenous damage associated molecular patterns (DAMPs) such as extracellular matrix fragments, releasing inflammatory cytokines (TNFα, IL-6). Activates the chondrocytes for cartilage degradation TLR, osteophyte formation via bone morphogenetic protein (BMP) and fibroblast-like synoviocytes. Phagocytosis.
T cell	Considerable number of cells in synovium. Recognises the pathogen or DAMP presented by macrophages, to start adaptive immune response.
B cell	Low number of cells in synovium. Synthetises the antibodies for adaptive immune response against the pathogen or DAMP.
Plasma cell	Low number of cells in synovium. Secretes the antibodies for DAMP synthesised by B cell.
Mast cell	Low number of cells in synovium. Releases cytokines and inflammatory products such as prostaglandins, responsible of pain.

(Mathiessen and Conaghan 2017; de Lange-Brokaar et al. 2012)

1.3.2. Rheumatoid arthritis

Joint swelling in RA reflects the synovial inflammation as a consequence of the infiltration of immune and inflammatory cells. The cellular composition of synovitis in rheumatoid arthritis includes innate immune cells (monocytes, dendritic cells, mast cells, and innate lymphoid cells) and adaptive immune cells (T-helper-1 and T-helper-17 cells, B cells, and plasma cells). The inflammatory milieu in the synovial compartment is regulated by a complex cytokine and chemokine network leading to the induction or aggravation of the inflammatory response by activating endothelial cells and attracting immune cells to accumulate within the synovial compartment. To start the mechanism is required that an autoantigen or foreign peptide is presented by an antigen-presenting cell

(APC) to the T cells via the major MHC class II. The T cell becomes activated releasing lymphokines that can activate macrophages and activate B cells that start producing autoantibodies against the antigen recognised in the synovium. The immune complex, formed when autoantibodies bind to its autoantigens, can bind to macrophages and other cells activating them and secreting pro-inflammatory cytokines TNFα and IL-6. Fibroblast from synovium that express RANKL can activate macrophages to differentiate to osteoclasts that resorb bone (Redlich and Smolen 2012). The presence of TNFα and IL-6 can also activate chondrocytes to secrete enzymes like prostaglandins and MMPs to degrade cartilage (See review Aletaha and Smolen 2018) (Figure 1.3).

As consequence of the development of inflammatory and immune mechanisms in the synovium and spreading to the joint, it is suggested that the cytokines released can also impact to other tissues such as skeletal muscle (Varadhan et al. 2017). TNFα influences satellite cell proliferation stimulating the production of catabolic cytokines, which is associated with loss of muscle mass (Farber and Mannix 2000). IL-6 levels increase after exercise and are an essential regulator of muscle stem cell-mediated hypertrophy (Pedersen and Febbraio 2008; Serrano et al. 2008). However, chronic inflammation and levels of IL-6 are associated with muscle wasting by decreasing pro-myogenic factor and IGF-1 (Ahmed et al. 2007). The anti-inflammatory cytokine IL-10 plays an important role in regulating inflammatory response in muscle, inhibiting TNFα and IL-6 amongst other pro-inflammatory cytokines (Fiorentino et al. 1991). The protective effects of IL-10 are linked to the ability of this cytokine to convert M1 macrophages

to the more regenerative M2 macrophages and the prevention of TNFα induced phosphorylation of JNK and upregulation of IL-6 (Strle et al. 2007). Muscle inflammation will be discussed in section 1.7.

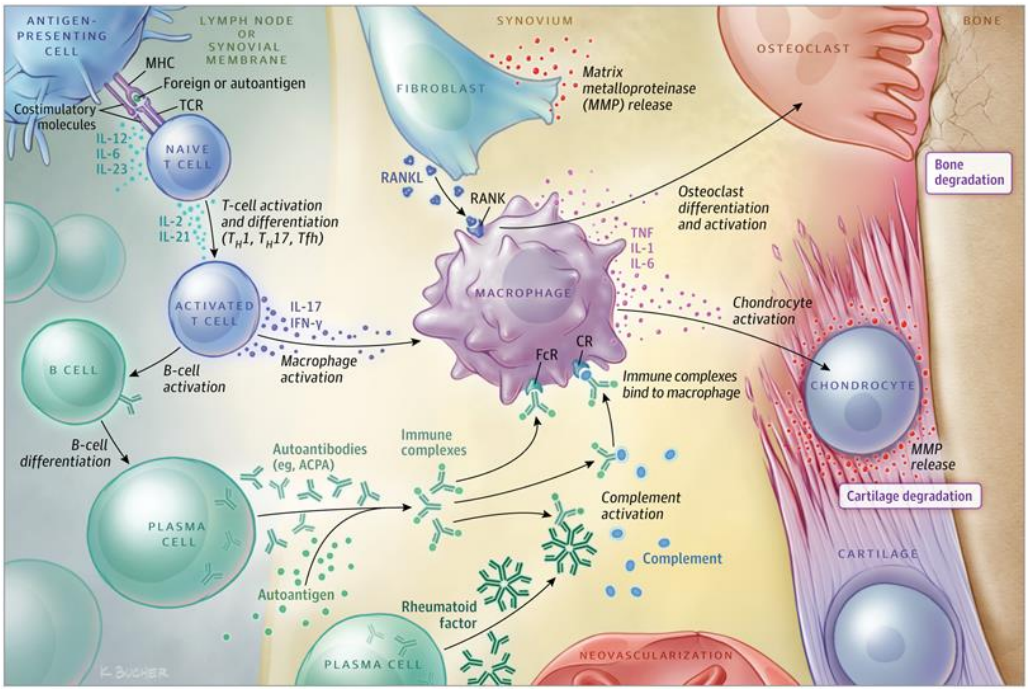


Figure 1.3: Inflammatory and immune response in the joint of RA. From left to right: activation of the immune system (T cells and B cells) via recognising the autoantigen generates autoantibodies and releases inflammatory cytokines that activate macrophages. The conjunction of cytokines differentiates macrophages to chondrocytes to degrade cartilage and osteoclasts for bone resorption. Refer to main text for abbreviations and detailed description of the mechanism. Image from (Aletaha and Smolen 2018).

1.4. Animal models of arthritis

Pre-clinical models are essential in research, allowing to do numerous experiments in a considerable short time and to extract any targeted tissue. They reproduce some aspects of the disease seen in patients with arthritis, mimicking symptomatic aspects and joint deterioration. Each animal model differs on advantages and disadvantages as they develop differently the pathological features of the disease. Therefore, it is critical to determine the hypothesis being tested in order to choose the appropriate model. Most models of arthritis are performed in rodents and small animals rather than big ones. Additionally there are non-animal alternatives such as cell lines culture from cartilage, synovium and other tissues relevant for the study originals from animal and patient samples.

1.4.1. Animal models of OA

The most used animal models for knee OA are mouse and rat, although models in rabbit, guinea pig, dog, sheep, horse and pig can be performed. Models of knee OA are induced by a chemical compound or surgery. The chemical compound used, generally, is the monosodium iodoacetate (MIA). The MIA model consists of an intra-articular injection of monosodium iodoacetate in the knee joint, which is and inhibitor of anaerobic glycolysis, inducing cartilage degradation by killing chondrocytes in the marginal zone (Bendele 2001). Results with the progressive loss of proteoglycans, the atrophy of the collagenous matrix and osteophytes formation (Guingamp et al. 1997). The MIA model is commonly used to study the morphological structure of the knee joint in OA and the development of pain, starting two

weeks after injections (Mapp et al. 2013a). This model was not adapted to this study due to the metabolic response induced by the monosodium iodoacetate.

The surgical models consist on destabilising the joint by transecting ligaments or the meniscus, causing post-traumatic OA and joint mechanical stress. A well stablish model is the medial meniscus transection (MNX), which consists on the transection of the medial collateral ligament (MCL) exposing the meniscus to cut it at its narrowest point (Janusz et al. 2002). It destabilises the joint for any movement, and the progressive degenerative changes start occurring by 3-6 weeks post-surgery. Cartilage degenerates quickly accompanied by proteoglycan loss, osteophytes formation and synovitis. Lesions are reasonable consistent if the surgery is also consistent. The lesions are morphologically similar to human disease occurring more rapidly. Therefore, it is extensively used for testing the protective effects of pharmaceutical treatments (Bendele 2001). MNX is also used as osteoarthritic pain model. Weight-bearing and paw withdrawal thresholds start becoming different than sham surgery from the second week after surgery (Mapp et al. 2013a). There is a variety of surgical models including anterior cruciate ligament transaction (ACLT) and combined with meniscus transection in rodents. Different strains respond differently to the surgeries, being Lewis, Sprague Dawley and Wistar rats the most used. They differ on the lesions of the joint pathology, being more severe in the outer proximal tibia in Lewis and in the middle and inner thirds in Sprague Dawley (Gerwin et al. 2010). In mouse, the destabilisation of the medial meniscus (DMM) model is the most used. Alternatively, OA can naturally

occur in the Dunkin Hartley Guinea pig and in big animals (pig, horse, etc) (Bendele 2001). The spontaneity of OA may appear by aging and due to heavy weight bearing as well as by genetic modifications.

1.4.2. Animal models of RA

Models of RA are induced by an autoimmune response against an agent, called rodent models of immune-mediated arthritis (RMIA). The susceptibility to immune-mediated arthritis induction is limited to certain strains. For rats, the inbred Sprague Dawley and Lewis strains are the most susceptible to arthritis induction, and they are not equally vulnerable to all arthritogenic agents. The induced RMIA result from the injection of a specific insult. The adjuvant-induced arthritis (AIA) model is induced by an injection of a specific chemical with incomplete Freund's adjuvant, most commonly the heat-killed *Mycobacterium tuberculosis*. Rats are susceptible to all the AIA models while mice are resistant to the majority of them (Yoshino, Murata, and Ohsawa 1998).

The collagen-induced arthritis (CIA) model of RA is induced by intradermal injection of emulsified collagen type II from porcine or bovine (in the majority) with IFA or complete Freund's adjuvant (CFA). It can be induced with two injections (100 µl) in the base of the tail or several injections (around 10) in the back, achieving a severer model. The onset of disease varies between animals, starting with the hind paws from day 14 after injections. It is characterised by body weight loss, progressive inflammation and skeletal erosion in the hind paws in the acute phase. After that, the chronical phase, the lesions reach the plateau point in both hind and fore

paws. This model is performed in female Lewis rats due to the high susceptibility (Bolon et al. 2011). It is used to study any aspect of immune progression of RA disease, pathological changes and pain development. Additionally, it is a good model to study the muscle wasting progression in RA, which mimics the rheumatoid cachexia identified in patients with RA (Alabarse et al. 2018).

1.5. Regulation of skeletal muscle mass

Skeletal muscle represents the largest organ in mammals and its atrophy can occur in catabolic states, such as denervation, energy restriction, inactivity, acute trauma and inflammation and chronic disease. Muscle atrophy is due to unbalanced protein turnover. It can occur as a result of decreased protein synthesis and/or increased protein degradation inducing loss of muscle mass and body weight, weakness and increased disability.

Muscle atrophy is conditioned by fibre composition, which influences the response to external stimuli such as during exercise, inflammation and muscle disuse. Classically, the fibre types are defined as slow-twitch (type 1) and fast-twitch (type 2) muscles, depending on the contractile properties. The fast fibres can be classified as type 2A, 2B and 2X, determined by the presence of different myosin heavy chain isoforms gene expression. However, humans only have the presence of fibres type 1, 2A and 2X while rodents have all four fibre types, including type 2B (Schiaffino and Reggiani 2011). Additionally, fibre composition can be classified regarding their metabolic energy production being type 2X and 2B the most glycolytic and

type 1 and 2A the most oxidative (Talbot and Maves 2016). Glycolytic fibres produce ATP mainly by anaerobic process due to restricted oxygen availability whereas oxidative fibres produces energy by aerobic conditions. Muscle fibres have the ability to remodel their phenotypes and adapt to different uses and conditions. Different muscle-related disorders affect specific skeletal muscle fibre types. Muscle dystrophies such as Duchene muscle dystrophy affects fibres type 2X (Pedemonte et al. 1999), obesity and type 2 diabetes presents a reduction of type 1 fibres and more type 2 fibres (Oberbach et al. 2006; Mootha et al. 2003), inactivity atrophies type 1 fibres and increases the presence of type 2 (Gallagher et al. 2005), aging cachexia and sepsis atrophies type 2 fibres (Tanner et al. 2002; Nilwik et al. 2013).

The atrophy of different fibre types are associated to the ability to regulate protein turnover. Muscle disuse, denervation and immobilisation cause muscle mass loss mostly reducing protein synthesis activity. These situations are associated with inhibition of protein synthesis in both human and animal models in slow-twitch muscles while fast-twitch muscles are associated with reduced protein synthesis and activated protein degradation under malnutrition and inflammatory states (fasting, diabetes, sepsis, cancer cachexia) (Ciciliot et al. 2013).

Animal models have been used extensively to determine the mechanisms underlying in muscle atrophy. However, some differences have been detected comparing to humans. Several studies in animal models have identified that muscle protein synthesis is less and protein breakdown greater following cast immobilisation (Kobayashi et al. 2006). Instead, in

humans, it is suggested that protein synthesis is the main mechanism leading to muscle loss after immobilisation (Murton and Greenhaff 2010). The reason for these controversies may become from the stress caused by the handling and manipulation inflicted in rodents compared than in humans.

In contrast, muscle atrophy under inflammatory conditions, where several pro-inflammatory cytokines (IL-6, IL-1, TNFα, CRP, etc) are released, is thought to be mediated by less protein synthesis and a marked protein breakdown in animals and humans. In rodents, high levels of the mentioned cytokines increased protein breakdown (Haddad et al. 2005; Frost et al. 2007), which was attenuated by their inhibitors (Zamir et al. 1992). In critical ill humans, muscle atrophy is associated with a slow decrease of protein synthesis and marked elevated protein breakdown (Puthucheary et al. 2013). Therefore, the main muscle protein synthesis and breakdown mechanisms regulating muscle mass and atrophy are described in this section.

1.5.1. Muscle protein synthesis

The control of muscle growth is mediated by the regulation of protein synthesis and degradation as well as myogenic factors. Dietary factors, such as amino acids, and exercise stimulate muscle protein synthesis (Kumar et al. 2009; Pasiakos and McClung 2011). Protein synthesis is initiated with the translation of the encoded mRNA to peptides by the ribosome complex and tRNAs (Pain 1996). The PI3K-Akt-mTOR signalling pathway and the negative regulator myostatin regulate muscle protein

synthesis (Bodine et al. 2001a; Lee and McPherron 2001), which are explained below.

1.5.1.1. The IGF1-PI3k-Akt signalling pathway

Insulin-like growth factor (IGF1) and insulin can bind to the IGF1 receptor and insulin receptor (InsR). The binding to IGF1 receptor leads to activation of the intrinsic tyrosine kinase and autophosphorylation. Then, insulin receptor substrate-1 (IRS1) is phosphorylated, which recruits and activates phosphatidylinositol-3-kinase (PI3K). PI3K catalyses the formation of phosphoinositide-3,4,5-triphosphate (PIP3) from PIP2. This leads to the phosphorylation and activation of Akt at threonine^{308} and serine^{473} sites by the phosphoinositide-dependent kinase 1 (PDK1), resulting with its translocation to the inner plasma membrane. Akt activates protein synthesis, via the mammalian target of rapamycin (mTOR), and glycogen synthase kinase 3β (GSK3β). Then, Akt also inhibits protein degradation by phosphorylating and repressing Forkhead box O (FOXO) (See review Manning and Toker 2017).

In protein synthesis, the phosphorylation of GSK3β by Akt releases the inhibition of the factor eukaryotic initiation factor 2B (eIF2B) to initiate protein synthesis (Rhoads 1999). Akt also activates mammalian target of rapamycin (mTOR) phosphorylating and activating p70^{S6K} and phosphorylating and releasing the inhibitory effect of eukaryotic initiation factor 4E binding protein 1 (4E-BP1) to dissociate from eIF-4E and initiate protein translation (Terada et al. 1994). Therefore, induced activation of Akt

in both *in vitro* and *in vivo* cause hypertrophy (Bodine et al. 2001a; Blaauw et al. 2009). See figure 1.4.

1.5.1.2. Myostatin

The loss of muscle mass can also be conducted by myostatin, a negative regulator of muscle growth member of the tumour growth factor-β (TGFβ) family and expressed predominantly in the skeletal muscle (Lee and McPherron 2001). When myostatin gene was modified in animal models, they developed hypertrophic phenotype in the mice, sheep and cattle and increased of muscle mass was found when loss of function of myostatin in humans (Clop et al. 2006; Schuelke et al. 2004). Thus, the overexpression of myostatin can mediate the loss of muscle mass.

1.5.2. Muscle protein breakdown

Numerous diseases whereby are conditioned by acute and chronic inflammatory states, protein synthesis declines and protein breakdown dominates muscle wasting (Williams, Sun, et al. 1999; Thomas and Mitch 2013) by the activation of both ubiquitin-proteasome system (UPS) (Gomes et al. 2001; LECKER et al. 2004) and lysosomal-autophagy proteolytic pathways (Zhao et al. 2007; Mammucari et al. 2007). Microarray studies have identified a set of atrophy-related genes called atrogenes, encoding ubiquitin, proteasome subunits, ubiquitin ligases and proteins that mediate lysosomal-autophagy activity, under various wasting conditions (Gomes et al. 2001; LECKER et al. 2004), which are also regulated by Akt-FOXO signalling pathway.

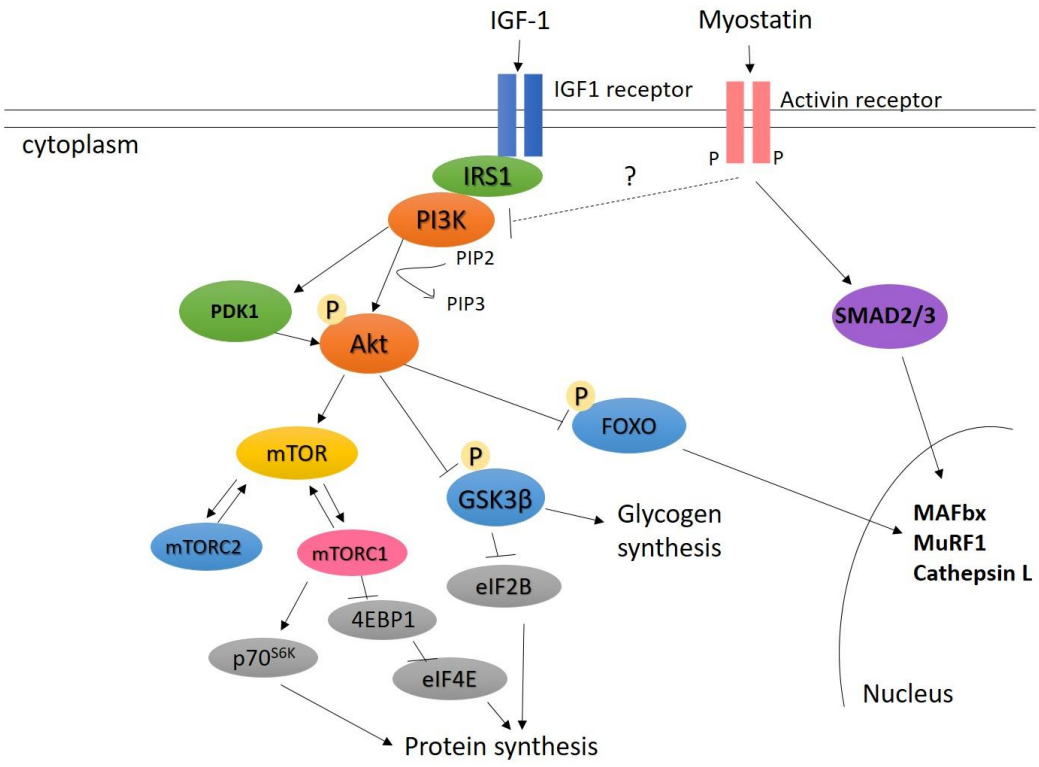


Figure 1.4: IGF1-PI3K-Akt signalling pathway regulating protein synthesis and degradation in the skeletal muscle. Activating PI3K-Akt signalling via phosphorylation from IGF1 receptor and IRS1 leads to protein synthesis and inhibits FOXO, which regulates the atrogenes expression for protein degradation. Myostatin has a role on inhibiting PI3K-Akt signalling and therefore activating protein degradation. For detailed information, refer to the text on sections 1.5.1. and 1.5.3. Arrows represent activation and bars represent inhibition.

The mentioned mechanisms regulating protein breakdown in muscle are described below.

1.5.2.1. Ubiquitin-proteasome system

There are two muscle ubiquitin ligases markedly induced in several types of muscle atrophy and used as markers of accelerated proteolysis: muscle-specific RING-finger 1 (MuRF1 also known as TRIM63) and muscle atrophy F-box (MAFbx also known as atrogin1 and Fbxo32) (Gomes et al. 2001).

When using knock out mice for MAFbx and MuRF1, they were resistant to muscle denervation-induced atrophy (Bodine et al. 2001). Consistent with these findings, it was suggested that MAFbx and MuRF1 might, in part, be responsible for the UPS-mediated muscle protein degradation observed during muscle atrophy conditions (Glass 2003). MAFbx catalyses the degradation of proteins promoting protein synthesis such as factor eukaryotic initiation factor 3 subunit 5 (eIF3-f) (Csibi et al. 2010) as well as MyoD, involved in muscle development and differentiation (Tintignac et al. 2005). MuRF1 catalyses the ubiquitination and degradation of myofibrils and components of the cytoskeleton (Clarke et al. 2007; Cohen et al. 2009). The UPS is required to remove sarcomeric proteins in response to changes in muscle activity (Bonaldo and Sandri 2013). Intact myofibrils are unable to be degraded directly by UPS thus an additional proteolytic system has been suggested to be responsible for the initial cellular degradation, specifically involving increased caspase-3 and/or calpain activity (WILLIAMS, DECOURTEN-MYERS, et al. 1999). The UPS is an ATP dependent process that involves degradation of target proteins by the addition of ubiquitin molecules via the activity of 3 enzymes (E1, E2 E3). Briefly, ubiquitin binds to Ub-activating enzyme E1 via ATP-dependent process and is transferred to the Ub-conjugating enzyme E2. Then Ub-ligase enzyme (E3) (MAFbx and MuRF1) transfers the ubiquitin to the target protein (Passmore and Barford 2004). The process is repeated until four ubiquitin residues are bound to the target protein to be recognised by the 26S proteasome, which degrades the proteins into short oligonucleotides (Thrower et al. 2000). The proteolytic UPS system is depicted in Figure 1.5.

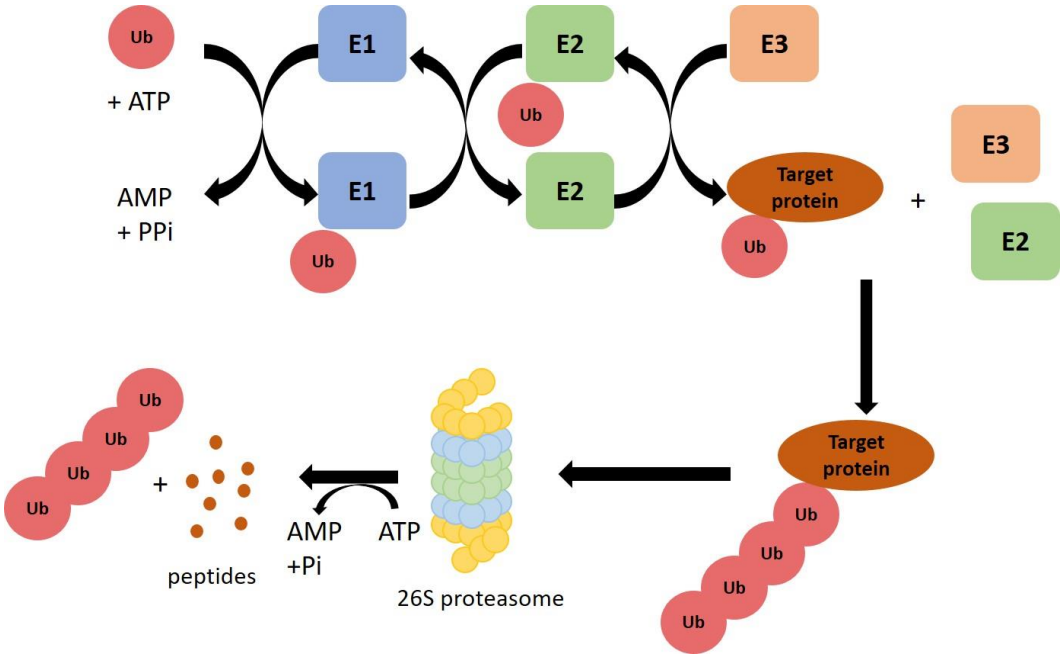


Figure 1.5: Representation of the ATP-dependent ubiquitin-proteasome system (UPS) pathway for protein degradation. The binding of 4 ubiquitin is needed to flag the target protein to be degraded. Ubiquitin is transported to the protein target by an ATP-dependent process involving three sets of enzymes: E1 (ubiquitin-activating enzymes, E2 (ubiquitin-conjugating enzymes) and E3 (ubiquitin-ligases). The flagged protein is degraded by the 26S proteasome, and ubiquitin is recycled.

1.5.2.2. Lysosome-autophagy system

Autophagy and endocytosis are important processes to select cell components to be degraded due to constitutive conditions and in response to various stimuli, such as cellular stress and cytokines amongst other pathologies (Mizushima et al. 2008). Extracellular and membrane components are delivered to lysosomes by endocytosis while cytosolic constituents and organelles are delivered through autophagy process. The lysosomes are membrane-bounded vesicles that have an acid lumen (pH 4-5) containing high concentrations of acid hydrolases and therefore able

to degrade a variety of macromolecules. Proteins are first denatured in the acid lumen of lysosomes and then degraded by cathepsins (Bechet et al. 2005). Cathepsins are the major ubiquitous lysosome proteases and expressed in low levels in the skeletal muscle to degrade myofibrillar proteins. It has been reported that cathepsin L is the major lysosome protease in skeletal muscle and it is upregulated under muscle atrophy conditions, being recognised as a general marker of atrophy (Deval et al. 2001). It was found up-regulated in models of muscle wasting such as sepsis rats treated with pharmacological doses of synthetic glucocorticoids (e.g. dexamethasone), disuse atrophy in rodents and type 2 diabetes (Deval et al. 2001; Taillandier et al. 1996; Huang et al. 2003).

1.5.3. Cross-talk between muscle protein synthesis and breakdown

The IGF1-PI3K-Akt signalling pathway regulates both protein synthesis and breakdown in muscle cells. The phosphorylation of the signalling pathway activates protein synthesis through Akt-mTOR activity and inhibits FOXO activity. When depleted Akt activity, muscle results in atrophy by reducing protein synthesis and activating FOXO and downstream atrogenes (Stitt et al. 2004). FOXO, recruited in the cytoplasm by Akt phosphorylation, becomes activated when is dephosphorylated and is translocated to the nucleus. It is then when FOXO downstream transcription factors are activated. Both, atrogenes MAFbx and MuRF1 mediating UPS activity and cathepsin L mediating lysosome activity, promote the degradation of proteins and thereby muscle atrophy (LECKER et al. 2004; Yamazaki et al. 2010). Simultaneously, it was reported that myostatin might upregulate atrogenes controlled by FOXO in muscle cell cultures. Indeed, treatment

with myostatin blocked the IGF-PI3K-Akt pathway activating FOXO1 and expression of MAFbx (McFarlane et al. 2006). Hence, the regulation of myostatin expression via FOXO supports the concept that the myostatin pathway synergies with Akt-FOXO signalling (Allen and Unterman 2007). However, the effects of myostatin inhibition on muscle growth are likely to be independent of the Akt pathway (Goncalves et al. 2010). For visual description see figure 1.4.

1.6. Regulation of skeletal muscle carbohydrate metabolism

In skeletal muscle atrophy conditions, energy metabolism becomes altered by modulated intermediary factors. Specifically, the IGF-PI3K-Akt signalling pathway regulates glucose uptake and carbohydrate utilisation. In several occasions, inflammation and atrophy results with insulin resistant states in skeletal muscle.

As mentioned earlier, insulin can bind to IGF receptor and insulin receptor. The binding of either insulin or IGF to both IGF receptor and InsR trigger the phosphorylation of IRS1 activating its downstream factors. Thus, insulin availability also inhibits protein degradation by the modulation of mTOR and FOXO factors in the PI3k-Akt signalling pathway explained in the section above. Indeed, protein degradation is decreased in skeletal muscle in response to physiological increases in plasma insulin (Gelfand and Barrett 1987). In numerous *in vitro* experiments have been demonstrated that high concentrations of insulin stimulates protein synthesis and reduces protein degradation in rodents (Kimball SR 1998). Conversely, reduced insulin availability reduces the rate of protein synthesis in rat skeletal muscle

(Kimball SR 1998). It is well established that insulin exerts a diverse range of metabolic effects including stimulation of glucose uptake and synthesis of glycogen in skeletal muscle and increase of lipids synthesis and a decrease of lipolysis in adipose tissue (Wilkes et al. 2009).

The phosphorylation and consequent activation of Akt lead to the translocation of glucose transporter-4 (GLUT4) receptors to the plasma membrane to allow glucose uptake into the muscle (Kohn et al. 1996). In muscle, glucose is then stored as glycogen by glycogen synthase (GS) or catabolised to pyruvate and lactate by glycolysis. In normal aerobic conditions, the pyruvate dehydrogenase complex (PDC) catabolises pyruvate to acetyl-CoA which is degraded by the tricarboxylic acid (TCA) cycle to generate reducing equivalents for the electron transport chain. In conditions of increase metabolic demand, pyruvate is catabolised to lactate when the rate of pyruvate production exceeds the rate of mitochondrial pyruvate use. The inhibition of PDC activity can result in hyperlactatemia. In normal conditions, PDC is regulated by pyruvate dehydrogenase phosphatase (PDP), which stimulates its activity. In inflammation, the activation of FOXO by its dephosphorylation initiates the transcription of pyruvate dehydrogenase kinase 4 (PDK4), which inhibits PDC (Constantin-Teodosiu 2013). PDC is localised in the mitochondrial membrane, which contains the pyruvate dehydrogenase (PDH) necessary to metabolise pyruvate from glycolysis to acetyl-CoA. See figure 1.6 for schematic representation.

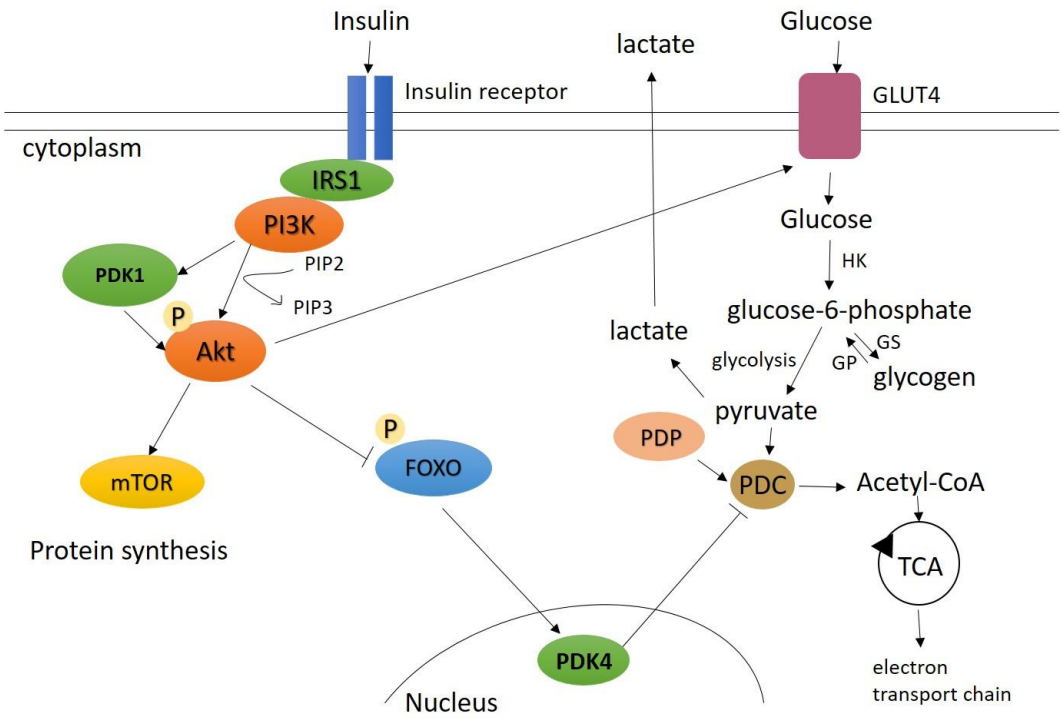


Figure 1.6: Signalling pathway regulating carbohydrate metabolism. PI3K-Akt signalling pathway regulated by IGF1 and IRS1 activates glucose uptake via GLUT4 receptor. Glucose catabolism is mediated via PDC to transform pyruvate to Acetyl-CoA and be metabolised by the TCA cycle to produce energy via electron transport chain (aerobic process). PDC activity is activated by PDP and inhibited by PDK4, which is regulated by FOXO. When PDC is inhibited, pyruvate is converted to lactate (anaerobic process). Refer to text for details and abbreviations on section 1.6.

1.6.1. Inflammation and muscle disuse-induced insulin resistance

Skeletal muscle is the main organ with glucose uptake activity in the body (80% in men) (Lorenzo et al. 2008). Therefore insulin sensitivity and insulin-stimulated glucose uptake are strongly regulated in the skeletal muscle being the major site for insulin resistance (IR). Muscle IR results from abnormal insulin concentrations in blood or a failure in the machinery of insulin-mediated glucose uptake in the muscle. Catabolic diseases, including sepsis, chronic kidney disease (CKD), ageing and immobilisation

are frequently associated with muscle IR (Dardevet et al. 1994; Kobayashi et al. 2005). Insulin resistance develops in reduced ambulatory activity, after 3-14 days (Olsen et al. 2008). The mechanism whereby muscle insulin resistance develops under inflammation and muscle disuse is associated with the PI3K-Akt pathway. In rodents, hind limb immobilisation resulted with a decline of IRS1 protein expression and Akt activity (Hirose et al. 2000). Immobilisation in humans blunted Akt phosphorylation and reduced GLUT4 protein expression resulting with less glucose uptake and muscle glycogen synthase activity (Mortensen et al. 2014; Bienso et al. 2012). In inflammation, such as sepsis, insulin resistance accompanied by hyperlactatemia may be triggered by impaired PDC activity as a result of PDK4 upregulation (Alamdari et al. 2008). It has been shown that insulin may suppress PDK4 upregulation by phosphorylating the PI3K-Akt-FOXO pathway (Kwon et al. 2004) and therefore IR states result in increased PDK4 and consequent inhibition of PDC activity in muscle (Furuyama et al. 2003; Kim et al. 2006).

1.7. Muscle atrophy and insulin signalling in inflammation and arthritis

Inflammation and muscle disuse are often associated with muscle wasting and important metabolic alterations. As mentioned in section 1.3, the low inflammatory response is associated with OA, which is locally found in the tissues belonging to the joint in OA, whereas severe systemic inflammation is found in RA. Both types of arthritis correlate with comorbidities appearing

in mid and late stages of disease (hypertension, obesity, diabetes, dyslipidaemia, etc) (Soubrier et al. 2014; Breedveld 2004).

Muscle weakness is commonly observed in patients with early and established OA (Lewek, Rudolph, and Snyder-Mackler 2004) and in patients with RA (Helliwell and Jackson 1994). Muscle atrophy and metabolic dysfunction are mediated by non-inflammatory conditions and muscle disuse including limb immobilisation, bed rest or spinal cord injury, and by inflammatory conditions including sepsis, cancer cachexia and chronic diseases such as CKD and COPD. Muscle dysfunction in OA mainly affects type II fast-twitch muscle fibres, which are atrophied in patient's quadriceps (Fink et al. 2007), as well as in RA (Gómez-SanMiguel et al. 2016).

In patients and several models of OA, muscle weakness has been correlated to loss of muscle strength rather than atrophy with a 12% reduction of cross-sectional area in quadriceps, which may be concomitant to muscle disuse (van der Poel et al. 2016; Slemenda et al. 1997; Ikeda, Tsumura, and Torisu 2005). In contrast, RA is a systemic disease with well-established inflammatory state and consequent muscle atrophy (rheumatoid cachexia) (Roubenoff et al. 1994) where there is a clear reduction of muscle mass as well as strength (Cooney et al. 2011). In both OA and RA, muscle wasting and insulin resistance could be driven not only by inflammation but also decreased physical activity attributable to pain. However, the trigger of immobilisation induced insulin resistance is unknown.

Since arthritis results in elevated joint and plasma concentrations of pro-inflammatory cytokines (at least in RA), it is possible that they are, at least in part, responsible for triggering the molecular changes that lead to muscle atrophy during arthritis. Studies in tumour-bearing animal models and sepsis demonstrated that pro-inflammatory cytokines are mediators for accelerated proteolysis, primarily by the UPS, and lysosomes with less extend (Gomes et al. 2001; Baracos et al. 1995). TNFα can induce genes involved in proteolysis by UPS in cultured muscle cells (Bhatnagar et al. 2010; Llovera et al. 1996). With more precision, local inflammation in the tibiotarsal joint of the rat resulted with increase TNFα, atrogenes MuRF1 and MAFbx and myostatin in the tibialis anterior muscle (Carolina Ramírez 2011). Accordingly, in models of RA, skeletal muscle resulted with a reduction of cross-sectional area as an indicator of muscle wasting and increased levels of atrogenes MuRF1, MAFbx and TNFα in gastrocnemius (Gómez-SanMiguel et al. 2016). The anti-TNFα therapy (DMARD) is used in patients with RA with a positive reduction of disease activity but does not improve body composition and muscle mass (Metsios et al. 2007). The anti-TNFα treatment in patients with cancer-associated did not prevent muscle atrophy (Jatoi et al. 2007) probably due to the contribution of other pro-inflammatory cytokines like IL-6, which correlate with weight loss in cancer (Ebrahimi et al. 2004). Indeed, the infusion of IL-6 in healthy volunteers led to muscle protein degradation (van Hall et al. 2008), and it can be ameliorated by IL-6 targeted antibodies (Strassmann et al. 1992). A good anti-IL6 treatment can be the tocilizumab, a DMARD currently administered in patients with RA (Tournadre et al. 2017). In parallel, pro-inflammatory

cytokines also regulate lysosome-autophagy complex. IL-6 mediates muscle atrophy and is associated with increased muscle cathepsin-L (Tsujinaka et al. 1995). Tumour-bearing animals treated with an inhibitor of TNFα reduced cathepsin-L in muscle (Tsujinaka et al. 1995). Keeping in line, muscle loss mediated by myostatin was seen in a model of RA (Castillero et al. 2011), being also associated with insulin resistance in muscle fibres (Hittel et al. 2010).

Accordingly, it is likely that cytokines also modulate muscle metabolic dysfunction associated with insulin resistance and carbohydrate oxidation during inflammation. Albeit alternative pathways may also be important, Akt-FOXO activity appears to be crucial in both muscle atrophy and insulin signalling. Catabolic states with acute and chronic inflammation strongly associated with insulin resistance and dysregulation of carbohydrate oxidation (Dardevet et al. 1994). A genetically modified insulin-resistant mouse (*db/db*) mediated by dyslipidaemia was found to have increased UPS-dependent protein degradation, which was correlated to impaired Akt-FOXO signalling. These effects were then reversed with the administration of an insulin sensitizer (rosiglitazone), whose anti-inflammatory effects improved insulin signalling through PI3K-Akt signalling and suppressed muscle proteolysis (Wang et al. 2006). In inflammatory states such as obesity and diabetes, IL-6 is correlative to IR (Al-Khalili et al. 2006). IL-6 induces IR by blocking PI3K-Akt signalling, which reduces glucose uptake by impaired GLUT4 and IRS1 as well as glycogen synthesis (Yin et al. 2014). In fact, in the CIA model of RA, the expression of sensitivity genes GLUT4, IRS1 and IRS2 were lower than in control rats (Arias de la Rosa et

al. 2018). In arthritis, patients tend to present symptoms of muscle weakness and insulin resistance, which may end with further complications resulting in diabetes and cardiovascular disease (Soubrier et al. 2014; Nicolau et al. 2017). The most common cause of premature death in arthritis is a cardiovascular disease (Radner et al. 2017). The physiological and molecular process whereby patients with arthritis develop alterations in muscle protein metabolism and insulin sensitivity are not yet identified. It is well known that there is a disruption on carbohydrate and lipids metabolism in metabolic tissues from RA models (Arias de la Rosa et al. 2018). The mechanisms whereby metabolic dysfunction is driven are numerous. However, it may be partly regulated by Akt-FOXO signalling. It was demonstrated in sepsis that FOXO-derived transcription factors might mediate carbohydrate oxidation. It was seen that a decrease of phosphorylated Akt and FOXO led to PDK4 accumulation, which regulates PDC activity (Crossland et al. 2008). Especially, IL-6 induced increased PDK4 and affected PDH activity in muscle from fed and fasted rats (Biensø et al. 2014). Patients with OA with decreased muscle strength presented increased FOXO expression in vastus lateralis (Levinger et al. 2016) as well as in a rat model of RA (Gómez-SanMiguel et al. 2016) but not Akt. Hence, it is unclear the existence of crosstalk on insulin-mediated protein turnover and carbohydrate metabolism in arthritis as seen previously in sepsis (Crossland et al. 2008).

1.8. Aims of thesis

It is well stablished that arthritis pathology involves a complex inflammatory response including pain and low physical activity that affects the quality of life. Moreover, inflammation and muscle disuse are factors contributing to muscle atrophy and insulin resistance increasing morbidities and mortality rates in arthritis. The complexity of mechanisms and comorbidities in patients with arthritis hinders the identification of treatments to combat the disease. Targeting muscle dysfunction will improve the overall health of an individual and allow them to undertake daily activities with better quality of life in patients with arthritis. Inflammation and muscle disuse are a major determinant of arthritis disease pathology, comorbidities, pain and muscle dysfunction. Therefore, in this thesis, I aimed to identify disease severity related to inflammation, locomotor activity and muscle deterioration to understand better the underlying mechanism(s), which may inform the identification of alternative treatment targets in arthritis. The primary aim of the thesis is to use established animal models of arthritis to identify the physiological (physical activity and inflammation) and muscle molecular events in the EDL (fast-twitch) leading to atrophy and dysregulation of carbohydrate metabolism, focusing mainly on the PI3K-Akt-FOXO signalling pathway, and where possible to confirm the translational relevance in clinical samples.

Objective 1: To identify muscle mass and carbohydrate metabolism function in a model of OA and its contribution to locomotor activity, pain and pathology. The experimental model of OA used is a surgical model MNX,

where the ipsilateral medial meniscus is transacted through its full thickness provoking the tear and wear of the cartilage (Janusz et al. 2002).

Objective 2: To identify the molecular pathways involved in the muscle mass loss and dysregulation of carbohydrate metabolism and its contribution to pain, locomotor activity and pathology in CIA rat model of early RA. A set of genes (46) from muscle atrophy and metabolic pathways and inflammation were quantified in the EDL muscle. The CIA model develops RA by an autoimmune response to bovine collagen type II inducing ankle swelling, which is more analogous to human RA (Bendele et al. 1999; Trentham, Townes, and Kang 1977).

Objective 3: To test the impact of the anti-inflammatory and insulin sensitising agent rosiglitazone (PPARɣ agonist) on ameliorating muscle wasting and metabolic dysfunction in the EDL muscle of CIA rats, identifying the relevant changes on the genes analysed in Chapter 4 including PI3K-Akt-FOXO signalling axis (Crossland et al. 2017). Simultaneously, the protective effects of rosiglitazone would be reflected to paw swelling and pathology as well as pain and physical activity levels.

Chapter 2:

General methods

2.1. Animals and subjects

In this project, we have used two different rat models of arthritis. In Nottingham, the Pain Centre of Arthritis Research in the UK has established surgical rat model of meniscal transection MNX, which results in pain behaviour and knee pathology, mimicking key aspects of the pathology in human osteoarthritis (Mapp et al. 2013b). This experimental model mimics the tearing of the medial meniscus in the knee, a common injury. The second model used is the CIA in rat, which is a model of autoimmune rheumatoid arthritis that affects the ankle joints in early stages with acute inflammation. The CIA model has been introduced recently in the ARUK Pain Centre in Nottingham to study the pain sensory neurons (Nieto et al. 2016). It consists of intradermal injection of bovine collagen type II to induce the autoimmune response against the collagen type II in the joints.

These two animal models were used for the first time to analyse the metabolic and molecular changes in skeletal muscle at the University of Nottingham.

All procedures were approved by the University of Nottingham Ethical Review Committee and were performed under Home Office Project and Personal Licence authority (Animal Scientific Procedures Act ASPA 1986). Male Sprague-Dawley rats, weighing 160-180 g, and female Lewis rats, weighing 150-170 g, were purchased from Charles River UK and housed in the Biomedical Services Unit, University of Nottingham, for at least seven days after delivery and before any procedure. Rats were housed in groups of 3-4 and had free access to standard rat chow and water. Room

temperatures were maintained at 21 ± 2^{o}C, and the light/dark cycle was 12 h from 7 am to 7 pm. All experiments were carried out under blind conditions to treatment. Body weights and health checks of rats were monitored before, during and after each experiment.

Quadriceps mRNA from patients with rheumatoid arthritis was provided by Dr Rowan Hardy (Institute of Metabolism and Systems Research, University of Birmingham) and Dr Andrew Filer (Institute of Inflammation and Ageing, University of Birmingham) as part of research collaboration. mRNA from vastus lateralis from age-matched healthy volunteers was provided by Prof Paul Greenhaff (MRC/ARUK Centre for Musculoskeletal Ageing Research, University of Nottingham).

2.1.1. Anaesthesia

General anaesthesia was administered by inhalation to allow the surgery and injections to rats (recovery procedures) and by intraperitoneal injection to harvest limb muscles (non-recovery). The selected inhalation anaesthetic agent was isoflurane (halogenated ether), a volatile compound which was delivered with oxygen (O_2). It induces and maintains general anaesthesia by depression of the central nervous system (CNS). The general anaesthesia was performed by placing the rats individually in a chamber with isoflurane 3% in 1 L/min of O_2 until no reflexes were observed. When confirmed, the anaesthetic effect was maintained by an inhalation tube with isoflurane 2% in 1 L/min of O_2 and the rat placed over a heating matt to maintain the body temperature. Once the surgery or the injections were completed, rats were placed on a warm heating pad in a new cage and kept

under observation until recovered. Non-recovery anaesthesia for harvesting muscles was performed by intra-peritoneal injection with the anaesthetic agent pentobarbital. One person restrained the rat by the scruff with one hand and hind limbs with the other hand while a second person injected the pentobarbital (50 mg/ml) with a 25G, 5/8 inch orange needle to the hub into the lower abdominal quadrant between the midline and leg at a 45^{o} angle. The volume injected depended on the body weight of the rat, administering 60 ml/kg (Overmyer et al. 2015).

2.1.2. Medial meniscus transection

OA was induced by surgical transection of the medial meniscus as described previously in Janusz *et al*. (2002) and Ashraf, Mapp, and Walsh (2011).

Briefly, rats underwent to general anaesthesia induced by inhalation with isoflurane (3%) and oxygen (1 L/min) prior to surgery and maintained (2% and 1L/min O_2) during surgery. The left leg was taken as ipsilateral, which was shaved and swabbed with chlorhexidine in order to sterilise the area under the surgical incision. Rats were placed on a heating matt to preserve the body core temperature during surgery and covered with a sterile op-cover with a hole over the area operated. All instruments were autoclaved before surgery and re-autoclaved in between. An incision on the skin over the medial part of the joint, by a pair of scissors, allowed access to find the medial collateral ligament (MCL), seen as a white shadow line under the muscle layers. The connective tissue and muscle covering the MCL was cauterised using small vessel cauteriser (InterFocus Ltd, Linton,

Cambridge, 18000-00). Bleeding and haemorrhage were stopped cauterizing the vessel and with a sterile swab or cotton. Then, the MCL was grasped with rat teeth forceps and cut using straight spring scissors held flat to the joint to remove it in order to expose partly the meniscus. The skin was sutured to obtain a Sham surgery of the model. For MNX surgery, the meniscus was cut through all thickness at its narrowest point with straight spring scissors. The connective tissue layer was closed with interrupted stitches using Ethicon coated vicryl 8/0 sutures (NHS supply chain), and the skin was closed with running suture stitches using Ethicon coated vicryl 4/0 sutures. Finally, some Gluture was administered at the end of the knot to secure the cicatrisation.

2.1.3. Intradermal injection of Bovine Collagen type II

Intradermal injections in the base of the tail were performed. Rats were under general anaesthesia (inhalation with isoflurane (3%) and 1 L/min O_2 before and during the procedure). The area at the base of the tail was shaved and swabbed with chlorhexidine to sterilise the skin. An emulsion was injected with a 1 ml syringe through 25G, 5/8 inch orange needle, piercing carefully only the top layer of the skin (epidermis). Hence, the emulsion remained in the surface in the form of a bubble under the skin. The emulsion contained bovine collagen type II (4 mg/ml; MD Bioproducts) dissolved in acetic acid 10 mM and emulsified 1:1 with Complete Freund's Adjuvant (CFA), which was made with 1 mg Mycobacterium Tuberculosis in 1 ml of Incomplete Freund's Adjuvant. Two hundred microliters of bovine collagen type II emulsion (2 mg/ml) was injected to induce the model of

arthritis, and 200 µl of CFA emulsified 1:1 in acetic acid 10 mM was injected as the control.

2.1.4. Blood withdrawal from the tail vein

Blood was collected from the tail vain before, during, and at the end of experiments. Rats were pre-warmed at 37ºC in a heating chamber for 3-5 min and then placed in a restriction red tube to immobilise the animals without anaesthesia. After checking the nose was well placed and the rat is breathing normally, the tail was swabbed with chlorhexidine to identify the lateral vein. Butterfly needles with 21G were injected into the vein to the tail with and angle <45º. Blood (approx. 0.5-1 ml) was collected in a 1.5 ml tube containing 50 µl of heparin (1,000 U/ml) on ice. Soon after, the plasma was extracted by centrifugation at 13.000 rpm for 5 min, and then the supernatant was transferred to a new tube. The volume of blood was calculated based on the LASA Guideline, collecting no more than 7.5% in any 1 week and 10% in any 2 weeks of total blood volume (65 ml/kg).

2.2. Oral gavage

The administration of drugs in rodent animals can be done by different techniques. The best technique was selected by considering different factors such as stress for the animal, blinding conditions, number of animals housing in a cage, experimental design and solubility. Due to blinding conditions, performing different in vivo techniques on the same day and maintaining the rats in groups of 4 in the same cage, the oral gavage was the method of choice. This method, with good training and experience,

provides convenience for most of the experimental conditions and time, although it might expose the rats to stress.

The drug was delivered directly into the stomach of animals by soft, flexible plastic catheters with a protective rounded tip to prevent any internal tissue puncture during the procedure. The maximum volume administered to a rat was calculated based on the LASA Good Practice Guidelines (10-20 ml/kg daily). The rat was restrained by scruffing with its neck extended so that the head was well controlled and the forelimbs immobilised. The distance from the oral cavity to the stomach was measured placing the catheter outside the rat and next to the cavity, and then the limit above the oral cavity was marked. The syringe (500 ml size) with the correct volume of the drug was attached to the catheter. It was then rotated slightly to enable smooth passage throughout the sphincter of the epiglottis and into the oesophagus until the mark. The liquid was passed gently down through the catheter placed on a lateral of the mouth, avoiding teeth contact not to perforate it. Then, it was gently removed in the opposite direction from insertion, and the rat returned to its cage. All rats were observed after the procedure for potential complications.

The drug administered to the experimental group contained rosiglitazone (Bepharm Ltd, China) dissolved in 0.5% (Hydroxypropyl) methylcellulose (HPMC) (Sigma). The dose given was 10 ml/kg of 8.5 mg Rosiglitazone suspended in 0.5%HPMC. Control rats received only 0.5%HPMC as a vehicle.

2.3. Joint swelling

Both OA and RA are diseases with joint inflammation. Knee joint swelling for each limb in OA operated rats was measured using digital electronic calliper (Miyutoyo UK Ltd Andover, UK) before surgery. For the OA model, joint swelling was only measured if the rat was limping or presented lameness to ensure the swelling did not exceed 50% of the starting diameter (adverse event limit). The diameter of the knee joint was measured placing each part of the calliper on each lateral and medial side of the knee joint. For the RA model, joint swelling was measured throughout the study, by placing one side of a digital electronic calliper on the instep and the other side between food pads. Rats were humanly terminated if the thickness of hind paws exceeded double of the starting diameter (adverse event limit).

2.4. Pain behaviour measurements

Measurements of weight bearing (WB) and paw withdrawal thresholds (PWT) were used in this thesis. Similar pain behaviour assessments are widely used in both arthritic patients and rats *(*Hendiani *et al*. 2003).

2.4.1. Weight-bearing

This method compares the difference in weight borne on the ipsilateral and contralateral limbs of the rat using an Incapacitance Meter (Linton Instruments, Norfolk, UK). Rats were placed in an angled Perspex box and were allowed to habituate. Hind paws need to be aligned in parallel such as each one rests on the corresponding transducer pad. The weight distribution between the hind paws is recorded during 3 s. The average of 3 consecutive readings was taken and expressed as the difference in

percentage between each hind limb following the equation bellow (Bove *et al*. 2003).

$$\frac{\text{Contralateral} - \text{Ipsilateral}}{\text{Contralateral} + \text{Ipsilateral}} * 100$$

2.4.2. Hind paw withdrawal thresholds

Alterations in hind paw withdrawal thresholds were assessed using calibrated von Frey monofilaments (Semmes-Weinstein monofilaments) bending forces from 2, 4, 6, 8, 10, 15, to 26 g in a logarithm scale. Rats were habituated individually in Plexiglas mesh bottom test cages 15 min before the test. The Dixon up-down method was used as previously described (Chaplan *et al.* 1994; Sagar *et al*. 2010). Briefly, the plantar surface of both hindpaws was stimulated with the 4 g filament for 3 s, commencing with the ipsilateral side. In the case of pain response, lifting and/or licking the affected paw and flinching, the next lower filament was used. If there was no pain response, the next upper filament was applied. After the first threshold response was observed, the lower monofilament with a stimuli respond was recorded as the PWT. The same procedure was applied to the contralateral side.

2.5. Physical activity measurements

There are several ways to record the physical activity of rats using either active (i.e. wheel) or passive methods (i.e. activity boxes). The active methods may interfere with the molecular and physiology parameters as it can be interpreted as exercising, whereas the activity boxes are more appropriate to count only the number of movements a rat normally performs

in a short time. Therefore, the physical activity test used in this project was the locomotor activity boxes (LMA). Rats were placed in individual automated infra-red activity boxes, which consisted of Plexiglas cages (39.0×23.5×24.5 cm) with wire mesh lids and exchangeable floors, fitted with a 4×8 horizontal photo-beam configuration (Photo-beam Activity System-Home Cage, San Diego Instruments, CA). The photo-beam activity system consists of eight parallel lower beams and four parallel upper beams in each box. The activity was counted when the consecutive breaking for two adjacent photo-beams (locomotion) and one upper beam (rear) break. The beam-break accumulation was automatically recorded over 5 min time intervals for a certain period.

2.6. Tissue collection

On the last day of the experiment, the tissue needed for further *ex vivo* analysis was collected. It included the EDL muscle, rich in type II muscle fibres (75.7%) (Soukup, Zachařová, and Smerdu 2002), and joints (knee and ankle).

2.6.1. Muscle dissection under terminal anaesthesia

The EDL muscle from both hind limbs was removed under terminal anaesthesia with an intraperitoneal injection of pentobarbital as described previously (section 2.1.1.). The rat was placed on a heating matt to preserve the body core temperature while harvesting the muscle. Upon the absence of the paw withdrawal reflex, elicited by pinching the fore and hind paws and checking eyes blinking movements, the muscle was removed and immediately snap-frozen in liquid nitrogen. A portion of muscle was stored

at -80^{o}C for wet muscle analysis and another portion was freeze-dried over 48 h and stored at -80^{o}C until analysed.

2.6.2. Dissection and mounting of rat tibiofemoral joint

Fresh tibiofemoral joints were collected by cutting mid-femur and tibia with a bone cutter and removing the excess of skeletal muscle. They were post-fixed in a tube containing neutral buffered formalin 4% formaldehyde, pH 7.4, at room temperature for 48 h and then it was replaced with phosphate-buffered saline (PBS). They were then decalcified with a chelating agent to obtain thin sections of the joints for histology staining. The decalcification allows to soften the heavy mineralised tissues, such as bone, to produce soluble calcium salts. The most common chelating agent, and used in the experiments, is the ethylenediaminetetraacetic acid (EDTA), which is less harsh than other agents and acts slowly, preserving most of the joint structures and some enzyme activity (Mepham 1991). The joints were immersed in 10% EDTA in 10mM Tris buffer with 7.5% [w/v] polyvinylpyrrolidone [PVP], pH 7, under continuous agitation during 6-8 weeks, changing the EDTA solution once a week.

After decalcification, the joints were split in frontal plane with a rectangular blade, taking the lateral collateral ligaments as guidance, in two halves and placed separately in plastic cassettes for processing and embedding. They were processed by standard histological techniques, in the Shandon Pathcentre enclosed tissue processor to undergo a series of dehydration (in alcohol) and clearing (in xylene). Then, the joint tissues were impregnated with molten wax for the final embedding stage. It consists of

placing the inner part of the joint facing down into the centre of a metal mould in a hot-plate, dispensing some warm wax in and the plastic cassette on the top of the mould. They were placed on a cold-plate to allow the wax to solidify and then removed from the metal mould. The excess wax was trimmed from the cassettes and stored at room temperature until required for sectioning.

2.6.3. Dissection and mounting of rat tibiotarsal joint

Fresh tibiotarsal joints were collected by removing the skin from mid-tibia to paw digits and cutting tibia with a bone cutter. They were post-fixed in a tube containing neutral buffered formalin 4% formaldehyde, pH 7.4, at room temperature for 48 h and then it was replaced with PBS. The decalcification process was similar to the previously described in section 2.6.2 (tibiofemoral joint). In this case, it was carried out with a weak acid fixation solution composed of 10% formic acid (90%) and 2% of formaldehyde in an aqueous solution. Decalcification occurs rapidly in 3 days.

After decalcification, the digits and excess tibia were removed to place only the ankle in plastic cassettes for processing and embedding as described previously for the tibiofemoral joint. In this case, the medial part of the joint was placed facing down into the mould.

2.7. Histopathology of joints

2.7.1. Histology

Once the joints are embedded with paraffin wax in the corresponded cassette, the sectioning for histopathology was carried out following the osteoarthritis research international (OARSI) histopathology initiative

recommendations for histological assessments of osteoarthritis and rheumatoid arthritis in the rat (Gerwin et al. 2010).

In knee joints, frontal sections are the most commonly used for microscopic evaluation (Janusz *et al*. 2002) with both femoral condyles, tibia plateaux, menisci and synovium (Gerwin *et al*. 2010). The blocks were trimmed to obtain a clear section of the tibia plateau and then eight 5 µm coronal sections of 3 different levels were cut by a manual microtome. The levels were spaced in 200µm.

In ankle joints, the medial part is the most commonly used to include the tibiotarsal joint. The blocks were trimmed until the surface of the joint was exposed. After testing a control joint, it was found that the tibiotarsal joint starts after 400-500 µm trimmed from an intact wax block. At this point, five 8 µm sections were cut from 3 different levels, spaced with 60 µm in-between.

The most frequent stain used for histology is the haematoxylin and eosin (H&E), which is sensitive enough for scoring following OARSI guideline. It is often used to analyse tissue morphology. The haematoxylin dye is basic and has a high affinity for acidic structures which are stained in blue whereas the eosin dye is acidic and stains the basic structures in pink (Mepham 1991). The paraffin wax tissue sections were first dewaxed in xylene and then dehydrated in graded ethanol 100% and 70% before being washed in distilled water to hydrate for 5 min each step. Then, the first staining was achieved with Mayer's haematoxylin for 15 min and rinsing tap water to differentiate it for 1 min following 20 s of 1% acid alcohol solution

and back into tap water for 3 min. The second staining was achieved with 1% eosin for 30 s and differentiated under running tap water for 5 min. In the end, the sections were dehydrated with graded ethanol 70% and 100% and xylene for 5 min each. They were then drained and covered with DePeX and cover-slips and allowed to dry.

2.7.2. Joint microscopic scoring

The samples were scored with a conventional microscope starting at 4x augments up to 40x if necessary.

The model used in this thesis for OA is the surgical MNX model whose most affected part of the joint is the medial tibia plateau of frontal sections (Mapp et al. 2013b). The scoring system used for chondropathy and osteophytosis was the previously described from Janusz *et* al. (2002), and synovitis was scored according to the thickness of the synovial lining layer and synovial cellularity (Mapp *et al*. 2008).

Chondropathy is the pathological stage of cartilage deterioration. The score is based on the scale of 0 to 5 where 0 = Cartilage of normal appearance; 1 = Minimal fibrillation in superficial zone; 2 = Mild, fibrillation extends to upper zone; 3 = Moderate, well into the middle zone; 4 = Marked, well and gasping into the deep zone; 5 = Severe, full thickness degeneration to the tidemark. Additionally, the involvement of the damage in the medial tibia plateau is considered: 1/3, 2/3, 3/3. The final cartilage damage score was the multiplication of the chondropathy and involvement (1, 2 or 3) with a maximum score of 15.

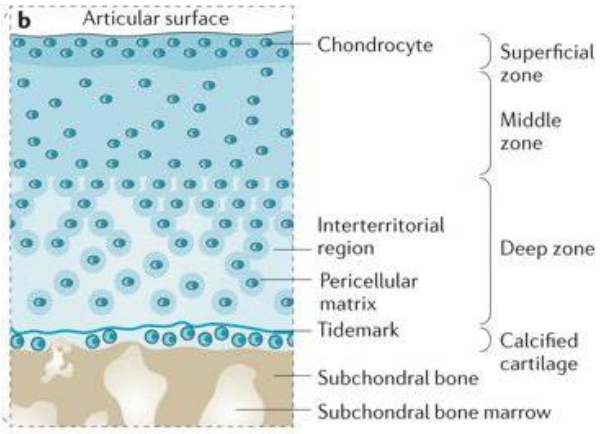


Figure 2.1. Zones of articular cartilage important to distinguish for an accurate scoring (Martel-Pelletier et al. 2016).

Osteophytosis is the formation of bone tissue from cartilage on the lateral side of the condyle. The score is on scale of 0 to 3 where 0 = No presence of osteophytes; 1 = Osteophytes <40 µm; 2 = Osteophytes 40-160 µm; 3 = Osteophytes >160 µm.

Synovitis is the synovium inflammation with the presence of inflammatory cells and increased thickness. The score is based on the scale of 0 to 3 where 0 = No cellularity and 1-2 synovial layers; 1 = Mild, no cellularity and 3-5 synovial layers; 2 = Moderate, mildly increased of cellularity and/or 6-8 synovial layers; 3 = Severe, cellularity and ≥ 9 synovial layers.

The model used for rheumatoid arthritis was the systemic inflammatory CIA model that has the presence of ankyloses (inflammation and deterioration of the ankle). As this is an inflammatory model, the purpose of the scoring in the tibiotarsal joint in my thesis was the severity of synovitis only. There are different scoring systems where some involve the whole joint pathology together, and others divide the different pathologies into different parts of the joint like in the tibiofemoral joint previously described. One of the

commonly used scoring methods for the synovitis of the ankle is the OARSI system (Gerwin et al. 2010), with some similarities to the knee joint scoring used in the MNX model (Janusz *et al*. 2002).

2.8. Enzyme-linked immunosorbent assay (ELISA) to determine cytokines in plasma

The ELISA kit employed for the detection of inflammatory cytokines levels in plasma, extracted as detailed on section 2.1.5., was the Quantikine ® ELISA (Rat IL-10, IL-6, TNFα) R&D Systems. This assay consists of the quantitative sandwich immunoassay technique, where the rat antibodies for the corresponding cytokine are attached to the microplate, the antigen (cytokine) from plasma binds to them and a specific enzyme and its substrate are added to quantify the product from its reaction by colour intensity, which is equivalent to the quantity of cytokine selected. A different kit per each cytokine was used following manufacturer's protocol, and samples were diluted 1:1 only for the TNFα quantification.

Firstly, 50 µl of Assay Diluent and 50 µl of standard, control and sample were added to each well. Standards were made in a range from 4000 to 62.5 pg/ml, and the samples were diluted 1:1 with Calibrator Diluent. The plate was mixed gently and incubated for 2 h at room temperature and then washed 5 times with Wash Buffer using 400 µl per wash. A hundred µl of Rat IL-6 Conjugate was added in each well and incubated for 2 h at room temperature. The plate was then washed 5 times, and 100 µl of Substrate Solution was added and protected from light. After 30 min incubation at room temperature, 100 µl of Stop Solution was added and gently mixed.

The optical density (OD) was determined within 30 min using a microplate reader with the wavelength set at 450 nm. In order to calculate the concentration of target cytokine, the OD from 0 pg/ml was subtracted as blank, and the standard logarithmic curve created. The analysis was performed by 4-Parameter Logistic Regression using online software.

2.9. *Ex vivo* analysis of muscle intermediary metabolites

2.9.1. Muscle metabolite extraction

Intermediary metabolite concentrations were analysed in freeze-dried muscle tissue. Frozen, freeze-dried muscle samples were brought to room temperature in silica gel to keep the muscle dry. Following this, muscle (5-10 mg) was powdered with a scalpel, curved forceps and a small mortar at room temperature. Visible connective tissue and superficial blood were then removed and muscle powder weighted. Muscle metabolite extraction was done with ice-cold perchloric acid (PCA) as previously described (Harris, Hultman, and Nordesjö 1974). The adequate volume of 0.5 M PCA, 1 mM EDTA solution was added to 5-10 mg powder (1 ml for every 12.5 mg powder) and incubated on ice for 10 min, mixing occasionally. It was then spun down at 24,000 g for 3 min at 4^{o}C, and the supernatant was removed and neutralised with 2.2 M $KHCO_3$ solution by adding a volume corresponding to 1/4 of PCA mixture recovered. The perchlorate mixture obtained was incubated for 10 min on ice and spun down at 24,000 G for 3 min at 4^{o}C. The supernatant was transferred into a new tube and stored at -80^{o}C for subsequent analysis. The extraction factor (EF) of each sample was determined using the following formula:

$$EF = \frac{V_{PCA} + V_{KHCO3}\ (\mu l)}{\text{Tissue (mg)}}$$

2.9.2. Muscle adenosine triphosphate and phosphocreatine determination

Muscle adenosine triphosphate (ATP) and phosphocreatine (PCr) content was measured in a tandem assay. The buffer used contained 1 M Triethanolamine, 0.1 M Mg $(CH3COO)_2$ and 10 mM EDTA Na_2, pH 7.5. This was mixed with 10 mM DTT, 10 mM $NADP^+$, 40 mM ADP and 5 mM glucose. Two hundred and twenty-five µl of the mixture containing glucose-6-phosphate dehydrogenase (G6PDH) were added to a well of a 96 well plate together with 25 µl of muscle extract in PCA, blank or standard (ATP+PCr). The initial absorbance (A_{340}) was measured in a spectrophotometer, and then 2 µl hexokinase (HK) was added to determine the ATP content. In this reaction, hexokinase catalyses ATP hydrolysis by transferring the phosphate group to a glucose molecule obtaining Glucose-6-P and $NADP^+$. The content of NADPH absorbance by G6PDH was used to quantify the muscle ATP content.

$$\text{Glucose-6-P} + \text{NADP} \xrightarrow{\text{G6PDH}} \text{P-gluconolactone} + \text{NADPH}$$

$$\text{ATP} + \text{Glucose} \xrightarrow{\text{HK}} \text{ADP} + \text{Glucose-6-P}$$

The plate was shaken and incubated for 20 min and the NADPH A_{340} was determined. Then, 2 µl creatine kinase (CK) dissolved in 0.5% NaHCO3 + 0.05% BSA (15 mg/ml) were added to catalyse the phosphorylation of ADP transferring a phosphate group from PCr. The change in NADPH

absorbance (A_{340}) was used to determine muscle PCr content after 30 min of incubation.

$$PCr + ADP \xrightarrow{CK} Cr + ATP$$

2.9.3. Muscle free creatine assay determination

Muscle free creatine (Cr) content was measured with the buffer 320 mM Glycine containing 16 mM Mg $(CH3COO)_2$, pH 9.01, 30 mM KCl, 1.5 mM ATP, 1 mM Phosphoenolpyruvate (PEP), 1 mM NADH, pyruvate kinase (PK) and lactate dehydrogenase (LDH). Three hundred µl of the mix were added to each well of a 96-well plate together with 20 µl of muscle metabolite extract, blank or standard. The initial A_{340} was determined and then 10 µl CK were added (dissolved in 0.5% NaHCO3 + 0.05% BSA (15 mg/ml) to determine free Cr content. Any free Cr was phosphorylated to PCr and ADP which served as substrate for PK reaction obtaining pyruvate which was reduced to lactate by LDH. The NADH A_{340} from LDH reaction was determined after 30 min incubation.

$$Cr + ATP \xrightarrow{CK} PCr + ADP$$

2.9.4. Muscle lactate determination

Muscle lactate content was measured using a modified method from Harris *et al*., (1974). The buffer used contained 1 M Glycine, 0.5 M Hydrazine sulphate, 5 mM EDTA, pH 9.5, and 2.5 mM NAD^+. One hundred µl of the mix were added into each well of a 96-well plate together with 150 µl of the sample (25 µl muscle metabolites extract in PCA diluted in 125 µl water), blank or standard. The initial A_{340} was determined, and then 2 µl LDH was

added to determine the lactate content. Lactate was converted to pyruvate and NAD^+ to NADH. The absorbtion of NADH at A_{340} was mesured after 30 min incubation.

$$\text{Lactate} + NAD^+ \xrightarrow{\text{LDH}} \text{pyruvate} + NADH$$

2.9.5. Calculations

Concentration of ATP, PCr, creatine and lactate in muscle extraction was measured with the following formula:

$$\text{“Metabolite” mmol/kg dry muscle} = \frac{((V_1*(A_1-B_1)-V_0*(A_0-B_0))*EF}{6.22*SV}$$

Where:

V = Total volume (0- initial; 1- after adding the corresponded enzyme)

A = Absorbance sample (0- initial; 1- after adding the corresponded enzyme)

B = Absorbance blank (0- initial; 1- after adding the corresponded enzyme)

EF = extraction factor (ml/g)

6.22 = millimolar extinction coefficient for NADH at 340 nm

SV = Sample volume

2.9.6. Muscle glycogen

Muscle glycogen was measured in powdered tissue using the modified spectrophotometric method (Harris *et al*., 1974). The extraction of glycogen in powdered muscle (0.5-2 mg) was performed solubilising the muscle

powder in 100 µl 0.1 M NaOH by shaking and heating at 80^{o}C for 10 min. It was then hydrolysed into glycosyl units with neutralisation solution (0.1 M HCl, 0.2 M citrate buffer, pH 5 containing 0.2 M Na_2HPO_4). Then, 18 µl amyloglucosidase (AGDase) were added and incubated at room temperature for 1 h. The supernatant was collected after being centrifuged for 2 min at 14,000 rpm and stored at -80^{o}C until required. The extraction factor was calculated by the following formula:

$$EF = \frac{V_{NaOH} + V_{Buffer} + V_{AGDase}}{\text{Tissue (mg)}}$$

Free glucose was then determined using 250 µl of triethanolamine, pH 8.2 containing 0.75 mM ATP, 1 mM DTT and 1 mM NAD^+ buffer mix. Two hundred fifty µl of buffer mix were added into each well in a 96-well plate together with 25 µl of glucose extract, blank or standard. The initial A_{366} was determined and then 2 µl of a mixture 1:1 of Glucose 6 phosphate dehydrogenase (G6PDH) from *Leuconostoc mesenteroides* and Hexokinase (HK) from *Saccharomyces cerevisiae* was added. The glycogen-derived glucose phosphorylated to G6P and it was oxidised to 6-P-gluconolactone. The NADH A_{366} was determined after 30 min incubation.

$$\text{ATP + Glucose} \xrightarrow{\text{HK}} \text{ADP + Glucose-6-P}$$

$$\text{Glucose-6-P + } NAD^+ \xrightarrow{\text{G6PDH}} \text{6-P-gluconolactone + NADH}$$

Concentration of glycogen in muscle extraction was then calculated using the following formula:

$$\text{Glycogen mmol/kg dry muscle} = \frac{((V_1*(A_1-B_1)-V_0*(A_0-B_0))*EF}{3.4*SV}$$

Where:

V = Total volume (0- initial; 1- after adding the corresponded enzyme)

A = Absorbance sample (0- initial; 1- after adding the corresponded enzyme)

B = Absorbance blank (0- initial; 1- after adding the corresponded enzyme)

EF = extraction factor

3.4 = millimolar extinction coefficient for NADH at 366 nm

SV = Sample volume

2.10. Muscle alkaline-soluble protein:DNA ratio

Quantifying the protein content can give a better view of the accuracy of protein breakdown and consequent muscle mass reduction (Puthucheary *et al*. 2013). There are different methods that can determine the content of specific protein properties depending on interests. The determination of muscle alkaline-soluble protein normalised to DNA has been applied for protein content in muscle biopsies of critically ill patients with more sensitive results (Soop *et al*. 1989). They demonstrated that there is a reduction of skeletal muscle protein in the extracellular space and this occurs in the face of an increase in the cellular water volume. Thus, this method is more sensitive to muscle protein breakdown than the muscle weight.

2.10.1. Muscle extraction

Powdered muscle (approximately 3 mg) was used to extract the alkaline-soluble proteins and the DNA in the same assay as previously described

(Forsberg *et al*. 1991). Samples were shaken at 4ºC for 10 min with 500 µl of 0.2 M PCA in a glass tube and then centrifuged at 3,000 g for 15 min at 4ºC. The supernatant containing the soluble acid metabolites was discarded, and the pellet was washed twice with 500 µl 0.2 M PCA (spun at 3,000 g for 2 min at 4ºC). The muscle residue was dissolved in 1 ml 0.3 M KOH by incubating at 37ºC and shaking sporadically for 1 h. Two samples of 10 µl of the dissolved solution were taken into a new tube containing 90 µl Millipore water to quantify the alkaline-soluble protein extract. To the remaining solution, the RNA was extracted by incubating with 1.2 M PCA incubated at 4ºC for 30 min and discarded after spinning at 3,000 g for 15 min at 4ºC. The pellet obtained contained the DNA and was washed twice with 500 µl 0.2 M PCA. The DNA was then hydrolysed with 250 µl 1 M PCA by incubating at 70ºC for 1 h and centrifuged at 3,000 g at 4ºC for 10 min. Two hundred of the digest was placed into a new glass tube, containing the DNA extract, and stored at -20ºC.

2.10.2. Protein quantification

The content of alkaline soluble proteins (ASP) was quantified by the method of Lowry et al. (1951). All reagents used were freshly prepared. One ml of 0.1 M NaOH containing 2% Na_2CO_3, 1% Potassium tartrate (50:1) and 0.5% $CuSO_4$ pentahydrate was added to 100 µl of sample and standards and incubated at room temperature for 10 min. The standards for the standard curve were made with bovine serum albumin (BSA) diluted in 0.03 M KOH in a range of 0 to 20 µg concentration. After 10 min incubation, 100 µl of Folin Ciocalteu's Phenol Reagent (diluted 1:1 with Millipore water) was added and incubated at room temperature for 40 min. The aromatic amino

acids resulted from the pre-treated samples with the solution containing $CuSO_4$ reduced the acid present in the Folin Ciocalteu Phenol Reagent obtaining a blue end product that can be quantified. The absorbance of the product was measured in a spectrophotometer at 747 nm. A standard curve was generated by plotting the BSA concentration at absorbance 747 nm minus the absorbance of blank and the concentration of protein was calculated by the following formula:

$$\text{Protein µg/mg dry muscle} = \frac{(A_2-B_2)*\text{Dilution factor}}{(\text{Slope of curve}*\text{mg muscle})}$$

Where:

A_2 = Absorbance sample

B_2 = Absorbance blank

2.10.3. DNA quantification

To quantify the DNA content was performed using the modified method using diphenylamine (Burton 1956; Giles and Myers 1965). All reagents were freshly made on the day of the assay. To 200 µl sample, 50 µl 1.7 M PCA was first added obtaining 250 µl volume. Standards were made with calf thymus DNA in 1 M PCA in a range of 0 to 45 µg/ml. Two hundred fifty µl of 4% diphenylamine in glacial acetic acid containing 4% acetaldehyde (0.2%) were added to samples and standards and incubated at 30^{o}C for 18-24 h. The diphenylamine reacts with the deoxyribose sugar producing a blue-coloured complex which absorbance was red at 595 nm and 700 nm. A standard curve was generated by plotting the DNA concentration at the

subtraction of A_{595}–A_{700} and the concentration of DNA were calculated with the following formula:

$$\text{DNA } \mu g/mg \text{ dry muscle} = \frac{(A_{595}-A_{700})*\text{Dilution factor}}{(\text{Slope of curve}*\text{mg muscle})}$$

2.11. Gene expression quantification in muscle tissue

Quantitative PCR (qPCR), a method developed by Higuchi *et al*. (1993), is commonly used to quantify selected mRNA transcripts in a sample. Before that mRNA needs to be retro-transcript to the complementary DNA (cDNA), which will be quantified by a quantitative PCR technique.

2.11.1. Muscle total mRNA extraction

The first thing to do in order to quantify the gene expression is to extract the messenger ribonucleotide acid (mRNA). The mRNA is a complementary copy of a single strand of the DNA double helix.

Total mRNA was extracted from 20-30 mg of frozen wet muscle with TRIzol reagent solution (Ambion, UK). The wet muscle was homogenised with 1 ml of cold TRIzol containing 10 µg/µl glycogen solution by using a Polytron homogeniser for 40 s. The homogenate was transferred to a new tube and incubated at room temperature for 5 min. The mRNA was isolated with 200 µl of chloroform and shaking twice vigorously for 15 s. After incubating at room temperature for 10 min, the tubes were spun down at 12,000 g for 15 min at 4ºC. The water top phase containing the mRNA was transferred to a new tube, and 500 µl of iso-propanol were added. After 20 min of incubation at room temperature, the samples were spun down at 12,000 g for 15 min at 4ºC to precipitate the mRNA. The supernatant was discarded, and the

pellet with mRNA washed with 1 ml of 75% Ethanol. Samples were spun down at 8,000 g for 10 min at 4ºC, and the supernatant was discarded. The mRNA was then isolated and left for 5 min to dry out and dissolved in 50-30 µl of molecular RNase free water to store at -80ºC.

Subsequently, the quality and quantity of the total mRNA were measured by spectrophotometry at 260 nm with the RNA integrity number (RIN); purity is determined as the ratio of 260/280 nm readings >1.7 using NanoDrop One ™.

2.11.2. cDNA synthesis by reverse transcription PCR (RT-PCR)

The mRNA extracted was copied to cDNA in order to quantify the expression of targeted genes. It is the complementary DNA from a single mRNA strand. The conversion of mRNA to cDNA is achieved by using a reverse transcriptase that functions as a polymerase by the transcription of de nucleotides from one strand (mRNA) to the complementary nucleotide for the new strand (cDNA). Thus, there is a DNA-RNA hybrid helix which RNA is hydrolysed creating some gaps. The pieces of mRNA remaining in the helix are used as primers to start sequencing the second strand of DNA by the polymerase and get a double-strand of cDNA. The remaining RNA is degraded during subsequent cycles.

For the cDNA synthesis, 1 µg of total mRNA extracted would be copied to 1 µg of cDNA. The corresponding volume of sample to make up 1 µg in RNase free water, containing 2 µl of Random Primers (50 µg/ml; Promega, Madison, USA) and 1 µl of a nucleotide mix (dATP, dGTP, dCTP and dTTP diluted 1:10 each), were added into a new tube and incubated at 70ºC for 5

min on a thermocycler to denature secondary structures and allow the primers to anneal. The samples were cooled down at room temperature for a couple of minutes, and a master mix containing 4 µl of enzyme buffer, 1 µl DTT and 1 µl RNase inhibitor (Promega) together with 1 µl of the reverse transcriptase SuperScript III (Invitrogen) were added. They were placed to the thermocycler again at 25ºC for 5 min, followed by 1h at 50ºC for the reverse transcription reaction and 40 min at 70ºC to inactivate the transcriptase enzyme. The generated cDNA was stored at -20ºC.

2.11.3. Quantitative PCR (qPCR)

The process consists of denaturing the double strand cDNA into two single strands at high temperature before its exponential amplification. The primers of the genes selected bind to the single strand at 3' and the polymerase start complementing its sequence on each strand in a 5' to 3' direction, in a way that the end product is two amplicons. This reaction is repeated on each cycle resulting in exponential amplification.

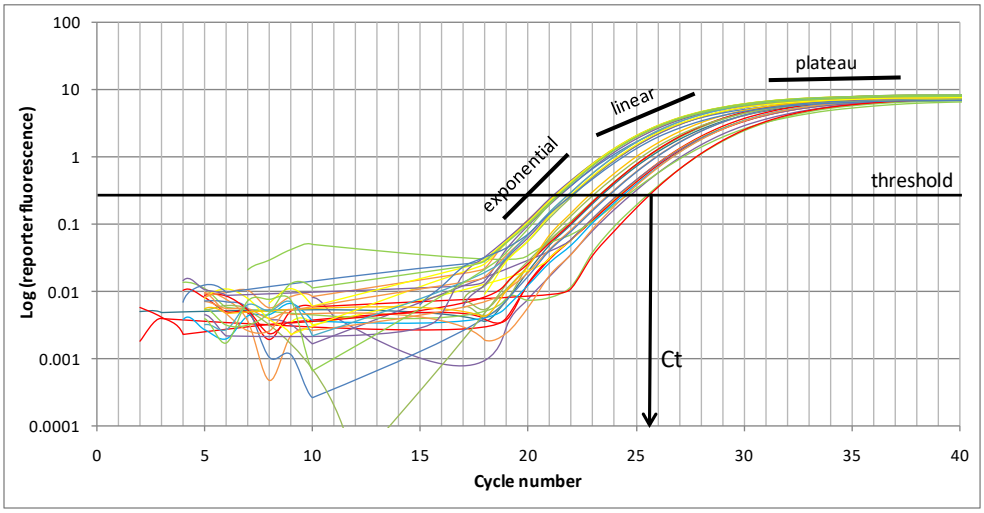


Figure 2.2: Typical real-time PCR plot showing the three main steps of the reaction; the exponential, linear and plateau phase. A threshold of fluorescence is set in the

exponential phase, and the cycle number at which reporter emission of the sample reaches this threshold is reported as the cycle threshold (Ct) value.

The quantification is measured by fluorescence released during the process. Briefly, the use of TaqMan® probes, which are short oligonucleotides with a fluorescent reporter dye and a corresponding quencher, bind to the target sequences. The DNA polymerase reaches the probe and hydrolyses it separating the reporter dye from the quencher dye, which emits fluorescence. The consecutive repetition (40 cycles) of this process per amplicon increases the fluorescence intensity by PCR technique exponentially, where the fluorescence detected is directly proportional to the cDNA quantity in the sample. There is a threshold value of fluorescence reached at specific cycle number in each sample, which is reported as cycle threshold (Ct) value generated by the Applied Biosystems 7900HT Fast-Real-Time PCR system, for the gene expression quantification. The Ct value of a housekeeping gene was used as internal control to normalise the concentration of each target gene. The relative expression can be determined by the following steps:

1. $\Delta Ct_{control} = \Delta Ct_{target\ gene} - \Delta Ct_{reference\ gene}$

   $\Delta Ct_{treated} = \Delta Ct_{target\ gene} - \Delta Ct_{reference\ gene}$
2. $\Delta\Delta Ct = \Delta Ct_{treated} - \Delta Ct_{control}$
3. Relative expression mRNA = $2^{-\Delta\Delta Ct}$

The housekeeping gene selected was hydroxymethylbilane synthase (HMBS), which has been shown in previous studies to be stable, i.e. not affected by the treatment.

There are different options to quantify the gene expression depending on the technique and the number of genes desired. In this project, the technique carried out was by TaqMan ® using probes for individual genes and microfluidic array cards for multiple genes.

2.11.3.1. Quantitative PCR (qPCR) by TaqMan®

To quantify the number of amplicons that are proportional to the gene expression from individual genes was used the TaqMan® technique with probes as previously described. It allows quantifying the expression of a gene in a determined sample at a real time. The relative levels of gene expression are determined from the fluorescence generated during the amplification by PCR method after 40 cycles.

The cDNA at a concentration of 1µg/20µl was diluted four times (1:4). The master mix was composed of 12.5 µl buffer, 1.25 µl probe and 9.25 µl RNase free water per each sample. Twenty-three µl of master mix was added to a 96 wells plate with 2 µl of diluted cDNA in each well.

2.11.3.2. Quantitative PCR (qPCR) by TaqMan® low-density array (TLDA)

To quantify the number of amplicons that are proportional to the gene expression from a large number of genes was used the TaqMan® low-density array (TLDA) technique. It allows quantifying in real time the expression of 48 genes altogether in one sample using the same technique as that described above. Each TLDA card is designed with 384 wells containing the primers of specific gene target in each well. Each sample is loaded in a row composed of two rows of 24 wells (48 wells for one gene

each). The relative levels of gene expression are determined from the fluorescence generated during the amplification by PCR method.

The cDNA obtained (1 µg/20 µl) was diluted to 250 ng with RNase free water to get a total of 50 µl of sample in a sterilised dark brown test tube containing 50 µl of TaqMan® Universal Master Mix II. The TLDA card stored at 4^{o}C was brought to room temperature previously for 15 min. One hundred µl of the mix was added to each channel in the TLDA card and centrifuged twice at 1,200 rpm for 1 min before being sealed. Then, the fluorescence was measured to generate the Ct value for each gene in each sample and calculated as previously described.

2.11.4. Ingenuity Pathway Analysis

Ingenuity Pathway Analysis (IPA) is a web-based commercial software application (Redwood City, CA, USA) that enables analysis, integration and understanding of data from gene expression as well as metabolomics, proteomics and RNA sequencing experiments amongst others. Data analysis and interpretation with IPA builds on the manually curated content of the Ingenuity Knowledge Base, identifying regulators, relationships, mechanisms, functions and pathways relevant to changes observed in the dataset analysed. IPA also generated novel networks of related genes and molecules based on the relationships present in the current literature. The log2 of the normalised fold change values were uploaded in IPA software.

2.12. Statistical analysis

Statistical analyses and graphs were performed using Prism v7 (GraphPad, San Diego CA). All data are presented as Mean ± S.E.M. Two-way ANOVA

was used for in vivo data. Parametric data were analysed by one-way ANOVA to compare 3 or more groups and t-student to compare two groups. Non-parametric data were analysed using Kruskal-Wallis to compare 3 or more groups and Mann-Whitney to compare two groups. A two-tailed P value of <0.05 was taken to indicate statistical significance.

Chapter 3:

Unaffected muscle mass and energy metabolism in the MNX model of knee OA

3.1. Introduction

OA is the most prevalent type of arthritis and is common in ageing (>50 years old) (Litwic et al. 2013) and obesity (Manek et al. 2003). Knee OA is caused by the degradation of collagen and proteoglycans in cartilage with joint inflammation and erosion of articular cartilage (Aurich et al. 2005). It is thought that it results from intrinsic alterations of the articular tissue, including pro-inflammatory cytokines (Kapoor et al. 2010), or as a response to mechanical stress such as extreme sporting activity (Fernandes et al. 2017). The degradation of cartilage triggers the formation of bone (osteophytes) and therefore the wear and tear of the joint with pain and inflammation as main symptomatic effects (Thorstensson et al. 2009). The destabilisation of the joint causing pain and inflammation can be a major deterrent and contributor to physical disability and sedentary behaviour in patients with OA (Dekker et al. 1993), which can contribute to further negative health effects (Fink et al. 2007). Patients with knee OA have increased levels of inflammatory and atrophy markers in muscle (vastus lateralis), such as MCP-1 protein, TNFα and atrogin-1 mRNAs, which are negatively correlated with muscle strength (Levinger, Levinger, et al. 2011). Therefore, muscle inflammation may also impact on muscle strength in OA through several indirect putative pathways, which is worthy of further investigation and may be relevant to the treatment of OA.

Muscle inflammation leads to skeletal muscle atrophy and dysregulated intermediate metabolism (Crossland et al. 2008; Constantin et al. 2011). The mechanisms underlying these events include reduced phosphorylation of PI3K/Akt1 signalling pathway, which blunts translation initiation of muscle

protein synthesis (Schiaffino and Mammucari 2011) and muscle FOXO1/3 phosphorylation (Stitt et al. 2004). Reduced FOXO1/3 phosphorylation increase FOXO transcriptional activity increasing mRNA expression of several downstream targets regulating muscle protein breakdown and carbohydrate oxidation (Crossland et al. 2008).

I hypothesised here that OA associated inflammation might alter muscle mass and metabolic fuel regulation, thereby reducing muscle integrity. In this study, the surgical model of OA was used involving transection of the medial meniscus (MNX) in the knee joint of the rat. This model causes the destabilisation of the knee, and is associated with cartilage damage, synovial inflammation and pain behaviour (Mapp et al. 2013a; Janusz et al. 2002). I investigated the extent to which robust markers of muscle atrophy and energy metabolism were altered in the MNX model and how these changes related to the time-course of progression of systemic inflammation, joint pathology, pain behaviour and physical activity levels.

3.2. Methods

Experiments were carried out following the methodology described in Chapter 2, where more details can be found.

3.2.1. Experimental design

Male Sprague Dawley rats (weighing 160-190 g, n=60) were used. Rats were randomly allocated to either MNX group, a sham group or a naïve control group (n=20 each group). Experiments were terminated in pre-determined time-points: 10 rats per group at day 28 post-surgery and 10 rats per group at day 55 post-surgery. Pain behaviour was measured at baseline (B) before intervention and then weekly on days 7, 14, 21, 28, 35, 42, 49 and 55 after surgery (Figure 3.1). Locomotor activity was measured at baseline the night before surgery and then weekly the evening before pain behaviour testing on days 6, 13, 20, 27, 34, 41, 48 and 54 after surgery (Figure 3.1). Venous blood (0.5 ml) was collected from the tail vain without anaesthesia before treatment and then 28 and 55 days after treatment when the study was terminated. The EDL muscle and knee joint were harvested from both limbs under terminal anaesthesia at day 28 and 55 (see section 3.2.7).

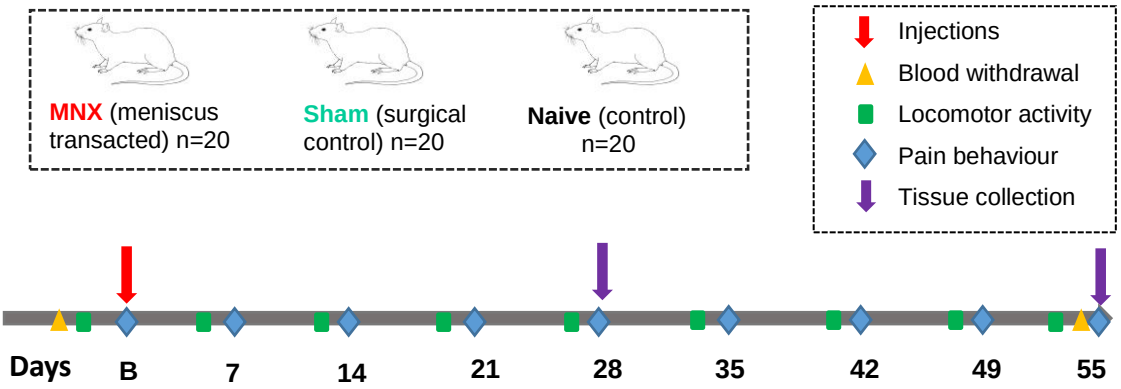


Figure 3.1: Experimental design scheme for *in vivo* study of the meniscus transacted model of osteoarthritis. The experimental design involved two time-points for tissue collection: 28 days n=10 each group and 55 days n=10 each group.

3.2.2. MNX model of osteoarthritis

The rodent model of OA was generated by surgical transection of the medial meniscus (Janusz et al. 2002). Rats were anaesthetised with isoflurane (3%) and oxygen (1 L/min). The left leg (ipsilateral) was shaved and surgically prepared, maintaining body core temperature with a heating matt underneath. The MCL was exposed by an incision on the skin and cauterising connective tissue and small vessel. A section of MCL was removed to expose the meniscus, which was cut through its full thickness at the narrowest point. The connective tissue layer and skin were closed with coated Vicryl 8.0 and 4.0 sutures, respectively. No post-operative analgesic drug was administered as pain behaviour was an outcome measure of the experiment. Sham-operated rats underwent an identical procedure with the exception that meniscus was not transected. Naïve rats underwent under general anaesthesia; the left leg was surgically prepared

and then allowed to recover. Rats were housed in groups of n=4 and n=3 per cage.

3.2.3. Pain behaviour

The weight-bearing asymmetry between limbs was tested using an Incapacitance Meter (Linton Instruments, Norfolk, UK). Rats were placed in an angled Perspex box and were allowed to habituate. The weight distribution between the hind paws placed in the corresponding transducer pad was recorded during 3 s. The average of 3 consecutive readings was taken and expressed as the difference in percentage following the equation: [(contralateral – ipsilateral) / (contralateral + ipsilateral)] x100.

Hind paw withdrawal thresholds were quantified in both limbs using calibrated Von Frey monofilaments (bending forces from 2-26 g in a logarithmic scale). Rats were habituated to pain assessment for two days before the model induction. The PWT measurements were performed as previously described in section 2.4.2.

3.2.4. Locomotor activity

Both vertical and horizontal movements were measured using locomotor activity boxes using an established method (Watson et al. 2012). Rats were placed in individual automated infrared activity boxes as previously described in section 2.5. The beam-breaks were counted in intervals of 5 min time epochs for 1 h under the red light the night before of PWT testing.

3.2.5. Plasma cytokines concentration

Tail vein blood (0.5 ml) was collected at the end of the experiment, and plasma was isolated from whole blood as previously described in section 2.1.5. The anti-inflammatory cytokine IL-10 and pro-inflammatory cytokines IL-6 and TNFα were quantified by ELISA (Quantikine ® ELISA, R&D systems) following the manufacturer's instructions as previously described in section 2.11.

3.2.6. Knee joint histopathology

The knee joints were harvested from both hind limbs in all rats at the end of the study to perform histopathology examination. The joints were processed as described in section 2.6.3 and the histology of tibiofemoral joints was performed with H&E staining. Frontal coronal sections (5 µm) were used for microscopic evaluation of the medial tibia plateau. The scoring system for chondropathy, osteophytosis and synovitis were following the described method in section 2.7.2. The data presented represent values from the ipsilateral limb.

3.2.7. Muscle analysis

The EDL muscle from both hindlimbs was harvested under terminal anaesthesia by intraperitoneal injection of pentobarbital and snap-frozen as described in section 2.6.1. Samples were stored at -80^{o}C until analysis was performed. Data presented represent values from the ipsilateral limb.

3.2.7.1. Muscle metabolites

A portion of EDL muscle was freeze-dried and powdered. Two aliquots of the powder were used to extract and measure muscle metabolites (ATP, PCr, creatine, and lactate; 5-10 mg) and muscle glycogen (0.5-2 mg) content, which was quantified using enzymatic spectrophotometry as previously described in section 2.8. PCr and creatine were normalised to the highest total creatine content (PCr+Cr) between left and right limbs following the formula:

$$(PCr_{left} / Total\ Cr_{left}) * Total\ Cr_{from\ limb\ with\ higher\ content}$$

3.2.7.2. Protein and DNA quantification

A portion of freeze-dried and powdered EDL muscle (~3 mg) was used to quantify total alkaline-soluble muscle protein and DNA contents in rats 55 days post-surgery as described in section 2.9. The protein : DNA ratio is a reliable marker of muscle mass (Forsberg et al. 1991; Crossland et al. 2010).

3.2.8. Statistical analysis

All data are presented as mean ± SEM and were analysed by Prism V.7 (GraphPad, San Diego, California, USA). The statistical analysis of differences amongst groups for PWT and locomotor activity was performed using two-way ANOVA with Bonferroni corrections. One-way ANOVA was used to compare plasma cytokines IL-10, IL-6 and TNFα, muscle intermediary metabolites (ATP, PCr, total Cr) glycogen and the muscle protein : DNA ratio. Kruskal-Wallis test was used to compare muscle lactate, cartilage damage, osteophytosis and synovitis due to the non-normal

distribution of data. Mean values were considered statistically different when $p<0.05$.

3.3. Results

The total n for weight-bearing, PWT and locomotor activity was n=20 per group (MNX, sham, naïve) from baseline to day 28 and n=10 per group from day 29 to day 55 after model induction. Two rats were excluded from analysis (1 MNX and 1 naïve) due to incomplete datasets (Table 3.1).

Table 3.1: Description of group size over the time-course of the weight-bearing test.

Treatment	Baseline-28 days	29-55 days	Excluded
Naïve	19	9	1
Sham	20	10	0
MNX	19	9	1

3.3.1. Pain behaviour in MNX model of OA

Weight-bearing was tested once a week following MNX, sham surgery or naïve. The MNX group had greater weight-bearing asymmetry throughout the study with significant differences compared to naïve rats on days 14, 28, 42 and 49 post-surgery and on day 14 compared to the sham group. The sham and naïve groups showed different profiles of weight-bearing asymmetry although there were no significant difference between the groups (Figure 3.2A).

PWT was tested once a week showed that the MNX group had significantly lower PWTs on day 21, 28, 35, 42 and 55 after OA induction compared to the naïve group and on day 55 compared to the sham group (Figure 3.2B).

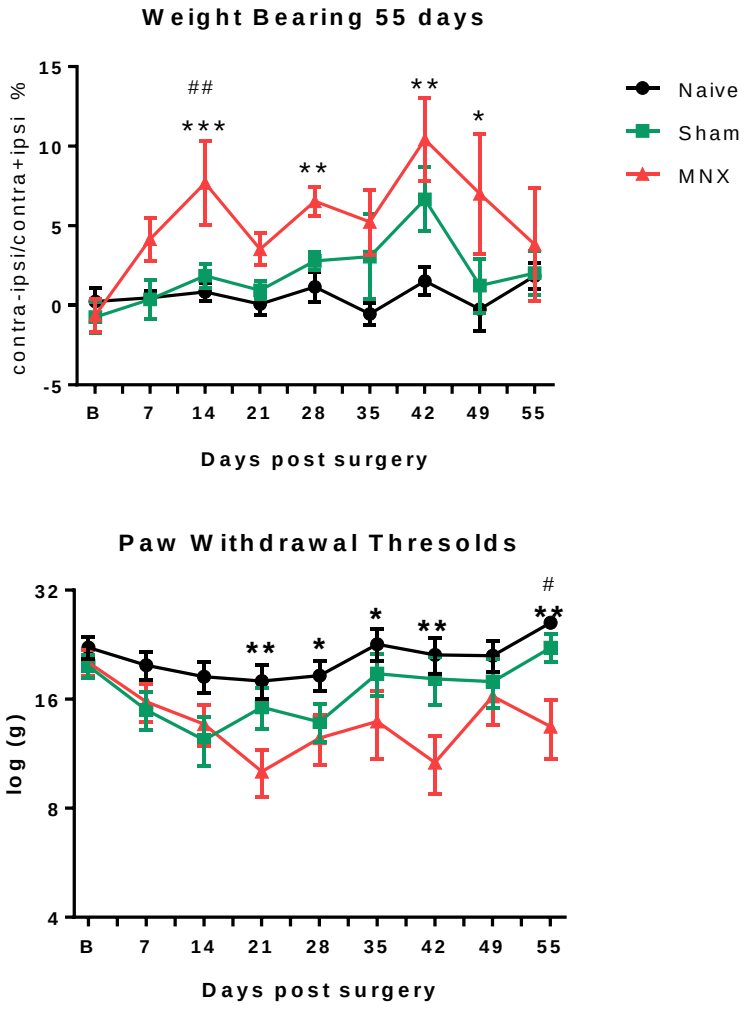


Figure 3.2: Weight-bearing (A) and paw withdrawal thresholds (B) in MNX, sham and naïve rats. Group sizes for weight-bearing are in table 3.1 and for PWT are n=20 each group on days B-28 and n=10 each group from days 29-55 after surgery. Results are mean ± SEM. Statistically analysed by two-way ANOVA with Bonferroni correction: naïve vs MNX: *p<0.05, **p<0.01, ***p<0.001; sham vs MNX: #p<0.05, ##p<0.01.

3.3.2. Locomotor activity in MNX rats

Horizontal locomotor activity was constant amongst the three groups MNX, sham and naïve over time (Figure 3.3A). On the other hand, vertical activity was more variable over the time-course of the study and levels were consistently lower in the sham and MNX rats compared to the naïve

(unoperated controls) (Figure 3.3B). On day 20, all rats showed an increase in vertical activity which may represent an environmental change altering this behaviour per se. At this time-point, there was a significant difference in vertical activity between the naïve and sham groups and the MNX rats (Figure 3.3B).

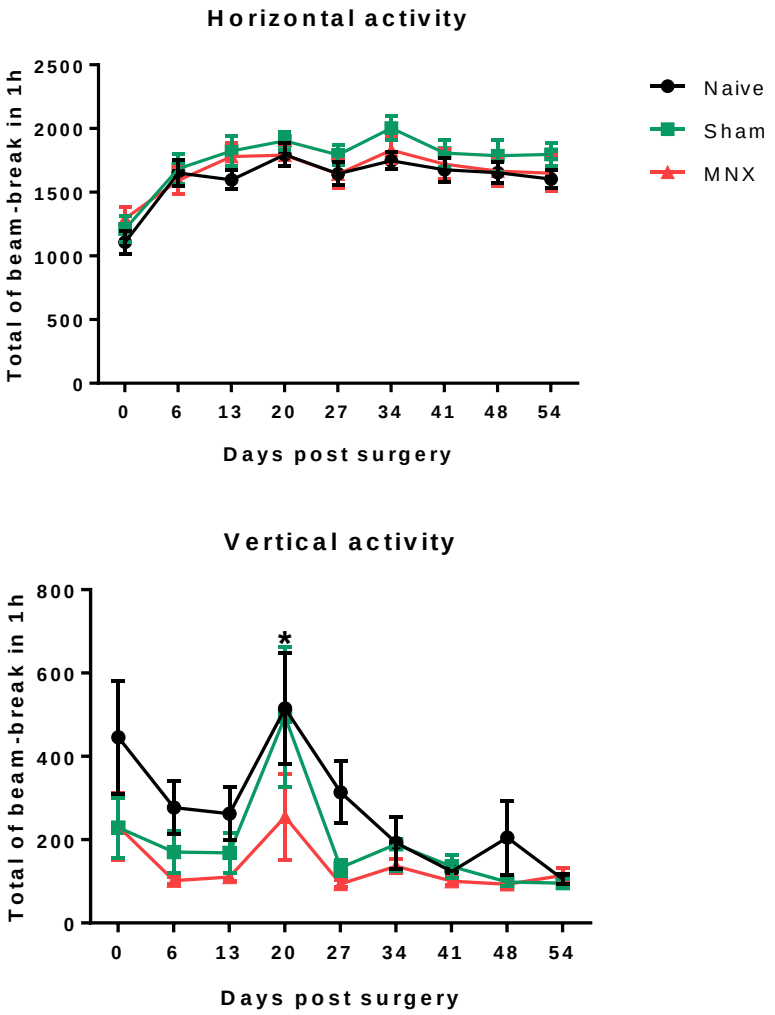


Figure 3.3: Locomotor activity during the dark cycle in MNX, sham and naïve rats. Group sizes: n=20 each group from baseline to 28 days and n=10 each group from 29-55 days after surgery. Results are mean ± SEM representing the total number of movements (beam-break) for 1 h in the dark cycle (night). Statistically analysed by two-way ANOVA with Bonferroni correction: naïve vs MNX *p<0.05; sham vs MNX #p<0.05.

3.3.3. Plasma inflammatory cytokine concentrations and EDL mRNA expression

Plasma concentrations of the anti-inflammatory cytokine IL-10 and pro-inflammatory cytokines IL-6 and TNFα were not different between MNX, sham and naïve rats at baseline or 55 days (Figure 3.4). Group sizes differed amongst groups and assays due to the limited volume of plasma (Table 3.2). The mRNA expression of cytokines in muscle was undetected (data not are shown).

Table 3.2: Description of group size for cytokine measurement for each group.

0 days (B)	Naïve	Sham	MNX
IL-10	9	9	9
IL-6	9	7	9
TNFα	8	8	9

55 days	Naïve	Sham	MNX
IL-10	9	9	10
IL-6	9	8	9
TNFa	8	9	9

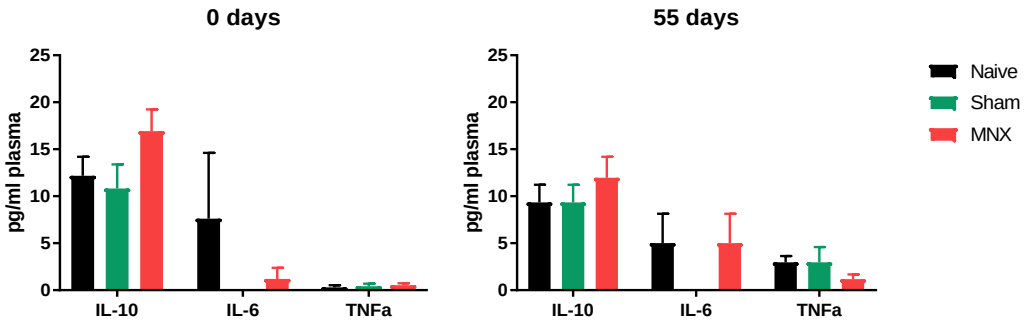


Figure 3.4: Plasma concentrations of IL-10, IL-6 and TNFα in MNX, sham and naïve rats. Plasma concentrations of cytokines at baseline (0 days) on figure A and 55 days after surgery on figure B. Group size represented in table 3.2. Results are mean ± SEM. Statistically analysed by one-way ANOVA.

3.3.4. Histopathology of tibiofemoral joint and scoring

The H&E staining of the tibiofemoral joint (knee) was performed at days 28 and 55 to score cartilage damage, osteophytes and synovitis in the medial tibia plateau. Due to the presence of damaged sections, the total scores for the naïve group was 10 (n=10) on day 28 and 8 (n=8) on day 55 after surgery, whereas sham and MNX groups were n=10 at both time-points.

Cartilage damage (chondropathy) was significant in MNX rats at both 28 and 55 days compared to naïve and sham groups (Figure 3.5A). Osteophyte formation (osteophytosis) was greater in MNX rats compared to naïve and sham groups (Figure 3.5B). On the other hand, synovitis was significantly higher in MNX rats than the naïve group at both 28 and 55 days, and higher than the sham group at day 28.

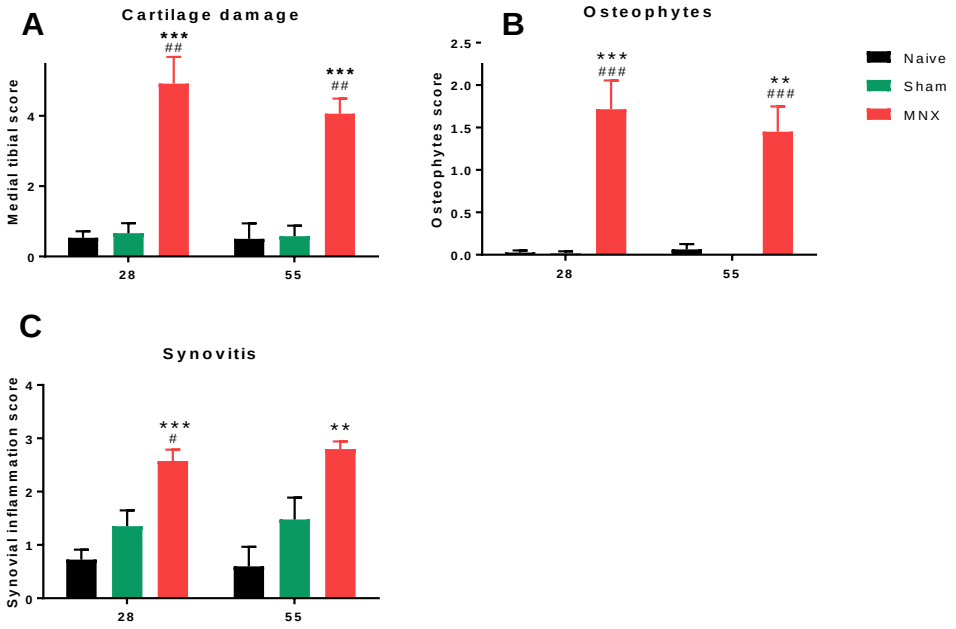


Figure 3.5: Scoring of cartilage damage (A), ostoephytosis (B) and synovitis (C) of the tibiofemoral joint at the end of the study. Group sizes were MNX (n=10) sham (n=10) at both 28 and 55 days and naïve (n=10) at day 28 and (n=8) at day 55 after surgery. Results are mean ± SEM. Statistically analysed using non-parametric Kruskal-Wallis test. naïve vs MNX: **p<0.01, ***p<0.001. sham vs MNX: #p<0.05, ##p<0.01, ###p<0.001.

On day 28 after surgery, the presence of osteophytosis and synovitis were separately correlated with weight bearing asymmetry. On day 55, cartilage damage and osteophyte score were correlated with paw withdrawal thresholds. Horizontal and vertical locomotor activity was not correlated to the knee pathology at any time-point measured (Table 3.2).

Table 3.3: Correlation of knee joint pathology to pain behaviour and activity tests. In bold, significant correlations by non-parametric Spearman test: *p<0.05, **p<0.01, ***p<0.001.

	28 days			**55 days**		
Variable	Cartilage	Osteophytes	Synovitis	Cartilage	Osteophytes	Synovitis
Weight bearing asymmetry	0.358	**0.537****	**0.392***	0.157	0.182	0.1632
Paw withdrawal thresholds	0.028	0.050	-0.290	**-0.590*****	**-0.502****	$-0.351^{0.07}$
Horizontal activity	-0.068	-0.192	0.082	-0.102	-0.187	0.172
Vertical activity	-0.272	-0.318	-0.253	0.018	-0.019	0.063

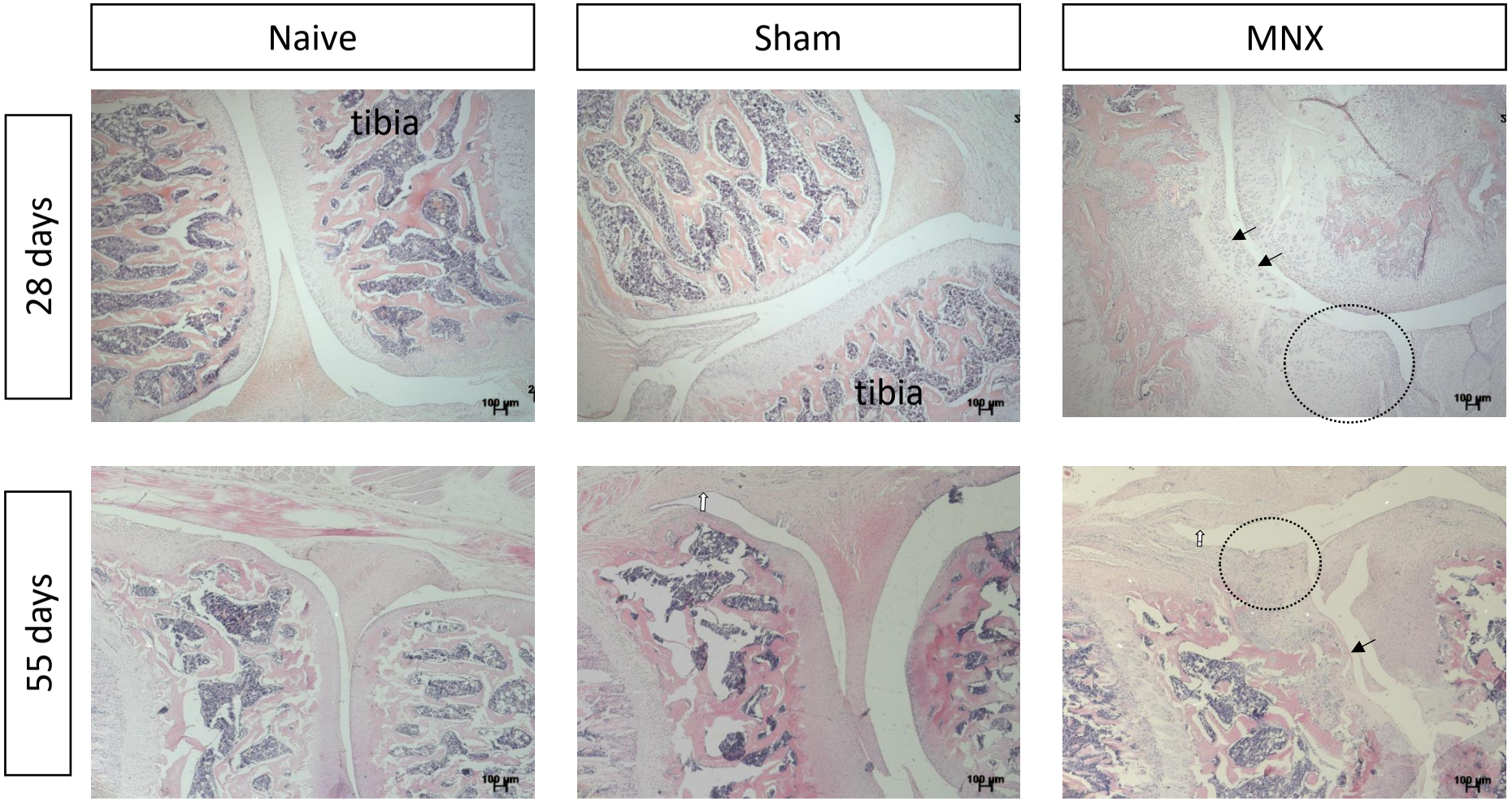


Figure 3.6: Histology of the medial tibiofemoral joint at days 28 and 55 after surgery. There was an increase in the cartilage degradation and osteophytes formation together with synovitis in the tibiofemoral joint of rats with meniscus transacted (MNX) (n=10) compared to the control Sham and naïve (n=10 each) groups (except naïve n=8 on day 55). Black arrows show cartilage damage, white arrows show synovium and ovals show osteophytes.

3.3.5. Muscle metabolites

Muscle metabolites were measured in the EDL muscle at 28 and 55 days post-surgery (Figure 3.7). Muscle ATP, PCr and total creatine content in the MNX group were not different from sham or naïve groups at either time-point (Figure 3.7 A and B). Values were comparable to those reported for resting rat EDL muscle (Alamdari et al. 2008), demonstrating good muscle tissue viability in this model. Additionally, muscle glycogen and lactate content in the EDL was comparable in MNX, sham and naive groups when comparing day 28 and day 55 time-points (Figure 3.7 A, B, C, D).

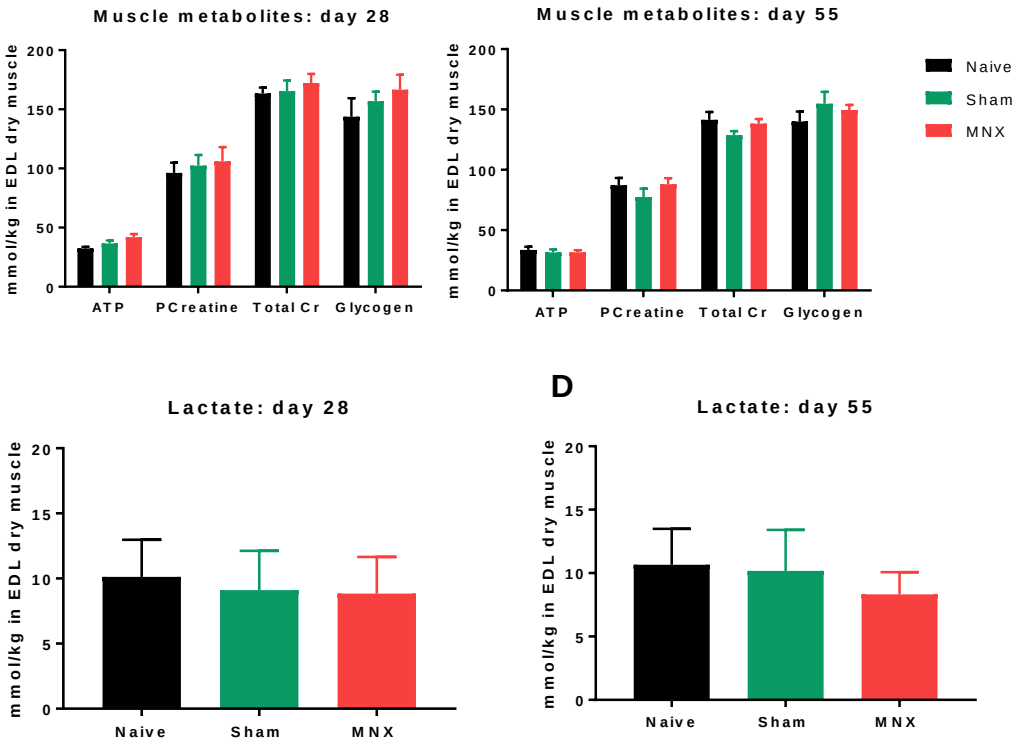


Figure 3.7: Muscle metabolites in the EDL muscle from MNX, sham and naive rats (n=10 each group). Results are presented as mean ± SEM in EDL dry muscle at day 28 and 55 after surgery. There were no differences between time-points within each group, or between groups at each time-point. Statistically analysed with parametric one-way ANOVA (ATP, PCr, Total Cr and glycogen) and non-parametric Kruskal-Wallis (lactate).

3.3.6. Muscle alkaline-soluble protein to DNA ratio

The content of alkaline-soluble protein in the EDL from the MNX, sham and naïve groups were similar. Hence, the protein : DNA ratios in the EDL muscle did not differ between groups at day 55 (Figure 3.8).

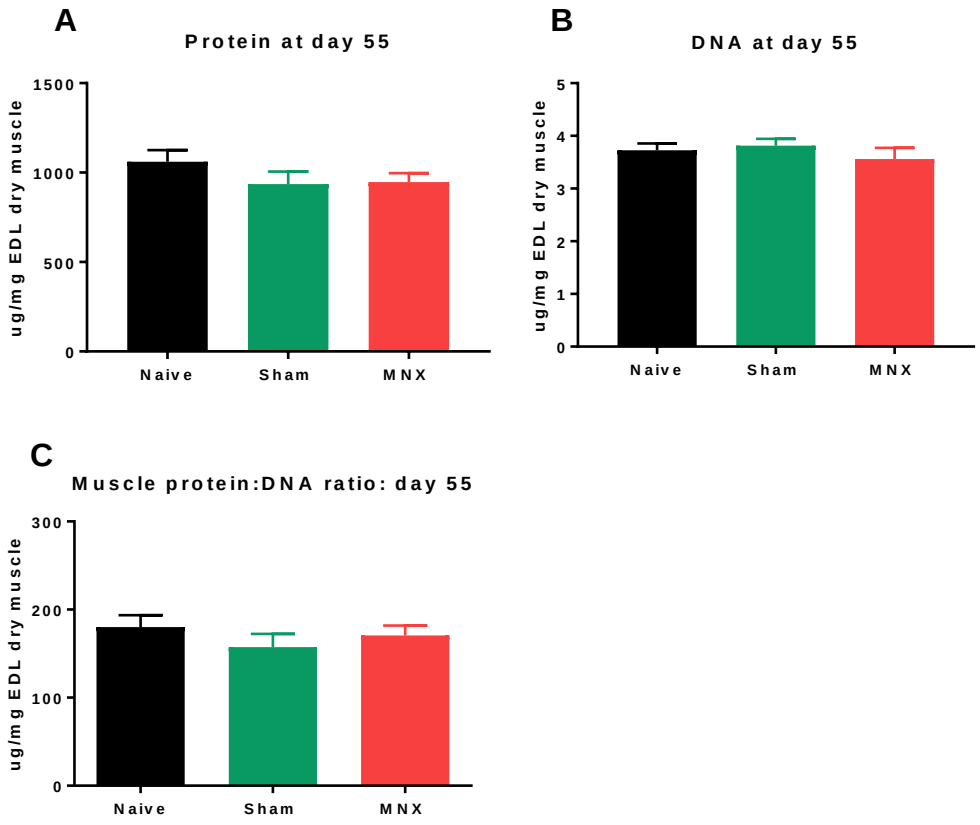


Figure 3.8: Alkaline-soluble protein to DNA ratio in EDL muscle of MNX, sham and naïve rats (n=10 each group) at 55 days after surgery. Results are mean ± SEM. Statistically analysed with parametric one-way ANOVA test.

3.4. Discussion

In this chapter, the progression of systemic inflammation, joint pathology, pain behaviour and physical activity levels were quantified in a surgical model of OA. Furthermore, whether changes observed were associated with changes in markers of muscle energy metabolism and atrophy in EDL muscle was investigated. Following MNX model induction, pain behaviour varied over the 55 days after surgery, with greatest changes in pain behaviour being observed on day 42 after model induction (Figure 3.2). The model was not associated with marked changes in locomotor activity, which remained fairly stable (Figure 3.3). The model exhibited significant pathology, including chondropathy, osteophytosis and synovitis (Figure 3.5). However, there were no significant changes in EDL muscle metabolite concentrations (Figure 3.6) and no evidence of muscle mass loss and inflammation (Figure 3.7) in this model of knee OA.

The rat MNX model has been extensively used to study the development and progression of knee pain in OA. For example, it has been reported that rats perceived discomfort which was accompanied by weight-bearing asymmetry from day 28 after induction with greater pain on day 49 (Mapp et al. 2013a). In the present study, it was found that MNX rats showed weight-bearing asymmetry earlier, from day 14 with a peak on day 42 post-surgery compared to sham and naïve groups which decreased on day 55 (Figure 3.2A). On the other hand, paw withdrawal thresholds were significantly lower in MNX than in the control groups from day 21 post-surgery until the end of the study (Figure 3.2B). Knee joint damage in MNX rats is likely to cause changes in pain behaviour as reflected by the clear

pathology evident in the subchondral bone, synovium and joint capsule. This contention is supported by the finding of a significant correlation between paw withdrawal thresholds and magnitude of chondropathy and ostoephytosis on day 55 as well as between weight-bearing and the magnitude of osteophytosis and synovitis on day 28 after surgery (Table 3.2). Nevertheless, non-correlated pain behaviour with structural pathology in a different model of OA induced by monosodium iodoacetate injection (MIA) was found (Nwosu et al. 2016), which may indicate that MNX is a more suitable model to study pain an pathology aspects of the disease.

Locomotor activity was assessed to quantify total movement over 1 h during the dark cycle. Given that pain may alter activity behaviour due to discomfort and that patients with OA show low physical activity or sedentary behaviour, it was hypothesised that low activity might alter muscle function. Both vertical and horizontal activity was similar amongst groups over the time-course of the study (Figure 3.3). A naïve group was tested due to the discomfort that the invasive surgery may cause in sham rats, whose MCL is removed. Naïve rats tended to rear more compared to sham and MNX at the majority of time-points, including baseline, which suggests that MNX surgery and OA progression may not have impaired daily activity levels. This novel finding is at odds with the reduced physical activity levels reported in patients with knee OA (Dekker et al. 1993). Pain and discomfort is a major stimulus to sedentary behaviour and physical disability, which may promote skeletal muscle deconditioning and atrophy (Dekker et al. 1993). Hence, the natural exploratory instinct from rats under moderate to mild conditions may have influenced the fact that MNX model does not

mimic the symptoms of low activity identified in patients with knee OA. It was reported instead, that the vertical activity in an OA model with anterior crucial ligament transection and partial medial meniscectomy (ACLT + pMMX), was significantly lower than in control after 8 weeks of surgery accompanied with weight-bearing asymmetry (Hamilton et al. 2015) whilst it was no different in the ACLT model without menisectomy (Silva et al. 2018). Therefore, different animal models may differ on severity, disease progression and results.

The molecular events underlying muscle atrophy in OA are still unresolved, and could be direct (e.g. inflammation) and/or indirect (e.g. reduced habitual physical activity). Patients with knee OA and quadriceps strength deficits, present with overexpression of muscle FOXO1 protein (Levinger et al. 2016). As mentioned in Chapter 1, FOXO1, which is regulated by the PI3K/Akt signalling pathway, is involved in the control of muscle protein turnover (Stitt et al. 2004). Thus, the activation (dephosphorylation) of FOXO1 protein triggers the transcription of genes involved in protein breakdown, such as atrogin-1 and MuRF1, which are accepted markers of muscle atrophy (Gomes et al. 2001). In animal models of OA, it has been difficult to demonstrate that muscle wasting occurs by the activation of FOXO and downstream atrogenes. For example, in the destabilisation of medial meniscus (DMM) model of post-traumatic OA, despite the loss of muscle function of tibialis anterior with specific force alteration and increased relaxation rate compared to sham mice after 8 weeks of surgery, there was no evidence of upregulation of muscle atrophy markers (atrogin-1 mRNA) or muscle histology (van der Poel et al. 2016).

Moreover, in the rat ACLT model of OA, expression of the atrophy markers MuRF1 and MyoD mRNA in gastrocnemius was not different from sham group (Silva et al. 2018). However, Silva *et al.* did show increased myostatin and decreased myogenin mRNA in the gastrocnemius of ACLT rats suggesting an impairment in the regeneration process after 12 weeks of disease (Silva et al. 2018). It is important to consider that disease progression is different between animal models. DMM mice with loss of muscle specific force developed mild-moderate cartilage damage after 4 weeks of surgery at which time-point synovitis improved (van der Poel et al. 2016). The ACLT + pMMx model exhibits pain behaviour and reduced vertical activity, and cartilage damage and osteophytosis on weeks 4 and 8 post-surgery (Hamilton et al. 2015). However, the ACLT model in rat which does not have altered MuRF1 and MyoD, but myostatin, showed cartilage degradation and synovial hyperplasia 12 weeks after surgery (Silva et al. 2018). In my study, MNX developed cartilage damage, osteophytosis and synovitis at both 28 and 55 days post-surgery (approximately 4 and 7 weeks) (Figure 3.5). Hence, the different animal models take varying amounts of time to develop OA pathology. Since no inflammatory markers were studied and identified in the previous studies, it is difficult to predict inflammatory-induced muscle changes in animal models, which may be due to pain induced lowering of physical activity. Accordingly, the protein:DNA ratio was not altered in MNX group compared to sham and naïve rats at the later point (55 days after surgery) (Figure 3.8), used as a marker of muscle mass loss in other models of inflammation and muscle atrophy (Crossland et al. 2008; Mallinson et al. 2015). Moreover, the inflammatory models with

muscle atrophy mentioned were associated with lactate accumulation. Inflammation dysregulates phosphorylation of PI3K-Akt signalling, activating FOXO1 which upregulates muscle atrogenes and PDK4 expression. Collectively this impairs PDC flux and carbohydrate oxidation, which is reflected with muscle lactate accumulation and greater glycogen degradation. In this study, I also sought to identify lactate accumulation due to inefficient use of muscle carbohydrate in the fast-twitch EDL from the MNX model of OA. In the MNX model, EDL muscle was dissected after 28 and 55 days of surgery with no differences in lactate and glycogen content from sham and naïve rats (Figure 3.7) contrary to catabolic states such as sepsis (Alamdari et al. 2008).

Since inflammation is a major driver of muscle atrophy and dysregulation of carbohydrate use, we quantified plasma cytokines and the mRNA expression of cytokines IL-10, IL-6 and TNFα in EDL muscle of MNX model. The expression levels of mRNA of inflammatory cytokines were too low to be detected in muscle (data not shown), and protein levels of cytokines in plasma were not different to control groups (Figure 3.4). Thus, these data demonstrate that the MNX model of OA does not result in systemic or muscle inflammation, and therefore one might not expect to see evidence of inflammation induced dysregulation of fuel and protein metabolism in EDL muscle, unlike more severe inflammatory conditions such as sepsis where marked increases in expression of IL-6 and TNFα in EDL was paralleled by muscle atrophy and dysregulated metabolism (Crossland et al. 2008). Our findings are consistent with recent reports of no changes in IL-6 in plasma and tibialis anterior muscle in the DMM model of OA pain,

and no differences in TNFα mRNA expression in gastrocnemius of ACTL of knee OA (van der Poel et al. 2016; Silva et al. 2018). In contrast, in patients with knee OA compared to healthy individuals serum IL-6 and TNF receptors 1 and 2 was associated with pain, disability and walking speed (Penninx et al. 2004). Muscle IL-6 protein and muscle MCP-1 and TNFα mRNAs are elevated and associate with reduced muscle strength, (Levinger, Levinger, et al. 2011) and muscle protein MCP-1 was positively correlated with stiffness, pain and physical function (Levinger, Caldow, et al. 2011).

The divergences of results across patients and animal models show the complexity of finding an adequate animal model for research and highlight the need to optimise the conditions to take benefit for a specific hypothesis. Patients with knee OA are usually diagnosed in a mid-late and chronic stage and is difficult to predict the time it started to develop in adults and elderly. Instead, research in animal models of OA is mostly done in early and acute stages in young-adult animals. It seems that systemic and muscle inflammation is evident in patients with knee OA, however, the MNX model of OA together with other animal models did not induce systemic and inflammatory muscle response as well as impaired locomotor activity, which may explain the differences with patients.

In conclusion, the MNX model resulted in the development of pain and knee OA with synovitis, but there was no evidence of systemic and muscle inflammation or reduced locomotor activity compared to control. As might be expected therefore, these responses were accompanied by no evidence

of muscle metabolic dysregulation or atrophy, despite this clear joint pathology.

Chapter 4:

Dysregulation of indices for muscle metabolism and wasting in a rat model and patients with rheumatoid arthritis

4.1. Introduction

RA is an autoimmune disease that causes joint inflammation and articular degradation following infiltration of inflammatory cells (See references in Ledingham, Snowden, and Ide 2017). The main regulators of the immune response are secreted inflammatory cytokines IL-1β, IL-6 and TNFα amongst other signals produced by macrophages to combat the autoimmune response against an external stimulus (see in Chapter 1). One consequence of this response is that the inflammatory response is associated with pain, which can be a major deterrent and contributor to a reduction in habitual physical activity levels and increased sedentary behaviour in patients with RA. This behaviour coupled with tissue inflammation is likely to a negative effect on muscle mass and insulin sensitivity (Fenton and Kitas 2016).

However, the extent to which muscle disuse and inflammation contribute to muscle dysfunction in RA is unclear. Severe inflammatory states (such as sepsis and COPD exacerbation) lead to a disruption of intermediary muscle metabolism and the molecular regulation of muscle mass and carbohydrate oxidation, leading to muscle atrophy and dysregulated fuel metabolism (Crossland et al. 2008; Constantin et al. 2011). The mechanisms underlying these events include suppression of PI3K/Akt1 signalling protein phosphorylation, which inhibits protein synthesis (Schiaffino and Mammucari 2011) and increases activation (dephosphorylation) of the FOXO family of transcription factors (Stitt et al. 2004). It is believed that PI3K signalling may be modulated by IRS-1, which is an important substrate for insulin receptor activation (Rui et al. 2001). In short, it is suggested that

inflammatory cytokines (such as IL-6, TNFα) may disrupt IRS-1 and its signalling cascade (Hotamisligil et al. 1996; Jian et al. 2014), triggering the activation of FOXO and downstream FOXO targets, such as PDK4, MAFbx and MuRF1, which are central to the regulation muscle carbohydrate oxidation and protein breakdown in skeletal muscle (Bodine et al. 2001a; Kwon et al. 2004). Muscle PDK4 inhibits PDC activity, reducing mitochondrial pyruvate flux leading to muscle lactate accumulation, as seen in a variety of inflammatory states, such as endotoxaemia (Alamdari et al. 2008), and in dietary-induced muscle insulin resistance (Furuyama et al. 2003; Constantin-Teodosiu 2013). The E3 ubiquitin ligases MAFbx, and MuRF, and cathepsin-L are key mediators of muscle protein catabolism via the ubiquitin-proteasome and lysosomal proteolytic pathways, respectively (Sandri et al. 2004; Deval et al. 2001).

In this study, I hypothesised that compared to control animals, inflammation in the CIA rat model of RA may contribute to the development of pain and reduced locomotor activity and that this would be associated with the dysregulation of muscle metabolism and muscle mass loss. The CIA model has been extensively used to study different aspects of arthritis, especially pain and joint pathology (Kuniaki Terato et al. 1982; Bendele et al. 1999), and it has been proven to be an adequate model to study rheumatoid cachexia (Alabarse et al. 2018). In addition, it was hypothesised that the pattern of differences in muscle metabolites in the CIA model would be paralleled with differences in muscle mRNA abundance of genes known to be intimately involved in reduced protein synthesis (such as Eif4ebp1), increased muscle protein breakdown (such as MAFbx, MuRF1) and

carbohydrate use (such as PDK4, FOXO1, IRS1) compared to controls. Furthermore, I had the opportunity to test whether differences in muscle gene expression from control in this CIA model were consistent with differences in muscle gene expression between healthy, age-matched control volunteers and patients with RA.

4.2. Methods

Experiments were carried out following the methodology described in Chapter 2, where more details can be found.

4.2.1. Experimental design

4.2.1.1. Rodent study

Female Lewis rats (weighing 160-180 g, n=18) were used. Rats were randomly allocated to either the CIA model group or a complete Freund's adjuvant control group (n=9 per group). Pain behaviour, locomotor activity and paw swelling were measured at baseline before intervention and on day 3, 7, 14, and 18 after induction of CIA and control intervention. Venous blood (0.5 ml) was collected from the tail vain without anaesthesia before and after 18 days of treatment. The study was terminated when rats presented with paw swelling at day 16-18 post-intervention. The EDL muscle, predominantly type II (fast twitch) in nature, was harvested under terminal anaesthesia and stored at -80^{o}C for further investigations, and ankle joints were fixed and preserved at room temperature. For clarity, the end time-point is represented as day 18 for all rats. All data represent means for both hind limbs in the control group and the inflamed hind limb in

the CIA group, except for the synovitis score where only one limb per animal was obtained.

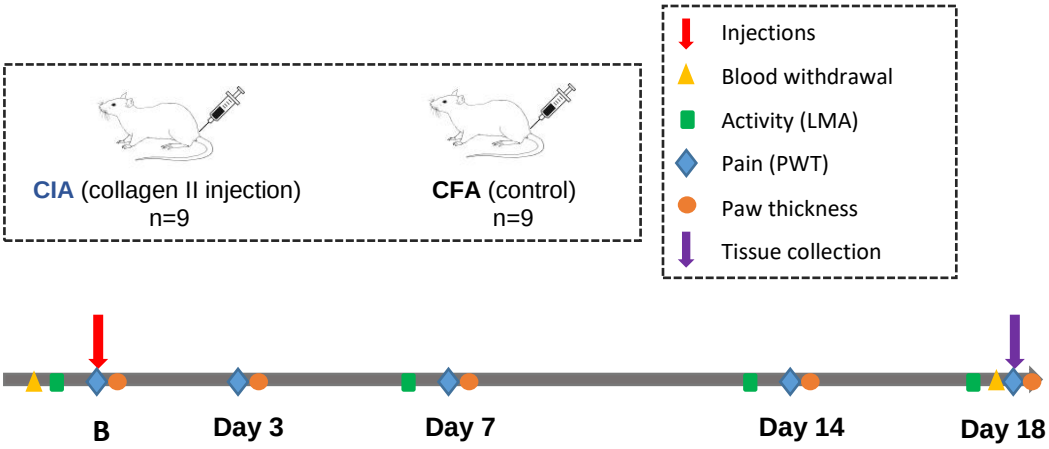


Figure 4.1: Experimental design scheme for *in vivo* study of the collagen-induced model of arthritis.

4.2.1.2. Human volunteer study

mRNA from quadriceps biopsies obtained from patients with RA (n=7) and age-matched healthy volunteers (n=6) was acquired via a collaboration with the University of Birmingham. The gender of the patients with RA was not provided, but relevant characteristics are summarised in Table 4.1.

Table 4.1: Clinical features from patients with rheumatoid arthritis whose muscle mRNA was used for gene expression quantification.

Patients	Age	Duration	Protein C-reactive (CRP)	Erythrocyte sedimentation rate (ESR)	Medication
JRP001	62	-	-	-	-
JRP006	63	35 years	11 mg/L	2 mm/h	Prednisolone
JRP036	67	>20 years	15 mg/L	13 mm/h	Infliximab
JRP039	67	>10 years	25 mg/L	46 mm/h	Methotrexate
JRP059	81	2 years	<3 mg/L	7 mm/h	None
JRP083	60	-	N/A	N/A	Unknown
JRP084	37	-	<3 mg/L	19 mm/h	Methotrexate

4.2.2. Collagen-induced model of arthritis

The rodent model of RA was generated by intradermal injection of bovine collagen type II in the base of the tail. Bovine collagen type II (4 mg/ml; MD Bioproducts, UK) was dissolved in acetic acid 10 mM and emulsified 1:1 with CFA, which was made with 1 mg *Mycobacterium Tuberculosis* in 1 ml of Incomplete Freund's Adjuvant. Two hundred µl of bovine collagen type II emulsion (2 mg/ml) was injected in the base of the tail to induce arthritis (n=9), and 200 µl of CFA emulsified 1:1 in acetic acid (10 mM) was injected in the control rats (n=9) under general anaesthesia. Rats were housed in groups of n=4 per cage.

4.2.3. Pain behaviour

Hind paw withdrawal thresholds were quantified using calibrated Von Frey monofilaments (bending forces from 2-26 g on a logarithmic scale). Rats were habituated to pain assessment for two days before the baseline measurement, which was measured on the same day as the model induction. The PWT method was performed as previously described in section 2.4.2.

4.2.4. Paw thickness

The increase of paw thickness during the development of arthritis in the ankle as measured with a digital electronic calliper as described in section 2.3.

4.2.5. Locomotor activity

Both vertical and horizontal movements were measured at the same time using locomotor activity boxes used as a reference method (Watson et al. 2012). Rats were placed in individual automated infrared activity boxes as previously described in section 2.5. The beam-breaks were counted at intervals of 5 min time epochs for 30 min under the red light the night before of PWT testing.

4.2.6. Plasma cytokines

Tail vein blood (0.5 ml) was collected at the end of the experiment, and blood plasma was isolated from whole blood as previously described in section 2.1.5. The anti-inflammatory cytokine IL-10 and pro-inflammatory cytokines IL-6 and TNFα were quantified by ELISA using R & D kits following the manufacturer's instructions as previously described in section 2.11.

4.2.7. Ankle histopathology

The ankle joints were harvested from both hind limbs in all rats at the end of the study to perform histopathology examination of synovia inflammation throughout the intervention. The joints were processed as described in section 2.6.3 and the histology of tibiotarsal joints was performed with H&E staining. The pathology for synovitis was scored using synovia lining layers and cellularity (0-3) as described in section 2.7.

4.2.8. Muscle analysis

The EDL muscle from both hind limbs was harvested under terminal anaesthesia by intraperitoneal injection of pentobarbital and snap-frozen as described in section 2.6.1.

4.2.8.1. Muscle metabolites

A portion of EDL muscle was freeze-dried and powdered. Two aliquots of the powder were used to extract and measure muscle metabolites (ATP, PCr, creatine, and lactate; 5-10 mg) and muscle glycogen (0.5-2 mg) content, which was quantified using enzymatic spectrophotometry as previously described in section 2.8.

4.2.8.2. Protein and DNA quantification

A portion of freeze-dried and powdered EDL muscle (~3 mg) was used to quantify total alkaline-soluble protein and DNA contents as described in section 2.9. The ratio protein : DNA is a reliable marker for muscle mass loss (Forsberg et al. 1991).

4.2.8.3. RNA extraction and quantitative PCR

Total mRNA from control and CIA animals was extracted from 20-30 mg of frozen wet EDL muscle, from which first strand cDNA was synthesised and quantified using qPCR. The protocols followed are described in section 2.10. Forty-eight genes were selected following literature searches and from in-house research interests in skeletal muscle energy metabolism, protein metabolism, inflammation and neurotrophic factors. The forty-eight

gene targets were identified for mRNA abundance quantification using Applied Biosystems TaqMan low-density array cards (Table 4.2).

Table 4.2: Genes included in the Tagman low-density array with its catalogue number.

Genes	Name	Catalogue number
Mitochondria		
Mtnd1	Mitochondrial subunit ND1	Rn03296764_s1
Ucp3	Mitochondrial uncoupling protein 3	Rn00565874_m1
Tfam	Transcription factor A mitochondrial	Rn00580051_m1
Tufm	Tu translational elongation factor mitochondrial	Rn01509017_g1
Tf2bm	Transcription factor B2 mitochondrial	Rn01412502_m1
Mtnd4	Mitochondrial subunit ND4	Rn03296781_s1
Bcl2l1	Bcl-2-like 1	Rn00437783_m1
Angiogenesis		
Vegfa	Vascular endothelial growth factor A	Rn01511602_m1
Carbohydrate metabolism		
Pdk2	Pyruvate dehydrogenase kinase 2	Mm00446681_m1
Slc2a4 (Glut4)	Glucose transporter 2	Rn00562597_m1
Pdk4	Pyruvate dehydrogenase kinase 2	Rn00585577_m1
Foxo1	Forkhead box protein 1	Rn01494868_m1
Lipid metabolism		
Cpt1a	Carnitine palmitoyltransferase 1A	Rn00682395_m1
Cpt1b	Carnitine palmitoyltrasnferase 1B	Rn00580702_m1
Insulin sensitivity		
Igf1	Insulin-like growth factor 1	Rn00710306_m1
Insr	Insulin receptor	Rn00690703_m1
Irs1	Insulin receptor substrate 1	Rn02132493_s1
Ppara	Peroxisome proliferator-activated receptor alpha	Rn00566193_m1
Ppard	Peroxisome proliferator-activated receptor delta	Rn00565707_m1
Pparg	Peroxisome proliferator-activated receptor gamma	Rn00440945_m1
Ppargc1a	Peroxisome proliferator-activated receptor gamma coactivator 1 alpha	Rn00580241_m1
Ppargc1b	Peroxisome proliferator-activated receptor gamma coactivator 1 beta	Rn00598552_m1
Endogenous genes		
Hmbs	Hydroxymethylbilane synthase	Rn01421881_m1
18S (Hs)	18 S ribosomal RNA	Mm04277571_s1
Myogenic factors		
Myf5	Myogenic factor 5	Rn01502778_m1
Myod1	Myogenic differentiation 1	Rn00598571_m1
Mstn	Myostatin	Rn00569683_m1
Protein synthesis		

Eif4ebp1	Eukaryotic translation initiation factor 4E binding protein 1	Rn00587824_m1
Mtor	Mammalian target of rapamycin	Rn00693900_m1
Murf1	Muscle RING-finger protein 1	Rn00590197_m1
Mafbx	Muscle atrophy f-box	Rn00591730_m1
Psma3	Proteasome subunit alpha type 3	Rn02587201_s1
Mt1A	Metallothionein 1A	Rn01536930_g1
Ctsl	Cathepsin L	Rn04341361_m1
Akt1	Serine/threonine-protein kinase 1	Rn00583646_m1
Atg9	Autophagy-related 9	Rn01400691_m1
Inflammation		
Nfkb1	Nuclear factor kappa-light-chain-enhancer of activated B cells	Rn01399572_m1
Il6	Interleukin 6	Rn01410330_m1
Il10	Interleukin 10	Rn01644839_m1
Tlr4	Toll-like receptor 4	Rn00569848_m1
Jak1	Janus kinase 1	Rn01763899_m1
Tnfa	Tumour necrosis factor alpha	Rn99999017_m1
Neurotrophic factors		
Ngf	Nerve growth factor	Rn01533872_m1
Bdnf	Brain-derived neurotrophic factor	Rn01484928_m1
Gdnf	Glial cell line-derived neurotrophic factor	Rn01402432_m1
Trka	Tropomyosin receptor kinase A	Rn00572130_m1
Trkb	Tropomyosin receptor kinase B	Rn01441749_m1
p75	Low-affinity nerve growth factor receptor	Rn00561634_m1

mRNA expression of 19 genes from the muscle of patients with RA and age-matched healthy volunteers was quantified by TaqMan probes from Applied Biosystems (Table 4.3). Theses 19 genes selected were chosen on the basis of being modulated from control in CIA rats.

The relative quantification of gene expression between control CFA and CIA rats, and between control healthy volunteers and RA patients, was calculated as fold change using the $2^{-\Delta\Delta Ct}$ method as described in section 2.10.3. The housekeeping gene used in both rats and humans was HMBS, used extensively in the past in similar muscle focussed studies (Alamdari et al. 2008).

Table 4.3: Genes selected to be quantified by Taqman probes in RA patients.

GENE	CATALOGUE NUMBER
PPARGC1A	Hs00173304_m1
IL6	Hs00174131_m1
IRS1	Hs00178563_m1
FOXO1	Hs00231106_m1
PSMA3	Hs00541061_m1
EIF4EBP1	Hs00607050_m1
HMBS	Hs00609297_m1
MURF1	Hs00822397_m1
MT1A	Hs00831826_s1
VEGFA	Hs00900055_m1
IL10	Hs00961622_m1
CTSL	Hs00964650_m1
MSTN	Hs00976237_m1
PPARGC1B	Hs00993805_m1
NTRK1	Hs01021011_m1
PDK4	Hs01037712_m1
MAFBX	Hs01041408_m1
TFAM	Hs01082775_m1
UCP3	Hs01106052_m1

4.2.9. Statistical analysis

All data are presented as mean ± SEM and were analysed by Prism V.7 (GraphPad, San Diego, California, USA). The statistical analysis of differences between control and CIA groups for PWT, locomotor activity and paw thickness was performed using two-way ANOVA with Bonferroni corrections. Student's unpaired t-test was used to compare muscle metabolites and the protein : DNA ratio between control and CIA groups. The Mann-Whitney test was used to compare plasma cytokines, histopathology scoring system and muscle mRNA expression. Ingenuity Pathway Analysis software (Redwood City, CA, USA) was used to interrogate differences in mRNA abundance from control as described in

section 2.10.4. Mean differences were considered statistically significant when $p<0.05$.

4.3. Results

4.3.1. Rodent study

Inflammation in the CIA model developed at slightly different rates in the rats, the manifestation of paw swelling was taken to indicate model success (Table 4.4).

Table 4.4: Description of group size and end-point based on paw swelling in each treatment group.

Treatment	Normal paw thickness	Paw swelling before day 16	Paw swelling between days 16-18	Total
Control	9	0	0	9
CIA	1	1	7	9

As a consequence of one CIA animal developing paw swelling earlier than the others, the group size was different for the last time-point of the behavioural experiments (Table 4.5 and 4.6).

Table 4.5: Group size during the time-course of paw withdrawal thresholds test. Note one rat developed paw swelling on day 15 in the CIA group and was terminated together with the accompanied rats in the same cage and one rat did not withdraw due to severe inflammation.

Treatment	Baseline	Day 3	Day 7	Day 14	Day 18
Control	9	9	9	9	7
CIA	9	9	9	9	6

Table 4.6: Group size during the time-course of the locomotor activity test. Note one rat developed paw swelling on day 15 in the CIA group and was terminated together with the accompanied rats in the same cage.

Treatment	Baseline	Day 3	Day 7	Day 14	Day 18
Control	9	9	9	9	7
CIA	9	9	9	9	7

4.3.1.1. Pain behaviour and paw thickness in the CIA model of RA

Baseline PWT between the two groups of rats were consistent (Figure 4.2). Paw withdrawal thresholds were quantified at 3, 7, 14, and 18 days following induction of the CIA model or control treatment. PWTs remained stable for the duration of the study for the control group, whereas the CIA group had significantly lower PWTs at 18 days (Figure 4.2.A). At this time point, there was also a significant increase in the paw thickness in the CIA group, compared to control (Figure 4.2.B). The change in PWT (indicative of pain) was significantly correlated with the increase of paw thickness (Table 4.6).

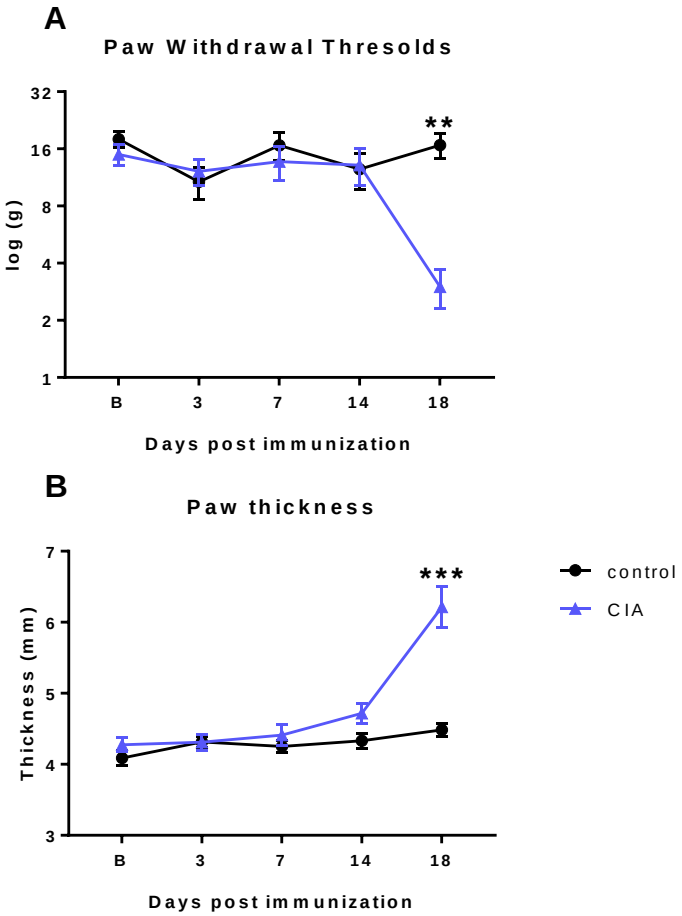


Figure 4.2: Paw withdrawal thresholds and thickness at baseline (B) and after treatment with CIA (n=9) or control (n= 9) rats. Results are mean ± SEM. Statistically analysed two-way ANOVA with Bonferroni correction. Differences between CIA and control groups during treatment **p<0.01, ***p<0.001.

4.3.1.2. Locomotor activity in CIA rats

At baseline, the horizontal and vertical activity of the two groups of rats were comparable (Figure 4.3). Following induction of the CIA model, locomotor activity remained relatively stable until the later time-points. There was a trend towards a reduction in the vertical activity of rats in the CIA group, compared to control on day 13. At day 17, there was a significant reduction in both the horizontal and vertical activity of the CIA group, compared to control (Figure 4.3 A, B). Changes in locomotor activity at day 17 were significantly correlated with the increase of paw thickness (Table 4.6).

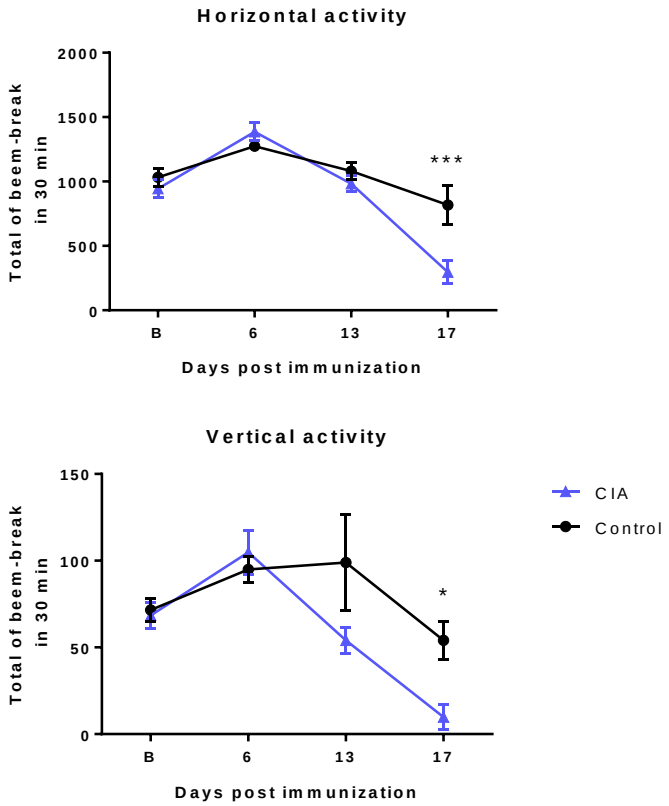


Figure 4.3: Locomotor activity at baseline and after treatment with CIA (n=9) or control (n=9) groups in 18 female rats. Results are mean ± SEM representing the number of movements (beam-break) for 30 min in the dark cycle (night). Statistical analysis using two-way ANOVA with Bonferroni correction. Differences between CIA and control groups on day 17: *p<0.05, ***p<0.001.

4.3.1.3. Plasma inflammatory cytokine concentrations

The plasma concentration of the anti-inflammatory cytokine IL-10 and the pro-inflammatory cytokine TNFα was very low in both CIA and control groups, with no difference between groups detected. However, the plasma concentration of the pro-inflammatory cytokine IL-6 was markedly and significantly increased in CIA rats, compared to control (Figure 4.4).

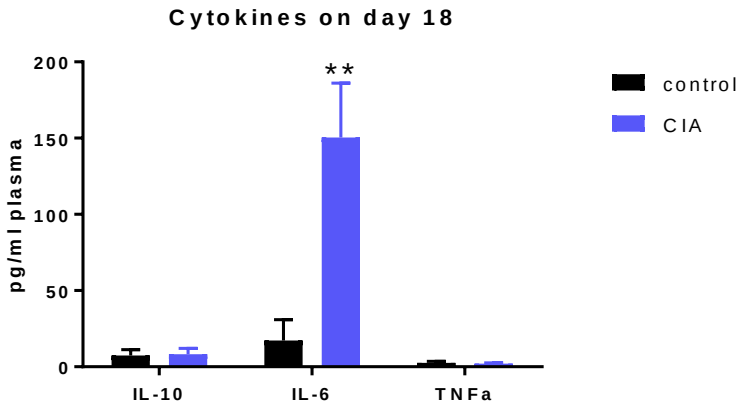


Figure 4.4: Plasma inflammatory cytokine concentrations from CIA rats (n=6) and control (n=7) rats at the end of the study. Results are mean ± SEM. Statistically analysed using Mann-Whitney non-parametric test. Differences between CIA and control groups on day 18: **p<0.01.

4.3.1.4. Histopathology of tibiotalus joint results in synovitis

The H&E staining of the tibiotalus joint (ankle) was performed at day 18, and a score of synovitis measured to quantify the extent of inflammation. There was a significantly greater number of cells in the talus and an increase in the cellularity in the synovium of CIA rats, compared to the control group (Figure 4.5).

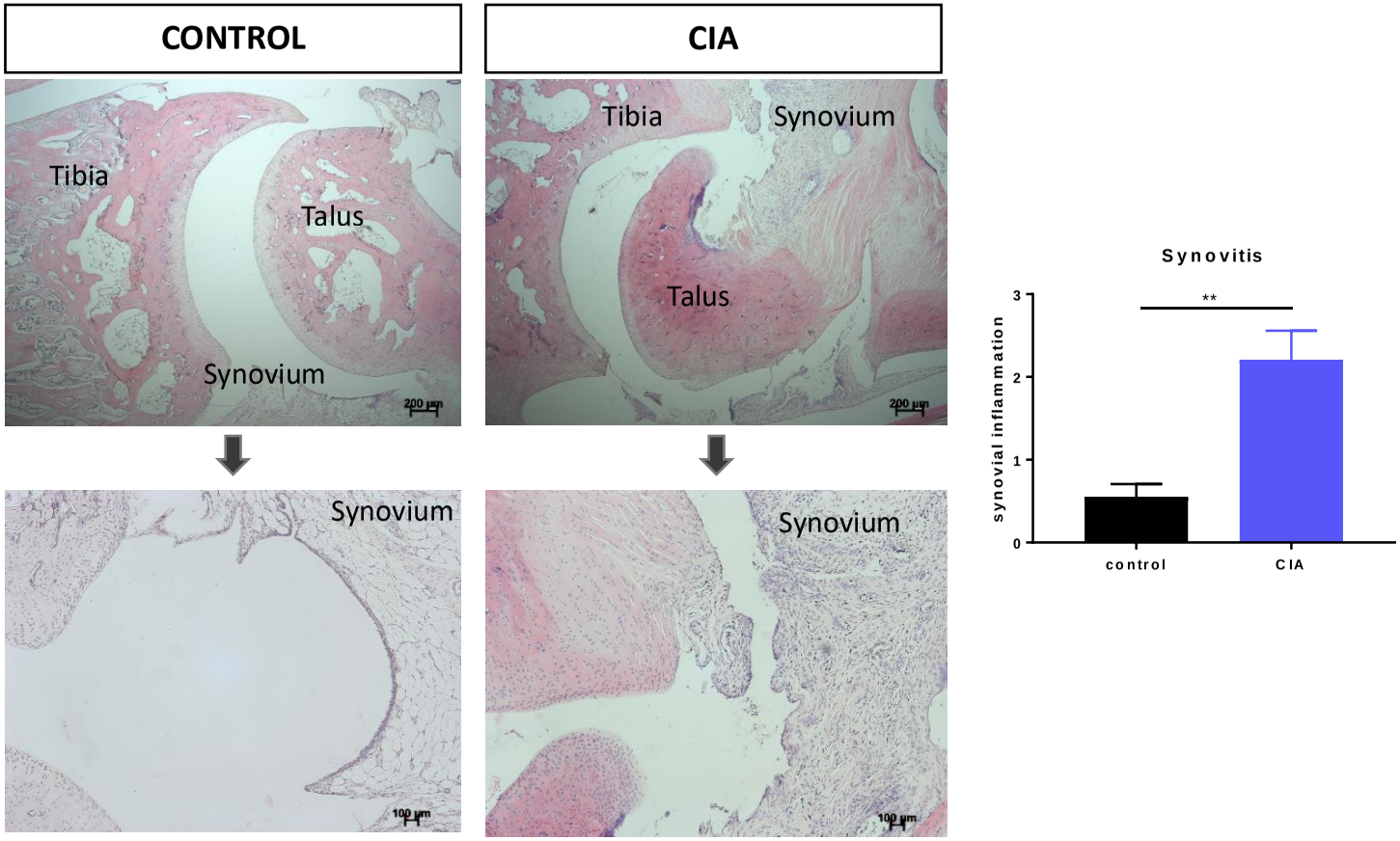


Figure 4.5: Histology and synovitis scoring of the tibiatarsal joint at the end of the study. There was an increase in the number of inflammatory cells in the tibiatalus joint of CIA rats (n=8) compared to the control (n=8) group. Results are mean ± SEM statistically analysed by non-parametric Mann-Whitney test: **p<0.01.

Synovitis, the main feature of inflammatory arthritis, was significantly correlated with paw thickness and both horizontal and vertical locomotor activity. However, synovitis was not correlated with plasma levels of IL-6, or pain behaviour (PWTs). In contrast, paw thickness was strongly correlated with pain behaviour (PWTs), locomotor activity and IL-6 in plasma as a marker of systemic inflammation (Table 4.7).

Table 4.7: Correlation of inflammatory synovitis and paw thickness with *in vivo* parameters in CIA rats. Data are shown as Pearson correlation coefficients. In bold are the levels of significance for each relationship.

Variable	Synovitis	P value	Paw thickness	P value
Paw withdrawal thresholds	-0.4446	0.0968	-0.6476	**0.0067**
Horizontal locomotor activity	-0.7403	**0.0007**	-0.7188	**0.0008**
Vertical locomotor activity	-0.7541	**0.0005**	-0.779	**0.0001**
Paw thickness	0.7081	**0.0015**	**-**	**-**
IL-6 in plasma	0.4444	0.1478	0.6807	**0.0130**

Additionally, pain behaviour (PWTs) was negatively correlated with systemic IL-6 ($p<0.01$). Interestingly, PWTs were not correlated with vertical ($p<0.1$) or horizontal ($p<0.085$) activity (Fig 4.6).

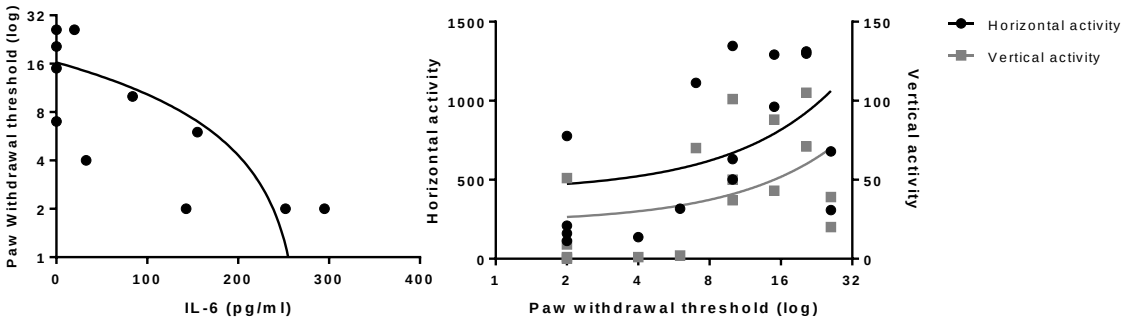


Figure 4.6. Correlations of paw withdrawal threshold as indicative of pain with systemic inflammation (A) and activity (B). Paw withdrawal threshold (PWT) axis is represented as a log scale. PWT vs IL-6: $r=-0.7883$, $p<0.01$. PWT vs horizontal activity: $r=0.444$. PWT vs vertical activity: $r=0.426$. Data are shown as the Pearson correlation.

4.3.1.5. Muscle glycogen and metabolites

Muscle glycogen and intermediary metabolites were measured in the EDL muscle at the end of the study in CIA rats with paw swelling (n = 9) and control rats (n = 9; Figure 4.7). Glycogen content in the EDL from the CIA rats was less than in the control rats. Similarly, muscle lactate content in the EDL was greater in the CIA rats, compared to the control group. Importantly, muscle ATP, phosphocreatine and total creatine contents were not different between the two groups of rats, indicating muscle viability and metabolic stress responses were comparable between the two groups (Figure 4.7.C).

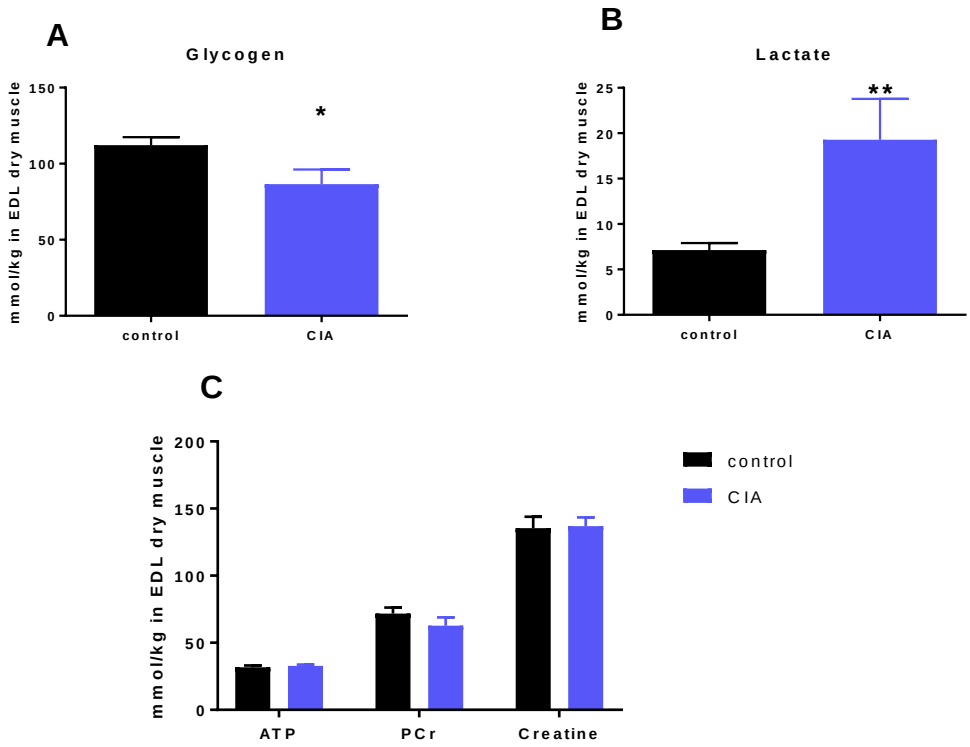


Figure 4.7: Levels of intermediate metabolites in the EDL muscle of CIA (n=9) and control (n=9) rats. Results are mean ± SEM representing glycogen (A), lactate (B), ATP, PCr and total creatine (C) content in EDL dry muscle. Statistically analysed using Student's t-test. Differences between CIA and control group on day 18: *p<0.05, **p<0.01.

4.3.1.6. Alkaline-soluble protein to DNA ratio

CIA rats tended to have less alkaline-soluble protein content (1052.45 µg/mg), compared to control rats (1119.8 µg/mg) and the muscle DNA content was similar between groups (2-2.1 µg/mg), therefore the protein:DNA ratio tended to be less (P=0.067) in CIA rats compared to control rats at the end of the study (Figure 4.8) pointing to greater muscle atrophy.

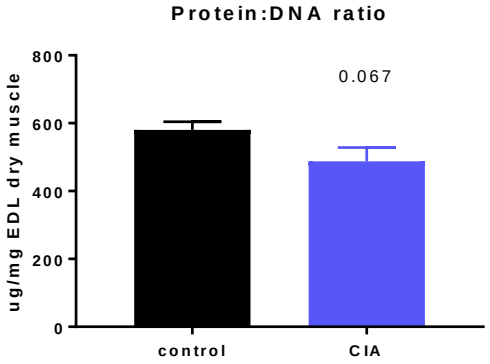


Figure 4.8: Alkaline-soluble protein to DNA ratio in the EDL muscle of CIA (n=9) and control (n=9) rats at the end of the study. Results are mean ± SEM. Statistically analysed using Student's t-test.

4.3.1.7. Muscle mRNA expression

Expression levels of 4 mRNAs known to regulate muscle protein breakdown and atrophy (Ctsl, Eif4bp1, Fbxo32, Trim63) were greater in EDL muscle in CIA rats, compared to CFA rats. Expression levels of mRNA related to neurotrophin receptor kinase 1 (Ntrk1) were less. Expression levels of 6 mRNAs associated with carbohydrate oxidation and insulin sensitivity were altered in the CIA rats, compared to control rats. Expression of FOXO1 mRNA was higher in the EDL of CIA rats, compared to controls. The expression of Irs1, PPARa, PPARgc1a, PPPARgc1b, Slc2a4 and Vegfa

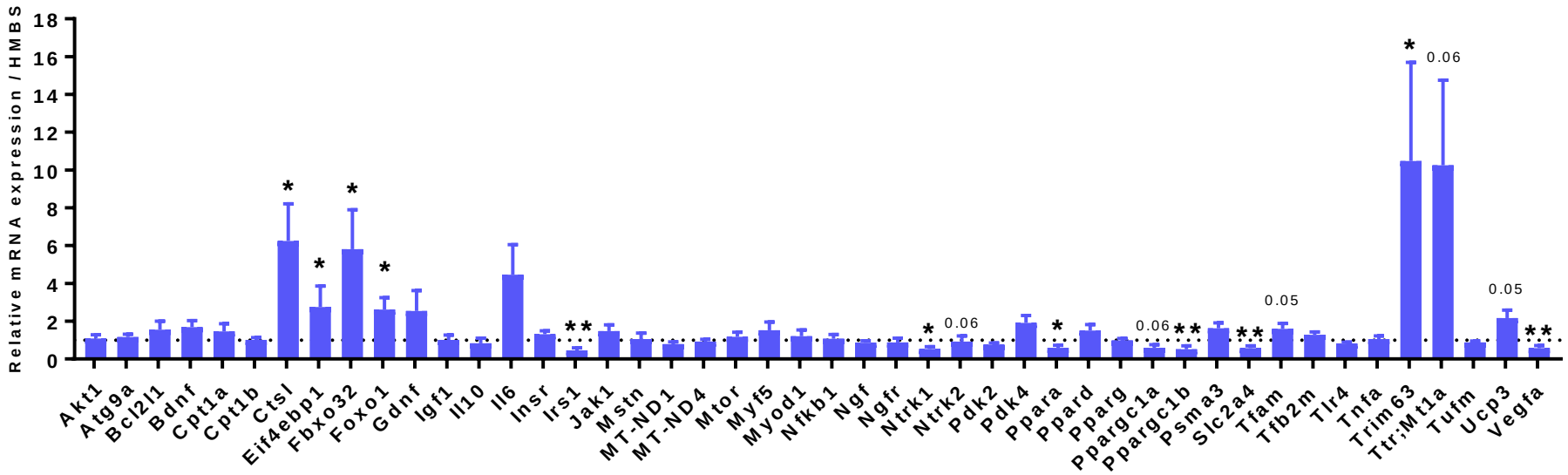


Figure 4.9: Fold-change in EDL mRNA abundance from control in CIA rats at day 18 (n=9). Results are mean ± SEM. Statistically analysed using non-parametric Mann-Whitney test. Differences between CIA and control group: *p<0.05, **p<0.01.

(hypoxia-related factor) mRNA was lower in the EDL of CIA rats, compared to CFA controls. There were no differences in the expression levels of IL-10 and IL-6 in the EDL between the two groups of rats.

In addition to identifying individual mRNA abundance differences, muscle mRNA abundance values for the whole cohort of genes identified in Table 4.2 were used to predict differences in metabolism from control in the CIA model using IPA bioinformatic software, thereby providing novel insight of metabolic pathways that might underpin any biochemical changes seen at a muscle level between groups. Fig 4.10 depicts the mRNAs most differentially regulated from control in the muscle of CIA treated animals (outer ring), and the centre predicts the changes expected in the CIA group based on these collective changes (see figure legend for a more detailed description). IPA predicted the inhibition of carbohydrate and fatty acid metabolism in the CIA group compared to control, with the confidence of predicted inhibition being greatest for carbohydrate metabolism (Figure 4.10A). Additionally, IPA predicted the activation of protein metabolism in CIA treated animals compared to control based on the differential mRNA abundance changes (Figure 4.10B). These predictions are in accordance with the other muscle level analyses performed in this study.

Importantly, provided that only 48 genes were introduced in the IPA analysis, and most were related to metabolic process, the system is subjected to highlight a metabolic dysfunction.

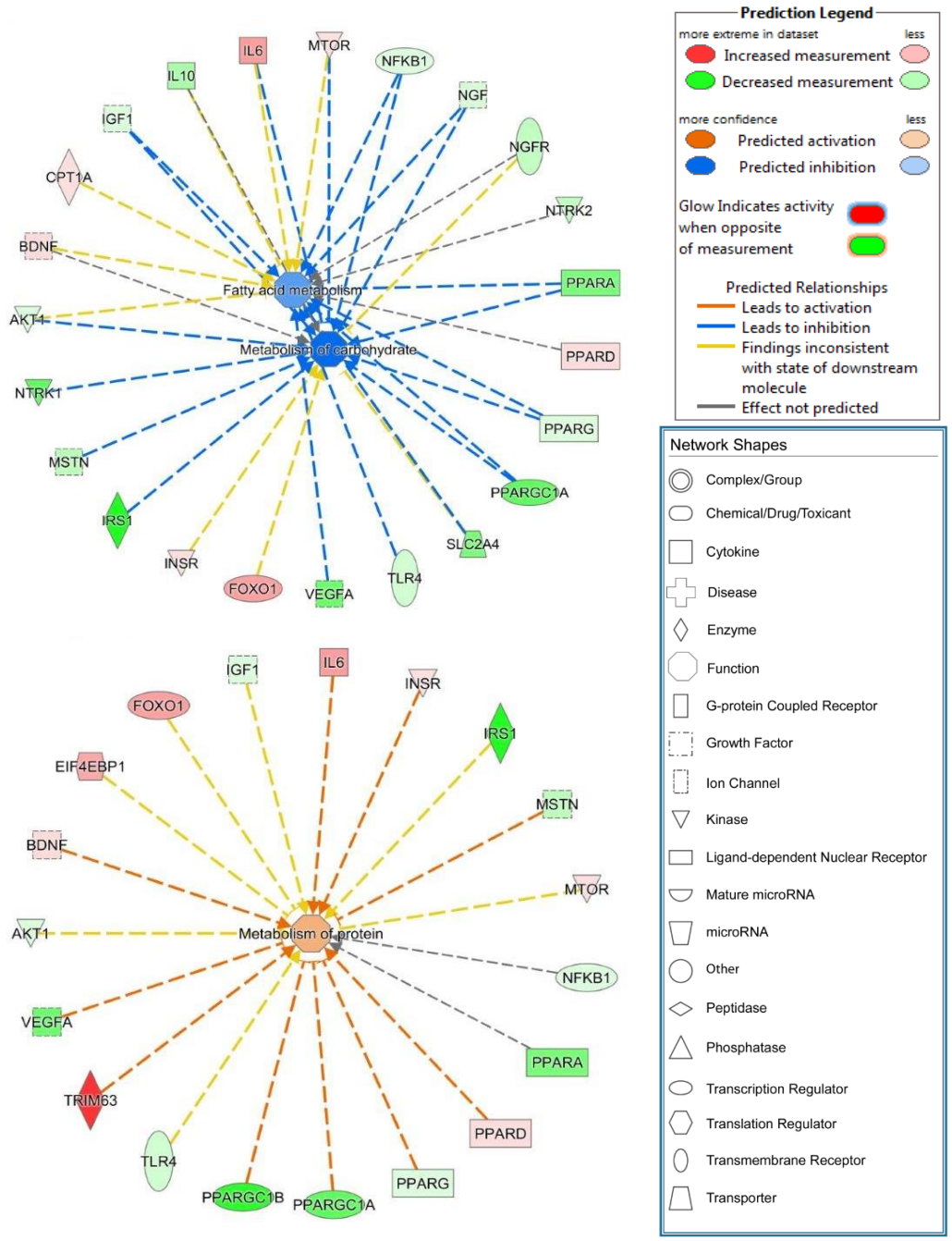


Figure 4.10: IPA prediction of energy metabolism including fatty acid and carbohydrate metabolism (A) and metabolism of protein (B) in EDL muscle based upon changes in mRNA expression from CIA rats (n=9) compared to control rats (n=9). In the outer ring: schematic representation of the most differentially regulated mRNAs in CIA compared to control rats, and with the colour intensity reflecting greater (red) or less expression (green) compared to control. The shape of the gens indicates the type of protein encoded. The centre of each ring indicates the network function connecting the genes by lines and arrows indicating the predicted relationship leading to activation (orange), inhibition (blue) or inconsistent (yellow).

4.3.2. Human volunteer study

Differences in muscle mRNA expression from control volunteers in rheumatoid arthritis patients are shown in Fig. 4.11. Expression levels of the anti-inflammatory cytokine IL-10 and pro-inflammatory IL-6 were higher in the muscle of RA subjects compared to control volunteers (Figure 4.11A). The expression of Mafbx mRNA was downregulated in the quadriceps muscle of RA subjects compared to controls, whilst MSTN and MT1A were upregulated in the muscle from RA patients compared to the control (Figure 4.11.B). PDK4 was highly upregulated, and PPARGC1b was downregulated in the quadriceps muscle of RA patients, compared to control volunteers (Figure 4.11.C).

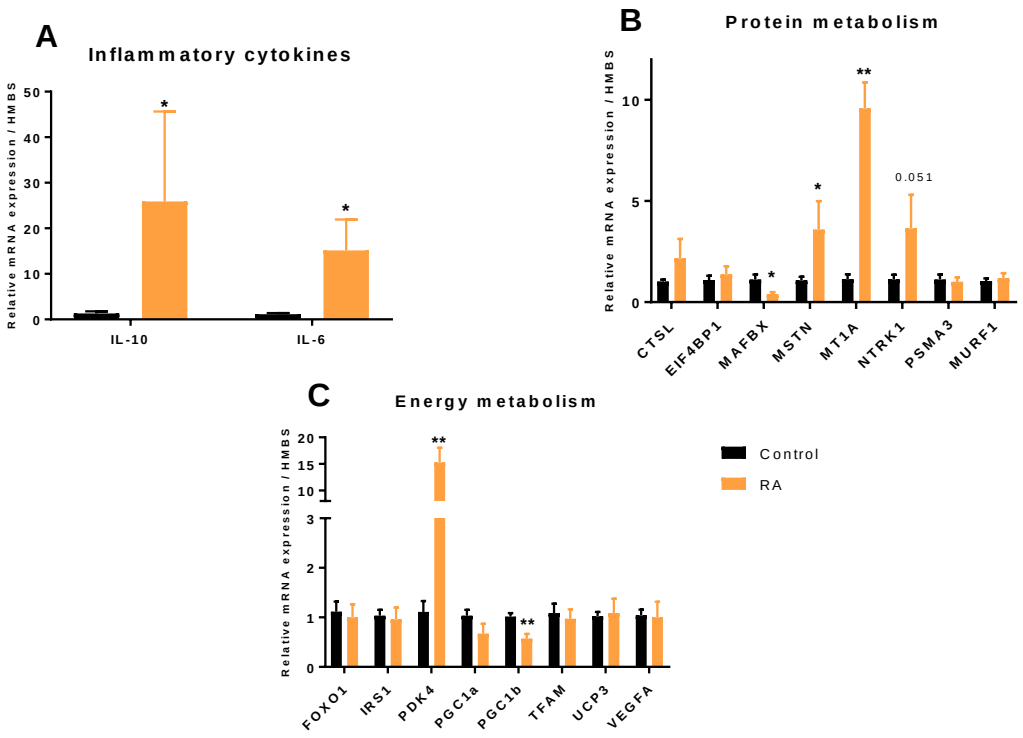


Figure 4.11: Expression of different clusters of genes in quadriceps from patients with RA (n=7) versus controls (n=6). Results are mean ± SEM representative of genes selected from results in muscle from CIA rats. Statistically analysed using non-parametric Mann-Whitney test. Differences between CIA and control groups at day 18: *p<0.05, **p<0.01.

4.4. Discussion

The studies undertaken in this chapter demonstrate the development of RA features, increase in pain behaviour, swelling and reduction of locomotor activity in the rat CIA model. New evidence for the presence of a systemic inflammatory response and metabolic and molecular changes in EDL muscle (from limbs with swollen hind paws) is presented herein. Joint swelling correlated with the decrease in paw withdrawal thresholds (indicative of pain), decreased locomotor activity and the elevation of plasma levels of the cytokine IL-6. Importantly, the evidence of systemic inflammatory response in the CIA model may be related to the changes in gene expression in the EDL muscle despite low muscle inflammation.

Increased pain and reduced locomotor activity in CIA at the stage of early acute inflammation supports the previous findings in models of rheumatoid arthritis and patients with the disease, where spontaneous locomotor activity decreased from day 14 in CIA and AIA rats coinciding with a fall of the pain threshold (Sasakawa et al. 2005; Tanimoto et al. 2015). However, the correlation between pain and locomotor activity was not significant, suggesting that low activity may be independent of pain and systemic inflammation, but more dependent on paw thickness and synovitis. Nevertheless, paw withdrawal thresholds were correlated with plasma levels of IL-6, and with paw thickness but not synovitis. These findings are consistent with evidence for a close relationship between pain behaviour and inflammation due to the role of cytokines, involved in the process of pathological pain modulating neuronal activity (Zhang and An 2007) in several diseases including rheumatoid arthritis (Bingham et al. 2009). In the

AIA model of RA, there is also an increase of IL-6 cytokine in serum and paw swelling by day 15 coinciding with low paw thresholds on day 22 (Tanimoto et al. 2015).

On the other hand, the locomotor activity may be affected by the discomfort of paw swelling and synovitis pathology in the CIA model. Therefore, as paw withdrawal thresholds is a test measuring pain sensitivity, it may not be representative of joint pain and thereby not correlated to locomotor activity. Pain tests focused locally to the joint, where the presence of swelling and synovitis is, could explain if the low activity may be due to pain in the inflamed joint.

There was a large increase in paw thickness, which correlated positively with plasma levels of IL-6. Previously, it was suggested that IL-6 has a key role in the inflammation associated with the early stages of RA, as plasma levels were extremely high in pre-arthritis patients and CIA model (Kokkonen et al. 2010; Alonzi et al. 1998). Furthermore, paw swelling was positively correlated with synovitis in the ankle joint of rats with early rheumatoid arthritis. However, plasma IL-6 levels did not correlate with levels of synovitis. Despite the evidence of systemic inflammation, cytokine levels were not significantly higher in the EDL muscle of CIA rats, compared to control CFA rats. Previous studies supported the concept that skeletal muscle dysfunction in CIA rats is triggered by inflammation and cytokine release, rather than muscle disuse (de Oliveira Nunes Teixeira et al. 2013). The metabolic and molecular changes in the muscle in the CIA model after 18 days of RA induction could potentially be due to a systemic inflammatory response at the muscle membrane (Peake et al. 2015). To better

understand and identify the grade of inflammation in the CIA model, it would be necessary to do a time-course of inflammatory development and cytokines during the disease progression in plasma, muscle and synovium.

Skeletal muscle integrity in the CIA model in this study was viable as muscle ATP, phosphocreatine and total creatine contents were similar to the control group. Nevertheless, glycogen content was lower while lactate content was greater in CIA rats compared to control, reflecting dysregulation of carbohydrate metabolism as seen in inflammatory states such as sepsis and COPD amongst other diseases (Crossland et al. 2008; Constantin et al. 2011). It has been proposed in these and other studies that muscle mitochondrial carbohydrate oxidation is impaired in inflammatory states, and via the Akt1/FOXO1 signalling pathway. Elevated cytokines have been proposed to reduce Akt phosphorylation thereby increasing FOXO1 activation (dephosphorylation) and the upregulation of downstream gene targets, including MAFbx, MuRF1 and PDK4 in rats with endotoxaemia (Crossland et al. 2008) and critically ill patients (Constantin et al. 2011). PDK4 phosphorylates and inactivates the pyruvate dehydrogenase complex PDC, which reduces mitochondrial pyruvate entry thereby decreasing muscle carbohydrate oxidation and increasing muscle lactate production. Considering the slight upregulation of PDK4 mRNA in this study, this may explain the greater muscle content of lactate compared to control, and the lower muscle glycogen content (which presumably resulted from less efficient glycogen use in the face of unchanged muscle ATP and phosphocreatine). In keeping with this observation, it has been demonstrated that some genes related to insulin sensitivity were

downregulated in muscle from different inflammatory and catabolic diseases, including a mouse CIA model (Arias de la Rosa et al. 2018). In this study, the following genes related to insulin signalling pathway were downregulated: insulin receptor substrate 1 (IRS1), glucose transporter type 4 translocation (Glut4), peroxisome proliferator-activated receptor PPARα, Peroxisome proliferator-activated receptor gamma coactivator 1 alpha (PPPARgc1a or PGC1α) and beta (PPPARgc1b or PGC1β). IPA analysis predicted its involvement to regulate carbohydrate metabolism.

Considering that RA is a disease characterised by the autoimmune and inflammatory response, we hypothesised that muscle mass and functionality would be reduced in this model. It has been reported that proteolytic pathways are regulated by Akt/FOXO1 signalling (Sandri et al. 2004), including the muscle-specific UPP ligases Mafbx and MuRF1. Expression levels of mRNAs involved in muscle protein breakdown and associated in muscle atrophy were increased in CIA treated animals compared to control. Expression of these genes has been previously shown to be increased in muscle from animal models of arthritis and inflammatory diseases (Castillero et al. 2009; Crossland et al. 2010; Constantin et al. 2011) suggesting the activation of ubiquitin-proteasome and autophagic-lysosomal proteolytic pathways (Gómez-SanMiguel et al. 2016) leading to muscle wasting. Furthermore, IPA analysis predicted the activation of protein metabolism in the CIA treated animals compared to control in the present study, and in keeping with the muscle alkaline-soluble protein:DNA ratio was less in the CIA rats compared to control. The activation of protein degradation pathways can be regulated by the dephosphorylation of

Akt1/FOXO1 signalling in different acute systemic inflammatory diseases, including sepsis, COPD and glucocorticoid treatments (Crossland et al. 2008; Doucet et al. 2007; Martín et al. 2014). Regardless, it remains unclear if the same mechanism exists in cachexia and arthritis due to normal Akt activity (Stephens et al. 2010; Castillero et al. 2011). These discrepancies may become from the severity grading between acute and chronic inflammatory states. However, I acknowledge that protein expression analysis would need to determine the levels of phosphorylated Akt1 and FOXO1 proteins in the CIA model.

Based on the IPA predictions, I could also associate the expression of different clusters of genes with muscle protein breakdown and carbohydrate metabolism. I documented lower expression of VEGFα, which has already seen to be associated with FOXO activation suppressing cellular metabolic flux, mitochondrial respiration and fatty acid synthesis (Domigan et al. 2015) as IPA predicted in this study. Neurotrophic receptor Ntrk1 (TrkA) for NGF neurotrophins has been suggested to be implicated in carbohydrate metabolism as shown in L6 muscle cells, where it was found its implication with pain and muscle regeneration (Rende et al. 2000). Additionally, TrkA is required to induce phosphorylation (activation) of Akt and insulin receptor complex by insulin stimulation (Geetha et al. 2013).

Overall, our study provides evidence of inflammation associated with pain, synovitis, and locomotor inactivity and provides a mechanism which may underlay the muscle wasting and metabolic dysregulation observed.

This approach can help to better understand the mechanisms of muscle mass loss and metabolic dysregulation in inflammation. It highlights the importance of muscle health in RA for its development as a disease and possible future treatments. However, further clinical experiments need to be undertaken to identify relevant similarities with the rodent model. In this study, mRNAs from quadriceps muscle of patients with RA was used to identify the more clinically relevant genes changed in the EDL muscle of CIA rats. In these clinical samples, levels of the IL-10 and IL-6 in the muscle from RA subjects were significantly higher than in healthy control, while mRNA markers of proteolytic pathways levels were not prominently changed. Interestingly, myostatin mRNA was upregulated in the RA muscle from clinical patients, which is a major indicator of muscle wasting as previously seen in critically ill patients (Constantin et al. 2011). On the other hand, the extremely high levels of mRNA PDK4 in clinical samples may indicate the impairment of carbohydrate oxidation in muscle from RA patients. Consistent with my data in the CIA rat model, PGC1b mRNA was downregulated in muscle from RA subjects, and Mt1a mRNA was upregulated. There are some key limitations of this study, patients used for the gene quantification in muscle had received treatments (NSAID and DMARD) which may have influenced the outcomes of this study. It would be an advantage to have more clinical parameters such as levels of cytokines in blood, disease progression and protein and metabolites content in muscle to better compare the stage of RA that the CIA model mimics. However, it will not be possible to compare directly the conditions of RA samples and CIA model as the duration of the disease is different. It

is yet to be known the equivalence of days in CIA model versus days in patients with RA.

In conclusion, the rat CIA model of RA is an inflammatory model with the development of disease pathology reflected on pain, low activity, paw swelling and synovitis. I evidenced that cytokine IL-6 is a major deterrent of the systemic inflammatory response in the CIA model and that it may trigger the activation of metabolic and molecular signalling pathways regulated by Akt/FOXO in the muscle. In accordance to previous research with inflammatory models, muscle from CIA rats are exposed to protein degradation and lactate accumulation with indices of carbohydrate metabolism impairment. Simultaneously, clinical samples of RA also showed muscle dysregulation by gene expression analysis.

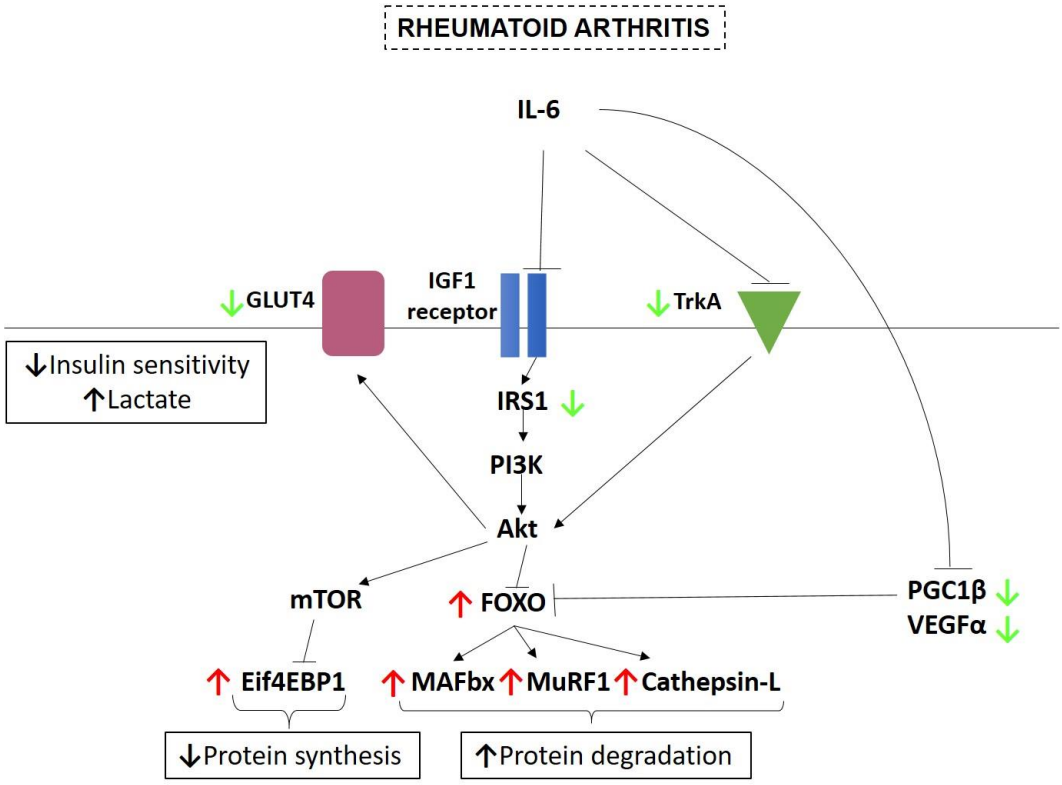


Figure 4.12: Proposed signalling pathway regulated by rheumatoid arthritis induced inflammation in the rodent model of CIA based on mRNA expression in muscle. IL-6 alters the phosphorylation cascade of the IGF1-PI3K-Akt axis by the downregulation of IRS1, activating FOXO and its downstream transcription factors. It triggers muscle atrophy by the protein imbalance (decreased protein synthesis and increased protein degradation) as well as decreased in muscle insulin sensitivity, which leads to a rise in muscle lactate levels.

Chapter 5:

Peroxisome proliferator-activated receptor ɣ agonist ameliorates inflammation and modifies muscle metabolism and lactate accumulation in a rat model of rheumatoid arthritis

5.1. Introduction

Skeletal muscle weakness, fatigue and weight loss are features of rheumatoid arthritis that impair the quality of life in patients. As it is demonstrated in chapter 4, collagen-induced arthritis model-related inflammation in rats resulted in arthritis-like symptoms such as ankle synovitis, pain, low locomotor activity and muscle dysfunction. It is widely reported that inflammation is a catabolic state that increases muscle protein breakdown via several pathways, including the ubiquitin-proteasome pathway and lysosomal-mediated autophagy (Bodine Sue C. et al. 2001b; Deval et al. 2001). Inflammation is also associated with muscle lactic acidosis, which is at least partly a result of reduced pyruvate dehydrogenase complex flux (Alamdari et al. 2008) arising from inflammation-induced increases in expression of PDK4, which inhibits PDC (Furuyama et al. 2003; Constantin-Teodosiu 2013). Reduced muscle PI3K-Akt phosphorylation by inflammatory cytokines results in dephosphorylation of FOXO transcription factors and their translocation to the nucleus resulting in increased transcription of downstream targets, such as PDK4, Mafbx, MuRF1 and cathepsin-L (Crossland et al. 2008). The physiological consequences of which include inhibition of muscle carbohydrate oxidation (Alamdari et al. 2008; Crossland et al. 2008) and promotion of muscle protein breakdown (Bodine et al. 2001a; Kwon et al. 2004; Sandri et al. 2004).

Rheumatoid arthritis patients and rodent models of this disease present with increased systemic inflammation, such as elevated concentrations of circulating IL-6 (both serum and plasma) (Alonzi et al. 1998; Heidi et al.

2010), which are associated with muscle wasting and altered body composition with a decrease in total and appendicular lean mass (Tournadre et al. 2017), increased fat mass (Khoja et al. 2018) and muscle function and physical inactivity (Huffman et al. 2017; Alabarse et al. 2018). Thus, it can be predicted that suppression of systemic inflammatory under these conditions may reduce muscle mass loss and preserve muscle carbohydrate oxidation. Indeed, this has shown to be the case in an animal model of endotoxaemia (Crossland et al. 2008; Crossland et al. 2010).

Disease-modifying anti-rheumatic drugs (DMARDs), such as cytokine antagonists, which suppress inflammatory response have beneficial effects on the severity of rheumatoid arthritis in some patients (Tournadre et al. 2017; Wilsdon and Hill 2017). Potential beneficial effects of these types of treatment upon the regulation of muscle mass and fuel metabolism in RA have yet to be evaluated.

Peroxisome proliferator-activated receptors (PPARs) are members of the nuclear hormone receptor superfamily, which act to regulate gene expression and metabolism (Berger and Moller 2002; Forman, Chen, and Evans 1996). They control the expression of networks of genes involved in adipogenesis, lipid metabolism, inflammation and maintenance of metabolic homeostasis (Ahmadian et al. 2013). PPARɣ regulates adipogenesis and whole-body lipid metabolism and insulin sensitivity (Evans, Barish, and Wang 2004; Tontonoz and Spiegelman 2008) as well as gene networks involved in glucose homeostasis. Additionally, PPARγ controls the expression of numerous factors secreted from adipose tissue, such as adiponectin, leptin and tumour necrosis factor-α (TNF-α), which

also influence insulin sensitivity (Ahmadian et al. 2013). Different tissues are directly involved with the mechanism and effects of thiazolidinediones (TZDs), which are synthetic agonists of PPARɣ, including adipose tissue, skeletal muscle and liver. Administration of synthetic agonists of PPARɣ, called thiazolidinediones (TZDs), can improve insulin sensitivity and glucose homeostasis in different tissues and have been extensively used to treat type II diabetes (Rizos et al. 2008; Rizos, Kei, and Elisaf 2016). PPAR ligands have anti-inflammatory effects in different diseases, such as diabetes and sepsis (Liu et al. 2005). Chronic pre-treatment with the selective PPARɣ agonist, rosiglitazone (8.5 mg kg^{-1} day^{-1}), suppressed lipopolysaccharide (LPS)-induced reductions in the phosphorylation status of Akt and FOXO, which was associated with reduced expression of muscle IL-6 and TNFα mRNA. Additionally, it preserved muscle mass and carbohydrate use by reducing the expression of MuRF1, Mafbx and PDK4 in the EDL muscle (Crossland et al. 2017). Similarly, rosiglitazone reduced circulating concentrations of TNFα, IL-1β and IL-6 in a mouse CIA model of RA (Cuzzocrea et al. 2003) and had anti-inflammatory effects reflected by a reduction in joint synovitis and bone erosions in adjuvant-induced polyarthritis rats (Koufany et al. 2008). However, the potential beneficial effects of PPARɣ agonists in preserving skeletal muscle mass and metabolic function in RA has yet to be reported.

This chapter addressed the hypothesis that the beneficial effects of rosiglitazone on inflammation improve skeletal muscle function in a rodent model of RA. The effects of rosiglitazone on inflammation, pain responses, locomotor activity, muscle energy metabolism pathways and muscle mass

were determined in the CIA model of RA. Finally, to understand better the pathways underlying the beneficial effects of rosiglitazone in this model of RA, targeted analysis of 48 gene transcripts was performed utilising a microfluidic, low-density array approach coupled with Ingenuity Pathway Analysis of expression data generated.

5.2. Methods

Experiments were carried out following the methodology described in Chapter 2, where more details can be found.

5.2.1. Experimental design

Female Lewis rats (weighing 170-190 g, n=40) were used. Rats were randomly allocated to either rosiglitazone (Rosi) or vehicle intervention (n=20 per group). Fourteen days after daily administration of either rosiglitazone or vehicle (see 5.2.2), rats were randomly allocated to CFA (control) or CIA (treatment) intervention (see 5.2.3), creating a total of 4 experimental groups (n=10 per group): control + vehicle; control + rosiglitazone; CIA + vehicle and CIA + rosiglitazone. Pain behaviour and paw thickness were measured before and at day 3, 8, and 17 following commencement of control and CIA intervention. Locomotor activity was measured the night before daily rosiglitazone and vehicle administration commenced, and before and on day 8 and 17 following commencement of control and CIA intervention. Venous blood (0.5 ml) was collected from the tail vain without anaesthesia before and 17 days after commencement of control and CIA intervention, and the study was terminated after 17 days.

At this time, the EDL muscle and ankle joints were harvested under terminal anaesthesia and stored at -80ºC.

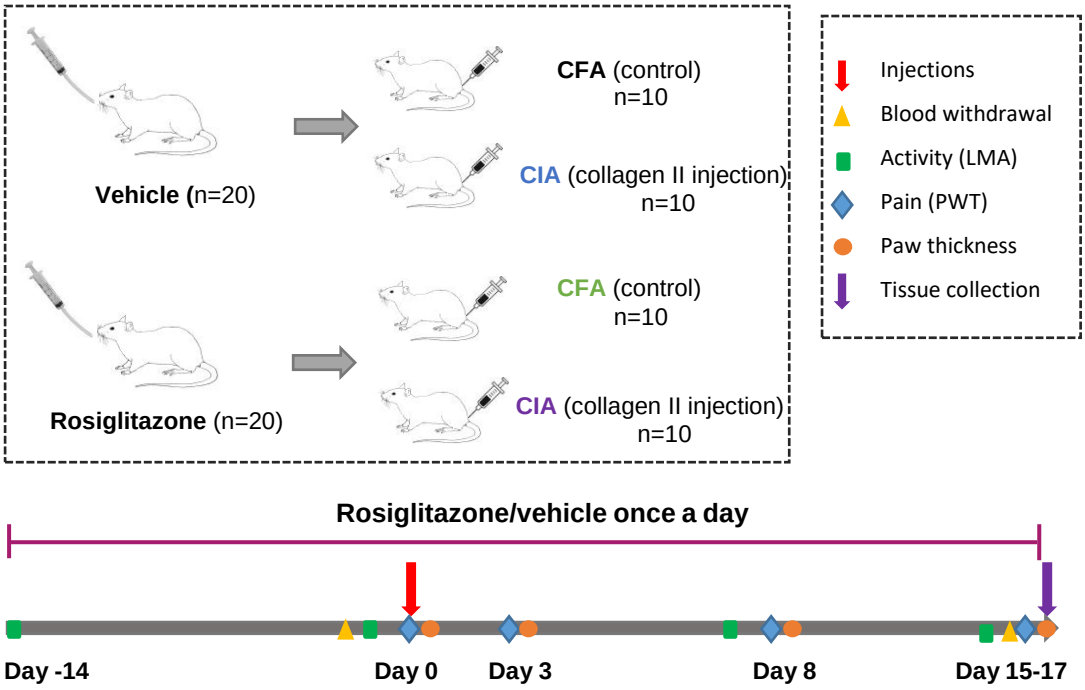


Figure 5.1: Experimental design scheme for *in vivo* study of the collagen-induced model of arthritis with daily treatment with rosiglitazone/vehicle.

5.2.2. Oral gavage

Rats were dosed via oral gavage as described in section 2.2. Rosiglitazone (8.5 mg/kg; Bepharm Ltd, China) was suspended in 0.5% HPMC (10 ml/kg; Sigma) and administered once per day for 14 days before commencement of control and CIA intervention and then every day until the end of the study. The control group received vehicle 0.5% HPMC identically.

5.2.3. Collagen-induced model of arthritis

The rodent model of RA was generated by intradermal injection of bovine collagen type II in the base of the tail. Bovine collagen type II (4 mg/ml; MD Bioproducts) was dissolved in acetic acid 10 mM and emulsified 1:1 with

CFA, which was made with 1 mg *Mycobacterium Tuberculosis* in 1 ml of Incomplete Freund's Adjuvant. Two hundred µl of bovine collagen type II emulsion (2 mg/ml) was injected in the base of the tail to induce arthritis (n=20) under general anaesthesia. The control for this model (200 µl of CFA emulsified 1:1 in acetic acid 10 mM) was injected into the base of the tail (n=20) under general anaesthesia. Rats were housed in groups of n=4 per cage.

5.2.4. Pain behaviour

Hind paw withdrawal thresholds were quantified for both limbs using calibrated Von Frey monofilaments (bending forces from 2-26 g in a logarithmic scale). Rats were habituated to pain assessment for two days before the intervention. The PWT method was performed as previously described in section 2.4.2 before and at day 3, 8, 17 after model induction (Figure 5.1).

5.2.5. Paw thickness

The paw thickness was measured in both hind limbs with a digital electronic calliper as described in section 2.3 before and at day 3, 8, 17 after the intervention (Figure 5.1.).

5.2.6. Locomotor activity

Both vertical and horizontal movements were measured using locomotor activity boxes using an established method (Watson et al. 2012). Rats were placed in individual automated infrared activity boxes as previously described in section 2.5. The beam-breaks were counted in intervals of 5

min time epochs for 30 min under the red light the night before starting oral gavage and then every night before PWT testing (Figure 5.1).

5.2.7. Plasma cytokine concentration

Tail vein blood (0.5 ml) was collected at the end of the experiment, and plasma was isolated from whole blood as previously described in section 2.1.5. The pro-inflammatory cytokine IL-6 was quantified by ELISA (Quantikine® ELISA, R&D systems) following the manufacturer's instructions as previously described in section 2.11.

5.2.8. Ankle histopathology

The ankle joints were harvested from both hind limbs in all rats at the end of the study to perform histopathology examination of synovia inflammation throughout the intervention. The joints were processed as described in section 2.6.3 and the histology of tibiotarsal joints was performed with H&E staining. Synovitis of the joint was scored using a cellularity scale (0-3) as described in section 2.7. Data presented represent values from the left hind limb in the control group and the most swollen limb of the CIA group measured by paw thickness.

5.2.9. Muscle analysis

The EDL muscles from both hind limbs were harvested under terminal anaesthesia by intraperitoneal injection of pentobarbital and snap-frozen as described in section 2.6.1. Data presented represent values from the left hind limb in the control group and the most swollen limb of the CIA group measured by paw thickness.

5.2.9.1. Muscle metabolites

A portion of EDL muscle was freeze-dried and powdered. Two aliquots of powder were used to extract and measure muscle metabolite (ATP, PCr, creatine, and lactate; 5-10 mg) and muscle glycogen (0.5-2 mg) content, which was quantified using enzymatic spectrophotometry as previously described in section 2.8.

5.2.9.2. Protein and DNA quantification

A portion of freeze-dried and powdered EDL muscle (~3 mg) was used to quantify total alkaline-soluble protein and DNA contents as described in section 2.9. The ratio protein : DNA is a reliable marker for muscle mass loss (Forsberg et al. 1991).

5.2.9.3. RNA extraction and quantitative PCR

Total mRNA from control and CIA animals was extracted from 20-30 mg frozen wet EDL muscle, from which first strand cDNA was synthesised and quantified using qPCR. The protocols followed are described in section 2.10. Forty-eight genes previously selected in Chapter 4 associated with the regulation of skeletal muscle energy metabolism, protein metabolism, inflammation and neurotrophic factors were quantified for mRNA abundance using Applied Biosystems TaqMan low-density array cards (Table 4.2). The relative quantification of gene expression amongst groups was calculated using the fold change from the $2^{-\Delta\Delta Ct}$ value as described in section 2.10.3 using control + vehicle group as a reference control. The housekeeping gene used was HMBS, which has been approved and used extensively (Alamdari et al. 2008).

5.2.9.4. Statistical analysis

All data are presented as mean ± SEM and were analysed by Prism V.7 (GraphPad, San Diego, California, USA). The statistical analysis of differences amongst groups for PWT, locomotor activity and paw thickness was performed with two-way ANOVA with Bonferroni corrections. Ordinary one-way ANOVA was used to compare metabolites (ATP, PCr, lactate, glycogen), protein : DNA ratio and synovitis. A Kruskal-Wallis test was used to compare muscle total creatine, plasma IL-6 and muscle gene expression due to non-normal distribution data. Ingenuity Pathway Analysis software (Redwood City, CA, USA) was used to interrogate differences in mRNA abundance from control + vehicle as described in section 2.10.4. Mean values were considered statistically different when $p<0.05$. Values in text, tables and figures are represented as mean ± SEM.

5.3. Results

Of the 20 CIA rats, one treated with rosiglitazone had eczema which was close to the severity limit to get infected and therefore the rat was humanly killed and not included in any analyses (final group size for CIA + rosiglitazone n=9). The manifestation of paw swelling was taken as a primary indication of CIA model success and was evident in 8 of the 10 rats in the CIA + vehicle group (Table 5.2).

Table 5.1: Description of group size and end-point based on paw swelling in each treatment group.

Treatment	No paw swelling	Paw swelling	Humanly killed	Total
Control + vehicle	10	0	0	10
Control + Rosi	10	0	0	10
CIA + vehicle	2	8	0	10
CIA + Rosi	5	4	1	10

Pain behaviour was quantified as a change in PWT. This commonly used measure is dependent upon the withdrawal of the hind limb. In some cases, in the CIA vehicle group, the swelling was judged to confound this measure with the inability of withdrawing, and this is evident in the group size of the last time-point for these data (Table 5.3).

Table 5.2: Description of group size over the time-course of PWT measurement. Note starting group size for CIA + Rosi was 9.

Treatment	Baseline	Day 3	Day 8	Day 17
Control + vehicle	10	10	10	10
Control + Rosi	10	10	10	10
CIA + vehicle	10	10	10	6
CIA + Rosi	9	9	9	7

There were no differences in PWT, paw swelling and locomotor activity in the control groups treated with vehicle or rosiglitazone, and therefore these two groups were merged as a single group (control n=20) to improve the clarity of line graphs.

5.3.1. Rosiglitazone reduced pain behaviour and blunted paw thickness

Baseline paw withdrawal thresholds amongst the groups of rats were comparable (Figure 5.2). PWTs were quantified at 3, 8, and 17 days following induction of the CIA model or control. In the control group, PWTs remained stable for the duration of the study, whereas the CIA + vehicle group had significantly lower PWTs at 17 days compared to the control group. The CIA group treated with rosiglitazone had significantly lower PWTs than the control group at day 17. There were no significant differences between CIA treated with rosiglitazone and CIA treated with vehicle although the mean of PWT always remained higher in CIA + rosiglitazone group (Figure 5.2.A). At this time-point, there was also a significant reduction in the paw thickness in the CIA group treated with rosiglitazone, compared to the CIA vehicle group and control (Figure 5.2.B). There was a significant negative correlation between paw thickness and PWT (Figure 5.3), with lowered PWTs (increased paw responses) correlated with paw thickness.

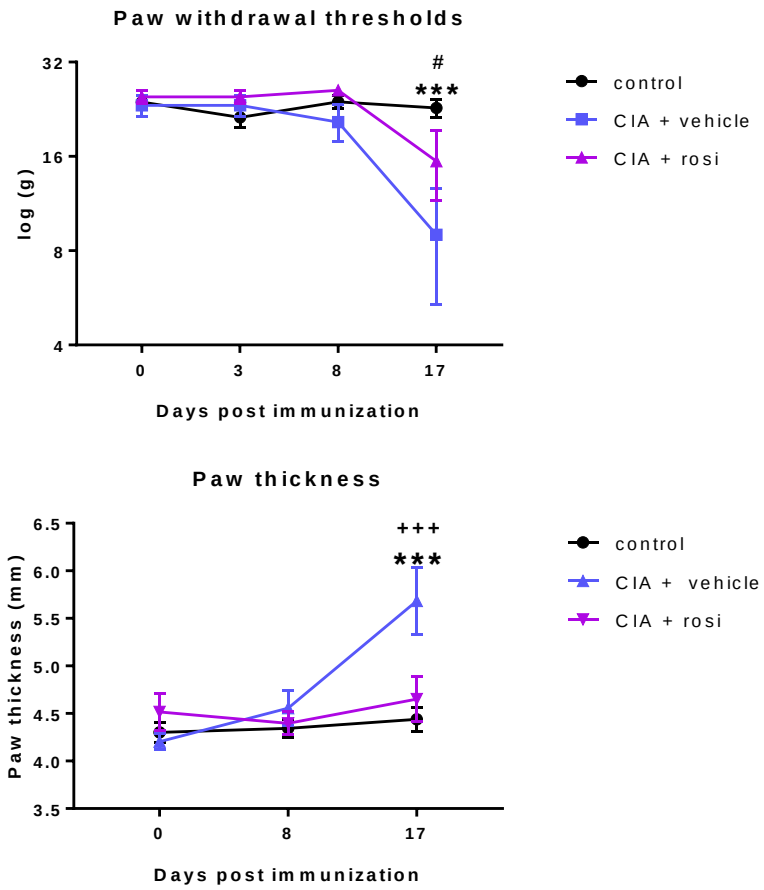


Figure 5.2: Effects of vehicle versus rosiglitazone (rosi) on paw withdrawal thresholds (A) and paw thickness (B) in CIA rats. Group sizes: control (n=20); CIA+vehicle (n=10); CIA+rosi (n=9). Results are mean ± SEM. Statistically analysed by two-way ANOVA with Bonferroni correction: control vs CIA+vehicle ***p<0.001; control vs CIA+rosi #p<0.05; CIA+vehicle vs CIA+rosi +++p<0.001.

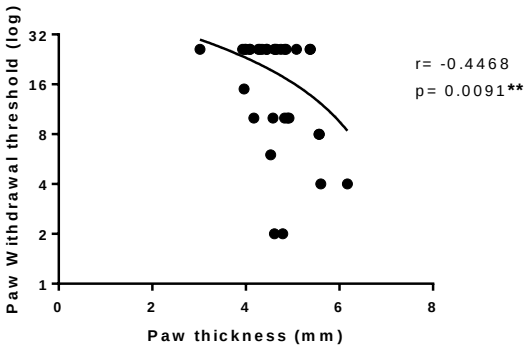


Figure 5.3: Correlation of paw withdrawal thresholds and paw thickness as indicative of pain responses and paw swelling. Paw withdrawal threshold axis is presented as a log scale. Data analysed with a Pearson correlation (r). *p<0.05.

5.3.2. Effects of rosiglitazone treatment on locomotor activity in CIA rats

At day -14 horizontal and vertical activity of rats was comparable between the three groups. Following CIA induction horizontal and vertical activity of rats remained stable and comparable to the control group until day 7. At day 17, horizontal and vertical activity was reduced in CIA rats treated with vehicle or rosiglitazone (Figure 5.4). Following induction of the CIA model, horizontal activity remained relatively stable until the later time-points (Figure 5.4.A). At day 17 there was a significant reduction in horizontal activity of rats in CIA rats treated with vehicle and the group treated with rosiglitazone, compared to the control group. Although there were changes in the vertical activity, significant differences between groups were not observed (Figure 5.4.B).

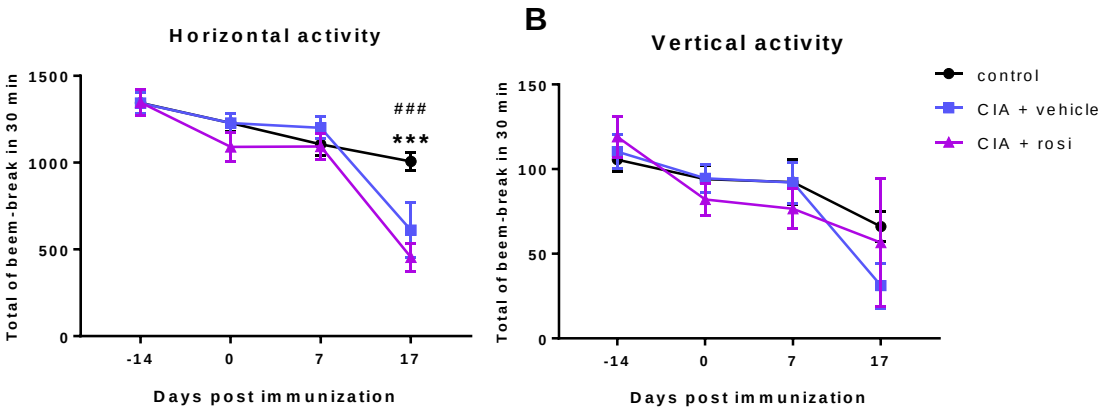


Figure 5.4: Effects of rosiglitazone (rosi) treatment on locomotor activity in CIA rats. Group sizes: control (n=20); CIA+vehicle (n=10); CIA+rosi (n=9). Results are mean ± SEM representing the total number of movements (beam-break) for 30 min in the dark cycle (night). Statistically analysed by two-way ANOVA with Bonferroni correction: control vs CIA+vehicle ***p<0.001; control vs CIA+rosi ###p<0.001.

Changes in horizontal activity at day 17 were significantly correlated with the paw thickness, but not with the PWT (Figure 5.5).

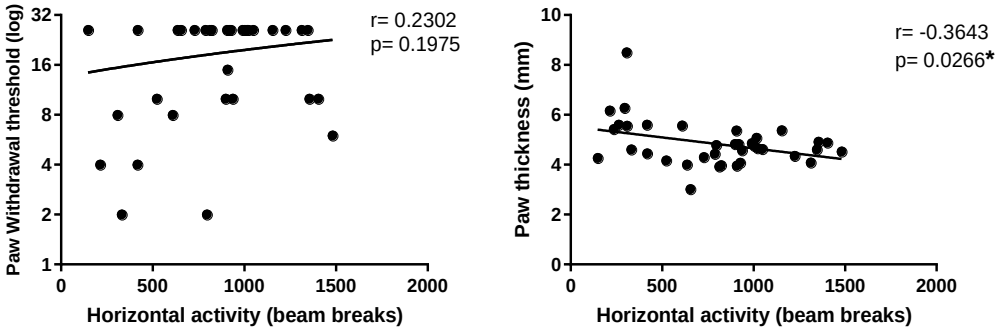


Figure 5.5: Correlation of horizontal activity with paw withdrawal thresholds and paw thickness, indicative of pain responses and paw swelling respectively. Paw withdrawal threshold axis is log scale. Data analysed with a Pearson correlation (r). *p<0.05.

5.3.3. Plasma levels of the inflammatory cytokine IL-6

Analysis of plasma at the end of the study revealed that IL-6 concentration was significantly increased in CIA + vehicle rats compared to the control group (Figure 5.6). Plasma levels of IL-6 in the CIA group treated with rosiglitazone were not significantly different to the control group treated with rosiglitazone. However, there was no significant difference between the vehicle CIA group and the rosiglitazone CIA group (Figure 5.5).

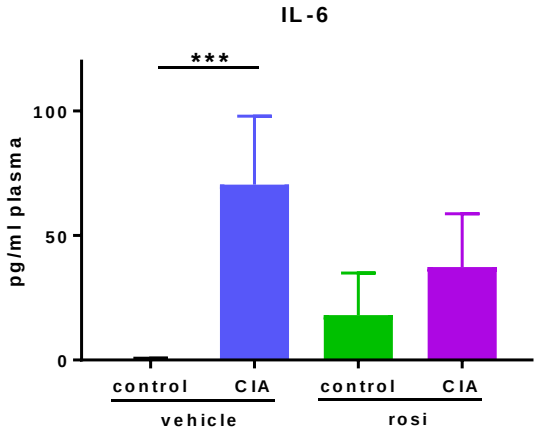


Figure 5.6: Plasma concentrations of IL-6 in CIA and control rats treated with rosiglitazone (Rosi) or vehicle on day 17. Group sizes: control (n=20); CIA+vehicle (n=10); CIA+rosi (n=9) Data are mean ± SEM. Statistically analysed using non-parametric Kruskal-Wallis test. Differences between CIA vehicle and control groups: ***p<0.001

Plasma concentration of IL-6 was significantly correlated with PWTs, but not with paw thickness (Figure 5.7).

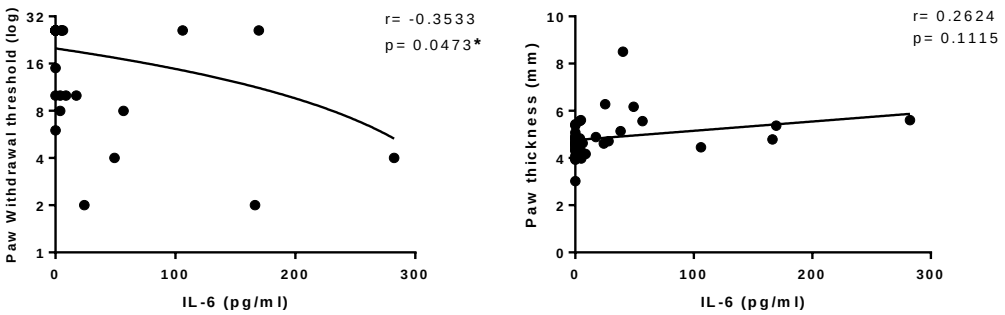


Figure 5.7: Correlation of plasma concentrations of IL-6 and paw withdrawal thresholds and paw thickness as indicative of pain and paw swelling. Paw withdrawal threshold axis is a log scale. Data analysed with Pearson correlation coefficient (r). *p<0.05.

5.3.4. Histopathology of tibiotalus joint and synovitis

The H&E staining of the tibiotalus joint (ankle) was performed at day 17 when the extent of inflammation was also analysed using semi-quantitative score of synovitis. The control + rosiglitazone group was not analysed and the control + vehicle group was used as the reference control. There was a significant increase in the cellularity in the synovium of CIA rats compared to control + vehicle group, indicative of synovitis (Figure 5.9). There was a trend towards a reduction in the cellularity in the CIA group treated with rosiglitazone, but there was no significant difference between CIA + vehicle and CIA + rosiglitazone (Figure 5.8).

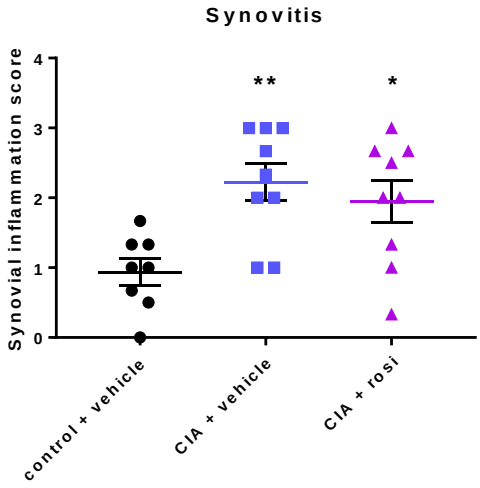


Figure 5.8: Synovitis scoring of the tibiatarsal joint at the end of the study. Group sizes: control + vehicle (n=8); CIA + vehicle (n=9); CIA + Rosi (n=8). Data are mean ± SEM. Statistically analysed using ordinary one-way ANOVA test. Differences compared to control + vehicle group on day 17: *p<0.05, **p<0.01.

Synovitis, the main feature of inflammatory arthritis, was significantly correlated with PWTs, horizontal activity and paw thickness (Table 5.3).

Table 5.3: Correlation of synovitis score with PWTs, horizontal activity and paw thickness. Data are shown as Pearson correlation coefficients and exact *P* values. In bold are the significant *P* value ($p<0.05$).

Variable	Synovitis	P value
Paw withdrawal thresholds	-0.7396	**0.0005**
Horizontal locomotor activity	-0.4535	**0.0340**
Vertical locomotor activity	-0.1631	0.4683
Paw thickness	0.525	**0.0101**
Plasma IL-6	0.0361	0.8733

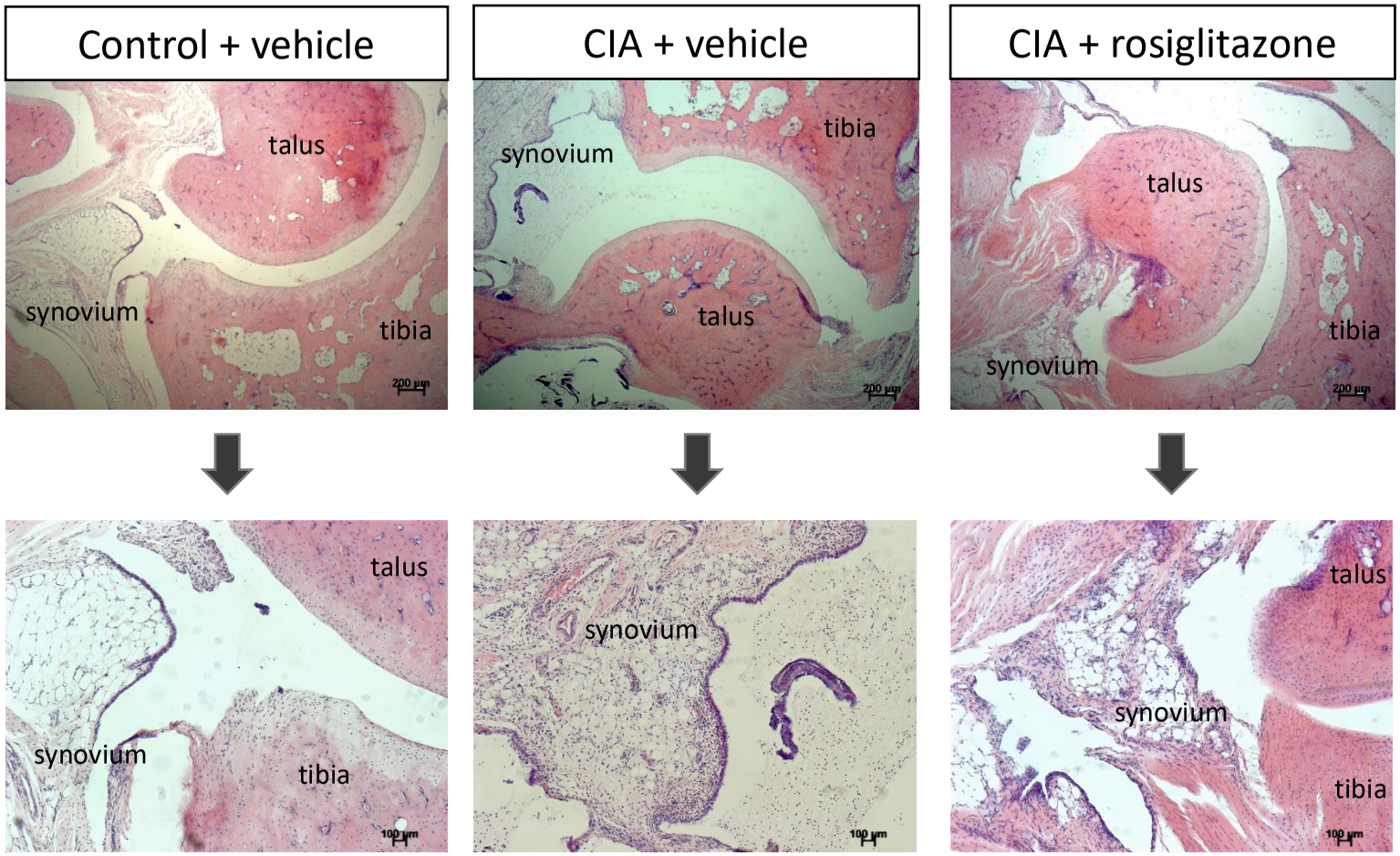


Figure 5.9: Histology of the tibiatarsal joint at day 17. There was an increase in the infiltration of inflammatory cells in the tibiotalus joint of CIA + vehicle rats (n=10) and CIA + rosi (n=9) compared to the control (n=10) group.

5.3.5. Muscle glycogen and metabolites

Muscle glycogen and intermediary metabolites were measured in the EDL muscle at the end of the study (Figure 5.10). There were no differences in muscle glycogen concentration between the four groups (Figure 5.10.A). Muscle lactate content in the EDL was significantly higher in the CIA + vehicle group compared to the control group (Figure 5.10.B). There were no differences in the muscle lactate content in the EDL between CIA + rosiglitazone group and the control rosiglitazone group (Figure 5.8.B).

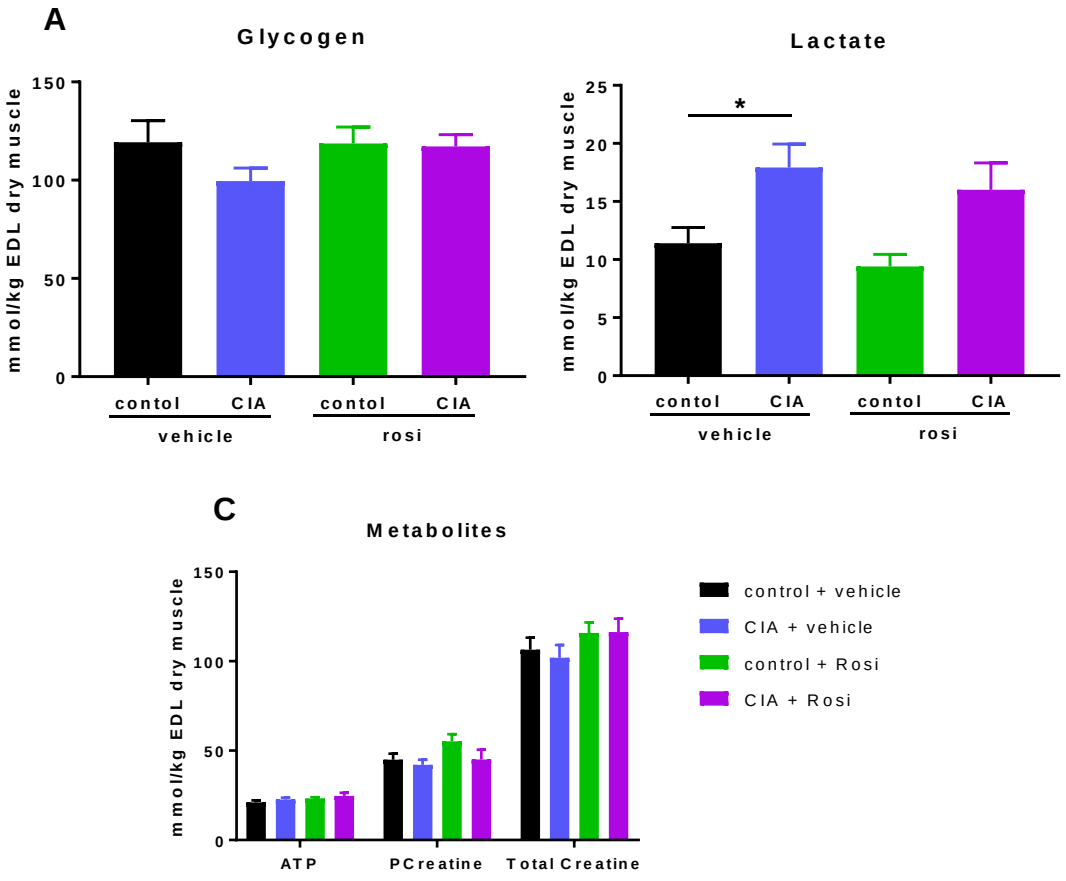


Figure 5.10: Glycogen and Intermediate metabolite content in the EDL muscle of CIA rats. Group size: control + vehicle (n=10); control + rosi (n=10); CIA + vehicle (n=10); CIA + rosi (n=9). Results are mean ± SEM representing glycogen (A), lactate (B), ATP, PCr and total creatine (C) content in EDL dry muscle. Statistically analysed using ordinary one-way ANOVA test. Differences between CIA + vehicle and control groups on day 17: *p<0.05.

Importantly, muscle ATP, PCr and total creatine content were not different between groups and representative of resting rat EDL muscle (Alamdari et al. 2008), demonstrating excellent muscle tissue viability (Figure 5.8.C).

5.3.6. Alkaline-soluble protein to DNA ratio

CIA rats and control rats treated with either vehicle or rosiglitazone had similar alkaline-soluble protein : DNA ratio content in EDL muscle (Figure 5.11).

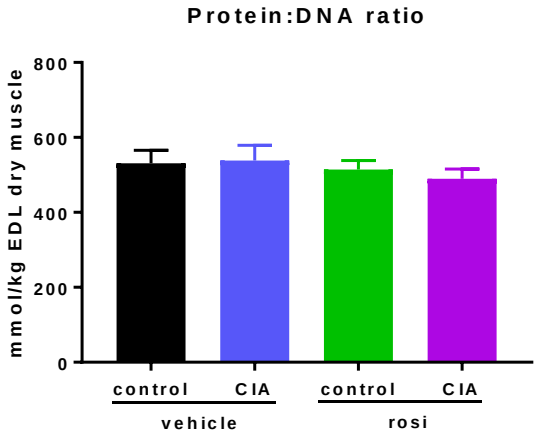
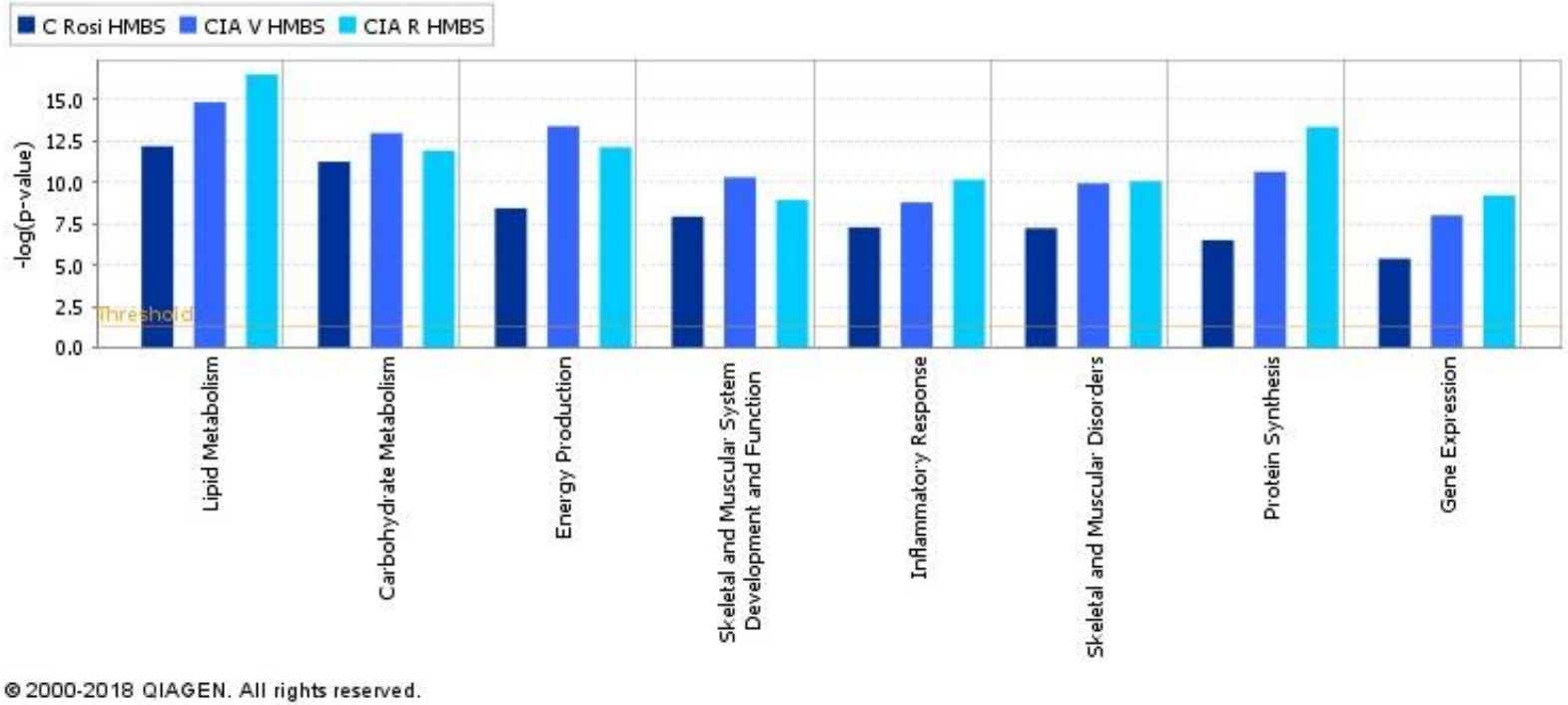


Figure 5.11: Alkaline-soluble protein to DNA ratio in EDL muscle of CIA rats. Group size: control + vehicle (n=10); control + rosi (n=10); CIA + vehicle (n=10); CIA + rosi (n=9). Results are mean ± SEM. Statistically analysed using one-way ANOVA.

5.3.7. Effects of rosiglitazone treatment on muscle mRNA expression

mRNA expression levels of 48 genes previously selected (Chapter 4, Table 4.2) were quantified to assess potential differences in gene expression between the CIA model treated with vehicle versus rosiglitazone.

Fig. 5.12 depicts changes in cellular function from the control + vehicle group response in the remaining three experimental groups. These changes in cellular function are predicted by IPA from the observed changes in EDL mRNA expression of the targeted genes compared to the control + vehicle group. IPA predicted changes in 8 cellular functions as a result of the CIA model and the effects of rosiglitazone in this model. The most affected cellular functions in the CIA rats (CIA V) were lipid metabolism, carbohydrate metabolism, and energy production ([-log (p-value) all >12.5]); skeletal muscular system development and function and protein synthesis ([-log (p-value) all >10]) (Figure 5.10). The most affected cellular functions associated with rosiglitazone treatment in CIA rats (CIA R) were lipid metabolism ([-log (p-value) >15]), protein synthesis ([-log (p-value) >12.5]), carbohydrate metabolism and energy production ([-log (p-value) both >10]), whereas in control rats (C Rosi) these were lipid and carbohydrate metabolism ([-log (p-value) both >10]) (Figure 5.12).



© 2000-2018 QIAGEN. All rights reserved.

Figure 5.12: Cellular functions identified by IPA as being different from control vehicle (n=10) in control + rosiglitazone (C Rosi, n=10), CIA + vehicle (CIA V, n=10) and CIA + rosiglitazone (CIA R, n=9) groups. Predictions are based on mRNA expression levels in EDL muscle. The X-axis displays cellular functions most affected while the Y-axis displays the –log of the p-values. The threshold in yellow line represents the control + vehicle group used as reference for foldchange. The –log of the p-value was calculated by Fisher's exact test right-tailed ($p<0.05$).

IPA illustrated the prediction of marked activation of muscle lipid oxidation (Fig 5.13) and specific lipid moieties (Fig 5.14), activation of carbohydrate metabolism to different degrees across groups (Fig 5.15) and synthesis of protein (again to different degrees across groups) (Fig 5.16) in CIA + vehicle, CIA + rosiglitazone and control + rosiglitazone groups compared to control + vehicle. The control + rosiglitazone group has represented a reduced number of genes whose expression was modified compared to CIA groups.

The outer ring of the 12 rosettes depicts the individual muscle mRNAs that collectively represent the altered cellular functions depicted in Fig. 5.12, along with the direction of mRNA expression change relative to control + vehicle (increased [red] or decreased [green] expression). The centre of each rosette depicts the IPA predicted change in metabolism based on the mutual changes in mRNA abundance (activation [orange] or inhibition [blue]). The level of confidence of this prediction is reflected by the colour intensity.

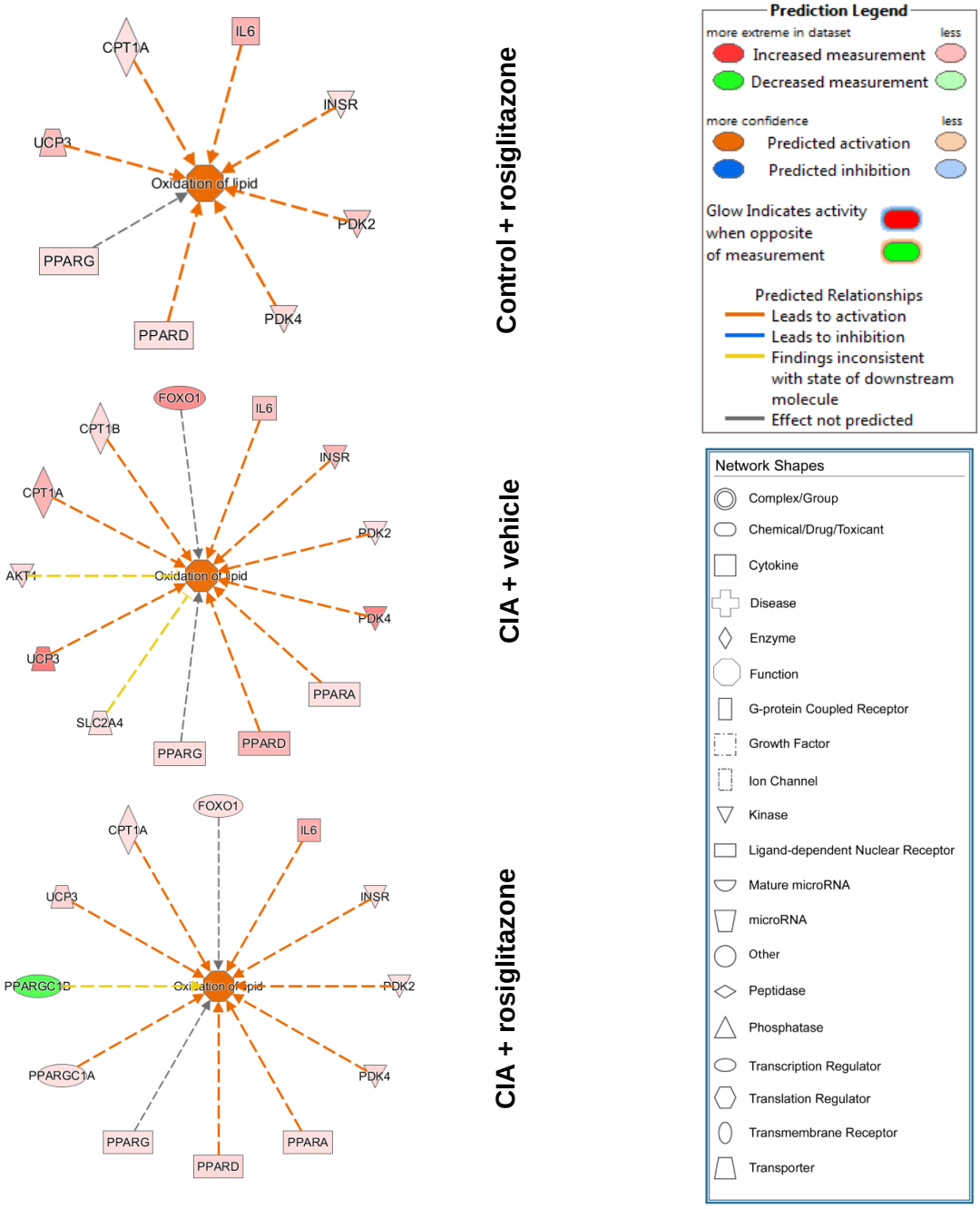
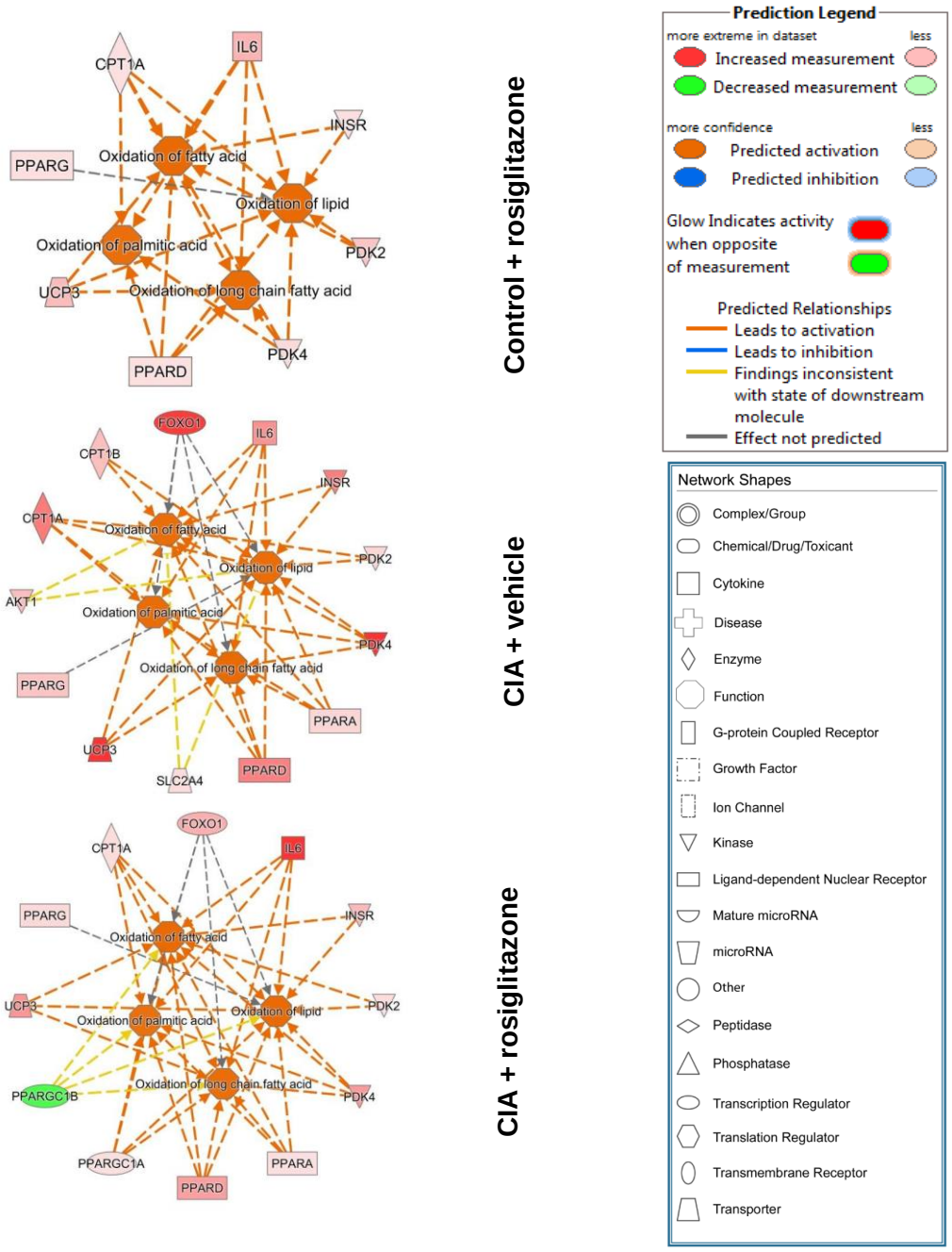
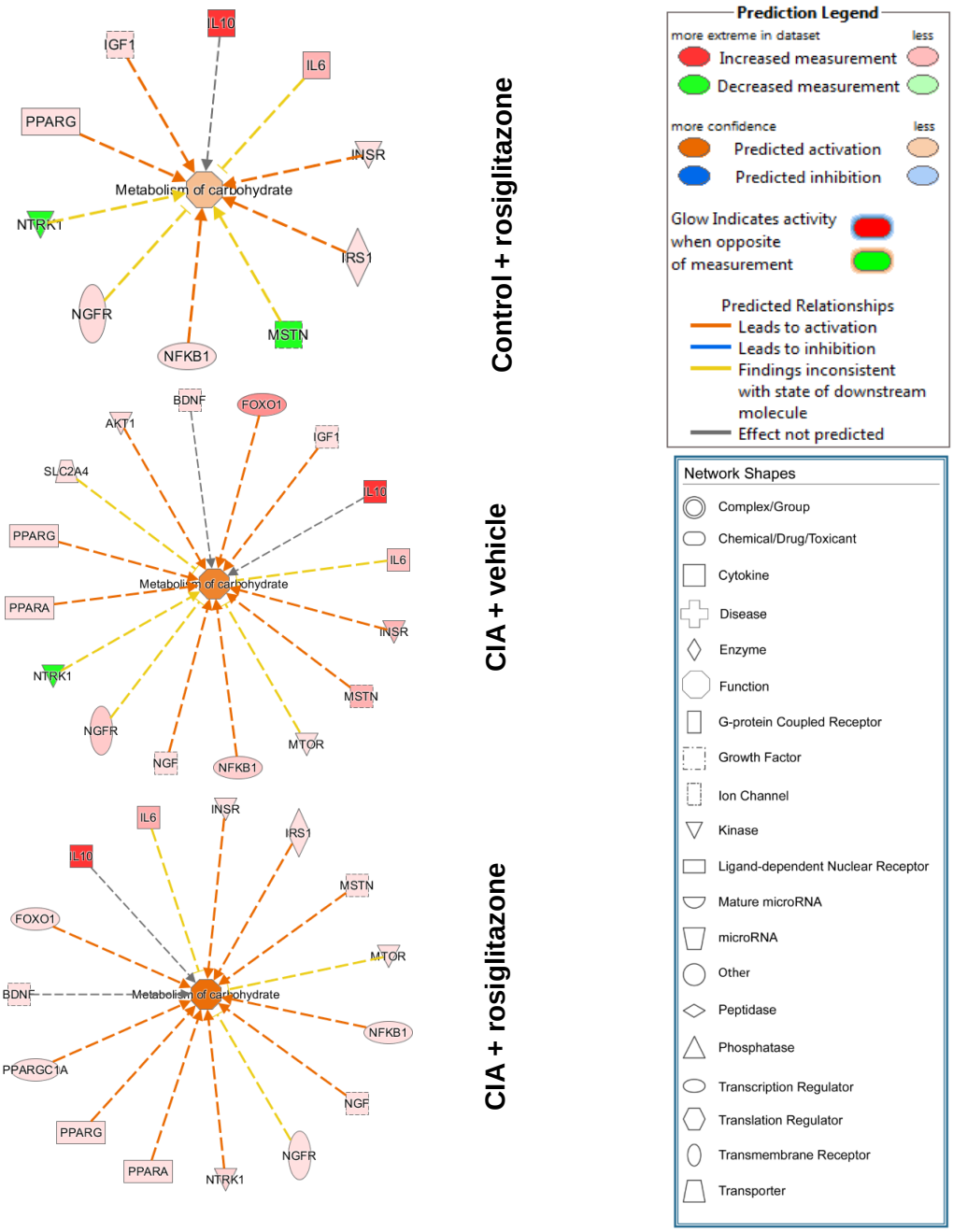


Figure 5.13: IPA prediction of oxidation of lipid in EDL muscle based upon changes in mRNA expression from control + rosiglitazone (n=10), CIA + vehicle (n=10) and CIA + rosiglitazone (n=9) compared to control + vehicle rats. In the outer ring are depicted schematic representation of the most differentially regulated mRNAs and with the colour intensity reflecting greater (red) or less expression (green) compared to control + vehicle. Oxidation of lipids is equally activated in all groups compared to control + vehicle. The centre of each ring indicates the network function connecting the genes by lines and arrows indicating the predicted relationship leading to activation (orange), inhibition (blue) or inconsistent (yellow).



5.14: IPA prediction of oxidation of lipid moieties (energy production) in EDL muscle based upon changes in mRNA expression from control + rosiglitazone (n=10), CIA + vehicle (n=10) and CIA + rosiglitazone (n=9) compared to control + vehicle rats. In the outer ring are depicted schematic representation of the most differentially regulated mRNAs and with the colour intensity reflecting greater (red) or less expression (green) compared to control + vehicle. Oxidation of lipid moieties is equally activated in all groups compared to control + vehicle. The centre of each ring indicates the network function connecting the genes by lines and arrows indicating the predicted relationship leading to activation (orange), inhibition (blue) or inconsistent (yellow).



5.15: IPA prediction of metabolism of carbohydrates in EDL muscle based upon changes in mRNA expression from control + rosiglitazone (n=10), CIA + vehicle (n=10) and CIA + rosiglitazone (n=9) compared to control + vehicle rats. In the outer ring are depicted schematic representation of the most differentially regulated mRNAs and with the colour intensity reflecting greater (red) or less expression (green) compared to control + vehicle. Metabolism of carbohydrates is mostly activated in CIA + rosiglitazone group compared to control + vehicle. The centre of each ring indicates the network function connecting the genes by lines and arrows indicating the predicted relationship leading to activation (orange), inhibition (blue) or inconsistent (yellow).

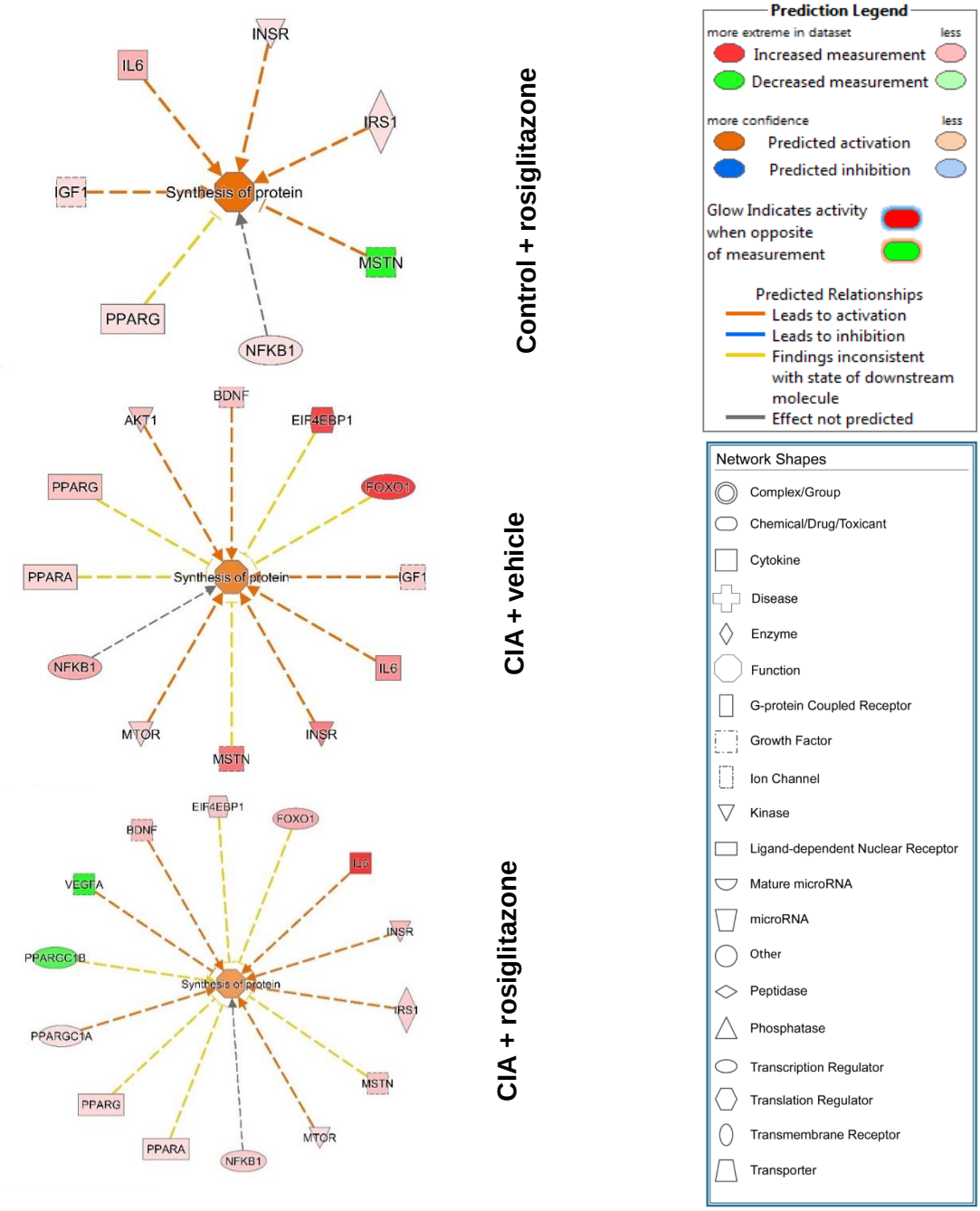


Figure 5.16: IPA prediction of protein synthesis in EDL muscle based upon changes in mRNA expression from control + rosiglitazone (n=10), CIA + vehicle (n=10) and CIA + rosiglitazone (n=9) compared to control + vehicle rats. In the outer ring are depicted schematic representation of the most differentially regulated mRNAs and with the colour intensity reflecting greater (red) or less expression (green) compared to control + vehicle. Protein synthesis is mostly activated in control + rosiglitazone group compared to control + vehicle. The centre of each ring indicates the network function connecting the genes by lines and arrows indicating the predicted relationship leading to activation (orange), inhibition (blue) or inconsistent (yellow).

Expression levels of the following mRNAs involved with lipid oxidation (Fig 5.13 and 5.14), carbohydrate metabolism (Fig 5.15) and synthesis of protein (Fig 5.16) were detected as the most altered genes in EDL muscle from CIA + vehicle and with a lesser extent in CIA + rosiglitazone, compared to control + vehicle rats.

There is a significant increase of Ctsl, Fbxo32, Trim63 and Mt1a in EDL of the CIA + vehicle group compared to controls, indicative of activation of protein degradation (Fig 5.17A). There is also an increase of FOXO1 and Ucp3 in EDL of the CIA + vehicle group compared to controls indicative of mitochondrial and metabolic disruption (Fig 5.17B). Due to variability, the standard error of the mean is wide in a considerably number of genes and the significance of potential dysregulation of expression of genes highlighted in the prediction rossetes is unreached (Fig 5.17).

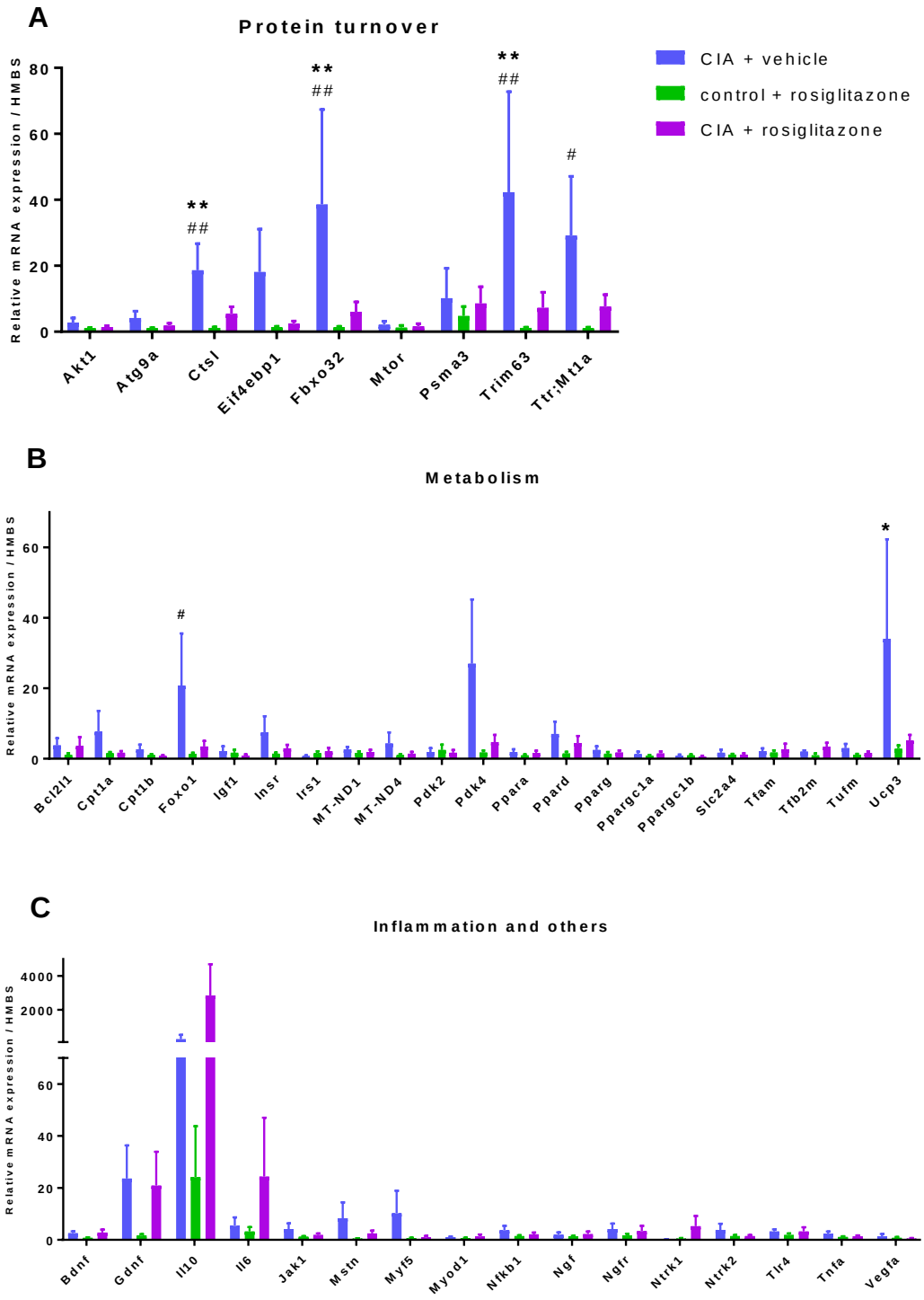


Figure 5.17: Fold-change in EDL mRNA abundance from control + vehicle group (n=10) in control + rosiglitazone (n=10), CIA + vehicle (n=10) and CIA + rosiglitazone (n=9) treated rats. Results are mean ± SEM. Statistically analysed suing non-parametric Kruskal-Wallis test. Differences between CIA + vehicle and control + vehicle groups: *p<0.05, **p<0.01; differences between CIA + rosiglitazone and CIA + vehicle groups: #p<0.05, ##p<0.01.

5.4. Discussion

Rosiglitazone is a PPARɣ agonist used as insulin sensitizer to maintain glucose homeostasis (Rizos et al. 2008; Rizos, Kei, and Elisaf 2016). Moreover, its anti-inflammatory effects have been reflected in the reduction of circulatory cytokines TNFα, IL-1β and IL-6 in different animal models including the CIA model in mouse (Cuzzocrea et al. 2003) as well as in synovium (Koufany et al. 2008) and muscle in a model of sepsis (Crossland et al. 2017). To my knowledge, this is the first study to comprehensively examine the impact of PPARɣ agonism (rosiglitazone) on pain behaviour, joint pathology and muscle metabolism in a rodent model of RA. The CIA model of RA developed inflammation with high levels of cytokine IL-6 in plasma, paw swelling and synovitis accompanied by heightened pain behaviour and altered locomotor activity. This study provides evidence that rosiglitazone administered 14 days before induction of the RA ameliorates inflammation, as evidenced by a reduced paw swelling in the rodent CIA model. However, PWT and locomotor activity in CIA rats did not change with rosiglitazone treatment. These effects of rosiglitazone in CIA rats were accompanied by lower muscle lactate content and unchanged glycogen content compared to CIA + vehicle group, keeping with the activation of muscle carbohydrate metabolism predicted by IPA. Collectively these data suggest a better matching of muscle glycolytic flux with mitochondrial carbohydrate use occurred in the CIA + rosiglitazone treated animals, which may be attributable to rosiglitazone anti-inflammatory properties (Crossland et al. 2017).

Paw swelling was evident in CIA rats, to a similar extent as reported in Chapter 4. Rosiglitazone had a marked effect on paw thickness, which was significantly greater in CIA rats treated with vehicle rather than rosiglitazone. Fewer of the CIA rats treated with rosiglitazone exhibited increases in paw thickness. However, paw thickness and cellular infiltration (synovitis) were significantly correlated ($r=0.525$, $p=0.0101$). Again, I demonstrated that paw thickness significantly correlated to pain ($r=-0.447$, $p<0.01$) and low activity ($r=-0.364$, $p<0.05$) in CIA rats, emphasising that paw swelling and synovitis may cause some discomfort and alter normal activity (Table 5.5).

It is widely believed that joint pain in arthritis leads to reduced locomotor activity and together with inflammation may cause muscle deconditioning and weakness in patients with RA. Although CIA rats exhibited lowered thresholds when testing with a mechanical punctate stimulus and reduced horizontal locomotor activity, these changes in behaviour were not correlated at least at the end of the study. However, the timing of the onset of changes in PWT and horizontal locomotor activity did coincide and it is possible that the study was not adequately powered to identify potential inter-dependencies of these two features of arthritis. The administration of rosiglitazone increased neither PWT nor locomotor activity in CIA rats enough to be significant. This finding is supported by the unmodified nocturnal mobility in adjuvant-induced arthritis (AIA) rats treated with glitazones (Koufany et al. 2008). Therefore there was not a significant positive effect of the PPARɣ agonist on *in vivo* traits of arthritis in the CIA model. It would be advantageous to test if different dose and routes of

rosiglitazone administration in the CIA model have a positive effect on pain relieve in RA. In a model of neuropathic pain, oral administration (30 mg/kg/day) of the thiazolidinedione PPARɣ agonist pioglitazone seven days before surgery and after, decreased mechanical pain responses by PWT test from 7 days after surgery (Morgenweck et al. 2013). Moreover, intrathecal injection of rosiglitazone (100-200 µg/15 µl) to the lumbar region of the spinal cord decreased mechanical pain responses by pinprick test after 30-60 min of injection in a model of neuropathic pain (Morgenweck et al. 2013; Churi et al. 2008).

There was evidence that rosiglitazone had an anti-inflammatory effect in the CIA model with a significant reduction in hind paw swelling and a trend towards a reduction in plasma IL-6 levels. These data support the existing evidence that rosiglitazone may ameliorate inflammation in arthritis, including a reduction in plasma IL-6 levels in a murine model of CIA after 15 days of treatment with rosiglitazone (10 mg/kg/day) from day 21 after CIA induction (Cuzzocrea et al. 2003). Previous findings also support the protective effects of PPARɣ agonists (pioglitazone and rosiglitazone) on the joint inflammation in the AIA rat model and a murine model of CIA respectively (Cuzzocrea et al. 2003; Koufany et al. 2008). However, in my study rosiglitazone did not reduce significantly the synovitis in the tibiotalus joint from CIA rats and it would be interesting to test with different doses and routes of administration. Furthermore, accelerated cartilage degradation and synovitis was evident in a cartilage-specific PPARɣ knock out mice, which suggests that this system controls cartilage homeostasis (Vasheghani et al. 2013).

It is important to study skeletal muscle integrity when employing animal models to induce muscle wasting and metabolic disturbance. In CIA rats, the viability of the muscle integration was maintained comparable to control rats with muscle ATP, PCr and total creatine levels in the normal range for resting EDL muscle in the rodent (Alamdari et al. 2008). Nevertheless, there was evidence of muscle dysregulation with an accumulation of lactate in the EDL muscle in the CIA rats compared to control. Rosiglitazone treatment in CIA rats reduced the lactate concentration in EDL muscle to a comparable level as seen in control rats, which is in keeping with the predicted increased carbohydrate metabolism via IPA. These data are consistent with earlier findings that LPS-induced impairment of carbohydrate oxidation in the rat is reversed by a PPARɣ agonist (Crossland et al. 2017).

Both CIA and rosiglitazone treatment had important effects on the muscle cellular functions compared to control + vehicle rats (Figure 5.10). The predictions in the cellular functions in each group of rats showed that lipid and specific lipid moieties oxidation, carbohydrate metabolism and protein synthesis were activated by CIA and rosiglitazone treatments, indicating that both interventions affected the muscle function independently. Alternatively, the vehicle (HPMC) in which rosiglitazone was suspended may have initiated a muscle metabolic response. Particularly, lipid and its moieties oxidation were activated similarly across groups whereas carbohydrate metabolism was more active and protein synthesis less in the CIA group treated with rosiglitazone (Figure 5.11). These results are in accordance with inflammatory diseases such as obesity, diabetes and sepsis resulting with altered lipid, fatty acid and carbohydrate oxidation (Al-

Khalili et al. 2006; Alamdari et al. 2008). Particularly, RA patients and CIA model have an increase of skeletal muscle fat, which is associated with inflammation and reduced physical function (Khoja et al. 2018; Alabarse et al. 2018). The increase of fat mass and adipose tissue stores are a constant source of lipolysis releasing circulatory fatty acids and triglycerides in plasma, which together with inflammatory cytokines contribute to dysregulated carbohydrate metabolism and insulin resistance in skeletal muscle (Andersson et al. 2008; Tsintzas et al. 2007). Furthermore, PPARɣ are known to regulate glucose homeostasis and lipid metabolism in skeletal muscle (Amin et al. 2010) in addition to its anti-inflammatory effects (Cuzzocrea et al. 2003; Crossland et al. 2017).

When reducing inflammation by rosiglitazone administration, it has a differential impact with the greatest activation on carbohydrate metabolism and reduced protein synthesis, consistent with the reduced lactate content and myostatin mRNA expression found in the CIA + rosiglitazone group. The upregulation of the anti-inflammatory cytokine IL-10, with high intensity in carbohydrate metabolism, and pro-inflammatory cytokine IL-6 influencing energy production, with different intensity in all groups compared to control + vehicle group may indicate the origin of the metabolic changes found in muscle. It was found that IL-6 promoted lipid and fat oxidation and together with IL-10, they modulated glycogen in primary skeletal muscle cultures, L6 myotubes and mouse gastrocnemius promoting insulin resistance (Carey et al. 2006; Al-Khalili et al. 2006; Kim et al. 2004).

The IPA predictions point that despite the activation of lipid oxidation, carbohydrate metabolism and protein synthesis in all groups compared to

control + vehicle, different altered genes may lead to those events in each group. The proposed signalling pathway in the hypothesis mediating inflammation-induced muscle metabolism and mass dysregulation, was the PI3K-Akt-FOXO axis as identified in catabolic states. Taking into account that other mechanisms may be involved, the mRNA upregulation of factors from the PI3K-Akt signalling were identified. Albeit PI3K and Akt were not dysregulated, whose phosphorylation would need to be determined by a different method, FOXO1 was highest in CIA + vehicle rats, suggesting an activation of lipid and carbohydrate oxidation and being inconsistent with protein synthesis, probably due to its role in activating protein degradation. As demonstrated previously in a sepsis model, Akt dephosphorylation activates FOXO, known to regulate the carbohydrate and protein metabolism via the expression of FOXO-dependent transcripts such as PDK4 and atrogenes (Crossland et al. 2008). Both the activation of lipid and fatty acid oxidation and activation of carbohydrate metabolism involves cross-talk in genes dysregulated on inflammatory states. It may be indicative that reduced of insulin signalling in skeletal muscle associated with inflammation in CIA rats may be induced not solely by carbohydrate metabolic pathway, as demonstrated in LPS-induced model (Crossland et al. 2017), but also by lipid and fatty acid metabolism, as long chain fatty acids induce PDK4 expression (Tsintzas et al. 2007; McGrath and Young 2015). In patients with RA and mouse CIA model, inflammation triggered IR, which was correlated to defective muscle carbohydrate and lipid metabolism (Arias de la Rosa et al. 2018). In RA is widely recognised the development of dyslipidaemia contributed to cardiovascular comorbidities

(Soubrier et al. 2014). Knowing that PPARs, especially PPARα and PPARɣ subtypes, regulate energy homeostasis through control of lipids and carbohydrate metabolism (Berger and Moller 2002), in addition to the anti-inflammatory effects (Ricote et al. 1998), rosiglitazone may alter dyslipidaemia. However, the mechanisms and mediators underlying the metabolic dysregulation in skeletal muscle in RA is unresolved.

RA and the CIA model have been associated with muscle atrophy, probably due to inflammation. RA patients tend to have sedentary behaviour and low physical activity in response to pain and fatigue. Muscle weakness and atrophy is reported in patients and animal models of RA. In patients with RA, muscle performance is reduced, maintaining body weight with an increase of fat mass (MATSCHKE et al. 2010) resulting with molecular alterations associated to disease activity and disability (Huffman et al. 2017). In the murine CIA model, there was a loss of muscle weight and reduced sarcoplasmic ratio and diameter, reduced cross-sectional area and increased MuRF1 (Alabarse et al. 2018; de Oliveira Nunes Teixeira et al. 2013). Also, AIA rats had reduced cross-sectional area and increased expression of muscle atrogenes MuRF1 and MAFbx (Gómez-SanMiguel et al. 2016) indicative of muscle atrophy.

In contrast, CIA rats in this study did not have altered muscle protein:DNA content. The protein:DNA ratio indicates the increase or decrease of muscle mass in total protein content. It has been demonstrated that reduced protein:DNA in systemic and inflammatory diseases are associated with the activation of protein degradation (Crossland et al. 2008; Mallinson et al. 2015). As IPA predicted, protein synthesis was activated in CIA rats and

reduced in rats treated with rosiglitazone. However, the genes involved most upregulated in CIA + vehicle rats were FOXO1 and Eif4bp1, which is inconsistent with protein synthesis. As mentioned, FOXO1 activates the downstream factors for protein degradation (i.e: MuRF1, MAFbx and Cathepsin-L) and Eif4bp1, which suppresses Eif4E (mRNA translation initiation factor) inhibiting protein synthesis (Sandri et al. 2004; Terada et al. 1994). However, no indices of muscle mass loss was found when studying protein:DNA content. Interestingly, myostatin tended to be upregulated in the CIA + vehicle group and was downregulated in CIA rats treated with rosiglitazone. Myostatin is a growth factor inhibitor that reduces muscle regeneration and contributes to the loss of skeletal muscle mass. Therefore, it is suggested that in CIA model, the dysregulation of skeletal muscular system development and function (figure 5.10) may be mediated by the increase of myostatin, whose mRNA expression was less in rats treated with rosiglitazone. It would be important to identify PPARɣ targets that reduce Mstn expression in RA as it is also reported that PPARα reduces Mstn in the AIA model of RA (Castillero et al. 2011).

In summary, the CIA model of RA is a robust model of inflammation exhibiting paw swelling and increases in plasma IL-6 and features of RA: pain, low locomotor activity, synovitis and muscle metabolic dysregulation but no atrophy. EDL muscle from CIA rats exhibited alterations in the mRNA expression of several genes involved in metabolic and protein metabolism reflected with the accumulation of lactate but no alkaline-soluble protein:DNA ratio. In CIA rats, the administration of PPARɣ agonist rosiglitazone reduced paw swelling, but effects on the other features of RA

did not reach significance. Interestingly, plasma IL-6 levels were ameliorated by the administration of rosiglitazone, which modulated the gene expression towards more active carbohydrate metabolism, lipid oxidation and protein synthesis. In this study, the identification of genes with altered expression due to inflammation can help future research to identify the cause of muscle dysregulation in the CIA model of RA with new targets.

Chapter 6:

General Discussion

6.1. Overview of findings

There are many physiological and pathophysiological changes associated with OA and RA, including muscle weakness in early and established disease (Lewek, Rudolph, and Snyder-Mackler 2004; Helliwell and Jackson 1994). The hypothesis of the thesis was that joint inflammation in arthritis will impact behavioural pain and activity, and skeletal muscle function. Therefore, this thesis aimed to identify whether dysregulated muscle metabolism is present in arthritis, which may contribute to associated dysregulation of muscle carbohydrate metabolism, wasting and weakness, similar to other inflammatory states, such as COPD and sepsis. Using established animal models of OA and RA, I investigated the potential contribution (s) of local and systemic inflammation to changes in muscle metabolism and muscle mass.

The surgical model of OA exhibited clear joint pathology and pain behaviour but did not result in reduced activity (Fig 6.1), and neither systemic or muscle inflammation was evident, nor was there any evidence of overt muscle necrosis/pathology based on muscle ATP and phosphocreatine levels. Muscle lactate and protein content in the fast-twitch EDL muscle of the model of OA was comparable to that of control rats, consistent with the unaltered activity and inflammatory status. By contrast, in the CIA model of RA there was overt paw swelling and systemic (Fig 6.2) and muscle inflammation, which coincided with the accumulation of lactate in the EDL muscle (Fig 6.3).

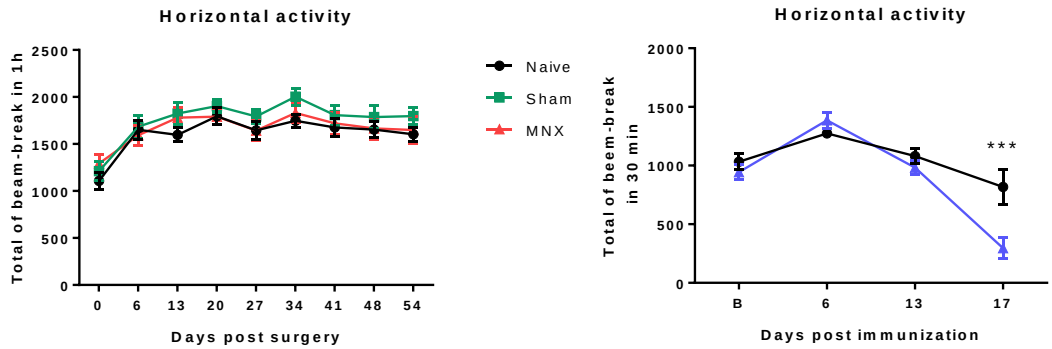


Figure 6.1: Comparison of locomotor activity in MNX rats with knee OA and CIA rats with RA. MNX (n=20 from day 0 to day 28; n=10 from day 29 to day 55) rats did not differed on locomotor activity compared to controls whilst it was reduced on CIA rats (n=9). ***p<0.001. For reference see Fig 3.3 and Fig 4.3.

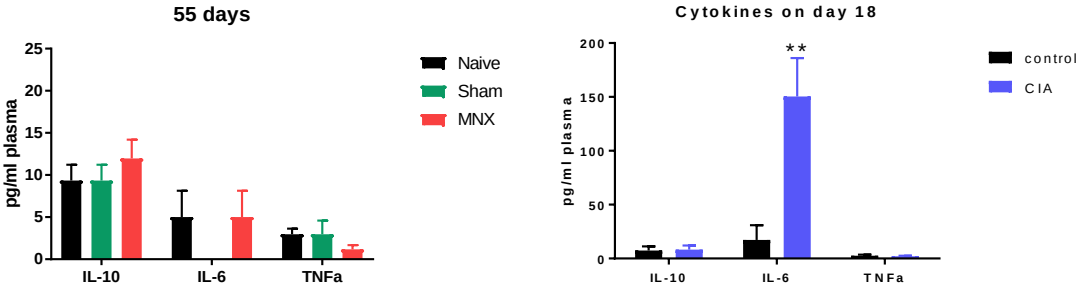


Figure 6.2: Comparison of systemic inflammatory markers in MNX rats with knee OA and CIA rats with RA. Cytokines IL-10 and TNFα were not significantly different in MNX and CIA rats compared to their respective controls whereas IL-6 content was high in plasma of CIA rats. **p<0.01. For reference see Fig 3.4 and Fig 4.4.

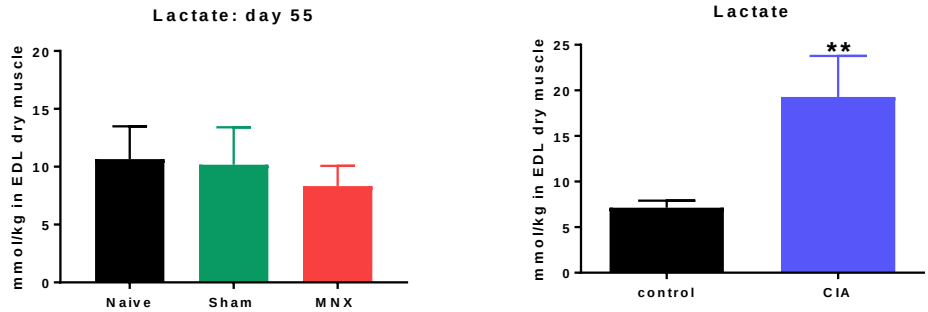


Figure 6.3: Comparison of lactate accumulation in EDL muscle from MNX rats with knee OA and CIA rats with RA. Lactate was stable compared to controls whereas was significantly increased in CIA rats. **p<0.01. For reference see Fig 3.7 and Fig 4.7.

Furthermore, changes in gene expression in the EDL muscle in the CIA model, compared to control, suggest the inhibition of carbohydrate metabolism and activation of protein metabolism. In the clinical study, genes altered in the CIA model were quantified in muscle from RA patients compared to age-matched healthy volunteers. There were some differences and similarities in gene expression and the findings in the clinical samples did not mirror those in the CIA model. Patients with RA had muscle inflammation and high levels of PDK4 suggesting disrupted muscle carbohydrate metabolism. Proteolytic factors in the human RA muscle were not significantly different to control samples. However, MT1A and myostatin levels were upregulated in the muscle samples from the RA patients, compared to the healthy volunteers.

PPARɣ is an insulin sensitising agent which has anti-inflammatory effects and has been shown to ameliorate muscle lactate accumulation, blunt increases in mRNAs and proteins associated with protein degradation and spare EDL muscle protein content in LPS-induced endotoxaemia (Crossland et al. 2017). It was hypothesised that rosiglitazone administration might alter the progression of the changes in the CIA model of RA. There was evidence that treatment with rosiglitazone had a blunting effect on inflammatory responses, reducing paw swelling (but not synovitis score) and reducing circulating levels of cytokines. Rosiglitazone treatment of CIA rats was associated with differences in muscle lactate levels and gene expression in the EDL muscle, compared to CIA rats treated with vehicle, predicting activation of carbohydrate metabolism and lipid oxidation as well as protein synthesis.

The effects of rosiglitazone in the model of RA are consistent with the anti-inflammatory effects of pioglitazone in RA patients, reducing levels of inflammatory markers in plasma, but not joint swelling (Ormseth et al. 2013). Previous pre-clinical studies have shown that pioglitazone and rosiglitazone reduced synovium inflammation but did not alter cartilage lesions in the ankle joint in the adjuvant-induced arthritis model in the rat (Koufany et al. 2008). My novel data that rosiglitazone alters muscle gene expression in the CIA model of RA advances understanding of the events underlying muscle wasting in RA and has the potential for the identification of new targets for treatment.

6.1.1. Inflammation and physical inactivity in arthritis

6.1.1.1. Inflammation

It is well established that different forms of arthritis impact differently on disease progression, symptoms and especially muscle functionality. OA was previously categorised as a mechanical disease, but nowadays it is considered that inflammation has an important role in disease progression (Scanzello and Goldring 2012). In accordance to the results in this thesis, the MNX and CIA models are good models for OA and RA, respectively, both from the perspective of pathology and pain showing similarities to human features. Despite synovitis being present in both MNX rats and patients with OA; there is a lack of evidence for systemic and muscle inflammation in animal models. Inflammation is a major indicator of muscle atrophy and dysregulation of metabolic flux, including insulin resistance. My findings are consistent with previous studies in other models of OA (DMM

and ACTL) which reported no change in muscle mRNA expression for inflammatory cytokines (van der Poel et al. 2016; Silva et al. 2018). Nevertheless, patients with OA exhibit muscle and systemic inflammation, with high levels of IL-6 protein and TNFα, MCP-1 mRNA in muscle and IL-6 in serum (Levinger, Levinger, et al. 2011; Penninx et al. 2004). These differences between the animal models and clinical OA may reflect the long duration that people have OA compared to the relatively short OA models. Another factor may be that the animal models of OA are generated in young animals whereas OA is a disease of older people, generally > 50 years old. RA is an autoimmune disease with a very high inflammatory response in different tissues including muscle and synovium. Consistent with my data generated in the CIA model in this thesis, multiple animal models of RA have identified high levels of IL-6 in serum (Alonzi et al. 1998; Tanimoto et al. 2015), consistent with data from RA patients (Kokkonen et al. 2010), as well as muscle inflammation (Gómez-SanMiguel et al. 2016). The changes in muscle mRNA for cytokines from RA patients identified in this thesis are consistent with changes in previous studies (Huffman et al. 2017).

6.1.1.2. Physical activity

Physical inactivity is an important determinant of muscle quality and functionality that is associated with muscle atrophy and metabolic flux dysregulation. The majority of pre-clinical models of OA, including MNX in this study, fail to reproduce the reduced physical activity seen in OA patients (Silva et al. 2018), except reduced vertical activity in the ACLT + pMMX model (Hamilton et al. 2015). The duration of the pre-clinical studies compared is the same, 8 weeks. Physical inactivity is a common feature in

patients with OA probably due to pain and associated inflammation (Dekker et al. 1993). Indeed, the inflammatory response of high IL-6 protein and increased TNFα mRNA in the vastus lateralis muscle of OA patients is associated with greater physical disability, slower gait velocity and impaired knee function during walking coinciding with a loss of muscle strength as seen in muscle disuse atrophy (Levinger, Levinger, et al. 2011; Levinger, Caldow, et al. 2011). Also, increased serum levels of IL-6 was associated with slow walking speed in patients with knee OA (Penninx et al. 2004). Reduced physical activity in OA is associated with increased mortality in patients, being at risk of death from cardiovascular diseases (Nüesch et al. 2011).

Physical activity was reduced in the CIA model implemented in this study coinciding with additional results from different pre-clinical models (Alabarse et al. 2018; Sasakawa et al. 2005; Tanimoto et al. 2015), as well as sedentary behaviour was persistent in patients with RA (Fenton et al. 2018). Low physical activity in RA patients is inversely correlated with disease activity and metabolic syndrome (Hernández-Hernández, Ferraz-Amaro, and Díaz-González 2014).

6.1.2. Muscle atrophy and metabolic flux in arthritis

Several studies identified that muscle wasting, and inflammation in chronic diseases results in cachexia, characterised by the loss of body cell mass (BCM) (Roubenoff et al. 1994). Rheumatoid cachexia differs from classic cachexia (muscle wasting with reduced body weight in chronic illness) as loss of body weight is unusual in patients with RA. Muscle wasting often

occurs alongside the maintenance or increase of total fat mass and maintained or reduced lean body mass (Elkan et al. 2009; Tournadre et al. 2017). In rheumatoid cachexia, reduced physical activity is associated with increased fat mass resulting from low energy expenditure and increased fatigue and weakness (Roubenoff et al. 2002), which would alter lipid storage and metabolism, consistent with lipid and fatty acid oxidation being the most altered cellular function seen in CIA in this thesis. Blunting inflammation with the PPARɣ agonist rosiglitazone resulted in increased lipid oxidation and carbohydrate metabolism at the gene expression level. Both physical inactivity, as seen in CIA rats, and PPARɣ intervention modulate lipid metabolism in skeletal muscle (Tontonoz and Spiegelman 2008).

An activated inflammatory system has energy demands that may be driven by cytokine-induced stimulation (mainly by IL-6) of the central nervous system, endocrine organs and energy storage organs such as skeletal muscle (Straub et al. 2010). Both fatty acid metabolites and inflammatory cytokines may lead to insulin resistance activating the serine phosphorylation of IRS1 that prevents the downstream insulin signalling cascade (Aguirre et al. 2002). In this thesis, the mRNA expression of genes associated with insulin signalling, including GLUT4 (Slc2a4) and IRS1, were downregulated in EDL muscle of CIA rats, consistent with the accumulation of lactate and less glycogen. Additionally, a contributing factor to metabolism regulation was the upregulation of the gene MT1A, a marker of stress oxidation that participates in the cellular defence against free radicals activated by cytokines (Nath et al. 2000). These findings suggest a role of

cellular stress conditions in the EDL muscle of CIA rats, probably caused by inflammation.

This study supports the hypothesis that in the CIA model of RA, inflammation accompanied by muscle disuse dysregulates muscle carbohydrate and lipid metabolism that may lead to insulin resistance. In RA patients, there is a large heterogeneity in different cohorts, but all them exhibit systemic inflammation and insulin resistance (Nicolau et al. 2017).

6.1.2.1. Regulation of muscle mass in CIA rats, a cross-talk with insulin signalling

Increased levels of circulating cytokines TNFα, IL-6 and IL-1β are associated with muscle wasting and insulin resistance in rheumatoid arthritis (Svenson et al. 1988; Yamaguchi et al. 2003). Given that insulin inhibits muscle protein degradation (Wang et al. 2006), the association of insulin resistance and muscle wasting via inflammatory response may explain the cross-talk found in RA and chronic diseases (Crossland et al. 2008). Total protein:DNA content of the EDL muscle tended to be lower, while total body weight was not significantly different in the CIA rats compared to controls on day 17 after immunisation (Annexe 2). At the mRNA level, there was evidence for dysregulation of genes involved in protein metabolism in the EDL of CIA rats, compared to controls. Overall, the data support the use of the CIA model to study muscle wasting in RA. This statement is supported by previous additional studies where decreased free exploratory locomotion, reduced muscle strength, fatigue

and muscle loss maintaining normal body weight were found in the CIA model in mice (Alabarse et al. 2018).

Insulin resistance is associated with unbalanced protein turnover accompanying muscle loss in obesity and diabetes (Wang et al. 2006) as well as in RA (Müller et al. 2017). The phosphorylation of downstream factors from insulin receptor is mandatory to regulate the signalling pathway PI3K-Akt-FOXO by IRS1 activity. In inflammatory conditions, the phosphorylation cascade in the signalling pathway is disrupted, leading to activated protein degradation, less protein synthesis and blunted insulin signalling (Aguila, Claffey, and Kirwan 1999; Wang et al. 2006). In CIA rats, there was a higher proteolytic and low protein synthesis and carbohydrate metabolic gene expression compared to control (LECKER et al. 2004; Crossland et al. 2010). Accordingly, the protein:DNA ratio tended to be low compared to control rats. Rosiglitazone treatment was predicted to increase gene expression associated with protein synthesis, potentially related to proteins involved in many cellular functions such as carbohydrate and lipid oxidation.

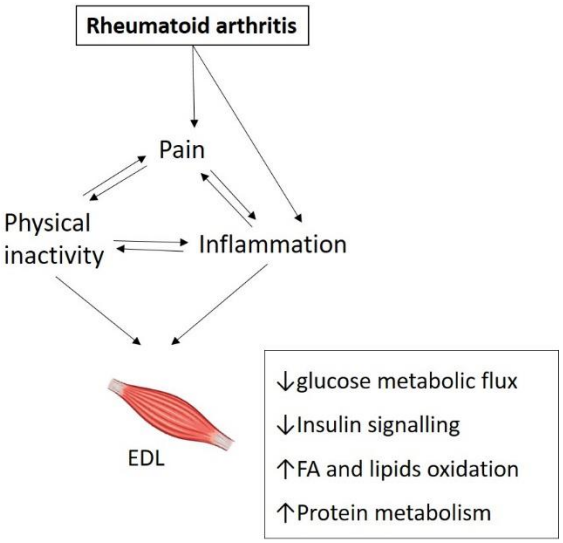


Figure 6.4: Schematic diagram of RA-induced muscle metabolic function in the EDL from CIA rats. RA is characterised for the development of pain and inflammation, both leading to reduced physical activity creating a vicious cycle. Muscle disuse and inflammation are causes for altered metabolic regulation leading to low glucose metabolic flux, insulin signalling and greater FA and lipid oxidation as well as protein metabolism.

6.2. Future directions for research

6.2.1. Adapting the MNX model of OA to human disease symptoms

The MNX model of knee OA seems to be a mild model unable to mimic the inflammatory and physical activity conditions occurring in patients with knee OA, at least up to 55 days of post-surgery. Given that the overweight is an important risk factor that widely affects patients developing knee OA, the introduction of fat high diet in MNX rats may aggravate the symptoms of the disease. Obesity can lead to mechanical stress in the joints as well as systemic inflammation with associated metabolic disorders. Obesity is classically defined as an imbalance of energy intake and energy expenditure but the underlying mechanisms from high fat diet are more complex (Murphy, Velazquez, and Herbert 2015). It is reported that high fat diet induces an inflammatory response in rats altering the gut microbiota and by direct effects of fatty acids on intestinal cells leading to systemic inflammation (Sanmiguel, Gupta, and Mayer 2015). Pro-inflammatory factors such as cytokines and fatty acids accumulates in plasma triggering inflammation to the peripheral tissues, including brain, liver, adipose tissue and skeletal muscle (this last including lipid accumulation) (Bleau et al. 2015). On the other hand, obesity is associated with the systemic release of adipocytokines and adipokines, which are pro-inflammatory cytokines, primarily by abdominal adipose tissue causing a low-grade inflammatory state involved in damage to many peripheral tissues, including joint tissues (Berenbaum 2013). It is stablished that high fat diet exacerbates OA development after transacted meniscus in mice, independently of weight gaining (Mooney et al. 2011). In patients, saturated fatty acids aggravates

structural knee OA, while unsaturated fatty acids may ameliorated its progression (Lu et al. 2017).

Additionally, aging is a major risk factor contributing to muscle atrophy (sarcopenia) and inflammation (Sanada et al. 2018). Since OA develops mainly >40 years old, aging is considered a risk factor associated to disease. Measuring muscle metabolic and atrophy factors after inducing OA in old rats could result in a model with a similar stage than patients.

6.2.2. Muscle disuse, fatigue and disability

Given that the CIA model resulted in reduced locomotor activity, which is related to sedentary life in patients with RA and associated with increase fat mass, measuring muscle strength and endurance exercise performance would add relevant information. LMA boxes are limited to measure only the number of movements, but it does not measure the capacity and disability of each rat with precision. Muscle strength and endurance exercise in a treadmill measures the distance walked, velocity and time that rats can spend, being able to identify fatigue and disability in the CIA rats compared to control and associate it with muscle dysfunction.

6.2.3. Effects on muscle function in CIA by inhibiting pain

Currently, the treatment of pain is a big problem for patients suffering from any form of arthritis. As described in Chapter 1, analgesics and anti-inflammatory treatments are not effective for the long-term treatment of OA and RA pain. In this study, blunting, at least partly, inflammation with rosiglitazone treatment in CIA rats resulted in less muscle lactate content and reduced dysregulation of metabolism. Despite of a partly reduction of

inflammation, locomotor activity was still reduced in CIA groups with rosiglitazone treatment, therefore both muscle disuse and inflammation may be involved with muscle metabolic dysregulation. Administering an analgesic drug to reduce pain but not inflammation, may improve locomotor activity in CIA rats. Therefore, it would be able to identify the metabolic muscle changes and gene expression induced only by inflammation. Given that slow-twitch muscles are more susceptible to changes conducted by muscle disuse and immobilisation, the analysis of Soleus muscle would need to be analysed too.

6.2.4. Overview of body homeostasis and the origin of metabolic dysregulation and inflammation in CIA

It would be advantageous to explore heterogeneity in skeletal muscle inflammation. Specifically, if different muscles respond in a similar manner in the CIA model. The metabolic flux and inflammation in muscle can be influenced by many circulatory factors coming from distant tissues induced by the autoimmune response. Using untargeted metabolomics would be interesting to explore tissue-specific metabolic finger prints and insulin resistance in response to CIA in different tissues, including skeletal muscle, adipose tissue, fat mass, blood, etc, during a time-course. It would help to identify the origin of its dysregulation and how it is spread to different tissues, quantifying the metabolites involved in the carbohydrate and lipid metabolism and protein turnover at once in each tissue and determine the cause of insulin resistance in RA. This could be achieved by measuring fat and carbohydrate oxidation rate using stable isotope tracers as well as energy expenditure using calorimetry chambers.

6.2.5. Molecular analysis for muscle atrophy in the CIA model

Myostatin is a negative regulator of muscle protein synthesis. Despite the unchanged protein:DNA ratio in EDL muscle from CIA rats, myostatin was downregulated in EDL muscle from rats treated with rosiglitazone and upregulated in patients with RA. Myostatin was identified to be upregulated in muscle from critically ill patients, which was accompanied with muscle atrophy, and it was reduced during rehabilitation after 2 weeks of bed rest (Constantin et al. 2011; JONES et al. 2004). The mechanism (s) by which myostatin modulate protein metabolism have not been studied in detail in models of RA. PPARα and ɣ agonists are known to downregulate myostatin expression in muscle in models of RA (Castillero et al. 2011). However, the involvement myostatin in muscle wasting and metabolism in RA is poorly understood. Determining the expression of myostatin receptors (ActRIIB) and downstream factors in a time course will help to identify its implication in muscle dysregulation in RA by muscle disuse and inflammation. Additionally, measuring the expression of IGF-PI3K-Akt signalling pathway at the protein level as well as its downstream factors, the overview of muscle disuse and inflammation induced muscle atrophy in CIA would be interpreted with more precision.

6.2.6. *In vitro* models

The *in vitro* models from human cell lines from different tissues could help understanding the metabolic dysfunction in muscle cells associated with the disease. Co-culturing muscle and synovial fibroblast cells from early and/or late stages of OA or RA patients would serve as a good model to study

signalling mechanisms of impaired carbohydrate oxidation. Using various genetic and pharmacological interventions, it would be possible to explore how synovial fibroblasts influence muscle function and metabolism.

6.3. Limitations in this study

In this thesis, the major objective was to identify potential changes in muscle metabolism and atrophy in the EDL muscle in models of arthritis. The use of animal models can be very beneficial for research, allowing the control of many variables present in clinical studies, as well as the short time needed for a single study, short breeding time and lifespan. Moreover, working with pre-clinical models allows analysis of multiple entire tissues from the same animal to explore the full body instead of a small biopsy as is the case in humans. However, in arthritis, even though MNX and CIA pathology are similar to human OA and RA respectively (Bendele et al. 1999; Bendele 2001), the findings do not strictly extrapolate to humans. For instance, rats grow throughout most of their lifespan with protein turnover and metabolic rate greater than in humans (Agoston 2017). Rat models develop rapidly in young-adult age whereas arthritis and pain progress slowly in humans predominantly from middle age.

Moreover, it is difficult to predict the start of the onset of disease in patients, which can be monitored in pre-clinical models. In MNX rats, disease pathology and symptoms develop quickly but progressively. In the rat CIA model implemented in this study, the onset of disease when swelling appears spontaneously is between 12-18 days, at which point the model

was used for the mechanistic studies. Therefore, these studies were performed in the early stages of RA instead of the mid and late-chronic stages, which is possibly most relevant to the human disease. The study could not be prolonged to later stages due to UON Home Office recommendations and rats were terminated when paw oedema appeared. Nevertheless, temporal changes in inflammation and muscle integrity before swelling appears may be important factors in the progression of the disease and muscle metabolism, as systemic inflammation is detected up to 10 years prior to the development of RA in humans, in the pre-clinical phase (Ridgley, Anderson, and Pratt 2018; Deane et al. 2010).

In both OA and RA, muscle biopsies are mainly from quadriceps in humans. In animal models, quadriceps is also a recurrent muscle due to its dimensions and proximity to human analysis. It is a muscle supporting a reasonable part of the body weight, composed of slow- and fast-twitch fibres. In this study, EDL was chosen due to its composition of fast-twitch fibres, which are the most susceptible to inflammatory-induced muscle changes (Tiao et al. 1997; Ciciliot et al. 2013). This is an additional limitation to take into account when comparing results from other studies, particularly with patients, as the type of muscle analysed may be different. Furthermore, in arthritis the modulation of muscle metabolism may arise not only due to inflammatory states, but also muscle disuse. Analysis of slow-twitch muscle such as soleus, would advance mechanistic understanding of the processes of atrophy and metabolism regulation in a muscle susceptible to changes related to muscle disuse, immobilisation and denervation (Ciciliot et al. 2013).

The composition of the skeletal muscle during disease can vary from healthy conditions, consisting of inflammatory cells and fat mass as well as muscle fibre cells. Infiltration of inflammatory cells into the muscle during inflammatory conditions likely alters the parameters measured. In RA, autoimmune and inflammatory cell function depends on metabolic conditions to regulate glucose utilisation for energy production and cell survival. Immune and inflammatory cells need glucose to complete their functions, such as cytokine synthesis and macrophage maturation, produce energy by glycolysis and activate lipid oxidation (Perl 2010; Michalek et al. 2011; Krawczyk et al. 2010; Roiniotis et al. 2009; Tannahill and O'Neill 2011). Therefore, although the greatest proportion of cells will be muscle cells compared to infiltrating inflammatory cells, it is not entirely evident my findings arise exclusively from muscle cells. An accumulation of lactate was also found in RA joints from increased inflammatory-induced glycolysis (Haas et al. 2015). Also, it is increasingly evident that there is an increase in fat mass in muscle from patients and models of RA (Tournadre et al. 2017; Alabarse et al. 2018).

Interpretation of my data must also consider that changes quantified at the mRNA level were not confirmed at the protein level. The PI3K-Akt-FOXO signalling pathway is a major regulator of carbohydrate and protein metabolism. However, AKT and FOXO phosphorylation were not measured to quantify its activation as well as PDC activity, which would help to interpret the lactate accumulation in the muscle. Moreover, carbohydrate and fatty acids oxidation rates and intermediary metabolites were not measured, except lactate and glycogen.

In this study, the number of samples and information received from patients with RA was limited. To better study the effects on gene expression in patients with RA, a larger number of samples and the analysis of the same genes as in the TLDA cards in CIA would give a better overview of muscle mechanisms regulating muscle mass and metabolism under disease. Although studies to identify the cause (s) of the molecular events in RA patients are of considerable research benefit, current drug treatments need to be considered when interpreting the findings. Additionally, in this study, the muscle samples were taken in different stages of disease. It would be important to differentiate between early and late stages as well as considering collecting muscle from patients during disease flare.

6.4. Conclusions

This thesis confirms that RA has a greater disease severity than OA. Muscle disuse and inflammation were only detected in the CIA model of RA with the consequent alterations in muscle mass and metabolic regulation. The changes in mRNA expression in RA depict the presence of muscle protein, carbohydrate and lipid metabolism activation modulated with rosiglitazone.

The findings in this study contribute to understand better the mechanism regulating muscle wasting and metabolism in RA, being the CIA model representative of rheumatoid cachexia. Muscle wasting and disability in arthritis are major problems in patients that need to be targeted and resolved for an accurate treatment in order to reduce morbidity and premature mortality.

Annexe 1

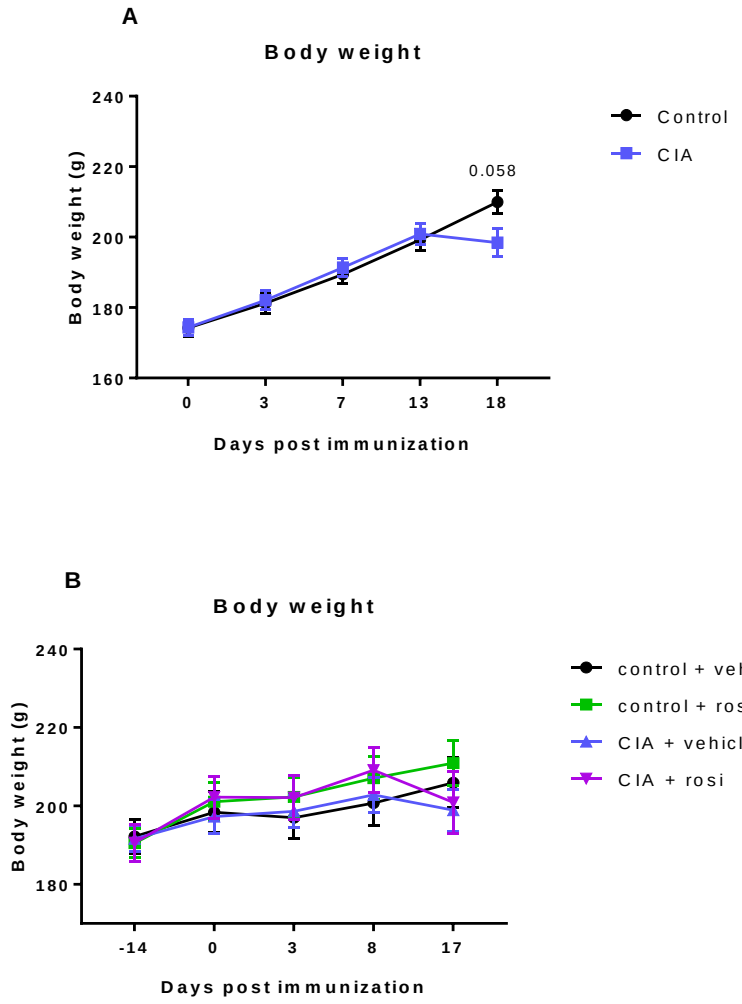
Chapter 4 - Correlations of genes investigated with carbohydrate metabolites, protein:DNA ratio and inflammation.

Variables	Lactate	Glycogen	Protein:DNA	IL-6	TNFα
Protein metabolism					
Ctsl	**0.7234*** **	**-0.5294***	**-0.4778***	0.4987	-0.1253
Eif4ebp1	**0.6928****	**-0.4935***	**-0.5648***	0.2664	-0.2596
Fbxo32	**0.7796*** **	**-0.5018***	**-0.5318***	0.3529	-0.1804
Mt1a	**0.5377***	-0.3622	-0.4241	0.5098	-0.3319
Psma3	**0.5638***	-0.3211	-0.3304	0.2734	0.0901
Trim63	**0.6474****	-0.4522	**-0.539***	0.3148	-0.3626
Energy metabolism					
Foxo1	**0.5992****	-0.2665	**-0.4721***	0.3259	-0.3366
Irs1	**-0.6085****	0.4463	**0.5207***	-0.4134	0.3194
Pdk4	0.4345	-0.2797	-0.4469	0.1059	**-0.5473***
Ppara	**-0.4799***	**0.5067***	**0.5232***	-0.3482	0.2923
Ppargc1a	-0.3748	0.3118	**0.4925***	-0.1142	0.4202
Ppargc1b	**-0.634****	**0.5111***	**0.5534***	-0.3487	0.2816
Slc2a4	**-0.4716***	0.3973	0.356	-0.3371	0.1077
Tfam	**0.4781***	-0.4399	-0.2943	0.4123	-0.0286
Ucp3	**0.5542***	-0.4324	**-0.5026***	0.2842	-0.3187
Vegfa	**-0.5885***	0.443	**0.475***	-0.3984	0.2747
Cytokines					
IL-6	0.0052	-0.2797	0.0155	**0.6547***	-0.0725
TNFa	-0.1115	-0.2261	-0.2261	0.0056	**-0.5956***

Data are shown as Pearson correlation coefficients. In bold are the significant *P*-value: *p<0.05, **p<0.01.

Annexe 2

Body weight in CIA rats compared to control in chapter 4 (A) and with interventions (B) in chapter 5.



References

Agoston, Denes V. 2017. 'How to Translate Time? The Temporal Aspect of Human and Rodent Biology', *Frontiers in neurology*, 8: 92-92.

Aguiar, Grazielle Cordeiro, Marcela Rêgo Do Nascimento, Aline Silva De Miranda, Natalia Pessoa Rocha, Antônio Lúcio Teixeira, and Paula Luciana Scalzo. 2015. 'Effects of an exercise therapy protocol on inflammatory markers, perception of pain, and physical performance in individuals with knee osteoarthritis', *Rheumatology International*, 35: 525-31.

Aguila, Luis F. del, Kevin P. Claffey, and John P. Kirwan. 1999. 'TNF-α impairs insulin signaling and insulin stimulation of glucose uptake in C2C12muscle cells', *American Journal of Physiology-Endocrinology and Metabolism*, 276: E849-E55.

Aguirre, Vincent, Eric D. Werner, Jodel Giraud, Yong Hee Lee, Steve E. Shoelson, and Morris F. White. 2002. 'Phosphorylation of Ser307 in Insulin Receptor Substrate-1 Blocks Interactions with the Insulin Receptor and Inhibits Insulin Action', *Journal of Biological Chemistry*, 277: 1531-37.

Ahmadian, Maryam, Jae Myoung Suh, Nasun Hah, Christopher Liddle, Annette R. Atkins, Michael Downes, and Ronald M. Evans. 2013. 'PPARγ signaling and metabolism: the good, the bad and the future', *Nature medicine*, 19: 557-66.

Ahmed, Tamer A., Mark D. Buzzelli, Charles H. Lang, John B. Capen, Margaret L. Shumate, Maithili Navaratnarajah, Murali Nagarajan, and Robert N. Cooney. 2007. 'Interleukin-6 inhibits growth hormone-mediated gene expression in hepatocytes', *American Journal of Physiology-Gastrointestinal and Liver Physiology*, 292: G1793-G803.

Al-Khalili, Lubna, Karim Bouzakri, Stephan Glund, Fredrik Lönnqvist, Heikki A. Koistinen, and Anna Krook. 2006. 'Signaling Specificity of Interleukin-6 Action on Glucose and Lipid Metabolism in Skeletal Muscle', *Molecular Endocrinology*, 20: 3364-75.

Alabarse, Paulo V. G., Priscila S. Lora, Jordana M. S. Silva, Rafaela C. E. Santo, Eduarda C. Freitas, Mayara S. de Oliveira, Andrelise S. Almeida, Mônica Immig, Vivian O. N. Teixeira, Lidiane I. Filippin, and Ricardo M. Xavier. 2018. 'Collagen-induced arthritis as an animal model of rheumatoid cachexia', *Journal of Cachexia, Sarcopenia and Muscle*, 9: 603-12.

Alamdari, N., D. Constantin-Teodosiu, A. J. Murton, S. M. Gardiner, T. Bennett, R. Layfield, and P. L. Greenhaff. 2008. 'Temporal changes in the involvement of pyruvate dehydrogenase complex in muscle lactate accumulation during lipopolysaccharide infusion in rats', *The Journal of Physiology*, 586: 1767-75.

Aletaha, D., and J. S. Smolen. 2018. 'Diagnosis and management of rheumatoid arthritis: A review', *JAMA*, 320: 1360-72.

Allen, David L., and Terry G. Unterman. 2007. 'Regulation of myostatin expression and myoblast differentiation by FoxO and SMAD transcription factors', *American Journal of Physiology-Cell Physiology*, 292: C188-C99.

Alnahdi, A. H., J. A. Zeni, and L. Snyder-Mackler. 2012. 'Muscle impairments in patients with knee osteoarthritis', *Sports Health*, 4: 284-92.

Alonzi, Tonino, Elena Fattori, Domenico Lazzaro, Patrizia Costa, Lesley Probert, George Kollias, Fabrizio De Benedetti, Valeria Poli, and Gennaro Ciliberto. 1998. 'Interleukin 6 Is Required for the Development of Collagen-induced Arthritis', *The Journal of Experimental Medicine*, 187: 461-68.

Alpízar-Rodríguez, Deshiré, Nicola Pluchino, Geraldine Canny, Cem Gabay, and Axel Finckh. 2017. 'The role of female hormonal factors in the development of rheumatoid arthritis', *Rheumatology*, 56: 1254-63.

Amin, Rajesh H., Suresh T. Mathews, Heidi S. Camp, Liyun Ding, and Todd Leff. 2010. 'Selective activation of PPARγ in skeletal muscle induces endogenous production of adiponectin and protects mice from diet-induced insulin resistance', *American Journal of Physiology-Endocrinology and Metabolism*, 298: E28-E37.

Andersson, Christian X., Birgit Gustafson, Ann Hammarstedt, Shahram Hedjazifar, and Ulf Smith. 2008. 'Inflamed adipose tissue, insulin resistance and vascular injury', *Diabetes/Metabolism Research and Reviews*, 24: 595-603.

Arend, William P., and Gary S. Firestein. 2012. 'Pre-rheumatoid arthritis: predisposition and transition to clinical synovitis', *Nature Reviews Rheumatology*, 8: 573.

Arias de la Rosa, I., Escudero-Contreras A., Rodríguez-Cuenca S., Ruiz-Ponce M., Jiménez-Gómez Y., Ruiz-Limón P., Pérez-Sánchez C., Ábalos-Aguilera M. C., Cecchi I., Ortega R., Calvo J., Guzmán-Ruiz R., Malagón M. M., Collantes-Estevez E., Vidal-Puig A., López-Pedrera Ch., and Barbarroja N. 2018. 'Defective glucose and lipid metabolism in rheumatoid arthritis is determined by chronic inflammation in metabolic tissues', *Journal of Internal Medicine*, 284: 61-77.

Ashraf, S., P. I. Mapp, and D. A. Walsh. 2011. 'Contributions of angiogenesis to inflammation, joint damage, and pain in a rat model of osteoarthritis', *Arthritis & Rheumatism*, 63: 2700-10.

Aurich, Matthias, Ginette R. Squires, Agnes Reiner, Juergen A. Mollenhauer, Klaus E. Kuettner, A. Robin Poole, and Ada A. Cole. 2005. 'Differential matrix degradation and turnover in early cartilage lesions of human knee and ankle joints', *Arthritis & Rheumatism*, 52: 112-19.

Baracos, V. E., C. DeVivo, D. H. Hoyle, and A. L. Goldberg. 1995. 'Activation of the ATP-ubiquitin-proteasome pathway in skeletal muscle of cachectic rats bearing a hepatoma', *American Journal of Physiology-Endocrinology and Metabolism*, 268: E996-E1006.

Bartok, Beatrix, and Gary S. Firestein. 2010. 'Fibroblast-like synoviocytes: key effector cells in rheumatoid arthritis', *Immunological reviews*, 233: 233-55.

Bechet, Daniel, Amina Tassa, Daniel Taillandier, Lydie Combaret, and Didier Attaix. 2005. 'Lysosomal proteolysis in skeletal muscle', *The International Journal of Biochemistry & Cell Biology*, 37: 2098-114.

Bendele, Alison, Jennifer Mccomb, TY Gould, Tracy Mcabee, Gina Sennello, Elizabeth Chlipala, and Michael Guy. 1999. 'Animal Models of Arthritis: Relevance to Human Disease', *Toxicologic Pathology*, 27: 134-42.

Bendele, AM. 2001. 'Animal models of osteoarthritis.', *J Musculoskelet Neuronal Interact*, 1: 14.

Benito, M. J., D. J. Veale, O. FitzGerald, W. B. van den Berg, and B. Bresnihan. 2005. 'Synovial tissue inflammation in early and late osteoarthritis', *Annals of the rheumatic diseases*, 64: 1263-67.

Berenbaum, F. 2013. 'Osteoarthritis as an inflammatory disease (osteoarthritis is not osteoarthrosis!)', *Osteoarthritis and Cartilage*, 21: 16-21.

Berger, Joel, and David E. Moller. 2002. 'The Mechanisms of Action of PPARs', *Annual Review of Medicine*, 53: 409-35.

Bhatnagar, Shephali, Siva K. Panguluri, Sanjay K. Gupta, Saurabh Dahiya, Robert F. Lundy, and Ashok Kumar. 2010. 'Tumor necrosis factor-α regulates distinct molecular pathways and gene networks in cultured skeletal muscle cells', *PloS one*, 5: e13262-e62.

Bienso, R. S., S. Ringholm, K. Kiilerich, N. J. Aachmann-Andersen, R. Krogh-Madsen, B. Guerra, P. Plomgaard, G. van Hall, J. T. Treebak, B. Saltin, C. Lundby, J. A. Calbet, H. Pilegaard, and J. F. Wojtaszewski. 2012. 'GLUT4 and glycogen synthase are key players in bed rest-induced insulin resistance', *Diabetes*, 61: 1090-9.

Biensø, Rasmus S., Jakob G. Knudsen, Nina Brandt, Per A. Pedersen, and Henriette Pilegaard. 2014. 'Effects of IL-6 on pyruvate dehydrogenase regulation in mouse skeletal muscle', *Pflügers Archiv - European Journal of Physiology*, 466: 1647-57.

Bingham, Brendan, Seena K. Ajit, David R. Blake, and Tarek A. Samad. 2009. 'The molecular basis of pain and its clinical implications in rheumatology', *Nature Clinical Practice Rheumatology*, 5: 28.

Blaauw, Bert, Marta Canato, Lisa Agatea, Luana Toniolo, Cristina Mammucari, Eva Masiero, Reimar Abraham, Marco Sandri, Stefano Schiaffino, and Carlo Reggiani. 2009. 'Inducible activation of Akt increases skeletal muscle mass and force without satellite cell activation', *The FASEB Journal*, 23: 3896-905.

Bleau, Christian, Antony D. Karelis, David H. St-Pierre, and Lucie Lamontagne. 2015. 'Crosstalk between intestinal microbiota, adipose tissue and skeletal muscle as an early event in systemic low-grade inflammation and the development of obesity and diabetes', *Diabetes/Metabolism Research and Reviews*, 31: 545-61.

Bodine Sue C., Esther Latres, Susanne Baumhueter, Venus K.-M. Lai, Lorna Nunez, Brian A. Clarke, William T. Poueymirou, Frank J. Panaro, Erqian Na, Kumar Dharmarajan, Zhen-Qiang Pan, David M. Valenzuela, Thomas M. DeChiara, Trevor N. Stitt, and George D. Yancopoulos and David J. Glass. 2001b. 'Identification of Ubiquitin Ligases Required for Skeletal Muscle Atrophy', *Science*, 294: 1704-08.

Bodine, Sue C., Esther Latres, Susanne Baumhueter, Venus K.-M. Lai, Lorna Nunez, Brian A. Clarke, William T. Poueymirou, Frank J. Panaro, Erqian Na, Kumar Dharmarajan, Zhen-Qiang Pan, David M.

Valenzuela, Thomas M. DeChiara, Trevor N. Stitt, George D. Yancopoulos, and David J. Glass. 2001. 'Identification of Ubiquitin Ligases Required for Skeletal Muscle Atrophy', *Science*, 294: 1704-08.

Bodine, Sue C., Trevor N. Stitt, Michael Gonzalez, William O. Kline, Gretchen L. Stover, Roy Bauerlein, Elizabeth Zlotchenko, Angus Scrimgeour, John C. Lawrence, David J. Glass, and George D. Yancopoulos. 2001a. 'Akt/mTOR pathway is a crucial regulator of skeletal muscle hypertrophy and can prevent muscle atrophy in vivo', *Nature Cell Biology*, 3: 1014.

Bolon, Brad, Marina Stolina, Caroline King, Scot Middleton, Jill Gasser, Debra Zack, and Ulrich Feige. 2011. 'Rodent preclinical models for developing novel antiarthritic molecules: comparative biology and preferred methods for evaluating efficacy', *Journal of biomedicine & biotechnology*, 2011: 569068-68.

Bonaldo, Paolo, and Marco Sandri. 2013. 'Cellular and molecular mechanisms of muscle atrophy', *Disease models & mechanisms*, 6: 25-39.

Bondeson, Jan, Shane D. Wainwright, Sarah Lauder, Nick Amos, and Clare E. Hughes. 2006. 'The role of synovial macrophages and macrophage-produced cytokines in driving aggrecanases, matrix metalloproteinases, and other destructive and inflammatory responses in osteoarthritis', *Arthritis research & therapy*, 8: R187-R87.

Bove, S. E., S. L. Calcaterra, R. M. Brooker, C. M. Huber, R. E. Guzman, P. L. Juneau, D. J. Schrier, and K. S. Kilgore. 2003. 'Weight bearing as a measure of disease progression and efficacy of anti-inflammatory compounds in a model of monosodium iodoacetate-induced osteoarthritis', *Osteoarthritis and Cartilage*, 11: 821-30.

Breedveld, F. C. 2004. 'Osteoarthritis—the impact of a serious disease', *Rheumatology*, 43: i4-i8.

Bruckner, Peter, and Michel van der Rest. 1994. 'Structure and function of cartilage collagens', *Microscopy Research and Technique*, 28: 378-84.

Burton, Kenneth. 1956. 'A study of the conditions and mechanism of the diphenylamine reaction for the colorimetric estimation of deoxyribonucleic acid', *Biochemical Journal*, 62: 315.

Carey, Andrew L., Gregory R. Steinberg, S. Lance Macaulay, Walter G. Thomas, Anna G. Holmes, Georg Ramm, Oja Prelovsek, Cordula Hohnen-Behrens, Matthew J. Watt, David E. James, Bruce E. Kemp, Bente K. Pedersen, and Mark A. Febbraio. 2006. 'Interleukin-6 Increases Insulin-Stimulated Glucose Disposal in Humans and Glucose Uptake and Fatty Acid Oxidation In Vitro via AMP-Activated Protein Kinase', *Diabetes*, 55: 2688-97.

Carolina Ramírez, Thiago Luiz Russo; María Cristina Sandoval, Adriana Abbade Dentillo, Marcela Abreu Silva Couto, João Luiz Quagliotti Durigan, Tania Fátima Salvini. 2011. 'Joint Inflammation Alters Gene and Protein Expression and Leads to Atrophy in the Tibialis Anterior Muscle in Rats', *Am J Phys Med Rehabil*, 90: 9.

Castillero, Estíbaliz, Ana Isabel Martín, María López-Menduiña, Miriam Granado, Mª Ángeles Villanúa, and Asunción López-Calderón. 2009. 'IGF-I system, atrogenes and myogenic regulatory factors in arthritis induced muscle wasting', *Molecular and Cellular Endocrinology*, 309: 8-16.

Castillero, Estíbaliz, María Paz Nieto-Bona, Carmen Fernández-Galaz, Ana Isabel Martín, María López-Menduiña, Miriam Granado, María Angeles Villanúa, and Asunción López-Calderón. 2011. 'Fenofibrate, a PPARα agonist, decreases atrogenes and myostatin expression and improves arthritis-induced skeletal muscle atrophy', *American Journal of Physiology-Endocrinology and Metabolism*, 300: E790-E99.

Chaplan, S. R., F. W. Bach, J. W. Pogrel, J. M. Chung, and T. L. Yaksh. 1994. 'Quantitative assessment of tactile allodynia in the rat paw', *J Neurosci Methods*, 53: 55-63.

Chatzidionysiou, Katerina, Sharzad Emamikia, Jackie Nam, Sofia Ramiro, Josef Smolen, Désirée van der Heijde, Maxime Dougados, Johannes Bijlsma, Gerd Burmester, Marieke Scholte, Ronald van Vollenhoven, and Robert Landewé. 2017. 'Efficacy of glucocorticoids, conventional and targeted synthetic disease-modifying antirheumatic drugs: a systematic literature review informing the 2016 update of the EULAR recommendations for the management of rheumatoid arthritis', *Annals of the Rheumatic Diseases*, 76: 1102-07.

Chu, I. J. H., A. Y. T. Lim, and C. L. W. Ng. 2018. 'Effects of meaningful weight loss beyond symptomatic relief in adults with knee osteoarthritis and obesity: a systematic review and meta-analysis', *Obesity Reviews*, 19: 1597-607.

Churi, Sajay B., Omar S. Abdel-Aleem, Kiranjeet K. Tumber, Heather Scuderi-Porter, and Bradley K. Taylor. 2008. 'Intrathecal rosiglitazone acts at peroxisome proliferator-activated receptor γ to rapidly inhibit neuropathic pain in rats', *The journal of pain : official journal of the American Pain Society*, 9: 639-49.

Ciciliot, Stefano, Alberto C. Rossi, Kenneth A. Dyar, Bert Blaauw, and Stefano Schiaffino. 2013. 'Muscle type and fiber type specificity in muscle wasting', *The International Journal of Biochemistry & Cell Biology*, 45: 2191-99.

Clarke, Brian A., Doreen Drujan, Monte S. Willis, Leon O. Murphy, Richard A. Corpina, Elena Burova, Sergey V. Rakhilin, Trevor N. Stitt, Cam Patterson, Esther Latres, and David J. Glass. 2007. 'The E3 Ligase MuRF1 Degrades Myosin Heavy Chain Protein in Dexamethasone-Treated Skeletal Muscle', *Cell Metabolism*, 6: 376-85.

Clop, Alex, Fabienne Marcq, Haruko Takeda, Dimitri Pirottin, Xavier Tordoir, Bernard Bibé, Jacques Bouix, Florian Caiment, Jean-Michel Elsen, Francis Eychenne, Catherine Larzul, Elisabeth Laville, Françoise Meish, Dragan Milenkovic, James Tobin, Carole Charlier, and Michel Georges. 2006. 'A mutation creating a potential illegitimate microRNA target site in the myostatin gene affects muscularity in sheep', *Nature Genetics*, 38: 813.

Coggon D, Reading I, Croft P, McLaren M, Barrett D, Cooper C. 2001. 'Knee osteoarthritis and obesity', *Int J Obes Relat Metab Disord*: 5.

Cohen, Shenhav, Jeffrey J. Brault, Steven P. Gygi, David J. Glass, David M. Valenzuela, Carlos Gartner, Esther Latres, and Alfred L. Goldberg. 2009. 'During muscle atrophy, thick, but not thin, filament components are degraded by MuRF1-dependent ubiquitylation', *The Journal of cell biology*, 185: 1083-95.

Constantin-Teodosiu, Dumitru. 2013. 'Regulation of Muscle Pyruvate Dehydrogenase Complex in Insulin Resistance: Effects of Exercise and Dichloroacetate', *Diabetes & Metabolism Journal*, 37: 301-14.

Constantin, Despina, Justine McCullough, Ravi P. Mahajan, and Paul L. Greenhaff. 2011. 'Novel events in the molecular regulation of muscle mass in critically ill patients', *The Journal of Physiology*, 589: 3883-95.

Cooney, Jennifer K., Rebecca-Jane Law, Verena Matschke, Andrew B. Lemmey, Jonathan P. Moore, Yasmeen Ahmad, Jeremy G. Jones, Peter Maddison, and Jeanette M. Thom. 2011. 'Benefits of exercise in rheumatoid arthritis', *Journal of aging research*, 2011: 681640-40.

Costenbader, Karen H., Shun-Chiao Chang, Immaculata De Vivo, Robert Plenge, and Elizabeth W. Karlson. 2008. 'Genetic polymorphisms in PTPN22, PADI-4, and CTLA-4 and risk for rheumatoid arthritis in two longitudinal cohort studies: evidence of gene-environment interactions with heavy cigarette smoking', *Arthritis research & therapy*, 10: R52-R52.

Crossland, Hannah, Dumitru Constantin-Teodosiu, Sheila Gardiner, and Paul Greenhaff. 2017. 'Peroxisome proliferator-activated receptor γ agonism attenuates endotoxaemia induced muscle protein loss and lactate accumulation in rats', *Clinical Science*.

Crossland, Hannah, Dumitru Constantin-Teodosiu, Sheila M. Gardiner, Despina Constantin, and Paul L. Greenhaff. 2008. 'A potential role for Akt/FOXO signalling in both protein loss and the impairment of muscle carbohydrate oxidation during sepsis in rodent skeletal muscle', *The Journal of Physiology*, 586: 5589-600.

Crossland, Hannah, Dumitru Constantin-Teodosiu, Paul L. Greenhaff, and Sheila M. Gardiner. 2010. 'Low-dose dexamethasone prevents endotoxaemia-induced muscle protein loss and impairment of carbohydrate oxidation in rat skeletal muscle', *The Journal of Physiology*, 588: 1333-47.

Csibi, Alfredo, Karen Cornille, Marie-Pierre Leibovitch, Anne Poupon, Lionel A. Tintignac, Anthony M. J. Sanchez, and Serge A. Leibovitch. 2010. 'The translation regulatory subunit eIF3f controls the kinase-dependent mTOR signaling required for muscle differentiation and hypertrophy in mouse', *PloS one*, 5: e8994-e94.

Cutolo, Maurizio, Barbara Villaggio, Chiara Craviotto, Carmen Pizzorni, Bruno Seriolo, and Alberto Sulli. 2002. 'Sex hormones and rheumatoid arthritis', *Autoimmunity Reviews*, 1: 284-89.

Cuzzocrea, Salvatore, Emanuela Mazzon, Laura Dugo, Nimesh S. A. Patel, Ivana Serraino, Rosanna Di Paola, Tiziana Genovese, Domenico Britti, Massimo De Maio, Achille P. Caputi, and Christoph Thiemermann. 2003. 'Reduction in the evolution of murine type II

collagen–induced arthritis by treatment with rosiglitazone, a ligand of the peroxisome proliferator–activated receptor γ', *Arthritis & Rheumatism*, 48: 3544-56.

Dahaghin, S., S. M. A. Bierma-Zeinstra, A. Z. Ginai, H. A. P. Pols, J. M. W. Hazes, and B. W. Koes. 2005. 'Prevalence and pattern of radiographic hand osteoarthritis and association with pain and disability (the Rotterdam study)', *Annals of the rheumatic diseases*, 64: 682-87.

Dardevet, D., C. Sornet, D. Attaix, V. E. Baracos, and J. Grizard. 1994. 'Insulin-like growth factor-1 and insulin resistance in skeletal muscles of adult and old rats', *Endocrinology*, 134: 1475-84.

de Lange-Brokaar, B. J. E., A. Ioan-Facsinay, G. J. V. M. van Osch, A. M. Zuurmond, J. Schoones, R. E. M. Toes, T. W. J. Huizinga, and M. Kloppenburg. 2012. 'Synovial inflammation, immune cells and their cytokines in osteoarthritis: a review', *Osteoarthritis and Cartilage*, 20: 1484-99.

de Oliveira Nunes Teixeira, Vivian, Lidiane Isabel Filippin, Paula Ramos Viacava, Patrícia Gnieslaw de Oliveira, and Ricardo Machado Xavier. 2013. 'Muscle wasting in collagen-induced arthritis and disuse atrophy', *Experimental Biology and Medicine*, 238: 1421-30.

Deane, Kevin D., Colin I. O'Donnell, Wolfgang Hueber, Darcy S. Majka, Ann A. Lazar, Lezlie A. Derber, William R. Gilliland, Jess D. Edison, Jill M. Norris, William H. Robinson, and V. Michael Holers. 2010. 'The number of elevated cytokines and chemokines in preclinical seropositive rheumatoid arthritis predicts time to diagnosis in an age-dependent manner', *Arthritis and rheumatism*, 62: 3161-72.

Dekker, Joost, Paolo Tola, Geert Aufdemkampe, and Marcus Winckers. 1993. 'Negative affect, pain and disability in osteoarthritis patients: the mediating role of muscle weakness', *Behaviour Research and Therapy*, 31: 203-06.

Deval, C., S. Mordier, C. Obled, D. Bechet, L. Combaret, D. Attaix, and M. Ferrara. 2001. 'Identification of cathepsin L as a differentially expressed message associated with skeletal muscle wasting', *Biochemical Journal*, 360: 143-50.

Dillon, Charles F, Elizabeth K Rasch, Qiuping Gu, and Rosemarie Hirsch. 2006. 'Prevalence of knee osteoarthritis in the United States: arthritis data from the Third National Health and Nutrition Examination Survey 1991-94', *The Journal of Rheumatology*, 33: 2271-79.

Dimitroulas, Theodoros, Tosin Lambe, Rainer Klocke, George D. Kitas, and Rui V. Duarte. 2017. 'Biologic drugs as analgesics for the management of osteoarthritis', *Seminars in Arthritis and Rheumatism*, 46: 687-91.

Domigan, Courtney K., Carmen M. Warren, Vaspour Antanesian, Katharina Happel, Safiyyah Ziyad, Sunyoung Lee, Abigail Krall, Lewei Duan, Antoni X. Torres-Collado, Lawrence W. Castellani, David Elashoff, Heather R. Christofk, Alexander M. van der Bliek, Michael Potente, and M. Luisa Iruela-Arispe. 2015. 'Autocrine VEGF maintains endothelial survival through regulation of metabolism and autophagy', *Journal of Cell Science*, 128: 2236-48.

Donahue, K. E., G. Gartlehner, D. E. Jonas, and et al. 2008. 'Systematic review: Comparative effectiveness and harms of disease-modifying medications for rheumatoid arthritis', *Annals of Internal Medicine*, 148: 124-34.

Doran, Michele F., Gregory R. Pond, Cynthia S. Crowson, W. Michael O'Fallon, and Sherine E. Gabriel. 2002. 'Trends in incidence and mortality in rheumatoid arthritis in Rochester, Minnesota, over a forty-year period', *Arthritis & Rheumatism*, 46: 625-31.

Doucet, Marième, Aaron P. Russell, Bertrand Léger, Richard Debigaré, Denis R. Joanisse, Marc-André Caron, Pierre LeBlanc, and François Maltais. 2007. 'Muscle Atrophy and Hypertrophy Signaling in Patients with Chronic Obstructive Pulmonary Disease', *American Journal of Respiratory and Critical Care Medicine*, 176: 261-69.

Ebrahimi, Behnam, Susan L. Tucker, Donghui Li, James L. Abbruzzese, and Razelle Kurzrock. 2004. 'Cytokines in pancreatic carcinoma', *Cancer*, 101: 2727-36.

Elkan, Ann-Charlotte, Inga-Lill Engvall, Tommy Cederholm, and Ingiäld Hafström. 2009. 'Rheumatoid cachexia, central obesity and malnutrition in patients with low-active rheumatoid arthritis: feasibility of anthropometry, Mini Nutritional Assessment and body composition techniques', *European Journal of Nutrition*, 48: 315-22.

Emery, P, C O Bingham, G R Burmester, V P Bykerk, D E Furst, X Mariette, D van der Heijde, R van Vollenhoven, C Arendt, I Mountian, O Purcaru, D Tatla, B VanLunen, and M E Weinblatt. 2017. 'Certolizumab pegol in combination with dose-optimised methotrexate in DMARD-naïve patients with early, active rheumatoid arthritis with poor prognostic factors: 1-year results from C-EARLY, a randomised, double-blind, placebo-controlled phase III study', *Annals of the Rheumatic Diseases*, 76: 96-104.

Englund, Martin, Ali Guermazi, Daniel Gale, David J. Hunter, Piran Aliabadi, Margaret Clancy, and David T. Felson. 2008. 'Incidental meniscal findings on knee MRI in middle-aged and elderly persons', *The New England journal of medicine*, 359: 1108-15.

Evans, Ronald M., Grant D. Barish, and Yong-Xu Wang. 2004. 'PPARs and the complex journey to obesity', *Nature medicine*, 10: 355.

Farber, Mark O., and Edward T. Mannix. 2000. 'TISSUE WASTING IN PATIENTS WITH CHRONIC OBSTRUCTIVE PULMONARY DISEASE, THE ACQUIRED IMMUNE DEFICIENCY SYNDROME, AND CONGESTIVE HEART FAILURE', *Neurologic Clinics*, 18: 245-62.

Felson, David T., Allan Naimark, Jennifer Anderson, Lewis Kazis, William Castelli, and Robert F. Meenan. 1987. 'The prevalence of knee osteoarthritis in the elderly. the framingham osteoarthritis study', *Arthritis & Rheumatism*, 30: 914-18.

Fenton, Sally A. M., and George D. Kitas. 2016. 'Sedentary behaviour in RA — a new research agenda', *Nature Reviews Rheumatology*, 12: 698.

Fenton, Sally A. M., Jet J. C. S. Veldhuijzen van Zanten, Joan L. Duda, George S. Metsios, and George D. Kitas. 2018. 'Sedentary behaviour in rheumatoid arthritis: definition, measurement and implications for health', *Rheumatology*, 57: 213-26.

Fernandes, Gwen Sascha, Sanjay Mukund Parekh, Jonathan Moses, Colin Fuller, Brigitte Scammell, Mark Edward Batt, Weiya Zhang, and Michael Doherty. 2017. 'Prevalence of knee pain, radiographic osteoarthritis and arthroplasty in retired professional footballers compared with men in the general population: a cross-sectional study', *British Journal of Sports Medicine*.

Fink, Bernd, Monika Egl, Joachim Singer, Martin Fuerst, Michael Bubenheim, and Eva Neuen-Jacob. 2007. 'Morphologic changes in the vastus medialis muscle in patients with osteoarthritis of the knee', *Arthritis & Rheumatism*, 56: 3626-33.

Fiorentino, D F, A Zlotnik, T R Mosmann, M Howard, and A O'Garra. 1991. 'IL-10 inhibits cytokine production by activated macrophages', *The Journal of Immunology*, 147: 3815-22.

Forman, Barry M., Jasmine Chen, and Ronald M. Evans. 1996. 'The Peroxisome Proliferator-activated Receptors: Ligands and Activatorsa', *Annals of the New York Academy of Sciences*, 804: 266-75.

Forsberg, A. M., E. Nilsson, J. Werneman, J. Bergström, and E. Hultman. 1991. 'Muscle composition in relation to age and sex', *Clinical Science*, 81: 249-56.

Frost, Robert A., Gerald J. Nystrom, Leonard S. Jefferson, and Charles H. Lang. 2007. 'Hormone, cytokine, and nutritional regulation of sepsis-induced increases in atrogin-1 and MuRF1 in skeletal muscle', *American Journal of Physiology-Endocrinology and Metabolism*, 292: E501-E12.

Furuyama, Tatsuo, Kazuko Kitayama, Hitoshi Yamashita, and Nozomu Mori. 2003. 'Forkhead transcription factor FOXO1 (FKHR)-dependent induction of PDK4 gene expression in skeletal muscle during energy deprivation', *Biochemical Journal*, 375: 365-71.

Gallagher, P., S. Trappe, M. Harber, A. Creer, S. Mazzetti, T. Trappe, B. Alkner, and P. Tesch. 2005. 'Effects of 84-days of bedrest and resistance training on single muscle fibre myosin heavy chain distribution in human vastus lateralis and soleus muscles', *Acta Physiologica Scandinavica*, 185: 61-69.

Geetha, Thangiah, Shraddha D. Rege, Salome E. Mathews, Susan O. Meakin, Morris F. White, and Jeganathan Ramesh Babu. 2013. 'Nerve Growth Factor Receptor TrkA, a New Receptor in Insulin Signaling Pathway in PC12 Cells', *The Journal of Biological Chemistry*, 288: 23807-13.

Gelfand, R. A., and E. J. Barrett. 1987. 'Effect of physiologic hyperinsulinemia on skeletal muscle protein synthesis and breakdown in man', *The Journal of clinical investigation*, 80: 1-6.

Gerwin, N, AM Bendele, S Glasson, and CS Carlson. 2010. 'The OARSI histopathology initiative–recommendations for histological assessments of osteoarthritis in the rat', *Osteoarthritis and Cartilage*, 18: S24-S34.

Giles, K Wv, and A Myers. 1965. 'An improved diphenylamine method for the estimation of deoxyribonucleic acid', *Nature*, 206: 93.

Glass, David J. 2003. 'Signalling pathways that mediate skeletal muscle hypertrophy and atrophy', *Nature Cell Biology*, 5: 87.

Goldring, Mary B. 2001. 'Anticytokine therapy for osteoarthritis', *Expert Opinion on Biological Therapy*, 1: 817-29.

Goldring, Steven R., and Mary B. Goldring. 2010. 'Bone and cartilage in osteoarthritis: is what's best for one good or bad for the other?', *Arthritis research & therapy*, 12: 143-43.

Gomes, M. D., S. H. Lecker, R. T. Jagoe, A. Navon, and A. L. Goldberg. 2001. 'Atrogin-1, a muscle-specific F-box protein highly expressed during muscle atrophy', *Proceedings of the National Academy of Sciences of the United States of America*, 98: 14440-45.

Gómez-SanMiguel, Ana Belén, Carolina Gomez-Moreira, María Paz Nieto-Bona, Carmen Fernández-Galaz, Maria Ángeles Villanúa, Ana Isabel Martín, and Asunción López-Calderón. 2016. 'Formoterol decreases muscle wasting as well as inflammation in the rat model of rheumatoid arthritis', *American Journal of Physiology-Endocrinology and Metabolism*, 310: E925-E37.

Goncalves, Marcus D., Emidio E. Pistilli, Anthony Balduzzi, Morris J. Birnbaum, Jennifer Lachey, Tejvir S. Khurana, and Rexford S. Ahima. 2010. 'Akt Deficiency Attenuates Muscle Size and Function but Not the Response to ActRIIB Inhibition', *PloS one*, 5: e12707.

Gregersen, Peter K., Jack Silver, and Robert J. Winchester. 1987. 'The shared epitope hypothesis. an approach to understanding the molecular genetics of susceptibility to rheumatoid arthritis', *Arthritis & Rheumatism*, 30: 1205-13.

Griffin, T. M., B. Fermor, J. L. Huebner, V. B. Kraus, R. M. Rodriguiz, W. C. Wetsel, L. Cao, L. A. Setton, and F. Guilak. 2010. 'Diet-induced obesity differentially regulates behavioral, biomechanical, and molecular risk factors for osteoarthritis in mice', *Arthritis Res Ther*, 12: R130.

Guingamp, Corinne, Pascale Gegout-Pottie, Lionel Philippe, Bernard Terlain, Patrick Netter, and Pierre Gillet. 1997. 'Mono-iodoacetate-induced experimental osteoarthritis. A dose-response study of loss of mobility, morphology, and biochemistry', *Arthritis & Rheumatism*, 40: 1670-79.

Haas, Robert, Joanne Smith, Vidalba Rocher-Ros, Suchita Nadkarni, Trinidad Montero-Melendez, Fulvio D'Acquisto, Elliot J. Bland, Michele Bombardieri, Costantino Pitzalis, Mauro Perretti, Federica M. Marelli-Berg, and Claudio Mauro. 2015. 'Lactate Regulates Metabolic and Pro-inflammatory Circuits in Control of T Cell Migration and Effector Functions', *PLOS Biology*, 13: e1002202.

Haddad, F., F. Zaldivar, D. M. Cooper, and G. R. Adams. 2005. 'IL-6-induced skeletal muscle atrophy', *Journal of Applied Physiology*, 98: 911-17.

Hamilton, C. B., M. A. Pest, V. Pitelka, A. Ratneswaran, F. Beier, and B. M. Chesworth. 2015. 'Weight-bearing asymmetry and vertical activity differences in a rat model of post-traumatic knee osteoarthritis', *Osteoarthritis and Cartilage*, 23: 1178-85.

Harris, R. C., E. Hultman, and L. O. Nordesjö. 1974. 'Glycogen, Glycolytic Intermediates and High-Energy Phosphates Determined in Biopsy Samples of Musculus Quadriceps Femoris of Man at Rest. Methods

and Variance of Values', *Scandinavian Journal of Clinical and Laboratory Investigation*, 33: 109-20.

Hart, Jaime E., Francine Laden, Robin C. Puett, Karen H. Costenbader, and Elizabeth W. Karlson. 2009. 'Exposure to traffic pollution and increased risk of rheumatoid arthritis', *Environmental health perspectives*, 117: 1065-69.

Haseeb, A., and T. M. Haqqi. 2013. 'Immunopathogenesis of osteoarthritis', *Clin Immunol*, 146: 185-96.

Heidi, Kokkonen, Söderström Ingegerd, Rocklöv Joacim, Hallmans Göran, Lejon Kristina, and Rantapää Dahlqvist Solbritt. 2010. 'Up-regulation of cytokines and chemokines predates the onset of rheumatoid arthritis', *Arthritis & Rheumatism*, 62: 383-91.

Helliwell, P. S., and S. Jackson. 1994. 'Relationship between weakness and muscle wasting in rheumatoid arthritis', *Annals of the rheumatic diseases*, 53: 726-28.

Hendiani, J. Amir, Karin N. Westlund, Nada Lawand, Niti Goel, Jeffrey Lisse, and Terry McNearney. 2003. 'Mechanical sensation and pain thresholds in patients with chronic arthropathies', *The Journal of Pain*, 4: 203-11.

Hernández-Hernández, Vanesa, Iván Ferraz-Amaro, and Federico Díaz-González. 2014. 'Influence of disease activity on the physical activity of rheumatoid arthritis patients', *Rheumatology*, 53: 722-31.

Higuchi, Russell, Carita Fockler, Gavin Dollinger, and Robert Watson. 1993. 'Kinetic PCR analysis: real-time monitoring of DNA amplification reactions', *Nature Biotechnology*, 11: 1026.

Hirose, M., M. Kaneki, H. Sugita, S. Yasuhara, and J. A. Martyn. 2000. 'Immobilization depresses insulin signaling in skeletal muscle', *Am J Physiol Endocrinol Metab*, 279: E1235-41.

Hittel, Dustin S., Michelle Axelson, Neha Sarna, Jane Shearer, Kim M. Huffman, and William E. Kraus. 2010. 'Myostatin decreases with aerobic exercise and associates with insulin resistance', *Medicine and science in sports and exercise*, 42: 2023-29.

Holers, V. Michael. 2013. 'Autoimmunity to citrullinated proteins and the initiation of rheumatoid arthritis', *Current opinion in immunology*, 25: 728-35.

Hotamisligil, Gökhan S., Pascal Peraldi, Adriane Budavari, Ramsey Ellis, Morris F. White, and Bruce M. Spiegelman. 1996. 'IRS-1-Mediated Inhibition of Insulin Receptor Tyrosine Kinase Activity in TNF-α- and Obesity-Induced Insulin Resistance', *Science*, 271: 665-70.

Huang, Xudong, Allan Vaag, Emma Carlsson, Mona Hansson, Bo Ahrén, and Leif Groop. 2003. 'Impaired Cathepsin L Gene Expression in Skeletal Muscle Is Associated With Type 2 Diabetes', *Diabetes*, 52: 2411-18.

Huffman, Kim M., Ryan Jessee, Brian Andonian, Brittany N. Davis, Rachel Narowski, Janet L. Huebner, Virginia B. Kraus, Julie McCracken, Brian F. Gilmore, K. Noelle Tune, Milton Campbell, Timothy R. Koves, Deborah M. Muoio, Monica J. Hubal, and William E. Kraus. 2017. 'Molecular alterations in skeletal muscle in rheumatoid arthritis are related to disease activity, physical inactivity, and disability', *Arthritis research & therapy*, 19: 12-12.

Hunter, David J, and David T Felson. 2006. 'Osteoarthritis', *BMJ*, 332: 639-42.

Hunter, David J., Jason J. McDougall, and Francis J. Keefe. 2008. 'The symptoms of osteoarthritis and the genesis of pain', *Rheumatic diseases clinics of North America*, 34: 623-43.

Hurley, M. V., D. L. Scott, J. Rees, and D. J. Newham. 1997. 'Sensorimotor changes and functional performance in patients with knee osteoarthritis', *Annals of the rheumatic diseases*, 56: 641-48.

Ikeda, Shinichi, Hiroshi Tsumura, and Takehiko Torisu. 2005. 'Age-related quadriceps-dominant muscle atrophy and incident radiographic knee osteoarthritis', *Journal of Orthopaedic Science*, 10: 121-26.

J. R. Vane, Y. S. Bakhle, and R. M. Botting. 1998. 'CYCLOOXYGENASES 1 AND 2', *Annual Review of Pharmacology and Toxicology*, 38: 97-120.

Janusz, M. J., A. M. Bendele, K. K. Brown, Y. O. Taiwo, L. Hsieh, and S. A. Heitmeyer. 2002. 'Induction of osteoarthritis in the rat by surgical tear of the meniscus: Inhibition of joint damage by a matrix metalloproteinase inhibitor', *Osteoarthritis and Cartilage*, 10: 785-91.

Jatoi, Aminah, Shaker R. Dakhil, Phuong L. Nguyen, Jeff A. Sloan, John W. Kugler, Kendrith M. Rowland, Gamini S. Soori, Donald B. Wender, Tom R. Fitch, Paul J. Novotny, and Charles L. Loprinzi. 2007. 'A placebo-controlled double blind trial of etanercept for the cancer anorexia/weight loss syndrome', *Cancer*, 110: 1396-403.

Jian, Yin, Hao Zhichao, Ma Yuanyuan, Liao Shuang, Li Xianxian, Fu Jing, Wu Yeke, Shen Jiefei, Zhang Ping, Li Xiaoyu, and Wang Hang. 2014. 'Concomitant activation of the PI3K/Akt and ERK1/2 signalling is involved in cyclic compressive force-induced IL-6 secretion in MLO-Y4 cells', *Cell Biology International*, 38: 591-98.

JONES, SIMON W., ROGER J. HILL, PHILIP A. KRASNEY, BARBARA O'CONNER, NICHOLAS PEIRCE, and PAUL L. GREENHAFF. 2004. 'Disuse atrophy and exercise rehabilitation in humans profoundly affects the expression of genes associated with the regulation of skeletal muscle mass', *The FASEB Journal*, 18: 1025-27.

Kapoor, Mohit, Johanne Martel-Pelletier, Daniel Lajeunesse, Jean-Pierre Pelletier, and Hassan Fahmi. 2010. 'Role of proinflammatory cytokines in the pathophysiology of osteoarthritis', *Nature Reviews Rheumatology*, 7: 33.

Khanna, Shweta, Kumar Sagar Jaiswal, and Bhawna Gupta. 2017. 'Managing Rheumatoid Arthritis with Dietary Interventions', *Frontiers in nutrition*, 4: 52-52.

Khoja, Samannaaz S., Charity G. Moore, Bret H. Goodpaster, Anthony Delitto, and Sara R. Piva. 2018. 'Skeletal Muscle Fat and Its Association With Physical Function in Rheumatoid Arthritis', *Arthritis Care & Research*, 70: 333-42.

Kim, Hyo-Jeong, Takamasa Higashimori, So-Young Park, Hyejeong Choi, Jianying Dong, Yoon-Jung Kim, Hye-Lim Noh, You-Ree Cho, Gary Cline, Young-Bum Kim, and Jason K. Kim. 2004. 'Differential Effects of Interleukin-6 and -10 on Skeletal Muscle and Liver Insulin Action In Vivo', *Diabetes*, 53: 1060-67.

Kim, Young I., Felix N. Lee, Woo S. Choi, Sarah Lee, and Jang H. Youn. 2006. 'Insulin Regulation of Skeletal Muscle PDK4 mRNA Expression Is Impaired in Acute Insulin-Resistant States', *Diabetes*, 55: 2311-17.

Kimball SR, Horetsky RL, Jefferson LS. 1998. 'Signal transduction pathways involved in the regulation of protein synthesis by insulin in L6 myoblasts.', *Am J Physiol.*, 274: 8.

Kobayashi, Hisamine, Hiroyuki Kato, Yuri Hirabayashi, Hitoshi Murakami, and Hiromi Suzuki. 2006. 'Modulations of Muscle Protein Metabolism by Branched-Chain Amino Acids in Normal and Muscle-Atrophying Rats', *The Journal of Nutrition*, 136: 234S-36S.

Kobayashi, S., H. Okamoto, T. Iwamoto, Y. Toyama, T. Tomatsu, H. Yamanaka, and S. Momohara. 2008. 'A role for the aryl hydrocarbon receptor and the dioxin TCDD in rheumatoid arthritis', *Rheumatology*, 47: 1317-22.

Kobayashi, Shuzo, Kyoko Maesato, Hidekazu Moriya, Takayasu Ohtake, and Toshio Ikeda. 2005. 'Insulin resistance in patients with chronic kidney disease', *American Journal of Kidney Diseases*, 45: 275-80.

Kohn, Aimee D., Scott A. Summers, Morris J. Birnbaum, and Richard A. Roth. 1996. 'Expression of a Constitutively Active Akt Ser/Thr Kinase in 3T3-L1 Adipocytes Stimulates Glucose Uptake and Glucose Transporter 4 Translocation', *Journal of Biological Chemistry*, 271: 31372-78.

Kokkonen, Heidi, Ingegerd Söderström, Joacim Rocklöv, Göran Hallmans, Kristina Lejon, and Solbritt Rantapää Dahlqvist. 2010. 'Up-regulation of cytokines and chemokines predates the onset of rheumatoid arthritis', *Arthritis & Rheumatism*, 62: 383-91.

Kostoglou-Athanassiou, Ifigenia, Panagiotis Athanassiou, Aikaterini Lyraki, Ioannis Raftakis, and Christodoulos Antoniadis. 2012. 'Vitamin D and rheumatoid arthritis', *Therapeutic advances in endocrinology and metabolism*, 3: 181-87.

Koufany, Meriem, David Moulin, Arnaud Bianchi, Mikhaela Muresan, Sylvie Sebillaud, Patrick Netter, Georges Weryha, and Jean-Yves Jouzeau. 2008. 'Anti-inflammatory effect of antidiabetic thiazolidinediones prevents bone resorption rather than cartilage changes in experimental polyarthritis', *Arthritis research & therapy*, 10: R6.

Krawczyk, Connie M., Thomas Holowka, Jie Sun, Julianna Blagih, Eyal Amiel, Ralph J. DeBerardinis, Justin R. Cross, Euihye Jung, Craig B. Thompson, Russell G. Jones, and Edward J. Pearce. 2010. 'Toll-like receptor-induced changes in glycolytic metabolism regulate dendritic cell activation', *Blood*, 115: 4742-49.

Kumar, V., P. Atherton, K. Smith, and M. J. Rennie. 2009. 'Human muscle protein synthesis and breakdown during and after exercise', *J Appl Physiol (1985)*, 106: 2026-39.

Kuniaki Terato, Ryoichi Hasi-Iida, Kazuyo Miyamoto, Tomiaki Morimoto, Yoshinori Kato, Seiichi Kobayashi, Tetsuya Tajimaz, and HISAE HORI and YUTAKA NAGAI SHINZABURO OTAKE. 1982. 'Histological, Immunological and Biochemicals Studies on Type II Collagen-Induced Arthritis in Rats', *Biomedical Research*, 3: 495-505.

Kwiatkowska, Brygida, Anna Kłak, Maria Maślińska, Małgorzata Mańczak, and Filip Raciborski. 2018. 'Factors of depression among patients with rheumatoid arthritis', *Reumatologia*, 56: 219-27.

Kwon, Hye-Sook, Boli Huang, Terry G. Unterman, and Robert A. Harris. 2004. 'Protein Kinase B-α Inhibits Human Pyruvate Dehydrogenase Kinase-4 Gene Induction by Dexamethasone Through Inactivation of FOXO Transcription Factors', *Diabetes*, 53: 899-910.

Lawrence, J. S., J. M. Bremner, and F. Bier. 1966. 'Osteo-arthrosis. Prevalence in the population and relationship between symptoms and x-ray changes', *Annals of the rheumatic diseases*, 25: 1-24.

Lawrence, Reva C., David T. Felson, Charles G. Helmick, Lesley M. Arnold, Hyon Choi, Richard A. Deyo, Sherine Gabriel, Rosemarie Hirsch, Marc C. Hochberg, Gene G. Hunder, Joanne M. Jordan, Jeffrey N. Katz, Hilal Maradit Kremers, Frederick Wolfe, and Workgroup National Arthritis Data. 2008. 'Estimates of the prevalence of arthritis and other rheumatic conditions in the United States. Part II', *Arthritis and rheumatism*, 58: 26-35.

LECKER, STEWART H., R. THOMAS JAGOE, ALEXANDER GILBERT, MARCELO GOMES, VICKIE BARACOS, JAMES BAILEY, S. RUSS PRICE, WILLIAM E. MITCH, and ALFRED L. GOLDBERG. 2004. 'Multiple types of skeletal muscle atrophy involve a common program of changes in gene expression', *The FASEB Journal*, 18: 39-51.

Ledingham, Joanna, Neil Snowden, and Zoe Ide. 2017. 'Diagnosis and early management of inflammatory arthritis', *BMJ*, 358.

Lee, David M., and Michael E. Weinblatt. 2001. 'Rheumatoid arthritis', *The Lancet*, 358: 903-11.

Lee, S. J., and A. C. McPherron. 2001. 'Regulation of myostatin activity and muscle growth', *Proceedings of the National Academy of Sciences of the United States of America*, 98: 9306-11.

Levinger, Itamar, Pazit Levinger, Marissa K. Trenerry, Julian A. Feller, John R. Bartlett, Neil Bergman, Michael J. McKenna, and David Cameron-Smith. 2011. 'Increased inflammatory cytokine expression in the vastus lateralis of patients with knee osteoarthritis', *Arthritis & Rheumatism*, 63: 1343-48.

Levinger, P., M. K. Caldow, J. R. Bartlett, J. M. Peake, C. Smith, D. Cameron-Smith, and I. Levinger. 2016. 'The level of FoxO1 and IL-15 in skeletal muscle, serum and synovial fluid in people with knee osteoarthritis: a case control study', *Osteoporosis International*, 27: 2137-43.

Levinger, Pazit, Marissa K. Caldow, Julian A. Feller, John R. Bartlett, Neil R. Bergman, Michael J. McKenna, David Cameron-Smith, and Itamar Levinger. 2011. 'Association between skeletal muscle inflammatory markers and walking pattern in people with knee osteoarthritis', *Arthritis Care & Research*, 63: 1715-21.

Lewek, Michael D., Katherine S. Rudolph, and Lynn Snyder-Mackler. 2004. 'Quadriceps femoris muscle weakness and activation failure in patients with symptomatic knee osteoarthritis', *Journal of Orthopaedic Research*, 22: 110-15.

Litwic, Anna, Mark Edwards, Elaine Dennison, and Cyrus Cooper. 2013. 'Epidemiology and Burden of Osteoarthritis', *British medical bulletin*, 105: 185-99.

Liu, D., B. X. Zeng, S. H. Zhang, and S. L. Yao. 2005. 'Rosiglitazone, an agonist of peroxisome proliferator-activated receptor γ, reduces pulmonary inflammatory response in a rat model of endotoxemia', *Inflammation Research*, 54: 464-70.

Llovera, Marta, Neus Carbó, Celia García-Martínez, Paola Costelli, Luciana Tessitore, Francesco M. Baccino, Neus Agell, Gregory J. Bagby, Francisco J. López-Soriano, and Josep M. Argilés. 1996. 'Anti-TNF Treatment Reverts Increased Muscle Ubiquitin Gene Expression in Tumour-Bearing Rats', *Biochemical and Biophysical Research Communications*, 221: 653-55.

Loeser, Richard F., Steven R. Goldring, Carla R. Scanzello, and Mary B. Goldring. 2012. 'Osteoarthritis: a disease of the joint as an organ', *Arthritis and rheumatism*, 64: 1697-707.

Lorenzo, M., S. Fernández-Veledo, R. Vila-Bedmar, L. Garcia-Guerra, C. De Alvaro, and I. Nieto-Vazquez. 2008. 'Insulin resistance induced by tumor necrosis factor-α in myocytes and brown adipocytes12', *Journal of Animal Science*, 86: E94-E104.

Lowry, O, N Rosebrough, A Farr, and R Randall. 1951. 'Protein measurement with the Folin phenol reagent', *J biol Chem*, 193: 265-75.

Lu, Bing, Jeffrey B. Driban, Chang Xu, Kate L. Lapane, Timothy E. McAlindon, and Charles B. Eaton. 2017. 'Dietary Fat Intake and Radiographic Progression of Knee Osteoarthritis: Data From the Osteoarthritis Initiative', *Arthritis Care & Research*, 69: 368-75.

Makrygiannakis, D, M Hermansson, A-K Ulfgren, A P Nicholas, A J W Zendman, A Eklund, J Grunewald, C M Skold, L Klareskog, and A I Catrina. 2008. 'Smoking increases peptidylarginine deiminase 2 enzyme expression in human lungs and increases citrullination in BAL cells', *Annals of the Rheumatic Diseases*, 67: 1488-92.

Malemba, Jean J., Jean M. Mbuyi-Muamba, Jean Mukaya, Xavier Bossuyt, Patrick Verschueren, and Rene Westhovens. 2012. 'The epidemiology of rheumatoid arthritis in Kinshasa, Democratic Republic of Congo—a population-based study', *Rheumatology*, 51: 1644-47.

Mallinson, Joanne E., Kanagaraj Marimuthu, Andrew Murton, Anna Selby, Kenneth Smith, Dumitru Constantin-Teodosiu, Michael J. Rennie, and Paul L. Greenhaff. 2015. 'Statin myalgia is not associated with reduced muscle strength, mass or protein turnover in older male volunteers, but is allied with a slowing of time to peak power output, insulin resistance and differential muscle mRNA expression', *The Journal of Physiology*, 593: 1239-57.

Mammucari, Cristina, Giulia Milan, Vanina Romanello, Eva Masiero, Ruediger Rudolf, Paola Del Piccolo, Steven J. Burden, Raffaella Di Lisi, Claudia Sandri, Jinghui Zhao, Alfred L. Goldberg, Stefano Schiaffino, and Marco Sandri. 2007. 'FoxO3 Controls Autophagy in Skeletal Muscle In Vivo', *Cell Metabolism*, 6: 458-71.

Manek, Nisha J., Deborah Hart, Timothy D. Spector, and Alexander J. MacGregor. 2003. 'The association of body mass index and osteoarthritis of the knee joint: An examination of genetic and environmental influences', *Arthritis & Rheumatism*, 48: 1024-29.

Manning, Brendan D., and Alex Toker. 2017. 'AKT/PKB Signaling: Navigating the Network', *Cell*, 169: 381-405.

Mapp, P. I., D. R. Sagar, S. Ashraf, J. J. Burston, S. Suri, V. Chapman, and D. A. Walsh. 2013a. 'Differences in structural and pain phenotypes in the sodium monoiodoacetate and meniscal transection models of osteoarthritis', *Osteoarthritis and Cartilage*, 21: 1336-45.

Mapp, PI, PS Avery, DF McWilliams, J Bowyer, C Day, S Moores, R Webster, and DA Walsh. 2008. 'Angiogenesis in two animal models of osteoarthritis', *Osteoarthritis and Cartilage*, 16: 61-69.

Mapp, PI, DR Sagar, S Ashraf, JJ Burston, S Suri, V Chapman, and DA Walsh. 2013b. 'Differences in structural and pain phenotypes in the sodium monoiodoacetate and meniscal transection models of osteoarthritis', *Osteoarthritis and Cartilage*, 21: 1336-45.

Martel-Pelletier, Johanne. 2004. 'Pathophysiology of osteoarthritis', *Osteoarthritis and Cartilage*, 12: 31-33.

Martel-Pelletier, Johanne, Andrew J. Barr, Flavia M. Cicuttini, Philip G. Conaghan, Cyrus Cooper, Mary B. Goldring, Steven R. Goldring, Graeme Jones, Andrew J. Teichtahl, and Jean-Pierre Pelletier. 2016. 'Osteoarthritis', *Nature Reviews Disease Primers*, 2: 16072.

Martín, Ana Isabel, Ana Belén Gómez-SanMiguel, Carolina Gómez-Moreira, María Ángeles Villanúa, and Asunción López-Calderón. 2014. 'αMSH Blunts Endotoxin-Induced MuRF1 and Atrogin-1 Upregulation in Skeletal Muscle by Modulating NF-κB and Akt/FoxO1 Pathway', *Mediators of Inflammation*, 2014: 179368.

Mathiessen, Alexander, and Philip G. Conaghan. 2017. 'Synovitis in osteoarthritis: current understanding with therapeutic implications', *Arthritis research & therapy*, 19: 18-18.

MATSCHKE, VERENA, PETER MURPHY, ANDREW B. LEMMEY, PETER MADDISON, and JEANETTE M. THOM. 2010. 'Skeletal Muscle Properties in Rheumatoid Arthritis Patients', *Medicine & Science in Sports & Exercise*, 42: 2149-55.

McFarlane, Craig, Erin Plummer, Mark Thomas, Alex Hennebry, Murray Ashby, Nicholas Ling, Heather Smith, Mridula Sharma, and Ravi Kambadur. 2006. 'Myostatin induces cachexia by activating the ubiquitin proteolytic system through an NF-κB-independent, FoxO1-dependent mechanism', *Journal of Cellular Physiology*, 209: 501-14.

McGrath, Catherine M., and Stephen P. Young. 2015. 'Lipid and Metabolic Changes in Rheumatoid Arthritis', *Current Rheumatology Reports*, 17: 57.

Mepham, B. L. 1991. 'Theory and practice of histological techniques, 3rd ed. J. D. Bancroft, A. Stevens (Eds). Churchill Livingstone, Edinburgh, 1990. No. of pages: 740. Price: £55. ISBN: 0 443 03559 8', *The Journal of Pathology*, 164: 281-81.

Metsios, G. S., A. Stavropoulos-Kalinoglou, K. M. J. Douglas, Y. Koutedakis, A. M. Nevill, V. F. Panoulas, M. Kita, and G. D. Kitas. 2007. 'Blockade of tumour necrosis factor-α in rheumatoid arthritis:

effects on components of rheumatoid cachexia', *Rheumatology*, 46: 1824-27.

Meulenbelt, I., C. Bijkerk, S. C. M. De Wildt, H. S. Miedema, H. A. Valkenburg, F. C. Breedveld, H. A. P. Pols, J. M. Te Koppele, V. F. G. Sloos, A. Hofman, P. E. Slagboom, and C. M. Van Duijn. 1997. 'Investigation of the association of the CRTM and CRTL1 genes with radiographically evident osteoarthritis in subjects from the rotterdam study', *Arthritis & Rheumatism*, 40: 1760-65.

Michalek, Ryan D., Valerie A. Gerriets, Sarah R. Jacobs, Andrew N. Macintyre, Nancie J. MacIver, Emily F. Mason, Sarah A. Sullivan, Amanda G. Nichols, and Jeffrey C. Rathmell. 2011. 'Cutting edge: distinct glycolytic and lipid oxidative metabolic programs are essential for effector and regulatory CD4+ T cell subsets', *Journal of immunology (Baltimore, Md. : 1950)*, 186: 3299-303.

Mizushima, Noboru, Beth Levine, Ana Maria Cuervo, and Daniel J. Klionsky. 2008. 'Autophagy fights disease through cellular self-digestion', *Nature*, 451: 1069-75.

Mooney, Robert A., Erik R. Sampson, Jaclyn Lerea, Randy N. Rosier, and Michael J. Zuscik. 2011. 'High-fat diet accelerates progression of osteoarthritis after meniscal/ligamentous injury', *Arthritis research & therapy*, 13: R198-R98.

Mootha, Vamsi K., Cecilia M. Lindgren, Karl-Fredrik Eriksson, Aravind Subramanian, Smita Sihag, Joseph Lehar, Pere Puigserver, Emma Carlsson, Martin Ridderstråle, Esa Laurila, Nicholas Houstis, Mark J. Daly, Nick Patterson, Jill P. Mesirov, Todd R. Golub, Pablo Tamayo, Bruce Spiegelman, Eric S. Lander, Joel N. Hirschhorn, David Altshuler, and Leif C. Groop. 2003. 'PGC-1α-responsive genes involved in oxidative phosphorylation are coordinately downregulated in human diabetes', *Nature Genetics*, 34: 267.

Morgenweck, J., R. B. Griggs, R. R. Donahue, J. E. Zadina, and B. K. Taylor. 2013. 'PPARγ activation blocks development and reduces established neuropathic pain in rats', *Neuropharmacology*, 70: 236-46.

Mortensen, B., M. Friedrichsen, N. R. Andersen, A. C. Alibegovic, L. Hojbjerre, M. P. Sonne, B. Stallknecht, F. Dela, J. F. Wojtaszewski, and A. Vaag. 2014. 'Physical inactivity affects skeletal muscle insulin signaling in a birth weight-dependent manner', *J Diabetes Complications*, 28: 71-8.

Müller, Raili, Mart Kull, Margus Lember, Kaja Põlluste, Annika Valner, and Riina Kallikorm. 2017. 'Insulin Resistance in Early Rheumatoid Arthritis Is Associated with Low Appendicular Lean Mass', *BioMed Research International*, 2017: 8.

Murphy, E. Angela, Kandy T. Velazquez, and Kyle M. Herbert. 2015. 'Influence of high-fat diet on gut microbiota: a driving force for chronic disease risk', *Current Opinion in Clinical Nutrition & Metabolic Care*, 18: 515-20.

Murton, Andrew J, and Paul L Greenhaff. 2010. 'Physiological control of muscle mass in humans during resistance exercise, disuse and rehabilitation', *Current Opinion in Clinical Nutrition & Metabolic Care*, 13: 249-54.

Myasoedova, Elena, Cynthia S. Crowson, Hilal Maradit Kremers, Terry M. Therneau, and Sherine E. Gabriel. 2010. 'Is the incidence of rheumatoid arthritis rising?: results from Olmsted County, Minnesota, 1955-2007', *Arthritis and rheumatism*, 62: 1576-82.

Nath, Ravindra, Dinender Kumar, Timao Li, and Pawan K. Singal. 2000. 'Metallothioneins, oxidative stress and the cardiovascular system', *Toxicology*, 155: 17-26.

Nelson, A. E. 2018. 'Osteoarthritis year in review 2017: clinical', *Osteoarthritis Cartilage*, 26: 319-25.

Nicolau, Julia, Thierry Lequerré, Hélène Bacquet, and Olivier Vittecoq. 2017. 'Rheumatoid arthritis, insulin resistance, and diabetes', *Joint Bone Spine*, 84: 411-16.

Nieto, F. R., A. K. Clark, J. Grist, G. J. Hathway, V. Chapman, and M. Malcangio. 2016. 'Neuron-immune mechanisms contribute to pain in early stages of arthritis', *J Neuroinflammation*, 13: 96.

Nilwik, Rachel, Tim Snijders, Marika Leenders, Bart B. L. Groen, Janneau van Kranenburg, Lex B. Verdijk, and Luc J. C. van Loon. 2013. 'The decline in skeletal muscle mass with aging is mainly attributed to a reduction in type II muscle fiber size', *Experimental Gerontology*, 48: 492-98.

Nüesch, Eveline, Paul Dieppe, Stephan Reichenbach, Susan Williams, Samuel Iff, and Peter Jüni. 2011. 'All cause and disease specific mortality in patients with knee or hip osteoarthritis: population based cohort study', *BMJ (Clinical research ed.)*, 342: d1165-d65.

Nwosu, L. N., P. I. Mapp, V. Chapman, and D. A. Walsh. 2016. 'Relationship between structural pathology and pain behaviour in a model of osteoarthritis (OA)', *Osteoarthritis and Cartilage*, 24: 1910-17.

Oberbach, Andreas, Yvonne Bossenz, Stefanie Lehmann, Josef Niebauer, Volker Adams, Ralf Paschke, Michael R. Schön, Matthias Blüher, and Karla Punkt. 2006. 'Altered Fiber Distribution and Fiber-Specific Glycolytic and Oxidative Enzyme Activity in Skeletal Muscle of Patients With Type 2 Diabetes', *Diabetes Care*, 29: 895-900.

Okada, Yukinori, Di Wu, Gosia Trynka, Towfique Raj, Chikashi Terao, Katsunori Ikari, Yuta Kochi, Koichiro Ohmura, Akari Suzuki, Shinji Yoshida, Robert R. Graham, Arun Manoharan, Ward Ortmann, Tushar Bhangale, Joshua C. Denny, Robert J. Carroll, Anne E. Eyler, Jeffrey D. Greenberg, Joel M. Kremer, Dimitrios A. Pappas, Lei Jiang, Jian Yin, Lingying Ye, Ding-Feng Su, Jian Yang, Gang Xie, Ed Keystone, Harm-Jan Westra, Tõnu Esko, Andres Metspalu, Xuezhong Zhou, Namrata Gupta, Daniel Mirel, Eli A. Stahl, Dorothée Diogo, Jing Cui, Katherine Liao, Michael H. Guo, Keiko Myouzen, Takahisa Kawaguchi, Marieke J. H. Coenen, Piet L. C. M. van Riel, Mart A. F. J. van de Laar, Henk-Jan Guchelaar, Tom W. J. Huizinga, Philippe Dieudé, Xavier Mariette, S. Louis Bridges, Jr., Alexandra Zhernakova, Rene E. M. Toes, Paul P. Tak, Corinne Miceli-Richard, So-Young Bang, Hye-Soon Lee, Javier Martin, Miguel A. Gonzalez-Gay, Luis Rodriguez-Rodriguez, Solbritt Rantapää-Dahlqvist, Lisbeth Arlestig, Hyon K. Choi, Yoichiro Kamatani, Pilar Galan, Mark Lathrop, Raci consortium, Garnet consortium, Steve Eyre, John Bowes, Anne Barton, Niek de Vries, Larry W. Moreland, Lindsey A.

Criswell, Elizabeth W. Karlson, Atsuo Taniguchi, Ryo Yamada, Michiaki Kubo, Jun S. Liu, Sang-Cheol Bae, Jane Worthington, Leonid Padyukov, Lars Klareskog, Peter K. Gregersen, Soumya Raychaudhuri, Barbara E. Stranger, Philip L. De Jager, Lude Franke, Peter M. Visscher, Matthew A. Brown, Hisashi Yamanaka, Tsuneyo Mimori, Atsushi Takahashi, Huji Xu, Timothy W. Behrens, Katherine A. Siminovitch, Shigeki Momohara, Fumihiko Matsuda, Kazuhiko Yamamoto, and Robert M. Plenge. 2014. 'Genetics of rheumatoid arthritis contributes to biology and drug discovery', *Nature*, 506: 376-81.

Olsen, R. H., R. Krogh-Madsen, C. Thomsen, F. W. Booth, and B. K. Pedersen. 2008. 'Metabolic responses to reduced daily steps in healthy nonexercising men', *JAMA*, 299: 1261-3.

Ormseth, Michelle J., Annette M. Oeser, Andrew Cunningham, Aihua Bian, Ayumi Shintani, Joseph Solus, S. Tanner, and C. Michael Stein. 2013. 'Peroxisome proliferator-activated receptor γ agonist effect on rheumatoid arthritis: a randomized controlled trial', *Arthritis research & therapy*, 15: R110-R10.

Overmyer, K. A., C. Thonusin, N. R. Qi, C. F. Burant, and C. R. Evans. 2015. 'Impact of anesthesia and euthanasia on metabolomics of mammalian tissues: studies in a C57BL/6J mouse model', *PLOS ONE*, 10: e0117232.

Pain, Virginia M. 1996. 'Initiation of Protein Synthesis in Eukaryotic Cells', *European Journal of Biochemistry*, 236: 747-71.

Pasiakos, S. M., and J. P. McClung. 2011. 'Supplemental dietary leucine and the skeletal muscle anabolic response to essential amino acids', *Nutr Rev*, 69: 550-7.

Passmore, Lori A., and David Barford. 2004. 'Getting into position: the catalytic mechanisms of protein ubiquitylation', *The Biochemical journal*, 379: 513-25.

Peake, J. M., P. Della Gatta, K. Suzuki, and D. C. Nieman. 2015. 'Cytokine expression and secretion by skeletal muscle cells: regulatory mechanisms and exercise effects', *Exerc Immunol Rev*, 21: 8-25.

Pedemonte, Marina, Claudia Sandri, Stefano Schiaffino, and Carlo Minetti. 1999. 'Early Decrease of IIx Myosin Heavy Chain Transcripts in Duchenne Muscular Dystrophy', *Biochemical and Biophysical Research Communications*, 255: 466-69.

Pedersen, Bente K., and Mark A. Febbraio. 2008. 'Muscle as an Endocrine Organ: Focus on Muscle-Derived Interleukin-6', *Physiological Reviews*, 88: 1379-406.

Penninx, Brenda W J H, Haider Abbas, Walter Ambrosius, Barbara J Nicklas, Cralen Davis, Stephen P Messier, and Marco Pahor. 2004. 'Inflammatory markers and physical function among older adults with knee osteoarthritis', *The Journal of Rheumatology*, 31: 2027-31.

Perl, Andras. 2010. 'Systems biology of lupus: mapping the impact of genomic and environmental factors on gene expression signatures, cellular signaling, metabolic pathways, hormonal and cytokine imbalance, and selecting targets for treatment', *Autoimmunity*, 43: 32-47.

Peschken, Christine A., and John M. Esdaile. 1999. 'Rheumatic diseases in North America's indigenous peoples', *Seminars in Arthritis and Rheumatism*, 28: 368-91.

Puthucheary, Z. A., J. Rawal, M. McPhail, and et al. 2013. 'Acute skeletal muscle wasting in critical illness', *JAMA*, 310: 1591-600.

Radner, Helga, Tamara Lesperance, Neil A. Accortt, and Daniel H. Solomon. 2017. 'Incidence and Prevalence of Cardiovascular Risk Factors Among Patients With Rheumatoid Arthritis, Psoriasis, or Psoriatic Arthritis', *Arthritis Care & Research*, 69: 1510-18.

Redlich, Kurt, and Josef S. Smolen. 2012. 'Inflammatory bone loss: pathogenesis and therapeutic intervention', *Nature Reviews Drug Discovery*, 11: 234.

Rende, Mario, Emanuela Brizi, Jim Conner, Susan Treves, Kathrin Censier, Carlo Provenzano, Giulio Taglialatela, Pietro Paolo Sanna, and Rosario Donato. 2000. 'Nerve growth factor (NGF) influences differentiation and proliferation of myogenic cells in vitro via TrKA', *International Journal of Developmental Neuroscience*, 18: 869-85.

Rhoads, Robert E. 1999. 'Signal Transduction Pathways That Regulate Eukaryotic Protein Synthesis', *Journal of Biological Chemistry*, 274: 30337-40.

Ricote, Mercedes, Andrew C. Li, Timothy M. Willson, Carolyn J. Kelly, and Christopher K. Glass. 1998. 'The peroxisome proliferator-activated receptor-γ is a negative regulator of macrophage activation', *Nature*, 391: 79.

Ridgley, Laura A., Amy E. Anderson, and Arthur G. Pratt. 2018. 'What are the dominant cytokines in early rheumatoid arthritis?', *Current opinion in rheumatology*, 30: 207-14.

Rizos, C. V., E. N. Liberopoulos, D. P. Mikhailidis, and M. S. Elisaf. 2008. 'Pleiotropic effects of thiazolidinediones', *Expert Opinion on Pharmacotherapy*, 9: 1087-108.

Rizos, Christos V., Anastazia Kei, and Moses S. Elisaf. 2016. 'The current role of thiazolidinediones in diabetes management', *Archives of Toxicology*, 90: 1861-81.

Roiniotis, John, Hang Dinh, Paul Masendycz, Amanda Turner, Caryn L. Elsegood, Glen M. Scholz, and John A. Hamilton. 2009. 'Hypoxia Prolongs Monocyte/Macrophage Survival and Enhanced Glycolysis Is Associated with Their Maturation under Aerobic Conditions', *The Journal of Immunology*, 182: 7974-81.

Rosillo, María Angeles, Marina Sánchez-Hidalgo, Susana Sánchez-Fidalgo, Marina Aparicio-Soto, Isabel Villegas, and Catalina Alarcón-de-la-Lastra. 2016. 'Dietary extra-virgin olive oil prevents inflammatory response and cartilage matrix degradation in murine collagen-induced arthritis', *European Journal of Nutrition*, 55: 315-25.

Roubenoff, R., R. A. Roubenoff, J. G. Cannon, J. J. Kehayias, H. Zhuang, B. Dawson-Hughes, C. A. Dinarello, and I. H. Rosenberg. 1994. 'Rheumatoid cachexia: cytokine-driven hypermetabolism accompanying reduced body cell mass in chronic inflammation', *Journal of Clinical Investigation*, 93: 2379-86.

Roubenoff, Ronenn, Joseph Walsmith, Nancy Lundgren, Laura Snydman, Gregory J. Dolnikowski, and Susan Roberts. 2002. 'Low physical activity reduces total energy expenditure in women with rheumatoid arthritis: implications for dietary intake recommendations', *The American Journal of Clinical Nutrition*, 76: 774-79.

Roubille, Camille, Jean-Pierre Pelletier, and Johanne Martel-Pelletier. 2013. 'New and emerging treatments for osteoarthritis management: will the dream come true with personalized medicine?', *Expert Opinion on Pharmacotherapy*, 14: 2059-77.

Rui, Liangyou, Vincent Aguirre, Jason K. Kim, Gerald I. Shulman, Anna Lee, Anne Corbould, Andrea Dunaif, and Morris F. White. 2001. 'Insulin/IGF-1 and TNF-α stimulate phosphorylation of IRS-1 at inhibitory Ser(307) via distinct pathways', *Journal of Clinical Investigation*, 107: 181-89.

Ryder, J J, K Garrison, F Song, L Hooper, J Skinner, Y Loke, J Loughlin, J P T Higgins, and A J MacGregor. 2008. 'Genetic associations in peripheral joint osteoarthritis and spinal degenerative disease: a systematic review', *Annals of the Rheumatic Diseases*, 67: 584-91.

Sagar, D. R., L. E. Staniaszek, B. N. Okine, S. Woodhams, L. M. Norris, R. G. Pearson, M. J. Garle, S. P. Alexander, A. J. Bennett, D. A. Barrett, D. A. Kendall, B. E. Scammell, and V. Chapman. 2010. 'Tonic modulation of spinal hyperexcitability by the endocannabinoid receptor system in a rat model of osteoarthritis pain', *Arthritis Rheum*, 62: 3666-76.

Sanada, Fumihiro, Yoshiaki Taniyama, Jun Muratsu, Rei Otsu, Hideo Shimizu, Hiromi Rakugi, and Ryuichi Morishita. 2018. 'Source of Chronic Inflammation in Aging', *Frontiers in cardiovascular medicine*, 5: 12-12.

Sandell, L. J., and T. Aigner. 2001. 'Articular cartilage and changes in arthritis. An introduction: cell biology of osteoarthritis', *Arthritis research*, 3: 107-13.

Sandri, Marco, Claudia Sandri, Alex Gilbert, Carsten Skurk, Elisa Calabria, Anne Picard, Kenneth Walsh, Stefano Schiaffino, Stewart H. Lecker, and Alfred L. Goldberg. 2004. 'Foxo Transcription Factors Induce the Atrophy-Related Ubiquitin Ligase Atrogin-1 and Cause Skeletal Muscle Atrophy', *Cell*, 117: 399-412.

Sanmiguel, Claudia, Arpana Gupta, and Emeran A. Mayer. 2015. 'Gut Microbiome and Obesity: A Plausible Explanation for Obesity', *Current Obesity Reports*, 4: 250-61.

Sartori-Cintra, A. R., P. Aikawa, and D. E. Cintra. 2014. 'Obesity versus osteoarthritis: beyond the mechanical overload', *Einstein (Sao Paulo)*, 12: 374-9.

Sasakawa, Tatsuya, Yuka Sasakawa, Yoshitaka Ohkubo, and Seitaro Mutoh. 2005. 'FK506 ameliorates spontaneous locomotor activity in collagen-induced arthritis: implication of distinct effect from suppression of inflammation', *International Immunopharmacology*, 5: 503-10.

Scanzello, Carla R., and Steven R. Goldring. 2012. 'The role of synovitis in osteoarthritis pathogenesis', *Bone*, 51: 249-57.

Scanzello, Carla R., Brian McKeon, Bryan H. Swaim, Edward DiCarlo, Eva U. Asomugha, Veero Kanda, Anjali Nair, David M. Lee, John C. Richmond, Jeffrey N. Katz, Mary K. Crow, and Steven R. Goldring. 2011. 'Synovial inflammation in patients undergoing arthroscopic meniscectomy: molecular characterization and relationship to symptoms', *Arthritis and rheumatism*, 63: 391-400.

Schett, Georg, and Ellen Gravallese. 2012. 'Bone erosion in rheumatoid arthritis: mechanisms, diagnosis and treatment', *Nature reviews. Rheumatology*, 8: 656-64.

Schiaffino, Stefano, and Cristina Mammucari. 2011. 'Regulation of skeletal muscle growth by the IGF1-Akt/PKB pathway: insights from genetic models', *Skeletal Muscle*, 1: 4-4.

Schiaffino, Stefano, and Carlo Reggiani. 2011. 'Fiber Types in Mammalian Skeletal Muscles', *Physiological Reviews*, 91: 1447-531.

Schuelke, Markus, Kathryn R. Wagner, Leslie E. Stolz, Christoph Hübner, Thomas Riebel, Wolfgang Kömen, Thomas Braun, James F. Tobin, and Se-Jin Lee. 2004. 'Myostatin Mutation Associated with Gross Muscle Hypertrophy in a Child', *New England Journal of Medicine*, 350: 2682-88.

Serrano, Antonio L., Bernat Baeza-Raja, Eusebio Perdiguero, Mercè Jardí, and Pura Muñoz-Cánoves. 2008. 'Interleukin-6 Is an Essential Regulator of Satellite Cell-Mediated Skeletal Muscle Hypertrophy', *Cell Metabolism*, 7: 33-44.

Silva, Jordana Miranda de Souza, Paulo Vinicius Gil Alabarse, Vivian de Oliveira Nunes Teixeira, Eduarda Correa Freitas, Francine Hehn de Oliveira, Rafael Mendonça da Silva Chakr, and Ricardo Machado Xavier. 2018. 'Muscle wasting in osteoarthritis model induced by anterior cruciate ligament transection', *PLOS ONE*, 13: e0196682.

Simon, Lee S. 1999. 'Role and regulation of cyclooxygenase-2 during inflammation', *The American Journal of Medicine*, 106: 37S-42S.

Sköldstam, L., L. Hagfors, and G. Johansson. 2003. 'An experimental study of a Mediterranean diet intervention for patients with rheumatoid arthritis', *Annals of the rheumatic diseases*, 62: 208-14.

Slemenda, C., K. D. Brandt, D. K. Heilman, and et al. 1997. 'QUadriceps weakness and osteoarthritis of the knee', *Annals of Internal Medicine*, 127: 97-104.

Smolen, Josef S., Daniel Aletaha, Anne Barton, Gerd R. Burmester, Paul Emery, Gary S. Firestein, Arthur Kavanaugh, Iain B. McInnes, Daniel H. Solomon, Vibeke Strand, and Kazuhiko Yamamoto. 2018. 'Rheumatoid arthritis', *Nature Reviews Disease Primers*, 4: 18001.

Smolen, Josef S., Daniel Aletaha, and Iain B. McInnes. 2016. 'Rheumatoid arthritis', *The Lancet*, 388: 2023-38.

Smolen, Josef S., Gabriele Eberl, Ferdinand C. Breedveld, Ieuan Jones, Michael Leeming, Graham L. Wylie, and John Kirkpatrick. 1995. 'Validity and reliability of the twenty-eight-joint count for the assessment of rheumatoid arthritis activity', *Arthritis & Rheumatism*, 38: 38-43.

Soop, M., E. Forsberg, A. Thörne, G. Cederblad, J. Bergström, A. M. Forsberg, and E. Hultman. 1989. 'Muscle alkali-soluble protein,

carnitine, water and electrolytes in patients with persistent post-operative infection', *Clinical Nutrition*, 8: 237-45.

Soubrier, Martin, Nicolas Barber Chamoux, Zuzana Tatar, Marion Couderc, Jean-Jacques Dubost, and Sylvain Mathieu. 2014. 'Cardiovascular risk in rheumatoid arthritis', *Joint Bone Spine*, 81: 298-302.

Soukup, Tomáš, Gisela Zachařová, and Vika Smerdu. 2002. 'Fibre type composition of soleus and extensor digitorum longus muscles in normal female inbred Lewis rats', *Acta Histochemica*, 104: 399-405.

Sparks, Jeffrey A., Shun-Chiao Chang, Katherine P. Liao, Bing Lu, Alexander R. Fine, Daniel H. Solomon, Karen H. Costenbader, and Elizabeth W. Karlson. 2016. 'Rheumatoid Arthritis and Mortality Among Women During 36 Years of Prospective Follow-Up: Results From the Nurses' Health Study', *Arthritis care & research*, 68: 753-62.

Stephens, Nathan A., Iain J. Gallagher, Olav Rooyackers, Richard J. Skipworth, Ben H. Tan, Troels Marstrand, James A. Ross, Denis C. Guttridge, Lars Lundell, Kenneth C. Fearon, and James A. Timmons. 2010. 'Using transcriptomics to identify and validate novel biomarkers of human skeletal muscle cancer cachexia', *Genome Medicine*, 2: 1.

Stitt, Trevor N., Doreen Drujan, Brian A. Clarke, Frank Panaro, Yekatarina Timofeyva, William O. Kline, Michael Gonzalez, George D. Yancopoulos, and David J. Glass. 2004. 'The IGF-1/PI3K/Akt Pathway Prevents Expression of Muscle Atrophy-Induced Ubiquitin Ligases by Inhibiting FOXO Transcription Factors', *Molecular Cell*, 14: 395-403.

Stolt, P., H. Källberg, I. Lundberg, B. Sjögren, L. Klareskog, L. Alfredsson, and Eira study group. 2005. 'Silica exposure is associated with increased risk of developing rheumatoid arthritis: results from the Swedish EIRA study', *Annals of the rheumatic diseases*, 64: 582-86.

Strand, Vibeke, Robert Kimberly, and John D. Isaacs. 2007. 'Biologic therapies in rheumatology: lessons learned, future directions', *Nature Reviews Drug Discovery*, 6: 75.

Strasser, Barbara, Gunther Leeb, Christoph Strehblow, Wolfgang Schobersberger, Paul Haber, and Edmund Cauza. 2011. 'The effects of strength and endurance training in patients with rheumatoid arthritis', *Clinical Rheumatology*, 30: 623-32.

Strassmann, G., M. Fong, J. S. Kenney, and C. O. Jacob. 1992. 'Evidence for the involvement of interleukin 6 in experimental cancer cachexia', *The Journal of clinical investigation*, 89: 1681-84.

Straub, R. H., M. Cutolo, F. Buttgereit, and G. Pongratz. 2010. 'Energy regulation and neuroendocrine–immune control in chronic inflammatory diseases', *Journal of Internal Medicine*, 267: 543-60.

Strle, Klemen, Robert H. McCusker, Lynn Tran, Alexandra King, Rodney W. Johnson, Gregory G. Freund, Robert Dantzer, and Keith W. Kelley. 2007. 'Novel activity of an anti-inflammatory cytokine: IL-10 prevents TNFalpha-induced resistance to IGF-I in myoblasts', *Journal of neuroimmunology*, 188: 48-55.

Suri, Sunita, Sarah E. Gill, Sally Massena de Camin, Deborah Wilson, Daniel F. McWilliams, and David A. Walsh. 2007. 'Neurovascular

invasion at the osteochondral junction and in osteophytes in osteoarthritis', *Annals of the rheumatic diseases*, 66: 1423-28.

Svenson, Karin L. G., Thomas Pollare, Hans Lithell, and Roger Hällgren. 1988. 'Impaired glucose handling in active rheumatoid arthritis: Relationship to peripheral insulin resistance', *Metabolism - Clinical and Experimental*, 37: 125-30.

Taillandier, P., F. Gilis, F. Ramon Portugal, P. Laforce, and P. Strehaiano. 1996. 'Influence of medium composition, pH and temperature on the growth and viability of Lactobacillus acidophilus', *Biotechnology Letters*, 18: 775-80.

Talbot, Jared, and Lisa Maves. 2016. 'Skeletal muscle fiber type: using insights from muscle developmental biology to dissect targets for susceptibility and resistance to muscle disease', *Wiley interdisciplinary reviews. Developmental biology*, 5: 518-34.

Tanimoto, Atsuo, Yuichi Shinozaki, Keisuke Nozawa, Yukari Kimoto, Wataru Amano, Akira Matsuo, Takayuki Yamaguchi, and Mutsuyoshi Matsushita. 2015. 'Improvement of spontaneous locomotor activity with JAK inhibition by JTE-052 in rat adjuvant-induced arthritis', *BMC Musculoskeletal Disorders*, 16: 339.

Tannahill, Gillian M., and Luke A.J. O'Neill. 2011. 'The emerging role of metabolic regulation in the functioning of Toll-like receptors and the NOD-like receptor Nlrp3', *FEBS Letters*, 585: 1568-72.

Tanner, Charles J., Hisham A. Barakat, G. Lynis Dohm, Walter J. Pories, Kenneth G. MacDonald, Paul R. G. Cunningham, Melvin S. Swanson, and Joseph A. Houmard. 2002. 'Muscle fiber type is associated with obesity and weight loss', *American Journal of Physiology-Endocrinology and Metabolism*, 282: E1191-E96.

Terada, N., H. R. Patel, K. Takase, K. Kohno, A. C. Nairn, and E. W. Gelfand. 1994. 'Rapamycin selectively inhibits translation of mRNAs encoding elongation factors and ribosomal proteins', *Proceedings of the National Academy of Sciences of the United States of America*, 91: 11477-81.

Thijssen, Eva, Arjan van Caam, and Peter M. van der Kraan. 2015. 'Obesity and osteoarthritis, more than just wear and tear: pivotal roles for inflamed adipose tissue and dyslipidaemia in obesity-induced osteoarthritis', *Rheumatology*, 54: 588-600.

Thomas, Sandhya S., and William E. Mitch. 2013. 'Mechanisms stimulating muscle wasting in chronic kidney disease: the roles of the ubiquitin-proteasome system and myostatin', *Clinical and experimental nephrology*, 17: 174-82.

Thorstensson, C A, M L E Andersson, H Jönsson, T Saxne, and I F Petersson. 2009. 'Natural course of knee osteoarthritis in middle-aged subjects with knee pain: 12-year follow-up using clinical and radiographic criteria', *Annals of the rheumatic diseases*, 68: 1890-93.

Thrower, J. S., L. Hoffman, M. Rechsteiner, and C. M. Pickart. 2000. 'Recognition of the polyubiquitin proteolytic signal', *The EMBO journal*, 19: 94-102.

Tiao, G., M. Lieberman, J. E. Fischer, and P. O. Hasselgren. 1997. 'Intracellular regulation of protein degradation during sepsis is different in fast- and slow-twitch muscle', *American Journal of*

Physiology-Regulatory, Integrative and Comparative Physiology, 272: R849-R56.

Tintignac, Lionel A., Julie Lagirand, Sabrina Batonnet, Valentina Sirri, Marie Pierre Leibovitch, and Serge A. Leibovitch. 2005. 'Degradation of MyoD Mediated by the SCF (MAFbx) Ubiquitin Ligase', *Journal of Biological Chemistry*, 280: 2847-56.

Tobón, Gabriel J., Pierre Youinou, and Alain Saraux. 2010. 'The environment, geo-epidemiology, and autoimmune disease: Rheumatoid arthritis', *Journal of Autoimmunity*, 35: 10-14.

Tombran-Tink, J., and C. J. Barnstable. 2004. 'Osteoblasts and osteoclasts express PEDF, VEGF-A isoforms, and VEGF receptors: possible mediators of angiogenesis and matrix remodeling in the bone', *Biochemical and Biophysical Research Communications*, 316: 573-79.

Tontonoz, P., and B. M. Spiegelman. 2008. 'Fat and beyond: the diverse biology of PPARgamma', *Annu Rev Biochem*, 77: 289-312.

Tore, F., and N. Tuncel. 2009. 'Mast Cells: Target and Source of Neuropeptides', *Current Pharmaceutical Design*, 15: 3433-45.

Tournadre, Anne, Bruno Pereira, Fréderic Dutheil, Charlotte Giraud, Daniel Courteix, Vincent Sapin, Thomas Frayssac, Sylvain Mathieu, Sandrine Malochet-Guinamand, and Martin Soubrier. 2017. 'Changes in body composition and metabolic profile during interleukin 6 inhibition in rheumatoid arthritis', *Journal of Cachexia, Sarcopenia and Muscle*, 8: 639-46.

Trelle, Sven, Stephan Reichenbach, Simon Wandel, Pius Hildebrand, Beatrice Tschannen, Peter M Villiger, Matthias Egger, and Peter Jüni. 2011. 'Cardiovascular safety of non-steroidal anti-inflammatory drugs: network meta-analysis', *BMJ*, 342.

Trentham, D. E., A. S. Townes, and A. H. Kang. 1977. 'Autoimmunity to type II collagen an experimental model of arthritis', *The Journal of experimental medicine*, 146: 857-68.

Trouw, L A, Tom W J Huizinga, and René E M Toes. 2013. 'Autoimmunity in rheumatoid arthritis: different antigens—common principles', *Annals of the Rheumatic Diseases*, 72: ii132-ii36.

Tsintzas, Kostas, Kamal Chokkalingam, Kirsty Jewell, Luke Norton, Ian A. Macdonald, and Dumitru Constantin-Teodosiu. 2007. 'Elevated Free Fatty Acids Attenuate the Insulin-Induced Suppression of PDK4 Gene Expression in Human Skeletal Muscle: Potential Role of Intramuscular Long-Chain Acyl-Coenzyme A', *The Journal of Clinical Endocrinology & Metabolism*, 92: 3967-72.

Tsujinaka, T., C. Ebisui, J. Fujita, M. Kishibuchi, T. Morimoto, A. Ogawa, A. Katsume, Y. Ohsugi, E. Kominami, and M. Monden. 1995. 'Muscle Undergoes Atrophy in Association with Increase of Lysosomal Cathepsin Activity in Interleukin-6 Transgenic Mouse', *Biochemical and Biophysical Research Communications*, 207: 168-74.

van der Poel, C., P. Levinger, B. A. Tonkin, I. Levinger, and N. C. Walsh. 2016. 'Impaired muscle function in a mouse surgical model of post-traumatic osteoarthritis', *Osteoarthritis and Cartilage*, 24: 1047-53.

Van Ede, Annelies E., Roland F. J. M. Laan, Maarten J. Rood, Tom W. J. Huizinga, Mart A. F. J. Van De Laar, Christiaan J. Van Denderen,

Toon A. A. Westgeest, Ton C. Romme, Dirk-Jan R. A. M. De Rooij, Marike J. M. Jacobs, Theo M. De Boo, Gert-Jan Van Der Wilt, Johan L. Severens, Margriet Hartman, Paul F. M. Krabbe, Ben A. C. Dijkmans, Ferdinand C. Breedveld, and Leo B. A. Van De Putte. 2001. 'Effect of folic or folinic acid supplementation on the toxicity and efficacy of methotrexate in rheumatoid arthritis: A forty-eight–week, multicenter, randomized, double-blind, placebo-controlled study', *Arthritis & Rheumatism*, 44: 1515-24.

van Hall, Gerrit, Adam Steensberg, Christian Fischer, Charlotte Keller, Kirsten Møller, Pope Moseley, and Bente K. Pedersen. 2008. 'Interleukin-6 Markedly Decreases Skeletal Muscle Protein Turnover and Increases Nonmuscle Amino Acid Utilization in Healthy Individuals', *The Journal of Clinical Endocrinology & Metabolism*, 93: 2851-58.

van Venrooij, Walther J., Albert J. W. Zendman, and Ger J. M. Pruijn. 2006. 'Autoantibodies to citrullinated antigens in (early) rheumatoid arthritis', *Autoimmunity Reviews*, 6: 37-41.

Varadhan, Krishna K., Dumitru Constantin-Teodosiu, Despina Constantin, Paul L. Greenhaff, and Dileep N. Lobo. 2017. 'Inflammation-mediated muscle metabolic dysregulation local and remote to the site of major abdominal surgery', *Clinical Nutrition*.

Vasheghani, F., R. Monemdjou, H. Fahmi, Y. Zhang, G. Perez, M. Blati, R. St-Arnaud, J. P. Pelletier, F. Beier, J. Martel-Pelletier, and M. Kapoor. 2013. 'Adult cartilage-specific peroxisome proliferator-activated receptor gamma knockout mice exhibit the spontaneous osteoarthritis phenotype', *Am J Pathol*, 182: 1099-106.

Wang, Xiaonan, Zhaoyong Hu, Junping Hu, Jie Du, and William E. Mitch. 2006. 'Insulin Resistance Accelerates Muscle Protein Degradation: Activation of the Ubiquitin-Proteasome Pathway by Defects in Muscle Cell Signaling', *Endocrinology*, 147: 4160-68.

Watson, David J. G., Charles A. Marsden, Mark J. Millan, and Kevin C. F. Fone. 2012. 'Blockade of dopamine D3 but not D2 receptors reverses the novel object discrimination impairment produced by post-weaning social isolation: implications for schizophrenia and its treatment', *International Journal of Neuropsychopharmacology*, 15: 471-84.

Wieland, Heike A., Martin Michaelis, Bernhard J. Kirschbaum, and Karl A. Rudolphi. 2005. 'Osteoarthritis — an untreatable disease?', *Nature Reviews Drug Discovery*, 4: 331.

Wilkes, Emilie A., Anna L. Selby, Philip J. Atherton, Rekha Patel, Debbie Rankin, Ken Smith, and Michael J. Rennie. 2009. 'Blunting of insulin inhibition of proteolysis in legs of older subjects may contribute to age-related sarcopenia', *The American Journal of Clinical Nutrition*, 90: 1343-50.

WILLIAMS, ARTHUR B., GABRIELLE M. DECOURTEN-MYERS, JOSEF E. FISCHER, GUANGJU LUO, XIAOYAN SUN, and PER-OLOF HASSELGREN. 1999. 'Sepsis stimulates release of myofilaments in skeletal muscle by a calcium-dependent mechanism', *The FASEB Journal*, 13: 1435-43.

Williams, Arthur, Xiaoyan Sun, Josef E. Fischer, and Per-Olof Hasselgren. 1999. 'The expression of genes in the ubiquitin-proteasome proteolytic pathway is increased in skeletal muscle from patients with cancer', *Surgery*, 126: 744-50.

Wilsdon, Tom D., and Catherine L. Hill. 2017. 'Managing the drug treatment of rheumatoid arthritis', *Australian Prescriber*, 40: 51-58.

Yamaguchi, Koichi, Katsuhiro Higashiura, Nobuyuki Ura, Hideyuki Murakami, Masaya Hyakukoku, Masato Furuhashi, and Kazuaki Shimamoto. 2003. 'The Effect of Tumor Necrosis Factor-α on Tissue Specificity and Selectivity to Insulin Signaling</B>', *Hypertension Research*, 26: 389-96.

Yamazaki, Yoshihiro, Yasutomi Kamei, Satoshi Sugita, Fumiko Akaike, Sayaka Kanai, Shinji Miura, Yukio Hirata, Bruce R. Troen, Tadahiro Kitamura, Ichizo Nishino, Takayoshi Suganami, Osamu Ezaki, and Yoshihiro Ogawa. 2010. 'The cathepsin L gene is a direct target of FOXO1 in skeletal muscle', *Biochemical Journal*, 427: 171-78.

Yin, Jian, Zhichao Hao, Yuanyuan Ma, Shuang Liao, Xianxian Li, Jing Fu, Yeke Wu, Jiefei Shen, Ping Zhang, Xiaoyu Li, and Hang Wang. 2014. 'Concomitant activation of the PI3K/Akt and ERK1/2 signalling is involved in cyclic compressive force-induced IL-6 secretion in MLO-Y4 cells', *Cell Biology International*, 38: 591-98.

Yoshino, Shin, Yuzo Murata, and Motoyasu Ohsawa. 1998. 'Successful Induction of Adjuvant Arthritis in Mice by Treatment with a Monoclonal Antibody Against IL-4', *The Journal of Immunology*, 161: 6904-08.

Zamir, O., P. Hasselgren, S. L. Kunkel, J. Frederick, T. Higashiguchi, and J. E. Fischer. 1992. 'Evidence that tumor necrosis factor participates in the regulation of muscle proteolysis during sepsis', *Archives of Surgery*, 127: 170-74.

Zhang, Jun-Ming, and Jianxiong An. 2007. 'Cytokines, Inflammation and Pain', *International anesthesiology clinics*, 45: 27-37.

Zhang, W., R. W. Moskowitz, G. Nuki, S. Abramson, R. D. Altman, N. Arden, S. Bierma-Zeinstra, K. D. Brandt, P. Croft, M. Doherty, M. Dougados, M. Hochberg, D. J. Hunter, K. Kwoh, L. S. Lohmander, and P. Tugwell. 2008. 'OARSI recommendations for the management of hip and knee osteoarthritis, Part II: OARSI evidence-based, expert consensus guidelines', *Osteoarthritis and Cartilage*, 16: 137-62.

Zhao, Jinghui, Jeffrey J. Brault, Andreas Schild, Peirang Cao, Marco Sandri, Stefano Schiaffino, Stewart H. Lecker, and Alfred L. Goldberg. 2007. 'FoxO3 Coordinately Activates Protein Degradation by the Autophagic/Lysosomal and Proteasomal Pathways in Atrophying Muscle Cells', *Cell Metabolism*, 6: 472-83.

Ziff, Morris. 1974. 'Relation of cellular infiltration of rheumatoid synovial membrane to its immune response', *Arthritis & Rheumatism*, 17: 313-19.